Developing an alveolar model to test the regenerative potential of placental membrane mesenchymal stem cells in bronchopulmonary dysplasia

Jessica A. J. Bratt

Institute of Science and Technology in Medicine

Keele University

Thesis submitted for the degree of

Doctor of Philosophy

December 2019

Abstract

Bronchopulmonary dysplasia (BPD) is a neonatal disease affecting the lungs of premature infants. Prematurely born infants have under-developed lungs and require invasive ventilation technologies to provide sufficient oxygen for survival. Artificial ventilation is thought to exacerbate BPD by causing mechanical and oxygen stress on the lung tissue. Despite improvements in paediatric respiratory management, BPD care is limited by a lack of appropriate treatment options and remains a key challenge for clinicians. The pathogenesis of BPD remains poorly understood and currently relies on animal models for investigation. This study looks at developing a hydrogel to provide a human relevant *in vitro* BPD model to investigate the potential regenerative capabilities of placenta mesenchymal stem cells as a cell-based therapy for BPD.

We successfully developed a collagen-elastin hydrogel representative of the human lung alveolus. This allows the co-culture of multiple lung cells in addition to an air-liquid interface which achieves hyperoxygen exposure (equivalent to clinical ventilation interventions) and allows assessment of output measures such as hydrogel contraction, imaging techniques and DNA quantification.

We identified a protocol to extract and expand cells from the tracheal suctions of ventilated infants. We cultured these cells within the previously developed model for assessment at hyperoxygen and compared cell function with human adult lung cells. We established that hyperoxygen had a detrimental effect on adult lung cell proliferation and the ability of cells to contract collagen-elastin hydrogels. Hyperoxygen had no observed effect on neonatal lung cells.

Finally, placenta derived MSCs (pMSCs) were isolated from the amnion and chorion membrane. We found hyperoxygen exposure has an adverse effect on the expression of MSC cell markers, cell proliferation and cell morphology. This could have implications when developing a cell therapy for the treatment of BPD. When co-cultured with adult lung fibroblast, pMSCs positively influenced the proliferation of adult lung fibroblasts through a paracrine mechanism. These results suggest that pMSCs have the potential to alleviate the oxygen stress that lung cells of BPD infants experience.

Keywords: Bronchopulmonary dysplasia, neonatal lung, cell therapy, regenerative medicine, placenta mesenchymal stem cell, in vitro model, hyperoxygen

Acknowledgments

I would like to sincerely thank my supervisors Dr Pensee Wu, Professor Nick Forsyth and Professor Alicia El Haj for their support and encouragement. At various stages of my PhD studies they have all significantly influenced my research. Their knowledge and guidance have helped me develop into an independent, self-confident scientist.

This study would not have been possible without the participation of patients from UHNM who kindly donated their placentas and tracheal suctionings. Their involvement during a vulnerable time was greatly appreciated and was a unique contribution to my studies. Patient recruitment and sample handling was achieved through the generous cooperation of clinical staff at the NICU unit of UHNM, particularly Dr Lee Abbott who allowed us to collect samples and provided a valuable clinical viewpoint.

This study was generously funded by ESPRC as part of the Loughborough, Nottingham and Keele Universities Centre of Doctoral Training (CDT) in Regenerative Medicine allowing me to complete my laboratory research and travel to numerous conferences. The education, guidance and friendly support I received from the CDT cohort has given me a unique understanding of clinical and industrial importance.

Many thanks go to my friends and colleagues at Guy Hilton Research Centre, Keele University. Their emotional and practical support has been invaluable during my studies. I was lucky to be part of three research teams who all contributed significantly with trouble-shooting and technical guidance. The friendly atmosphere I experienced at Guy Hilton made my time there a happy and amusing one.

I'd like to thank all my family for their continued love and support. My dad Brian, sister Lisa and partner Matt gave me the confidence to pursue a PhD. Whilst they continue to celebrate with me through my successes, their love and encouragement during my 'grumpy days' kept me motivated and helped to provide perspective.

Finally, I'd like to acknowledge my late mummy who is my continued inspiration.

Abbreviations

αSMA	Alpha-smooth muscle actin
2D	Two-dimensional
35FL	Adult lung fibroblasts
3D	Three-dimensional
A549	Lung epithelial cell line
AEC1	Type 1 alveolar pneumocyte
AEC2	Type 2 alveolar pneumocyte
AM	Amnion membrane
aMSC	Amnion mesenchymal stem cell
BADJ	Broncho-alveolar duct junction
BMSC	Bone marrow stem cell
BPD	Bronchopulmonary Dysplasia
CD	Cluster of differentiation
CM	Chorion membrane
cMSC	Chorion mesenchymal stem cell
COL1A	Collagen type 1 A
COPD	Chronic obstructive pulmonary dysplasia
dH_2O	Distilled water
DMEM	Dulbecco's Modified Eagle Medium
DMSO	Dimethyl sulfoxide
DNA	Deoxyribonucleic acid
EC	Endothelial cell
ECM	Extracellular matrix
ELBW	Extremely low birth weight
ELN	Elastin

EMT	Epithelial-mesenchymal transition
EPC	Endothelial progenitor cell
ESC	Endothelial stem cell
FACS	Fluorescence-activated cell sorting
FBS	Foetal bovine serum
FGF	Fibroblastic growth factor
GA	Gestational age
GAPDH	Glyceraldehyde 3-phosphate dehydrogenase
hMSC	Human mesenchymal stem cell
HTA	Human tissue act
Ig	Immunoglobulin
IMR90	Foetal lung fibroblasts
iPSC	Induced pluripotent cell
LIF	Lipofibroblasts
MSC	Mesenchymal stem cell
MYF	Myofibroblasts
NHS	National health service
NICU	Neonatal intensive care unit
NLF	Neonatal lung cells
NQO1	NAD(P)H Quinone Dehydrogenase 1
OCT	Optical coherence tomography
PBS	Phosphate buffered saline
PCR	Polymerase chain reaction
pMSC	Placenta derived mesenchymal stem cells
PS	Penicillin-Streptomycin
PSA	Penicillin-Streptomycin-Amphotericin B
RDS	Respiratory distress syndrome

RNA	Ribonucleic acid
ROS	Reactive oxygen species
RT	Room temperature
SMA	Smooth muscle actin
TC	Tissue culture plastic
TEER	Transepithelial electrical resistance
TGFβ	Transforming growth factor beta
UCB	Umbilical cord blood
VEGF	Vascular endothelial growth factor
VLBW	Very low birth weight

Contents

Figures

Tables

Schematics

Dedicated to my mummy

and all the premature children who passed away during my PhD

Chapter 1

Introduction

1.1 Prematurity and Bronchopulmonary Dysplasia

Prematurity is defined by the World Health Organisation (WHO) as babies born before 37 weeks gestational age (GA). It is the leading cause of death in new-borns[1] and is associated with significant long-term morbidity and financial expense[2]. Amongst other health problems respiratory complications account for a large majority of neonatal intensive-care unit deaths[3]. Bronchopulmonary Dysplasia (BPD) is a chronic paediatric lung disease affecting very premature babies usually receiving prolonged oxygen ventilation. Originally described in 1967, BPD was recognised in infants with lungs which failed to recover after being given mechanical ventilation to alleviate respiratory distress syndrome (RDS)[4]. The high oxygen content and excessive pressure from artificial ventilation resulted in fibrosis and inflammation of the lungs[5]. This is now referred to as "classic" BPD.

In the last 30 years there have been substantial improvements in the care for preterm babies with the introduction of incubators, surfactant treatment, steroids and the use of less invasive respiratory support[6,7]. These improvements in neonatal care have resulted in the high survival rate of very low birth weight (VLBW, <1,500g) or extremely low birth weight (ELBW, <1,000g) infants. Between 1995 and 2006 there was a 13% increase in survival of babies born between 22 weeks and 25 weeks GA. Infants born at 25 weeks GA now have a 75% chance of survival[8]. This increase in survival is a trend seen at each week of GA[8]. These vulnerable babies are delivered several weeks premature when the lungs are still under-developed and incapable of providing the respiratory support necessary for survival. This is referred to as "new" BPD which still remains one of the leading morbidities associated with premature birth with around 40% of extremely premature infants (<29 weeks GA) developing BPD[8]. A comparison of "new" BPD versus "classic "BPD" is shown in Table 1.1. The pathophysiology of new BPD includes a dysmorphic lung

development and an arrest in alveolar formation due to interrupted secondary septation resulting in a reduction in surface area for gas exchange. The lungs are unable to provide sufficient oxygen to the body for normal function and rely on artificial ventilation (Table 1.2)[9]. The most severe BPD infants require an endotracheal tube which supplies oxygen directly into the lungs using pressure. The oxygen percentage supplied is based on the patients arterial blood oxygen saturation and can vary from atmospheric oxygen (21%) to over 40% oxygen in the most severe cases.

Table 1.1 Old BPD versus New BPD

Old BPD	New BPD
Larger preterm infants (>30 weeks GA)	Extremely premature infants (<30 weeks GA)
Smooth muscle hypertrophy	Abnormal vascularization
Alveolar oedema	Arrested alveolarisation
Airway fibrosis and inflammation	Less inflammation and fibrosis

Table 1.2 The common types of ventilation methods used clinically for premature infants

Ventilation type	Description
Endotracheal tube	A tube is inserted through the nose/mouth and oxygen is mechanically blown in/out.
Continuous positive airway pressure (CPAP)	Prongs/mask positioned over the nose and oxygen in at a constant pressure to keep the alveoli inflated.
Nasal prong oxygen	Prongs positioned over the nostrils to deliver higher oxygen levels directly into the respiratory system
Incubator	Oxygen supplied into an incubator which the baby can breathe by their own means

1.1.1 Incidence

BPD is the most common morbidity associated with premature infants [10] with an inverse correlation between the risk of developing BPD and GA. There are few reports providing accurate details of the incidence of BPD. The EPICure is a series of studies examining the survival and health of babies born between 22 and 26 weeks GA.[8]. Data were collected from almost 200 maternity hospitals in England in 1995 and then again in 2006. The 2006 study revealed 39% and 61% infants born between 22 and 26 weeks GA and still receiving oxygen at 36 postmenstrual age were diagnosed as having moderate and severe BPD respectively[8]. A similar picture is seen in a Norwegian study which found 45.1% of infants born between 22 and 27 weeks GA were diagnosed with moderate/severe BPD [11]. Of note, the proportion of premature survivors suffering with BPD did not change in 11 years (between 1995 and 2006) [8]. It is likely that this is because the incidence of "classic" BPD has fallen but the incidence of "new" BPD has risen.

1.1.2 Diagnosis, causes and treatment

In June 2000 National Institute of Child Health and Human Development/National Heart, Lung, and Blood Institute Workshop proposed a severity-based definition of BPD for infants <32 weeks GA (Table 1.3)[12]. This has been acknowledged as an accurate definition for the BPD spectrum[13] and represents the current clinical diagnosis for BPD.

Table 1.3 Severity based definition of BPD

Diagnosis	Description at <32 weeks GA
Mild	Supplemental oxygen for over 28 days but not at 36 weeks' PMA
Moderate	Supplemental oxygen for over 28 days plus treatment with <30% O_2 at 36 weeks' PMA
Severe	Supplemental oxygen for over 28 days plus >30% oxygen and/or positive pressure at 36 weeks' PMA

BPD aetiology is thought to be a multifactorial disease with genetic[14], post-natal infection[15], prenatal infection[16], intrauterine epigenetics[17], and placenta abnormalities[18] all associated as predisposing factors. The most significant predisposing factors are low birth weight and extreme immaturity[19]. BPD is not just a neonatal disease but has consequences long-term. Patients often continue to suffer with long-term morbidities such as respiratory problems[20], reduced lung function into adulthood[21], and retinopathy (Figure 1.1). There is also an increased risk of complications later in life including early-onset emphysema and COPD (chronic obstructive pulmonary disease)[22]. This longevity of the BPD takes a considerable hit on health care resources with an estimated cost of a premature baby with BPD being between £40,000 and £100,000 (figures based on data from the Spanish Ministry of Health)[5,23]. Currently there are no effective treatment

options for BPD, only preventative and supportive measures exist for the management of BPD. Surfactant treatment was introduced in 2008[6] and is routinely given to premature babies at risk of RDS (respiratory distress syndrome)[24]. The surfactant reduces the need for prolonged aggressive respiratory support and therefore prevents injury. Antenatal corticosteroids are often considered for women who are at risk of pre-term birth[25,26] however the long-term effects have been scrutinized with emerging evidence they are associated with neurological developmental problems and reduced cognitive function later in life[27,28].
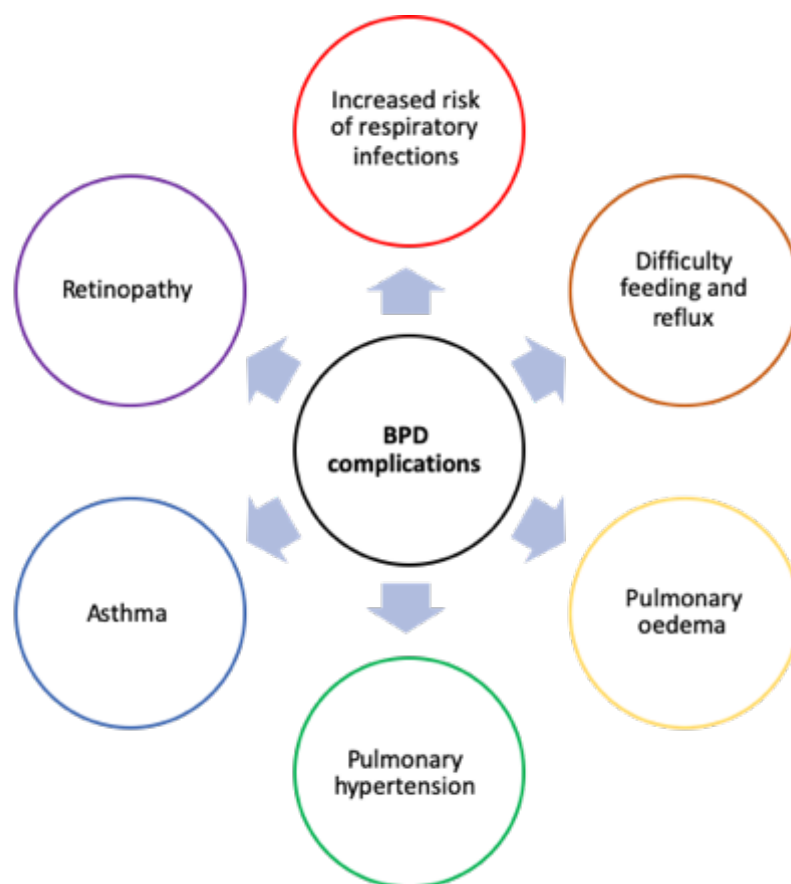
Figure 1.1 Complications associated with BPD

1.1.3 Lung development and BPD pathogenesis

Comprising of over 40 cell types[29], the lung is a complex organ and can be described as two sections: the proximal airway which consists of the trachea and the bronchus and the distal airway which consists of the bronchioles and the gas exchange units, the alveoli. Embryonic lung development is a complex and rapid process beginning from embryogenesis. The process is described as having five overlapping stages (Table 1.4). The beginning phase of lung development consists of the Embryonic and Pseudoglandular stages, which form the conducting airways. In the later stages of development (Canalicular, Saccular and Alveolar stages), there is a reduction in the mesenchyme and the functional respiratory portions of the lung form.

Table 1.4 The development of the lung consists of 5 over-lapping stages [30]

Stage	Gestational age (weeks)	Main events
Embryonic	3-7	The primitive lung bud forms from the foregut endoderm
Pseudoglandular	7-16	Branching morphogenesis completes. Cartilage and smooth muscles forms around the airways. Columnar epithelium, and some ciliated and goblet cells line the airways.
Canalicular	16-24	Capillarization and pulmonary acinar units develop
Saccular	24-36	Thinning of the epithelium and differentiation of type 1 and 2 alveolar epithelial cells to provide the air-liquid interface.
Alveolar	36-104 (2 years)	Alveolar expansion and septation continues. Parenchyma remodelling

As described earlier, advances in perinatal care have improved the survival for extremely preterm babies, allowing survival at just 22-24 weeks GA. At this age the lungs have only

reached the Canalicular/Saccular stage of development when the functional respiratory units are just beginning to develop (Figure 1.2). This results in "new" BPD which is characterized by the following:

- Dysmorphic lung development with abnormal collagen-elastin deposition/arrangement[31]
- Arrest in alveolar formation due to interrupted secondary septation resulting in fewer, simplified alveoli[32]. This can be seen in Figure 1.3 which shows a biopsy taken from a healthy infant's lung compared with a BPD lung.
- Abnormal pulmonary vascular development[33]
- Reduced inflammation as with "classic" BPD[34]
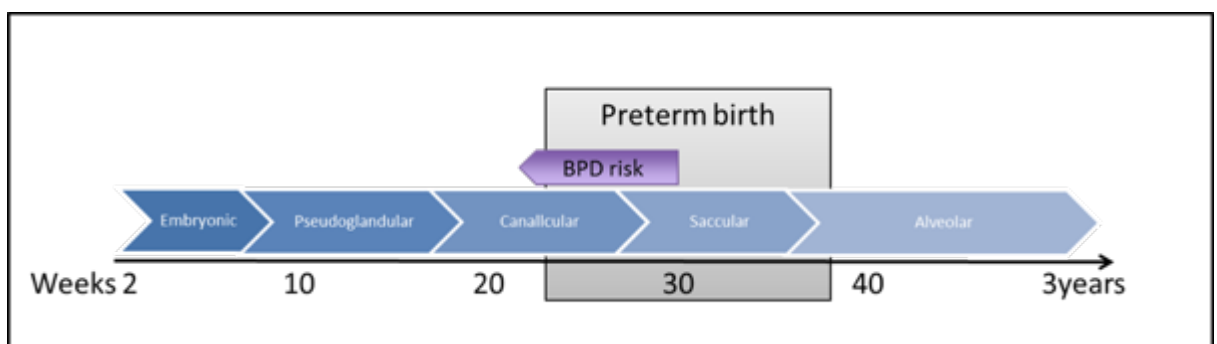
Figure 1.2 The development of the lung consists of 5 main stages. Premature birth can occur as early as 22 weeks gestational age (GA). As GA decreases the risk of bronchopulmonary dysplasia (BPD) increases. Image adapted from C. McEvoy *et al.* [35].
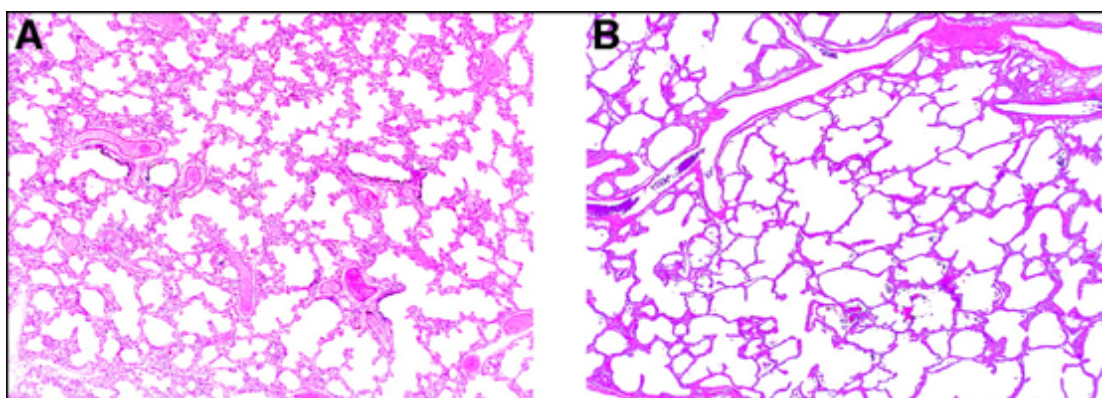
Figure 1.3 Lungs of a normal full-term infant and a BPD infant. Haematoxylin and eosin stained biopsies from the lung of a normal healthy baby **(A)** and a BPD infant born at 28 weeks GA **(B)**. The alveoli of BPD infants are more simplified in structure causing enlarged air spaces and a reduced surface area. Image taken from A. H. Jobe[36].

1.1.3.1 Disruption to alveologenesis

In premature birth lung development is interrupted during the final stages. In these final stages of development, the distal airway and alveoli are being formed. To understand disease pathogenesis, it is necessary to understand the alveolus development including cellular interaction and the alveolus structure.

Alveologenesis relies on the co-ordination of multiple specialised cell types (listed in Table 1.5). The alveolar epithelium is lined by 2 cell types: type 1 alveolar epithelial cells (AEC1) and type 2 alveolar epithelial cells (AEC2). AEC1 occupy a large surface area of around 93% and mediate gas exchange[37]. AEC2 are cuboidal cells containing lamellar bodies which produced surfactant, a vital substance for reducing surface tension during gas exchange[38]. These cells have long been recognized as the progenitor cells for AEC1[39,40]. Research by Desai *et al.* suggests that during lung development bipotent progenitors give rise to both AEC1 and AEC2 cells, however after birth only a sub-set of AEC2 cells function as the progenitor cells for AEC1 cells which contribute to repair[41]. These bipotent progenitor cells express bronchiolar and alveolar markers and possess stem cell properties[42]. This means during normal cell turnover or following injury AEC2 have the capacity to proliferate and differentiate into AEC1 to repopulate the damaged epithelium[43]. Surrounding the alveoli is a capillary network lined with endothelial cells which allows blood oxygenation and the lung interstitium. The interstitium contains other cells like macrophages and a fibroblast population which are thought to predominantly control the synthesis of the non-cellular components, such as collagen and elastin, providing the lung with its mechanical properties[44,45]. Lipofibroblasts (LIF) reside in the mesenchyme containing lipid droblets[46]. It is speculated that the LIF communicate with AEC2 to stimulate the production of surfactant[47]. Also residing within the mesenchyme are alpha-smooth muscle actin (α-SMA) expressing myofibroblasts (MYF) which are thought to be the driving force behind alveolus maturation through secondary septation

(Figure 1.4). It is speculated that PDGFRA (Platelet Derived Growth Factor Receptor Alpha) expressing myofibroblasts progenitor cells migrate towards sites of septae initiation[48]. The theory of septation has been based on the appearance of finger-like protrusions (septae) in 2D lung sections. The co-location of MYF and elastin deposits at the tips of the septae suggested that these cells were driving septae towards the lumen of the alveolus. However, Branchfield *et al.* examined alveologenesis using 3D imaging and speculates septal ridges underlined by a network of α-SMA and elastin are a more accurate representation of alveologenesis[49]. The work suggestions that a "fishnet" of elastin surrounds the alveolus and allows the alveolus epithelial wall not lined by elastin to bulge outwards through the pores creating mature alveoli with a large-surface area. In BPD this elastin network is defective and creates a "cheese cloth" preventing the epithelial walls form bulging reducing the surface area of the alveolus.

The molecular and cellular processes of BPD still remain poorly understood. The expression of many growth factors has been investigated as contributing to the development of BPD including keratinocyte growth factor[50,51], fibroblast growth factor (FGF)[52], transforming growth factor (TGF)[53] and interrupted cytokine synthesis such as Interlukin-10[54–56]. Vascular endothelial growth factor (VEGF) is a stimulator of alveolarisation and vascularization and is therefore likely to be a key modulator in BPD. Many studies have revealed abnormal levels of VEGF associated with the development of BPD[57]. Many of the molecular and cellular processes involved in lung development are likely to be involved in lung repair and regeneration. Therefore lung development is an important framework for understanding lung repair and potential therapeutic options[58].

Table 1.5 Cell types involved in alveologenesis.

Cells	Acronym	Location	Function
Myofibroblasts	MYF	Tip of septae formation	Express alpha-smooth muscle actin and produce extracellular matrix fibres.
Lipofibroblasts	LIF	Close to AECII	Source and transport lipids to AECII for surfactant production.
Endothelial cell	EC	Lung mesenchyme	Provides surface area of blood vessels.
Alveolar epithelial cell type 1	AEC1	Alveolar epithelium	Provides most of the surface of the alveoli to facilitate gas exchange.
Alveolar epithelial cell type 2	AEC2	Alveolar epithelium	Stem cell to AEC1, covers a small area of alveolus surface area and produces surfactant.
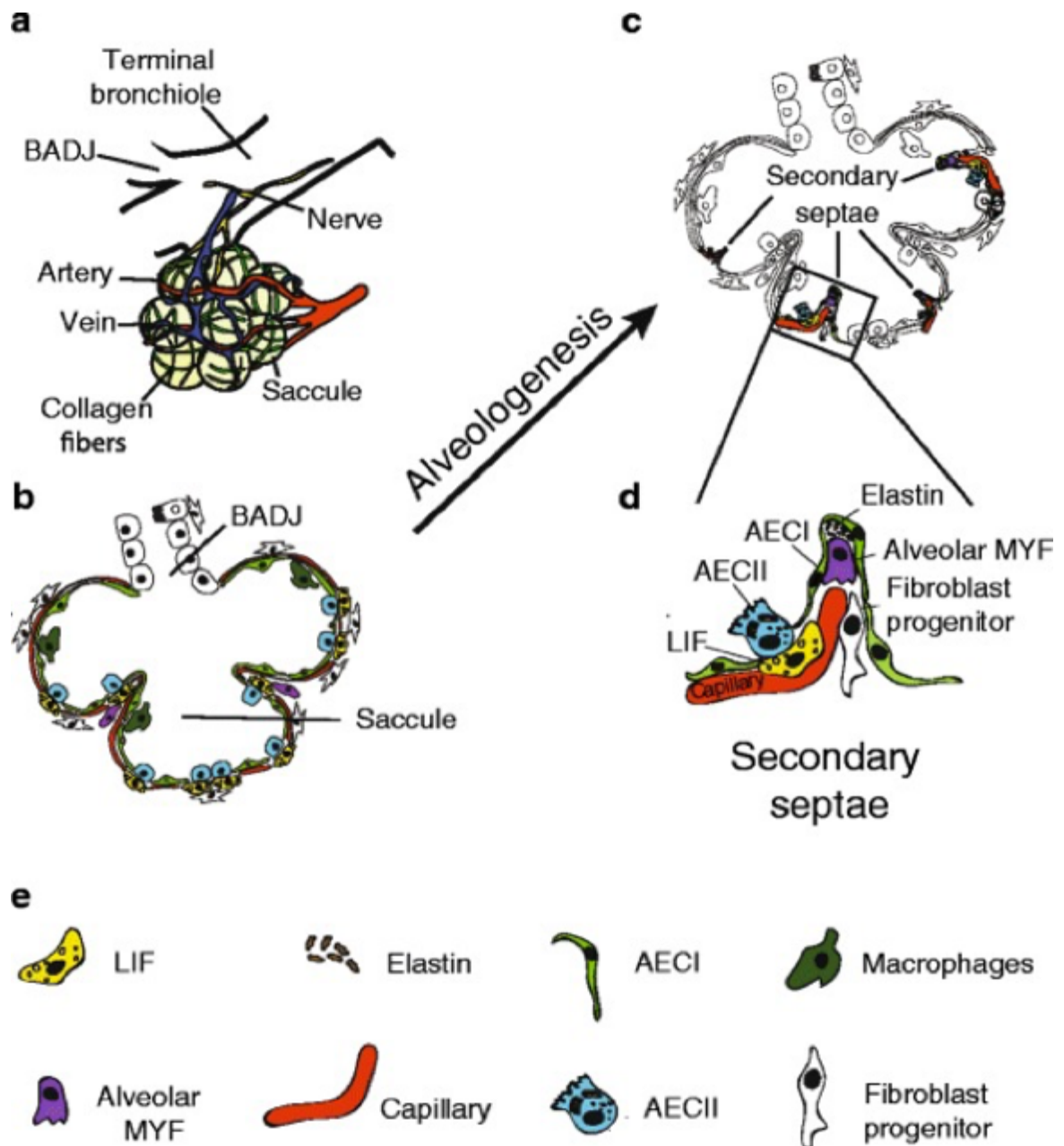
Figure 1.4 Diagram showing the Saccular and Alveolar stages of lung development. Primitive alveoli are formed during the saccular stage (a) which are surrounded by collagen fibres and blood vessels. AEC1 and AEC2 are present, forming the saccule walls and producing surfactant. Fibroblasts produce collagen and elastin (b). Secondary septation occurs which subdivides the saccules and forms mature alveoli (c). One theory suggests this process is driven by the deposition of elastin by the myofibroblasts (d). Later, double layer capillaries fuse to become thinner for efficient gas exchange. Shown are the AEC1 and 2 alveolar epithelial cells, BADJ broncho-alveolar duct junction, LIF lipofibroblasts (e). Image taken directly from Chao *et al.* [59].

1.2 BPD research

The pathogenesis of BPD remains poorly understood. Research has relied significantly on the use of animal models, cadavers and some *in vitro* cell culture[60]. Figure 1.5 summarises the various methods BPD research has utilised. Here, we describe the use of animal models and *in vitro* study in detail.
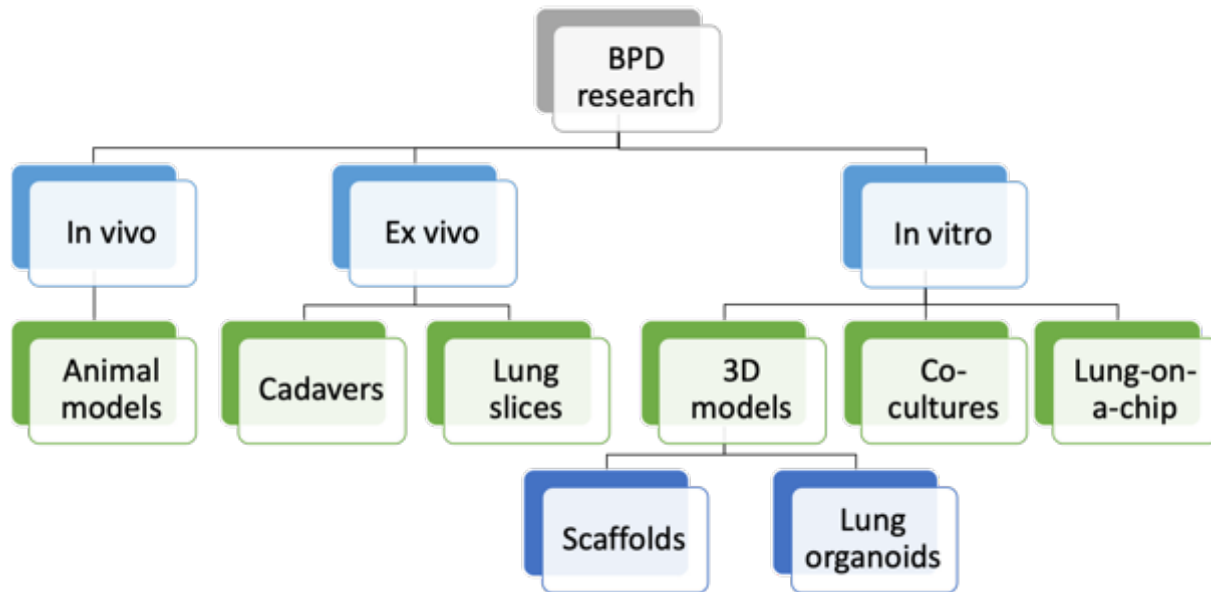
Figure 1.5 Schematic showing the various methods utilised in BPD research.

1.2.1 Animal models

Early experiments using animal models have helped shape our understanding of BPD[61]. This originated in 1932 when Smith *et al*. exposed rats to compressed air conditions[62]. Since then other animals have been used to model BPD, including rodents[61], rabbits[31], lambs[63], sheep[64] and baboons[65]. Animal models are currently the most favoured research method for lung research due to the complexity of respiratory diseases, however they are limited in terms of clinical utility due to interspecies variation.

1.2.1.1 Rodents

Rodents are a popular animal model in all areas of medical research due to their small size, short life span, the large availability of reagents and low upkeep cost. They have provided significant insight into the effects of oxygen toxicity. Rodents are considered an ideal model for BPD since their lungs are at the saccular stage of development at birth (postnatal day 5-30[66]), which is the same stage of lung development as premature babies. However, unlike humans, birth at this stage of lung development is normal for rodents, they are surfactant sufficient and able to exchange gas normally without any intervention. In contrast, human alveologenesis should normally begin in the uterus before birth. Premature VLBW infants may have only progressed to the canalicular stage of lung development[58] and the lungs are classed as under-developed.

Hyperoxia-induced neonatal rodents are the most commonly used BPD model. New-born rodents are kept in chambers containing high oxygen levels, usually 90% or over[53,56,67–69]. Human babies are rarely exposed to oxygen levels higher than 40%. Therefore, though the hyperoxia exposure is clinically relevant, the levels of oxygen are not[60]. There is also a lack of standardisation with rodent models. Investigators have employed various strains of mouse including BALB/c, C57BL/6 and FVB/N, making comparisons difficult[70]. Although often considered interchangeable, mice and rats are dissimilar in their lung anatomy with mice displaying a smaller lung capacity and alveoli[71].

Hyperoxygen exposure is a key tool used in BPD research, a disease exacerbated by oxygen toxicity. Exposure of new born mouse pups to hyperoxygen is a key *in vivo* method to model BPD. However, there is no standardised oxygen regime (oxygen percentage, exposure time and exposure window) which has caused some difficulties when drawing study conclusions. Exposed mice also do not experience mechanical stretch that endotracheal ventilated babies will experience[70].

1.2.1.2 Baboons and lambs

Larger animals are considered an expensive option; however, the preterm models of baboons or lambs are an attractive alternative to rodents. Their large size means they can be mechanically ventilated easily and have a very similar lung development making them clinically relevant for "new" BPD [60,72]. The baboon and lamb models has consistently shown similar pathological findings as that of BPD in human infants, including interrupted alveolarization and vascularization[63,65,73,74]. These animals also allow the use of pharmacology interventions such as vitamin A supplementation[75] and surfactant treatment[76].

1.2.1.3 Rabbit

The rabbit models have similar advantages to rodents in that they have a short gestation period, a large number of offspring and are easy to handle. Their kitten size is larger, which permits the use of certain instruments such as ventilation equipment[63]. Rabbit models have a similar lung development to humans in that full-term rabbits are born in the early to middle alveolar stage and have a mature surfactant system. Moreover, the rabbit lung is anatomically more similar to human lungs and can provide preterm delivery whilst maintaining a reduced alveoli number[77].The animals show pathological injuries on the lung architecture which are similar to those found in BPD[31]. New-born rabbits have also demonstrated hyperoxia resistance which is lost during adulthood, a phenomenon not shared by other animals[31,78]. The rabbit model is inhibited by a lack of rabbit-specific reagents to allow for scientific assessment.

1.2.2 *In vitro* models

In the past there has been a reliance on animal models that mimic key features of the disease due to availability of only basic *in vitro* cell culture techniques to model

alveolarization. The rapidly developing field of tissue engineering has enabled cell culture to become a feasible alternative to model disease. This is due to the employment of tissue engineered constructs that can mimic the native 3D environment of *in vivo* structures and the improvement of research analysis techniques and equipment[79]. In the last 60 years the 3Rs has come at the forefront of medical research as ethical values to strive for[80,81]. Standing for Replacement, Reduction and Refinement the principals hope to employ alternative strategies to promote research without the reliance of animal models. This has helped to catapult advances with *in vitro* modelling. In lung research, development of *in vitro* models has focused on the conducting zone of the respiratory tract[82], an easier tissue to model with simpler architecture. Some of these models are now commercially available[83]. Modelling the respiratory section of the lung is a more complicated task due to the intricate architecture of the alveoli, the multicellular components and the functional aspect (illustrated in Figure 1.6). The ideal alveolus *in vitro* model would encompass 4 key elements: a 3D structure, human relevant cell co-culture, mechanical stimulation and oxygen exposure. These aspects have now been described in more detail.

1.2.2.1 3D models

Current *in vitro* research of the respiratory system lacks biological relevance. Single cell type monolayer cultures are becoming out-dated as they lack the physiological complexity of the multi-cellular lung[79] and they often fail to translate to *in vivo.* 3D *in vitro* modelling of the respiratory system was first seen in 1970[84] and since then has become a popular choice in the laboratory. Materials which have been used as lung tissue constructs included synthetic polymers[85], Gelfoam sponges[86], electrospun polymer fibres[87] and collagen hydrogels[88]. 3D models of lung tissue offer the ability to investigate the biological interactions leading to BPD and potential therapeutic application. The functional importance of the lung ECM means that incorporation into any lung model is important.

Engineering functional 3D engineered constructs is a rapidly developing area of research for most tissue types. The conducting airway has been successfully engineered and implanted *in vivo*[89]. However, modelling the complex functional alveoli *in vitro* is a bigger challenge that so far, remains unmet.

The respiratory zone of the lung is a complex architecture composed of bronchioles terminating at alveoli air sacs. Secondary septation during the final stages of lung development increases the surface area of the alveoli considerably. The surrounding lung interstitium goes through remodelling to provide a collagen and elastin rich environment which impacts on lung development[90], structural integrity and mechanical capabilities[45,91–93]. Disrupted synthesis and assembly of collagen and elastin network has been a histological finding in both animal models and human infants with BPD[32,66,94–96]. Hyperoxia exposure has been shown to affect the cross-linking of collagen and elastin[66]. Surprisingly, few studies have examined the possibility of including these 2 components in an *in vitro* construct. Dunphy *et al.* created cell seeded collagen-elastin constructs to assess the Young's modulus[97]. The study found that the Young's modulus of the hydrogels was similar to the theoretical Young's modulus value of an alveolus. The mechanical properties of such a construct makes it an ideal 3D construct to include in an alveolus model.

Another possible approach to this challenge could be to use decellularized lung tissue. Studies have shown that when the decellularised tissue is re-popularised, the mechanical, topography, tissue architecture and functional aspects of the tissue remain the same[98,99]. The mechanical and chemical cues have been shown to influence cell behaviour, influencing cell proliferation, differentiation and gene expression[100–103]. This could be a more accurate method to use in lung research where hierarchical structure is complex. This technique of decellularizing and re-introducing native cells has proved successful

with rat lungs[104] and porcine lungs[105] however currently the technique may be unsuitable for research purposes due to its costly and time consuming approach and doesn't allow high-throughput.
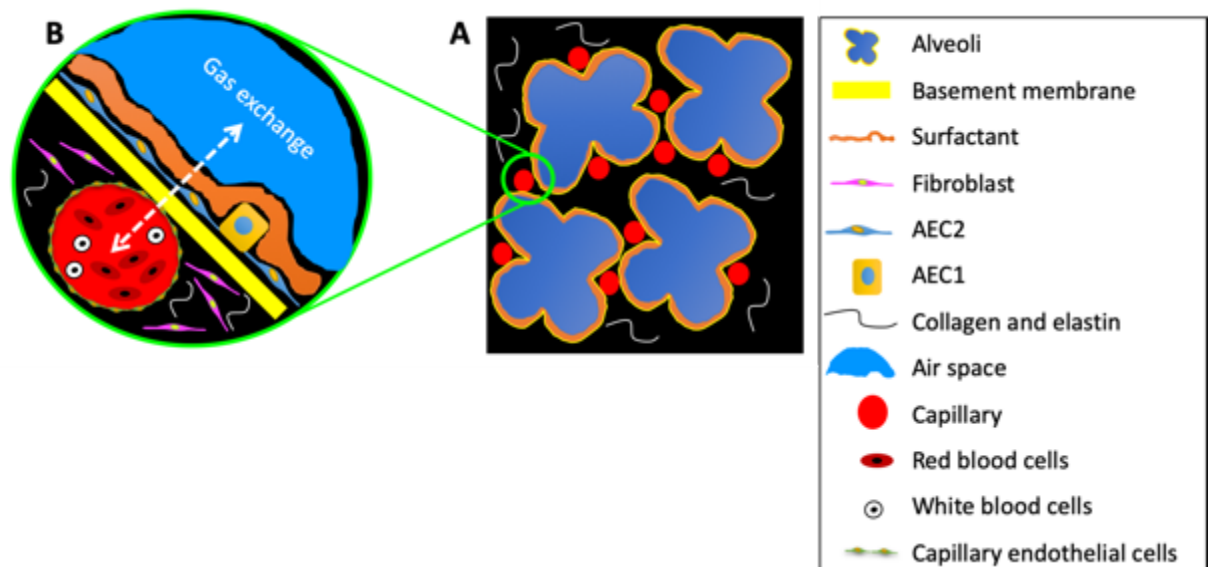
Figure 1.6 Diagram of the lung alveolus and surrounding interstitium. There are an estimated 480 million alveoli in each lung of a human adult[106]. Each alveolus is surrounded by the lung parenchyma composed of extracellular matrix (collagen and elastin mostly) produced by lung fibroblasts, and a vast network of blood capillaries (A). Each alveolus is composed of AEC1 and AEC2 which sit on a basement membrane. AEC2 produce surfactant to decrease surface tension during breathing (B).

1.2.3 Cell type and co-culture

Most *in vitro* BPD research uses a single cell culture in a hyperoxic environment which doesn't allow for cell-cell interactions to be assessed. The A549 cell line is a popular choice for modelling lung biology[107]. First derived by Giard *et al.* in 1973, it is a human alveolar cell carcinoma cell line regularly used to represent AEC2 *in vitro*[108]. The cells express lamellar bodies capable of producing surfactant. However the suitability of the cell line has come under scrutiny with questions regarding their surfactant protein

composition[109], expression markers[110] and their lack of ability to differentiate into a

AEC1. Interruption of differentiation of AEC2 to AEC1 may be a contributing factor to BPD

development and is therefore an important factor to consider[43]. Immortalised alveolar

type 1 cell line (TT1) developed by Kemp *et al.* has been suggested as a possible lung

model [111]. In 2010, Swain *et al* investigated the cell markers by using Raman microscopy

and showed they made a suitable candidate for the modelling of AEC1[110]. Animal cell lines

MLE-12 (mouse lung epithelial cell line) and RFL-6 (rat foetal lung fibroblast cell line)

have also been used in BPD models but are less common and usually only used as a cell

culture comparison to animal models[53].

As previously described (section 1.1.3.1) the lung parenchyma is a multicellular tissue

involving sophisticated cross-talk between AEC1, AEC2, myofibroblasts, lipofibroblasts

and macrophages. Cell-cell interactions are likely to be an important factor when

considering an *in vitro* model for any disease. Despite this, few BPD studies have

incorporated co-culture techniques in BPD research. A lung fibroblast-tracheobronchial

epithelial cell co-culture model was employed by Chetty *et al*. to investigate the migration

of fibroblasts through collagen gels in hyperoxia conditions[112]. The epithelial cells

promoted cell migration of the lung fibroblast and indicated the importance of

understanding cell-cell interactions. More recently in 2014, an epithelial (A549) cell line

and foetal mouse lung mesenchymal co-culture was employed by Greer *et al*.[113]. Tall peaks

were formed consisting of a mesenchyme cell core covered by epithelial cells. The study

demonstrated that a co-culture model could be used to test mesenchymal-epithelial

interactions following injury.

Lung-on-chip methodologies provide a platform to assess cell-cell interactions for

example replicating alveolar-capillary barrier [114]. This is a similar story for precision cut

organ slices which allow the assessment of tissue-tissue interaction such as airway and

vessels in the lung[115]. These models are still limited by a lack in availability of the appropriate tissue source.

Providing a platform to allow co-culture of human lung specific cells would allow the analysis of cell-cell interactions and could provide vital information into lung development and lung repair.

1.2.4 Mechanical stretching

Artificial ventilation has long been thought of as a contributing factor to BPD pathogenesis causing inflammation and ROS (reactive oxygen species) injury due to over-inflation of alveoli[116]. Although gentler respiratory aids are now employed in clinical practice, the under-developed premature lung is suddenly exposed to continuous inflation leading to a danger of overstretching. This may have an important consequence on lung interstitium deposition and maturation. Multiple studies have shown that mechanical forces between the lung ECM and cells directly influence cell signalling during lung development, surfactant release and tissue remodelling[117–120].

The lung ECM provides mechanical stability through collagen and elastin cross-linking which is a continuous process during the later stages of lung development. Elastin turnover is thought to be a slow process and as such the deposition of elastin during foetal development must sustain normal tissue function throughout a lifetime[121]. Therefore, interrupted elastin deposition during development may cause irrevocable damage. At 22-26 weeks GA the premature lung parenchyma is potentially not mechanically stable enough to sustain the physical forces experienced when the infant begins to breath for the first time. Despite its importance, few studies have incorporated mechanical stimulus *in vitro*[122]. In recent years novel bioreactors have been developed in other areas of

research to create physiological relevant mechanical stimuli[123]. In BPD research, there are few examples of the incorporation of bioreactor systems *in vitro*. Strain units such as the Flexcell strain unit (Flexcell International) and the Bio-Stretch System from ICCT[124] have been used to expose lung cells to cyclic strain regimes. Pro-inflammatory cytokines, chemokines, cell apoptosis and MMP release have all been shown to increase when foetal lung cells are exposed to stimulation[54,125,126]. Mechanical stretching has also been shown to affect airway smooth muscle-cell phenotype[127] and promotes the secretion of surfactant from AEC2[128]. Although predominately used for bone and cartilage research, the hydrostatic bioreactor[129] possess attributes which may bode well for lung research[130]. It can provide cyclic influxes of air pressure that mimic clinical ventilators. The hydrostatic bioreactor allows alteration of pressure and frequency to provide clinically relevant environments[131].

1.2.5 Oxygen exposure

Although BPD is considered a multifactual disease, it is largely associated with oxygen toxicity. Oxygen requirements form the basis of BPD diagnosis and are an essential treatment for premature infants. The most premature infants require oxygen ventilation of >40% to maintain healthy blood saturation levels. Oxygen toxicity was first reported by Northway *et al.* who demonstrated that exposing mice pups to 100% oxygen caused a BPD-like injury[4]. Studies have expanded this further by showing preterm baboons exposed to 30% oxygen had less lung injury than those exposed to 100% oxygen[132]. This highlights the importance of employing relevant oxygen exposure in an *in vitro* BPD model. The demand for oxygen control has increased in recent years due to the more recent understanding of replicating physiological oxygen. This has allowed the development of technologies that provide ambient oxygen control. The simplest form is a re-sealable chamber that can hold cell culture plates, be flushed with a pre-mixed gas of

the desired gas mixture, sealed with a tight stopper and placed inside an incubator. The most expensive technologies included whole incubators which maintain a constantly supply of the desired gas mix[133].

1.2.6 Developed *in vitro* models

Previous studies, as listed in Table 1.6 have made attempts to include one or two of the described elements to mimic the alveolus *in vitro*. This includes using collagen hydrogels to provide a 3D scaffold, using co-culture cell culture techniques and incorporating mechanical stimulus. Despite this, there is still much to be desired. The complexity of the respiring lung requires the development of an advanced model to include most if not all of the aspects previously described.

Table 1.6 Examples of *in vitro* studies which have attempted to model the lung alveoli. All the studies include co-culture techniques, mechanical stimulus or hydrogel scaffolds to mimic the complex lung alveoli.

Description	Authors	Year
Fibroblast cultured on collagen gel substrates and covered by a second layer of collagen gel. Epithelial cells then cultured on collagen gel surface and exposed to 95% oxygen [112].	Chetty A. *et al.*	1999
Lung-on-a-chip microdevice. Epithelial and endothelial cells cultured either side of a porous membrane. The membrane is mechanically stretched using a vacuum [134].	Huh D. *et al.*	2010
Foetal pulmonary cells resuspended in 1.2mg/ml collagen solution. Fibroblast growth factors 10, 7 and 2 were added to culture medium in various combinations [88].	Mondrinos M. *et al.*	2007
Primary foetal lung mesenchymal cells grown to confluency then A549 cells overlaid to cover underlying primary cells and cultured at 95% air [113].	Greer R. *et al.*	2014
A549 cells, rat alveolar epithelial cells, human bronchial epithelial cells and human foetal lung fibroblast cell line were cultured with collagen gels and on the surface of collagen gels. Gel contraction was examined under various conditions [135].	Umino T. *et al.*	2000
Foetal mouse lung fibroblast exposed to 20% cyclic stretch using Flexcell Strain Unit [54].	Hawwa R. *et al.*	2011
Collagen–elastin constructs seeded with lung fibroblasts possess lung modulus similar to the theoretical value of a lung alveolus [97].	Dunphy S. *et al.*	2014

1.3 Stem cells as therapies

Stem cells are a valuable cell type capable of self-renewal and differentiation into multiple cell lineages. They are a critical component for tissue generation during development and tissue repair[136]. Due to these properties, they are being harnessed for use as cell therapies in human disease, including BPD.

The complex lung structure, cell diversity and varying cell niches has made it difficult to identify the key progenitor cells in the lung[137]. Research examining the effect of stem/progenitor cells has shown potential for the prevention or the alleviation of BPD. Since BPD is a multifactorial disease, it may be difficult to determine the most appropriate cell type and ultimately a combination of cell types may be required for optimal cell therapy.

1.3.1 Endothelial progenitor cells

Endothelial progenitor cells (EPC) are circulating cells that have been described as contributing to angiogenesis[138]. The lung vasculature houses a population of EPCs that are proliferative and capable of vasculogenesis[139]. As previously mentioned, simplified pulmonary vascularization is a hallmark of BPD so EPCs are an attractive candidate as a therapeutic treatment for BPD[69]. Impaired or low numbers of EPC have been found to contribute to alveolar growth arrest[69] and BPD pathogenesis[140–142].

1.3.2 Amnion epithelial stem cells

The advantage of using amnion epithelial cells is that they possess stem like features, they are readily available from the placenta, and they do not form teratomas[143,144].There is emerging evidence that amnion epithelial cells have the capability to repair lung injury. One investigation examined the effect of amnion epithelial cells to protect lambs from

ventilation induced lung injury. The cells helped maintain the lung architecture and prevent injury[145]. Recently, the first-in-human clinical trial of hAECs in infants with BPD was completed and no adverse effects were seen[146]. Further trials are likely to be planned to assess the efficacy of these cells.

1.3.3 Pluripotent stem cells

Pluripotent stem cells are capable of differentiating into multiple cell lineages. They include induced pluripotent stem cell (iPSC)[147] and embryonic stem cells (ESC)[148]. iPSCs offer the ability to provide patient-specific lung progenitor cells. ESC and iPSCs have been successfully differentiated into lung progenitor cells which were able to form airway and alveolar cells[149,150]. Research into the use of pluripotent stem cells in BPD is still developing but is continually growing. Although there are concerns with the tumorigenicity and ethical considerations[151], their therapeutic potential is showing great promise[152].

1.3.4 Mesenchymal stem cells

Mesenchymal Stem cells (MSC) offer a promising cell type and are the most widely researched stem cell. Their wide distribution, ability to home to sites of injury[153], immunosuppressive properties[154], differentiation and proliferative capabilities makes them an attractive progenitor cell. MSCs have been identified in human lungs[155–157]. Although little is known about their function in the lung, they are regarded as having a great therapeutic potential for the treatment of BPD. Researchers have investigated various sources of MSCs for BPD including bone marrow[158,159] adipose tissue[160] and gestational tissue[161]. Gestational tissues (the placenta, Wharton's jelly and the umbilical cord) are particularly attractive sources of MSCs since the tissues are considered waste material and therefore possess few ethical dilemmas. Gestational tissue-derived MSCs can

be easily extracted from the tissues and they show less immunomodulatory effects[162]. Animal studies have demonstrated that umbilical cord blood derived MSCs attenuate hyperoxic injury in rats[163]. A recent study by Ahn *et al.* examined the optimal cell type to protect against neonatal rat hyperoxic lung injury. Human umbilical cord blood-derived MSCs have been shown to have a protective effect against hyperoxic stress when compared to bone marrow MSC and adult tissue MSC[107]. This was supported by Chang *et al.* who found intratracheal transplantation of umbilical cord blood MSC is more effective than intraperitoneal transplantation[163]. Similarly, the placenta is a valuable source of stem cells where a variety of stem cell types can be isolated, including haematopoietic, amniotic epithelial, chorionic mesenchymal and amniotic mesenchymal stem cells[164,165]. Of particular interest are placental MSCs which have been shown to have similar properties to bone marrow MSCs[166] with a high capacity for self-renewal, the capability to differentiate into multiple lineages[161,167,168] and promote angiogenesis[169].

The therapeutic effect of MSCs has been frequently investigated in rodent models[158,159,163]. Translation of MSCs into the clinic has already begun. PNEUMOSTEM® is an allogeneic umbilical cord blood derived MSC medicine[170]. It is currently in the US phase 1/2a clinical trial for the treatment of BPD in premature infants. The treatment still has a long way to go before being established safe and effective. However early results suggest the treatment is well tolerated, the severity of BPD in transplanted subjects is lower and there is a reduction in interleukin-6, interleukin-8, matrix metalloproteinase-9, tumour necrosis factor α, and TGF β1 in tracheal aspirates[171]. These promising results demonstrate the effectiveness of harnessing MSC attributes.

Recent reports have suggested that MSC transplantation is not necessarily required but that MSCs potentially alleviate BPD through paracrine mediators rather than regenerative capabilities [107,158,172–174]. Knoll *et al* employed a co-culture technique to culture foetal rat

fibroblasts or type II cells with bone marrow stem cells (BMSCs) using a transwell insert. The results indicated that BMSCs promote AEC2 maturation via a paracrine mechanism[173]. On a clinical point of view, this may allow cell-free conditioned media to be used therapeutically which would remove the risk of tumorigenesis[174].

1.4 The future for BPD and remaining challenges

There is still much to be learned about BPD. The disease mechanism remains unknown and is limited by the complex nature of the lung. Animal models have provided most of our current knowledge however are limited by cost, ethical considerations, biological variability, inconsistent experimental set-up and differences in animal lung development[60]. Furthermore, BPD research in animals has used non-clinically relevant and inconsistent oxygen concentrations to cause hyperoxic injury. With the development of tissue engineering, 3D *in vitro* models are becoming an attractive research tool, as it is possible to more accurately mimic the lung architecture and allow co-culture. This will enable researchers to accurately examine the molecular, cellular and ECM interactions. Finding the most appropriate scaffold design will require extensive research.

In recent years extensive knowledge about stem/progenitor cells has been uncovered. As previously described, there are various cell types which have the potential to offer a therapeutic treatment for BPD. Phase I UCB-MSC dose-escalated clinical study for the prevention of BPD have been reported. Although the efficacy has not been established, the report did demonstrate the short-term safety of MSC administration in premature babies[171]. There are still questions remaining regarding dose, timing, mechanisms, long-term safety and efficacy of MSC therapy for BPD. Standardized techniques for cell definition, extraction and expansion are yet to be achieved before routine translation of cell therapies to the clinic. Translating stem cell therapies will rely on partnership

between industry and funding bodies and incentives for companies to research the neonatal population[35].

1.5 Summary and hypothesis

In the last 50 years there have been considerable improvements in neonatal health care resulting in the survival of extremely premature infants at a high risk of developing BPD. The disease results from interruption to alveolarisation, vascularization and extracellular matrix arrangement. Current therapeutic options are limited and intended for palliative management rather than to be curative. The disease remains a major cause of morbidity and a burden on health resources due to the long term health impact on the affected population[175]. There is a significant clinical need to develop novel strategies for the treatment of BPD. The complex and poorly understood pathogenesis of BPD instigates challenges for developing a successful therapeutic treatment. Identifying and understanding the role of the lung stem and progenitor cells in the developing lung may offer new understanding into BPD pathogenesis and new therapeutic avenues. MSCs possess the potential to prevent injury, promote repair/regeneration in the immature lung and are a promising therapeutic option. The development of clinical therapies for BPD will likely rest on our understanding of the repair and regenerative capacity of lung progenitor cells[176].

BPD research has been restricted by a lack of adequate research methodologies. Animal studies have provided much of what is currently known about the disease, but they are limited by a lack of biological relevance and promotion of the 3Rs initiative. Although a cheaper option, rodent models do not represent the same lung development as humans. Larger animals such as rabbits and mammals over come this limitation but are associated with much higher costs. *In vitro* models can provide a controlled way of modelling

biologically relevant respiratory disease. This would allow researchers to examine the molecular and cellular interactions that lead to BPD. The use of engineered mechanically relevant 3D constructs and co-culture techniques offers a promising research tool by allowing the investigation of cell-cell and cell-ECM interaction.

The work described in this thesis investigates the possibility of developing an alveolus *in vitro* model capable of providing a BPD relevant environment in terms of cell-cell interaction, cell-ECM interaction and clinically relevant oxygen toxicity. The potential of extracting and culturing cells from BPD infants undergoing ventilation is examined for use in the model to provide disease relevance. In addition, the model is used as a platform to assess the therapeutic potential of placenta derived MSCs for BPD and the effect that clinically relevant hyperoxygen has on cell performance.

Chapter 2

Materials and Methods

2.1 Materials and equipment

This chapter details the fundamental methods used throughout the thesis. Table 2.1 and

Table 2.2 list the materials and equipment which were used.

Table 2.1 List of materials, catalogue code and suppliers used for experimental work

Materials	Order number	Supplier
3-isobutyl-1-methylxanthine (IBMX)	I7018	Sigma-Aldrich
Agarose	BP1356-500	Fisher Scientific
Alamar Blue Cell viability reagent	10161053	Invitrogen
Alcian blue	A3157	Sigma-Aldrich
Alizarin red S	A5533	Sigma-Aldrich
Ascorbic acid phosphate	A8960	Sigma-Aldrich
BEGM Bullet kit	CC-3170	Lonza
Beta-glycerophosphate disodium salt hydrate	G5422	Sigma-Aldrich
Ciprofloxacin	13541640	Fisher Scientific
Collagen type i rat tail high concentration 100mg	354249	Corning Scientific
Collagenase type IV	10780004	ThermoFisher Scientific
Dexamethasone	D2915	Sigma-Aldrich
Dimethylsulphoxide (DMSO)	D2650	Sigma-Aldrich
DNA ladder	CSL-MDNA-100BP	Cleaver Scientific
Dulbecco's Modified Eagle Medium (DMEM) 4.5g/L glucose w/ LG	LZBE12-604F	Lonza
Dulbecco's Modified Eagle Medium (DMEM) 4.5g/L glucose w/ LG powder	D5648-10L	Sigma-Aldrich
Elastin soluble from bovine neck ligament	E6527	Sigma-Aldrich
EpiVita w/ supplements	511-500	Cell Applications
Ethanol (absolute)	E0650/17	ThermoFisher Scientific
Ethidium bromide	E1510	Sigma-Aldrich
Ethylene diamine tetra-acetic acid (EDTA)	BP2482-1	ThermoFisher Scientific
Foetal bovine serum (FBS)	FB-1001/500	Biosera
Gel loading dye	G2526-5ML	Sigma-Aldrich
Gentamicin sulphate 600I.U./mg	15435139	Fisher Scientific
High Capacity cDNA Reverse Transcription Kit	4368814	Applied Biosystems
Human TGF-beta 3 (E. coli)	100-36E	PeproTech
Indomethacin	I7378	Sigma-Aldrich
Insulin, Transferrin, Selenium (ITS)	I3146	Sigma-Aldrich

L-Glutamine	BE17-605E	Lonza
L-Proline	P5607	Sigma-Aldrich
LHC-9	12680013	ThermoFisher scientific
LIVE/DEAD Viability/Cytotoxicity Kit	10237012	Invitrogen
MEM Eagle NEAA (100X)	LZBE13-114E	Lonza
Oil Red O	O0625	Sigma-Aldrich
Pen/Strep/Fungizone 10K/10K/25ug	LZ17-745E	Lonza
Penicillin/Streptomycin	LZDE17-603E	Lonza
Phosphate buffered saline	LZBE17-516F	Lonza
Phycoerythrin conjugated antibodies CD105	130-098-845	Miltenyi Biotec
Phycoerythrin conjugated antibodies IgG1isotype	130-098-849	Miltenyi Biotec
Phycoerythrin conjugated antibodies IgG2a isotype	130-098-849	Miltenyi Biotec
Phycoerythrin conjugated antibody CD14	130-098-167	Miltenyi Biotec
Phycoerythrin conjugated antibody CD19	130-098-168	Miltenyi Biotec
Phycoerythrin conjugated antibody CD34	130-098-140	Miltenyi Biotec
Phycoerythrin conjugated antibody CD45	130-098-141	Miltenyi Biotec
Phycoerythrin conjugated antibody CD73	130-097-932	Miltenyi Biotec
Phycoerythrin conjugated antibody CD90	130-098-906	Miltenyi Biotec
Phycoerythrin conjugated antibody HLA-DR	130-098-177	Miltenyi Biotec
PicoGreen dsDNA quantification kit	10398702	Invitrogen
Proteinase K	EO0491	Thermo Fisher
QuantiFast SYBR Green PCR kit	204054	Qiagen
RNeasy Minikit	74104	Qiagen
Sodium pyruvate	S8636	Sigma-Aldrich
Thincerts cell culture inserts, 0.4µm pore diameter	665641	Greiner Bio-one
Tris Acetate-EDTA buffer	T9650-4L	Sigma-Aldrich
TRIzol Reagent	15596026	ThermoFisher Scientific
TrypLE Express Enzyme	12604013	ThermoFisher scientific
Trypsin/Versene (EDTA)	LZBE02-007E	Lonza
UltraPure DNase/RNase-Free Distilled Water	10977049	ThermoFisher Scientific

Table 2.2 List of equipment and suppliers used in experimental work

Equipment	Supplier
TEER	Millicell ERS-2
Plate reader	BioTek Synergy 2
OCT	Thorlabs
PCR machine	Agilent Technologies Stratagene Mx3000P
Thermal cycler	MJ Research PTC-200 Thermal Cycler
Laser confocal microscope	Olympus FluoView 1200
Phase contrast inverted microscope	Olympus CKX41
Nanodrop	ThermoScientific

2.2 Cell culture

To maintain sterility all cell procedures were handled in a class II microbiology safety cabinet using sterile equipment. Unless otherwise stated all cells were cultured in media high glucose DMEM 4.5g/L glucose with L-glutamine supplemented with 10% FBS and 1% Penicillin 5.000 U/ml Streptomycin 5.000 U/ml, henceforth referred to as culture media. All cells were expanded in a humidified incubator at 37°C in the presence of 5% CO_2 and 95% air. The cell lines and primary cells used for experiments are detailed in Table 2.3.

Table 2.3 Cells cultured for experiments.

Cell type	Description	Origin
A549	Human lung type II alveolar epithelial cell line	ATCC
35FL	Human lung fibroblasts originating from a 35-year-old female lung. The cells have been retrovirally infected to express telomerase rendering the cells immortal.	Coriell Institute for Medical Research [177].
IMR-90	Human lung fibroblast originating from a 16-week gestational aged foetus.	ATCC
NLF	Human lung cells extracted from the tracheal aspirate of endotracheal ventilated babies.	Tracheal aspirates from suctioning of ventilated neonates as part of clinical care during NICU admission.
aMSCs	Human amnion mesenchymal stem cells	Extracted from the amniotic membrane of a healthy human term placenta.
cMSCs	Human chorion mesenchymal stem cells	Extracted from the chorion membrane of a healthy human term placenta.

2.2.1 Trypsinisation and sub-culture

Cells were sub-cultured when 70-90% confluency was achieved. Cells in a T75 flask were gently washed with PBS before adding 0.05% (w/v) trypsin/0.02% (w/v) EDTA solution and incubated at 37°C. Trypsinisation was checked under a light microscope to observe cells becoming rounded and detached from the flask surface. The flask was tapped against

the hand palm to ensure all cells were dislodged. Cell culture medium was added to the flask to neutralize the trypsin. The cell suspension was removed into a 15ml centrifuge tube and centrifuged at 1200 rpm for 3 minutes to form a cell pellet. The supernatant was aspirated and cells re-suspended in culture media. Cells 35FL, IMR90, aMSCs, cMSCs and NLF were sub-cultured at a split ratio of 1:4. Cells A549 were sub-cultured at a ratio of 1:20. Medium was changed every 2-3 days

2.2.2 Cell cryopreservation and recovery

For cell preservation, all cells were trypsinised as described in 2.2.1 and resuspended in 1ml freezing medium (composed of culture medium supplemented with 10% DMSO) per $1x10^6$ cells. 1ml cell suspension was placed into cryovials and frozen at -80°C using a CoolCell cell freezing container (BioCision) to control cooling at a rate of -1°C per minute. Cells were transferred to liquid nitrogen 24 hours later for long term storage. When necessary cryopreserved cells were recovered by removing the required cryovial from liquid nitrogen and thawing in a water bath at 37°C. Once thawed the cells were resuspended in cell culture medium in T75 flasks. The cells were incubated at 37°C for 24 hours after which the medium was replaced to remove the remaining DMSO.

2.2.3 Haemocytometer cell counting

All cell counts were achieved by trypsinizing (as described in 2.2.1) to attain a uniform cell suspension. 10µl of cell suspension was pipetted under the cover slip on a Neubauer haemocytometer by capillary action. If trypan blue exclusion assay was being used 10µl of trypan blue was added to 10µl cell suspension before being added to a Neubauer haemocytometer. The mean average cell count was achieved by counting the cells within 4, $1mm^2$ corner regions under a phase contrast microscope. The mean average cell number was multiplied by 10^4 to give cells/ml and then multiplied by the volume of cell

suspension in ml to give total cell count. If trypan blue was used the dilution factor was taken into account.

2.3 Human neonatal tracheal cell extraction and culture

2.3.1 Sample collection

Ethical approval was sought for a pilot study to collect lung tracheal aspirates from infants on endotracheal ventilation at UHNM NICU, REC reference number 16/WA/0265 (appendix A and B). Once informed consent was achieved the tracheal suctioning was collected from patients as per routine practice. Samples were labelled by medical staff with a unique ID number and stored at room temperature ready for collection and transportation to the Guy Hilton research Centre Laboratory for processing immediately (Figure 2.2). Once the suctioned material entered the laboratory, samples were logged and given a unique HTA (Human Tissue Act) appropriate number. This number was designed by using the following information (Figure 2.1): initials of research group lead (PW), patient number (1-6), sample number from that patient (1-4), cell culture surface (tissue culture plastic, P or collagen, C). Patients remained anonymous throughout the experiment work.
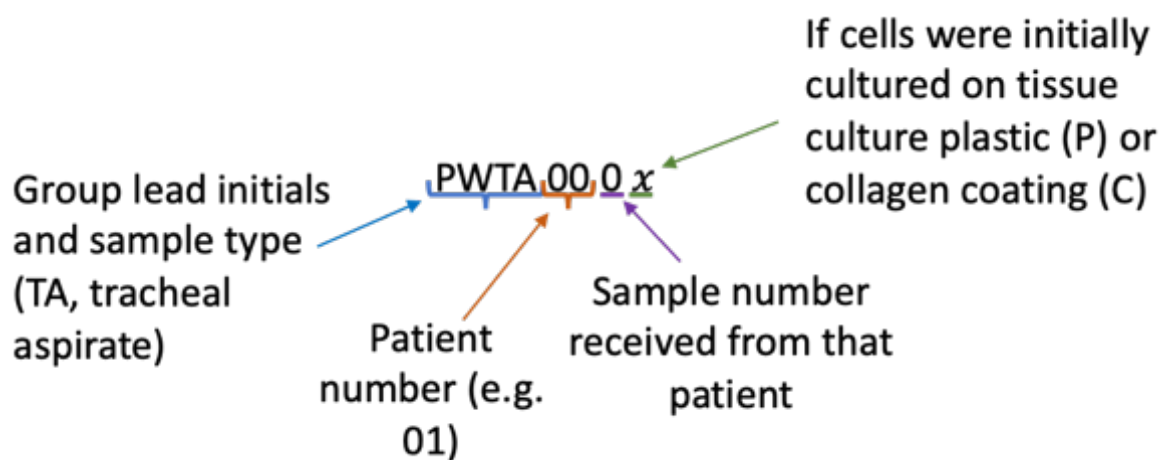
Figure 2.1 Human tissue labelling method.
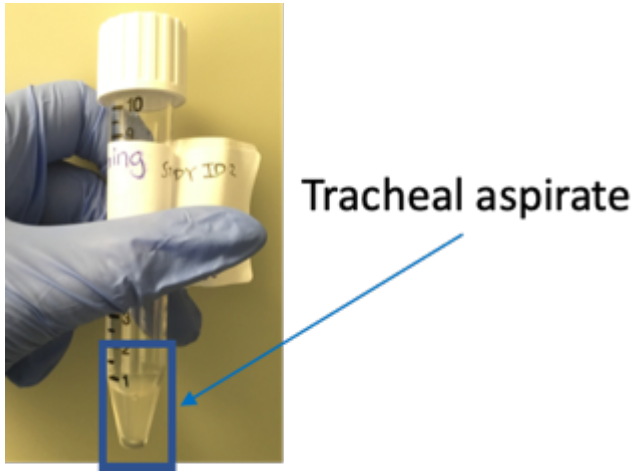
Figure 2.2 Tracheal aspirate collected from an infant on ventilation at UHNM NICU

2.3.2 Sample processing

Tracheal suctions were transfer to a 12ml centrifuge tube and centrifuged at 400 g for 20 minutes. Supernatant was aspirated and stored at -80°C. The pellet was resuspended in 1ml growth medium and a cell count was performed with trypan blue as described in section 2.2.3. Cells were seeded at 200,000 cells/well of a 24 well plate with 1ml of culture medium (high glucose DMEM 4.5g/L glucose with L-glutamine supplemented with 10% FBS and 1% Pen/Strep/Fungizone) at 37°C. After 1 hour of culture it was anticipated fibroblasts would have attached so the supernatant of each well was aspirated and transferred to a collagen coated well of a 24 well plate to encourage the attachment of epithelial cells. A representative flow diagram of the sample processing can be seen in Figure 2.3. Samples were checked daily with phase contract microscopy to observe cell attachment and proliferation.
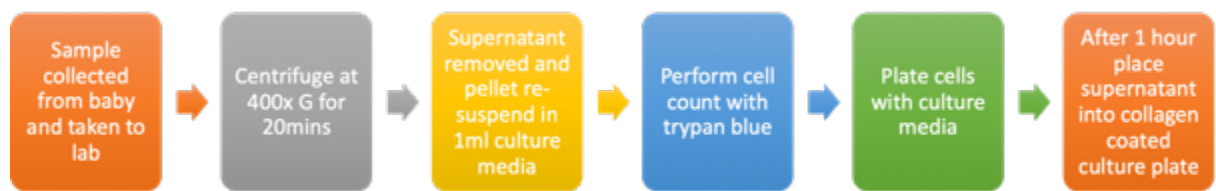
Figure 2.3 Flow diagram demonstrating the processing of tracheal aspirates.

2.3.3 Fibroblast cell culture

Cells isolated from the lung tracheal aspirates, henceforth called NLF, were cultured at 37°C in a humidified incubator with growth media at 5% CO_2 and 95% air 37°C. Once 90% confluency was achieved cells were trypsinised, counted and reseeded (as described in section 2.2.1) in a T75 culture flask at a 1:4 split ratio. At each passage cells were also cryopreserved as described previously in section 2.2.2.

2.3.4 Epithelial cell culture

To encourage epithelial cell growth 3 types of commercially available lung epithelial cell culture media were obtained (Table 2.4). The samples were processed as described in 2.3.2 but this time the pellet was resuspended in specific epithelial cell culture media to encourage lung epithelial growth. Media changes were completed every 3-4 days.

Table 2.4 Commercial culture media used to promote the growth of human lung epithelial cells.

Epithelial media name	Description	Source
LHC-9	Serum free media used for bronchial epithelial cells	ThermoFisher Scientific, UK
EpiVita w/ supplements	EpiVita Basal Medium used in conjunction with Human Bronchial/Tracheal Epithelial Cell Growth Supplement	Cell Applications, Inc. San Diego, US
BEGM bullet kit	BEGM™ Bronchial Epithelial BulletKitTM containing BEBM™ Bronchial Epithelial Cell Growth Basal Medium and BEGM™ Bronchial Epithelial Cell Growth Medium SingleQuots™ Supplements and Growth Factors.	Lonza, UK

2.4 Human placenta MSC extraction and culture

2.4.1 Placenta processing and MSC extraction

Ethical approval was sought to collect placentas from routine caesarean sections at UHNM, REC reference number 15/WM/0342 (appendix C). The term placentas were collected and processed immediately, following the arrival of the placenta at the laboratory, in a class II laminar flow hood to prevent contamination. The MSC isolation procedure was based on a previous published protocol[165]. An X-shaped incision was made from the umbilical cord towards the outer sides of the placenta. The amnion membrane was gently peeled off and placed in PBS to prevent drying. The chorion membrane was cut away from the placenta and placed into PBS (Figure 2.4). Both membranes were

thoroughly washed in PBS, cut into smaller pieces (around 2cm² squares) and any blood clots gently removed. The membranes were placed into trypsin-EDTA for 1 hour with vigorous shaking every 20 minutes, after which the maternal tissue was removed from the chorion membrane using tweezers. All membranes were washed thoroughly in PBS and placed into serum free medium containing 10% collagenase IV and incubated at 37°C until the membranes were digested. The digest solution was centrifuged at 250G for 5 minutes. The supernatant was removed, the pellet resuspended in PBS and the solution centrifuged as before. The pellet was resuspended in culture media (high glucose DMEM 4.5g/L glucose with L-glutamine supplemented with 10% FBS and 1% Pen/Strep) divided into three T175 cell culture flasks for each membrane and incubated at 37°C. A medium change was performed 2 hours after plating the cells to remove any contaminating epithelial cells.
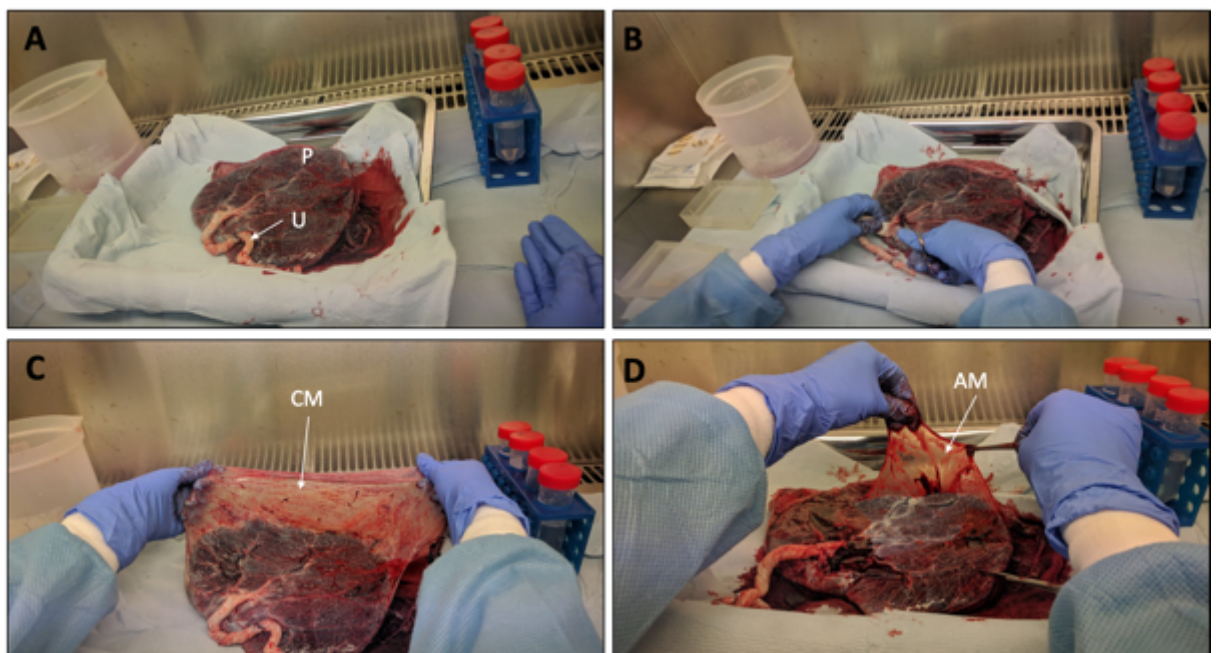
Figure 2.4 Isolation of Placenta derived MSCs. Whole placenta (labelled P) at arrival into laboratory with the umbilical cord (labelled U) **(A).** An X-shaped incision was made into the amnion membrane where the umbilical cord met the placenta **(B),** the chorion membrane (labelled CM) **(C),** and the amnion membrane (labelled AM) were lifted away **(D).**

2.4.2 Placenta MSC culture and expansion

Placenta derived amnion MSCs (aMSCs) and chorion MSCs (cMSCs) were cultured in a humidified incubator at 37°C in the presence of 5% CO_2 and 95% air (Figure 2.5). Culture medium (high glucose DMEM 4.5g/L glucose with L-glutamine supplemented with 10% FBS and 1% Pen/Strep) was changed every 2-3 days and cells were sub-cultured once 80-90% confluency was achieved using the previously described method (section 2.2.1).
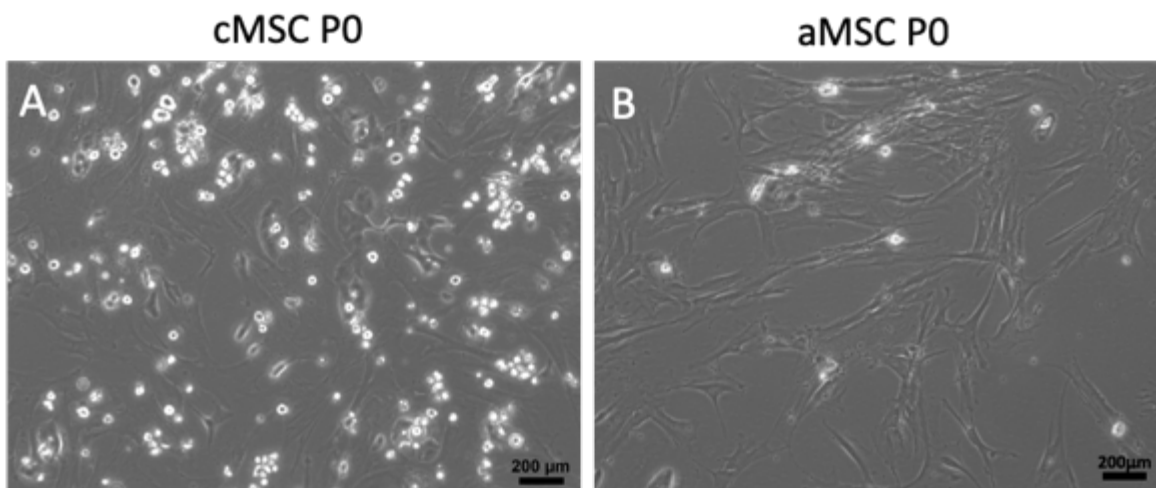
Figure 2.5 Isolated placenta MSCs. MSCs were isolated from the chorion membrane (A) and the amnion membrane (B) of a healthy full-term placenta. The MSC cells are elongated with a spindly-morphology. Smaller rounded cells can be observed with the cMSCs (A). These cells are likely to be epithelial cells which would later be removed through media changes.

2.5 Tri-lineage differentiation to assess MSC functionality

The differentiation potential of placenta derived MSCs was determined by seeding 4×10^4 cells/well in a 24 well plate in culture media. Cell were incubated overnight to allow for cell attachment. Cells were then cultured in the appropriate differentiation media for 21 days with media changes every 3-4 days. For controls, cells were seeded in the same manner and maintained with culture media.

2.5.1 Chondrogenic differentiation

For chondrogenic differentiation 1×10^5 cells in 7µl of medium was seeded as a micromass in the centre of a well. After 1-2 hours for cell attachment cells were cultured with chondrogenic media consisting of DMEM high glucose, 1% FBS (v/v), 1% ITS (v/v), 0.1µM dexamethasone, 50µM ascorbic acid phosphate, 40µg/ml L-proline and 10ng/ml TGF-β3.

2.5.2 Adipogenic differentiation

Adipogenesis was induced with DMEM high glucose supplemented with 10% FBS, 0.5µM dexamethasone, 0.5mM 3-isobutyl-1-methylxanthine, 10µg/ml insulin and 0.1mM indomethacin.

2.5.3 Osteogenic differentiation

Cells seeded for osteogenesis were cultured with DMEM supplemented with 50µM ascorbic acid phosphate, 10mM β-glycerophosphate and 0.1µM dexamethasone.

2.6 Histological staining of tri-lineage differentiation

Following 3 weeks of culture cells were fixed using 10% formalin for 20 minutes at room temperature, washed with PBS and stored at 4°C until staining.

2.6.1 Stain preparation: alizarin Red, oil red O and alcian Blue

1% Alizarin Red solution was prepared by dissolving 0.5g of Alizarin Red in 50ml of dH$_2$O and filtered through Whatman filter paper grade 1 . A stock solution of Oil Red O was prepared by dissolving 0.175g of Oil Red O powder in 50ml of 100% isopropanol and filtered using filter paper. Before each use, a 40% working solution was prepared by dissolving the stock solution in dH$_2$. O. 1% Alcian Blue solution was prepared by

dissolving 0.5g of Alcian Blue 8GX in 50ml of 3% acetic acid (pH 1.5). Solution was filtered using filter paper.

2.6.2 Histological staining

Mineral deposition of osteo-induced cells was determined using Alizarin Red solution. Stain was added to cells and incubated at room temperature for 10 minutes. The stain was removed, and cells were washed 3 times with tap water and imaged. For adipogenesis cells were washed with isopropanol before adding Oil Red O solution for 10 minutes at room temperature. The stain was removed, and the cells washed with isopropanol. Cells were imaged immediately. The chondrogenic cells were incubated with Alcian Blue over night at room temperature. Samples were then washed three times were tap water and imaged. All samples were imaged using an inverted light microscope with attached colour CCD camera.

2.7 LIVE/DEAD viability/cytotoxicity assay Kit

The LIVE/DEAD Viability/Cytotoxicity Assay Kit for mammalian cells (Invitrogen) allows the simultaneous determination of live and dead cells. The kit encompasses 2 probes, calcein AM and ethidium homodimer (EthD-1), which detect intracellular esterase activity and plasma membrane integrity respectively. Cells were prepared by removing culture media and washing samples twice with PBS. The staining solution was prepared by diluting 2μl of 2mM EthD-1 stock solution and 0.5μL of the 4mM calcein AM stock solution into 1ml of PBS. An appropriate volume of the staining solution was added to cover samples. The samples were left at 37°C for 30-45 minutes. Before imaging on a confocal microscope, the staining solution was aspirated and samples were gently washed with PBS. A small volume of PBS was left on the samples to prevent them drying out whilst imaging.

2.8 Flow cytometry

Placenta derived MSCs were cultured in growth media in T25 culture flasks at 37°C until confluency was achieved (as described in section 0). Cells were trypsinised (section 2.2.1) and the cell pellet resuspended in 11ml flow cytometry buffer (PBS with 0.5% (w/v) BSA and 2mM EDTA) and approximately $1x10^5$ cells aliquoted into microcentrifuge tubes. The samples were centrifuged at 300 g for 5 minutes and supernatant discarded. Each pellet was resuspended in PE (phycoerythrin)conjugated antibodies (CD14, CD19, CD34, CD45, CD73, CD90 and CD105, HLA-DR, IgG1 and IgG2a isotype controls) diluted in flow cytometry buffer and incubated in at 4°C for 15minutes. 1ml buffer was added to each samples and samples were centrifuged again. The supernatant was discarded, and the pellet was resuspended in 200μl PBS and transferred to the Beckton Dickinson FC500 flow cytometer for analysis. A minimum of 50,000 events was recorded and analysed by gating positive events to exclude 99% of the appropriate isotype control events (IgG1: CD19, CD73, CD90 and CD105, IgG2a: CD14, CD34, CD45, HLA-DR)

2.9 Hydrogels

Collagen hydrogels were prepared according to the manufactures protocol except that 10X DMEM replaced 10X PBS to provide the cells with appropriate nutrients for cell survival and proliferation. 10X DMEM was prepared by dissolving 50g DMEM powder and 3.7g sodium bicarbonate into 100 mL sterile deionised water. Elastin solution was also included into the collagen gelation procedure as described in previous published work[97]. A 10mg/ml elastin stock solution was prepared by dissolving 0.1g soluble elastin in 10ml sterile deionised water. 1N NaOH which neutralises the collagen to allow gelation was prepared by dissolving 2g of NaOH in 25 mL sterile deionised water. All solutions were sterile filtered in a flow hood using a syringe and 0.2 micron filter (Millipore, USA) to remove impurities. The collagen, 10X DMEM, sterile dH_2O and 1N NaOH were placed on

ice until ready to use. The appropriate volumes of each reagent were calculated using the following formulas:

$$Volume\ of\ 10XDMEM = \frac{Final\ volume\ of\ gel\ solution}{10}$$

$$Volume\ of\ collagen = \frac{final\ volume\ of\ solution \times final\ collagen\ concentration}{starting\ collagen\ solution}$$

$$Volume\ of\ 1N\ NaOH = volume\ of\ collagen\ gel\ solution \times 0.023$$

$$Volume\ of\ elastin\ solution = \frac{final\ volume\ of\ gel\ solution \times final\ elastin\ concentration}{starting\ elastin\ concentration}$$

$$Volume\ of\ dH2O = Final\ gel\ solution\ volume - (collagen\ volume + $$
$$10 \times DMEM\ volume + 1N\ NaOH\ volume + elastin\ volume)$$

Each component was added to a sterile tube held on ice in the following order: 10xDMEM, 1N NaOH, elastin, dH_2O and finally the collagen. For collagen only hydrogels (i.e. no elastin) elastin was omitted from the calculations. The contents were mixed thoroughly but caution was taken to avoid introducing bubbles. For hydrogels containing cells, the appropriate number of cells was trypsinised (as described in 2.2.1) and pelleted by centrifugation. The supernatant was aspirated and 200-300μl of collagen solution was then added to the cell pellet and mixed before adding to the remaining collagen solution. The solution was mixed by pipetting up and down gently but swiftly to avoid the gel setting. An appropriate volume of collagen solution was then pipetted into the tissue culture plate or cell culture well insert (Figure 2.6). The gels were allowed to set at 37°C for 30 minutes to 1 hour before culture medium was added. Medium changes were performed every 2-3 days being careful not to disturb the gel.
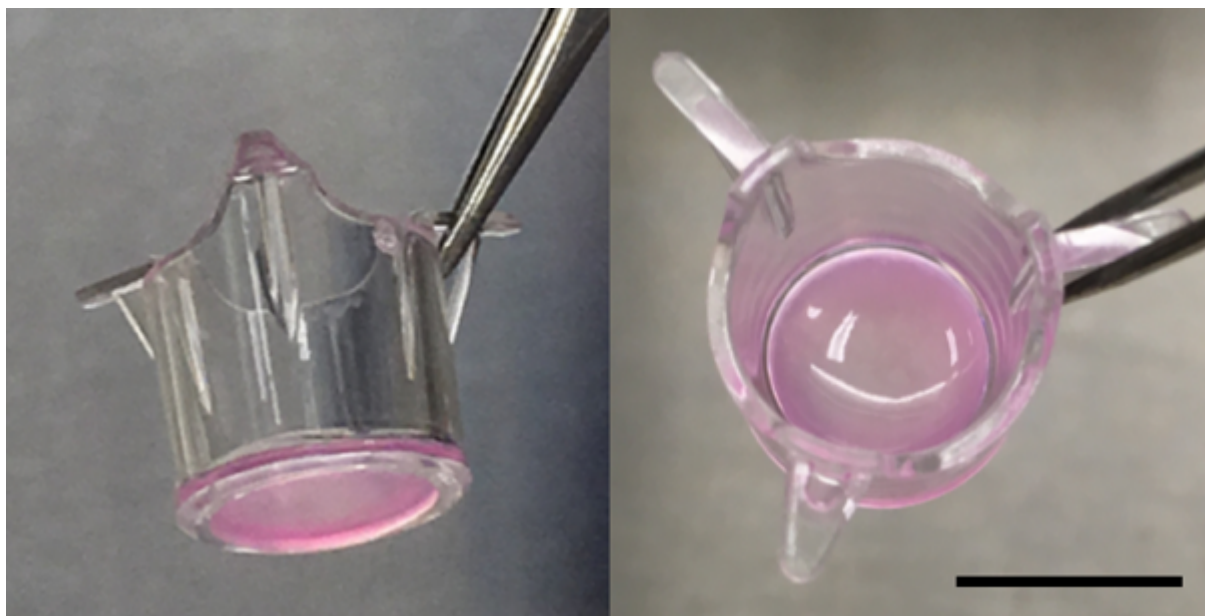
Figure 2.6 Cell seeded collagen-elastin hydrogel. Collagen-elastin hydrogels (concentration 3.5mg/ml) seeded with 35FL were set within ThinCert™ 12 well cell culture inserts PET (polyethylene terephthalate), 0.4μm pore size. Scale bar 15mm.

2.10 Gel measurements

Hydrogel depth and diameter were measured noninvasively every 5 days during culture (Figure 2.7). Hydrogel diameter was measured using a ruler placed underneath the culture plate (Figure 2.7 **B**). A commercially available spectral domain optical coherence tomography (OCT) (Thorlabs) was used to determine the gel depth. Changes in hydrogel dimensions were measured in millimetres and percentage change was calculated using the following equation (where day χ can represent any other day a measurement was taken):

$$\% \, change \, in \, depth = day \, 0 \, measurement \, (mm) \div day \, \chi \, measurement \, (mm) \times 100$$
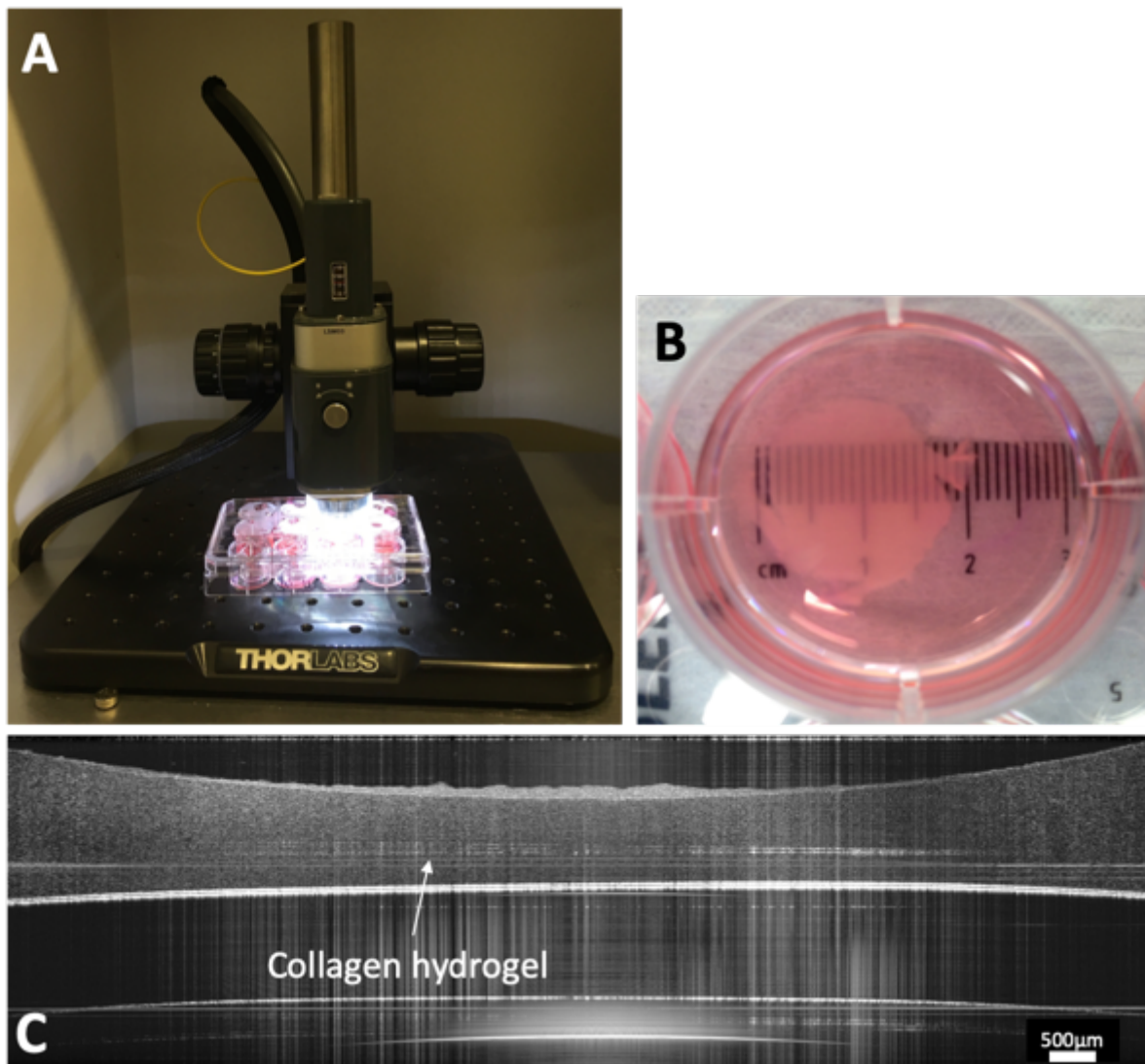
Figure 2.7 Measuring hydrogel depth and diameter. The Thorlabs OCT imaging system **(A)** scans a collagen hydrogel within a tissue culture well plate **(B)** and provides a computerised 2D cross-sectional image of the collagen hydrogel **(C)** that can be measured using the ThorImageOCT software. Hydrogel diameter is measured using a ruler placed underneath the tissue culture plate of the hydrogel **(B).**

2.11 Two-step real-time PCR

2.11.1　　RNA extraction

Two different methods of RNA extraction were compared: the TRIZOL method and the RNeasy kit. Six 3.5mg/ml collagen-elastin (at a 1:1 ratio) hydrogels seeded with 35FL were made using the protocol described in section 2.9. Before gelation 1×10^5 cells/gel were resuspended in the solution and 500µl was pipetted into a 12 well plate. The

samples were incubated at 21% oxygen 37°C for 24 hours. Three hydrogels for each group underwent the appropriate treatment for either the TRIZOL RNA extraction procedure or the RNeasy kit.

2.11.1.1   RNA extraction: TRIZOL method

Hydrogels were placed into 1ml of TRIZOL reagent in a microcentrifuge tubes and incubated for 5 minutes at room temperature. 200μl of chloroform was added to the samples and shaken vigorously for 15 seconds. The samples were centrifuged at 10,000 rpm for 15 minutes at 4°C at which point the mixture separates into lower organic, interphase and upper aqueous phase containing the RNA. The upper aqueous phase was transferred into a fresh microcentrifuge tube. 500μl of 100% isopropanol was added to each sample and incubated at room temperature for 20 minutes. The samples were centrifuged at 10,000rpm for 10 minutes at 4°C. The supernatant was removed by tipping to avoid disturbing the precipitated pellet. 1ml of 75% ethanol was added to the pellet and the samples were vortexed briefly. The samples were centrifuged at 7500 rpm for 5 minutes at 4°C and the remaining ethanol was aspirated. The pellets are left to air dry until the ethanol has evaporated. The remining pellet were gently mixed in 15μl RNase/DNase free H_2O and incubated at 55°C in a water bath. The RNA concentration was measured using a NanoDrop 2000 spectrophotometer (Thermo Scientific) instrument and the samples stored at −80°C.

2.11.1.2   RNA extraction: RNeasy kit

Total RNA extraction was performed using the RNeasy mini kit (Qiagen). For collagen gels medium was aspirated and discarded. The gels were gently removed using tweezers and placed into microcentrifuge tubes containing 350μl RLT lysis buffer. Samples were left for

20-30 minutes and briefly vortexed occasionally until the gels had been digested. For cells in monolayer, medium was removed and 350μl RLT buffer was added directly to cells and left for 20-30 minutes. Cell lysate was pipetted into microcentrifuge tubes. All samples were stored at -80°C until ready for extraction protocol.

Hydrogel RLT buffer lysate were placed on ice for thawing. 350μl of 70% ethanol was added to lysate and mixed by pipetting. The solution was added to the RNeasy spin column and centrifuged for 15 seconds at 17,000 g. The flow through was discarded and the column membrane was washed using the appropriate buffers according to the manufactures protocol and centrifuged at 17,000 g. All flow through was discarded after each centrifugation. After the final buffer was discarded the collection tube was replaced with a clean 1ml centrifuge tube. 15μl of RNase free water (provided by the manufacture) was added to the spin column to elute the RNA. The spin column was centrifuged for 1 minute at 17,000 g. The eluted water was then re-added onto the spin column membrane and the tube was centrifuged again at 17,000 g for 1 minute. Extracted RNA concentration was quantified using the Nanodrop and stored at -80°C freezer.

Table 2.5 RNA extracted from collagen hydrogels seeded with 35FL human lung fibroblasts. Two RNA extraction methods were compared; TRIZOL method and RNeasy kit. One sample from the TRIZOL method was lost during the procedure so no quantification could be achieved.

	TRIZOL method		RNeasy method	
Sample	Nucleic acid (ng/μl)	260/280nm	Nucleic acid (ng/μl)	260/280nm
1	14.2	1.92	19.1	2.07
2	15.8	1.94	20.4	2.09
3	-	-	13.8	2.05

2.11.2   Comparing RNA extraction methods

Both the TRIZOL method and RNeasy kit extracted RNA from the collagen-elastin hydrogels. One sample from the TRIZOL method was lost during the procedure so no quantification could be achieved. This method required more handling time and was a more difficult procedure compared with the RNeasy method. The RNeasy kit produced higher quantities of nucleic acid whilst maintaining a high purity (Table 2.5, indicated by the 260/280nm ratio) and was used henceforth for RNA extraction.

2.11.3   Reverse transcription- cDNA synthesis

The RNA samples were diluted in RNase/DNase free water to a concentration of 1μg/μl. The Thermo Fisher high capacity cDNA reverse transcription kit was used. The appropriate volume of 2x reverse transcription master mix was made by preparing a solution of RT buffer, dNTP mix, 10x RT random primers, MultiScribe™ Reverse Transcriptase and Nuclease-free H_2O. This master mix was added to a microcentrifuge tube with the extracted RNA to make a 1x solution. The samples were then placed into a thermal cycler and set to the following conditions:

1. 25°C for 10 minutes
2. 37°C for 120 minutes
3. 85°C for 5 minutes
4. 4°C ∞

Samples were stored at -20°C until ready for processing.

2.11.4   Primer design and optimisation

Appropriate primers associated with BPD were narrowed down by examining previous published *in vitro* and *in vivo* work and specificity was checked using NCBI Primer-BLAST. Markers which were most strongly associated with BPD were chosen (listed in Table 2.6) and purchased from Integrated DNA Technologies. RT-PCR was run with all the

established primers to check for product amplification. The housekeeping gene *GAPDH* was included. Primers were dissolved in RNase/DNase-free water according to the manufactures instructions to achieve 100μM. 10μM stock solutions were stored at -20°C.

Table 2.6 RT-PCR primer sequences. The sense and antisense sequence of primers, their annealing temperature for PCR and the product length

Gene	Sense sequence (5' to 3')	Antisence sequence (5' to 3')	Annealing temperature	Product length
GAPDH (Glyceraldehyde-3-phosphate dehydrogenase)	ACTTCAACAGCACACCCACT	GCCAAATTCGTTGTCATACCAG	58	103
ACTA2 (α-smooth muscle actin)	CCGACCGAATGCAGAAGGA	ACAGAGTATTTGCGCTCCGGA	60	88
ELN (Elastin)	GCAGGAGTTAAGCCCAAGG	TGTAGGGCAGTCCATAGCCA	60	148
COL1A1 (Collagen type 1)	GTCACCCACCGACCAAGAAAC	AAGTCCAGGCTGTCCAGGGATG	60	121
TGFB1 (Transforming Growth Factor Beta 1)	GCGACTCGCCAGAGTGGTTA	GTTGATGTCCACTTGCAGTGTGTTA	58	143
NQO1 (NAD(P)H quinone dehydrogenase 1)	GGTCGGCAGAAGAGCACTGA	CCAGAACAGACTCGGCAGGA	60	221

2.11.5   Real time-qPCR

The QuantiFast SYBR Green PCR Kit was used to determine the relative gene expression of mRNA *COL1A, ELN, ACTA2, TGFB1* and *NQO1.* In short, 1μl forward primer, 1μl reverse primer, 4μl RNase free water, 1.5μl cDNA and 7.5μl 2X QuantiFast SYBR Green PCR Master Mix were mixed in PCR tubes. The thermal cycling protocol is demonstrated in Figure 2.8. Relative gene expression in the form of $2^{-\Delta CT}$ fold change values were calculated.
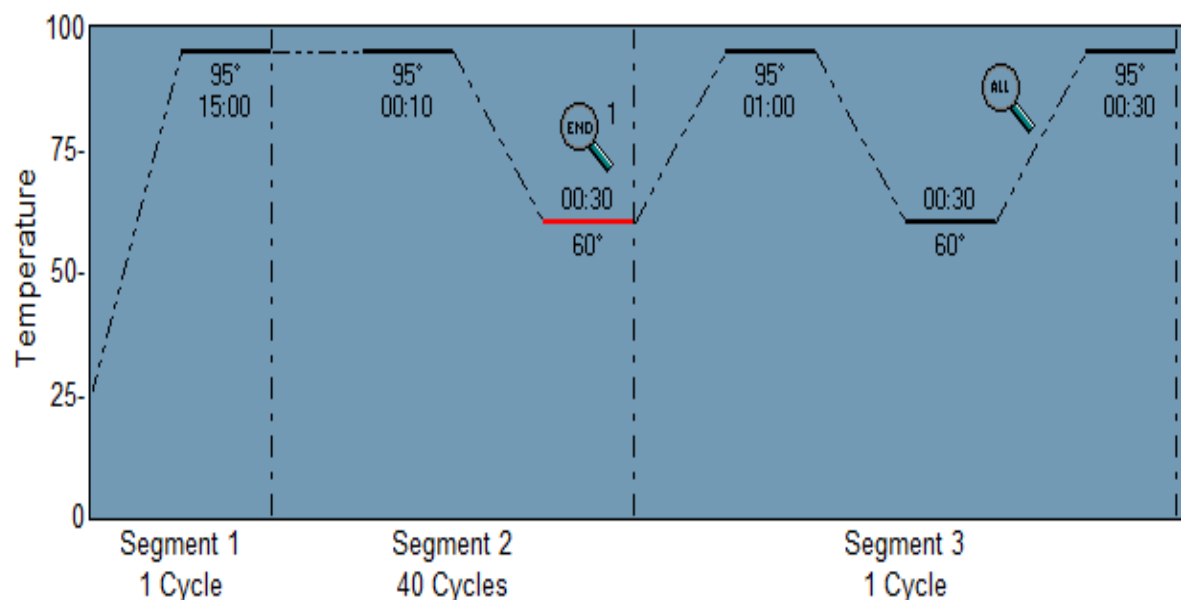
Figure 2.8 qRT-PCR thermal cycle programme. Segment 1 corresponds to the PCR initial activation step, segment 2 and 3 correspond to denaturing and annealing.

2.11.6   Gel electrophoresis

Gel electrophoresis was used to validate the primer design and PCR optimisation. A 2% (w/v) agarose gel was prepared by dissolving agarose in 1xTAE (tris-acetate-EDTA) buffer using a microwave to gently heat the solution. Once the agarose had dissolved, 8µl of ethidium bromide was mixed into the solution by swirling. The agarose solution was poured into the gel setting chamber, a comb was secured into the chamber and the gel was allowed to set for 45 minutes. The comb was removed and the gel was released from the chamber and transferred to BioRad electrophoresis clear chamber. 1xTAE solution was added to the electrophoresis chamber until the gel was covered. 2.5µL of loading buffer was added directly to PCR samples and 8µl of each sample was pipetted into respective wells of the gel. 5µl of DNA ladder was pipetted into the end wells (Figure 2.9). The chamber lid was attached, and conditions were set to 100v, 250mA, 25W for 1 hour.
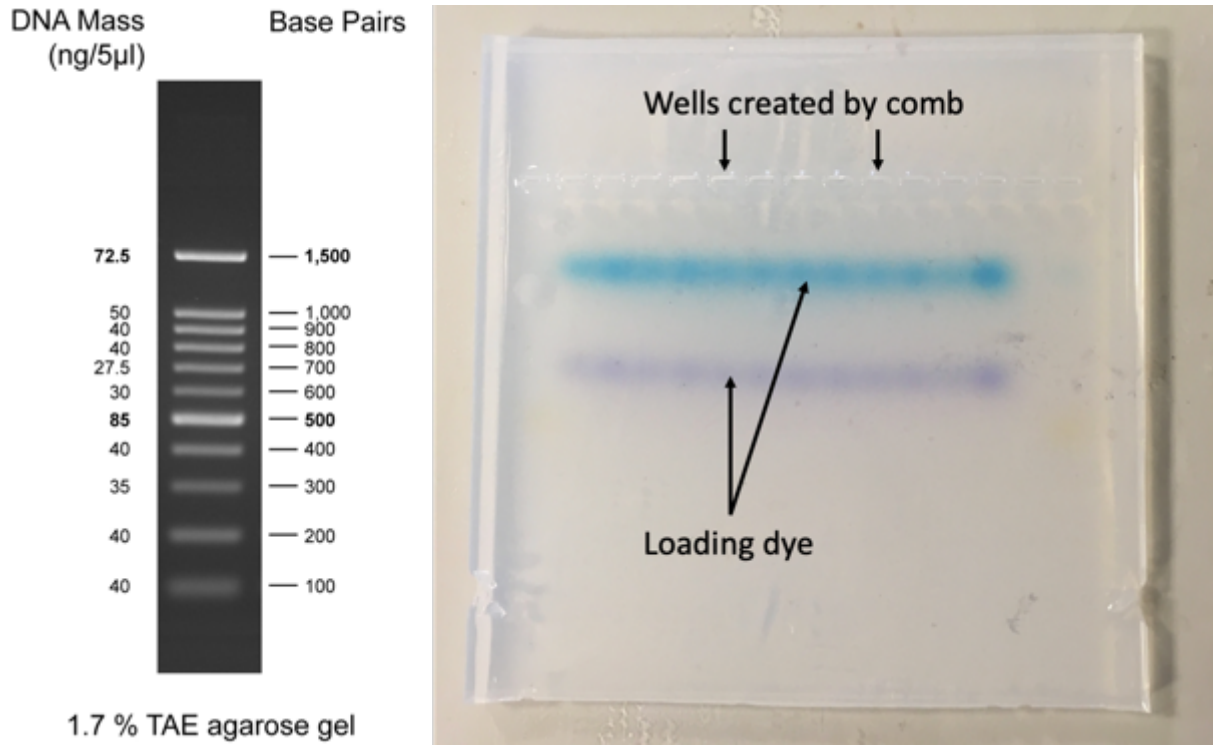
Figure 2.9 Gel electrophoresis. The DNA ladder used to compare DNA sizes and a photo of a 2% gel electrophoresis ran with PCR products with loading dye.

Figure 2.10 shows a completed gel electrophoresis used to verify product length, primer specificity and annealing temperature (A and B). Negative controls (containing no cDNA during amplification) were included (B). Amplified genes produced single bands which corresponded with product length. No bands were visualised for negative controls.
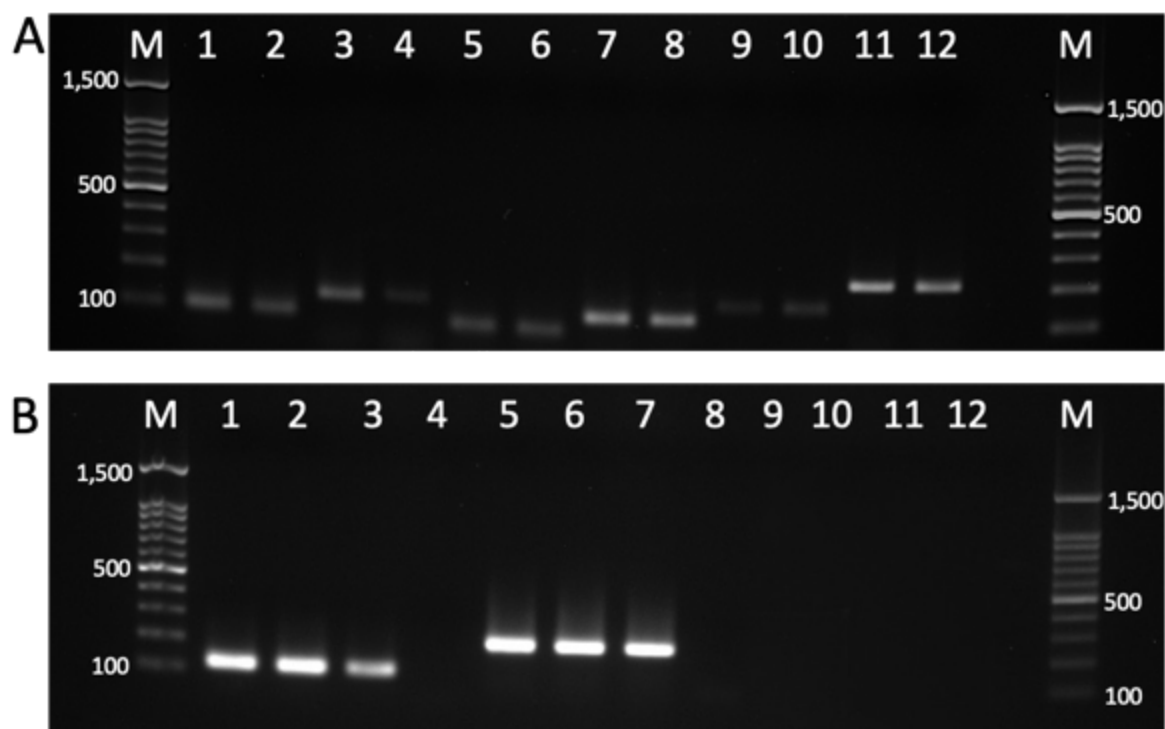
Figure 2.10 Agarose gel electrophoresis of PCR products for optimised primers GAPDH, TGFβ, COL1A1, ACTA, ELN and NQO1. Showing the migration of RT-PCR products as follows for image A: Lanes 1 and 2: GAPDH, 3 and 4: TGFβ1, 5 and 6: ACTA2, 7 and 8: COL1A1, 9 and 10: ELN, 11 and 12: NQO1. RT-PCR products for image B: 1, 2 and 3: COL1A1, 4: COL1A1 negative, 5, 6 and 7: NQO1, 8: NQO1 negative, 9: ELN negative, 10: ACTA2 negative, 11: GAPDH negative, 12: TGFβ negative. A molecular marker was included (M).

2.12 Proteinase K digestion

Proteinase K is a broad range protease which digests proteins. It can therefore be used to break-down collagen hydrogels and cell lysis. The proteinase K solution is provided at a concentration of 20mg/ml and was diluted with dH_2O to a stock concentration of 2.5mg/ml, aliquoted and stored at -20°C. Once ready to be used, the stock concentration is thawed at room temperature and diluted with dH_2O to a working concentration of 50µg/ml. Medium was aspirated from samples and using sterile tweezers collagen gels were carefully placed into sterile microcentrifuge tubes containing 0.5ml proteinase K working solution, vortexed briefly and placed in a 60°C oven for 1-2 hours until gels were

digested. For cells in monolayers, medium was aspirated off and 0.5ml proteinase K working solution was pipetted onto cell monolayer. Samples were left at 37°C for a few minutes until cell lysis was observed under phase contrast microscope. The cell lysate solution was pipetted into microcentrifuge tubes and vortexed briefly. Following digestion all samples were stored at -20°C until use.

2.13 Quant-iT™ PicoGreen™ dsDNA assay

The PicoGreen dsDNA assay allows the quantification of double stranded DNA from cell lysate. Cell lysate from proteinase K digestion (section 2.12) was left to thaw on ice. 1X Tris-EDTA (TE) buffer was prepared by diluting 20x TE in sterile deionised H_2O. A standard curve was created using the stock DNA provided with the kit (Table 2.7). The PicoGreen solution was prepared by diluting the PicoGreen stock solution 1:200 with 1X TE buffer. 50µl of the standards and cell lysate samples were pipetted into a 96 well plate in duplicate. Blanks were included which consisted of the acellular gels digested using the same proteinase K digestion method. 50µl of the PicoGreen working solution was then added to each sample. The samples were protected from light before measuring fluorescence at excitation 480 nm, emission 520nm on a plate reader. Concentrations were determined by plotting fluorescence emission intensity versus known DNA concentration using GraphPad Prism 7.0a (Figure 2.11).

Table 2.7 PicoGreen standard curve created to quantify DNA in unknown samples

Standard (µg/ml)	Volume of DNA 3µg/ml working solution (µl)	Volume of 1x TE buffer (µl)
0	0	300
0.005	0.375	299.625
0.01	0.75	299.25
0.05	1.5	298.5
0.1	7.5	292.5
0.5	15	285
1.0	75	225
2.0	150	150
3.0	300	0
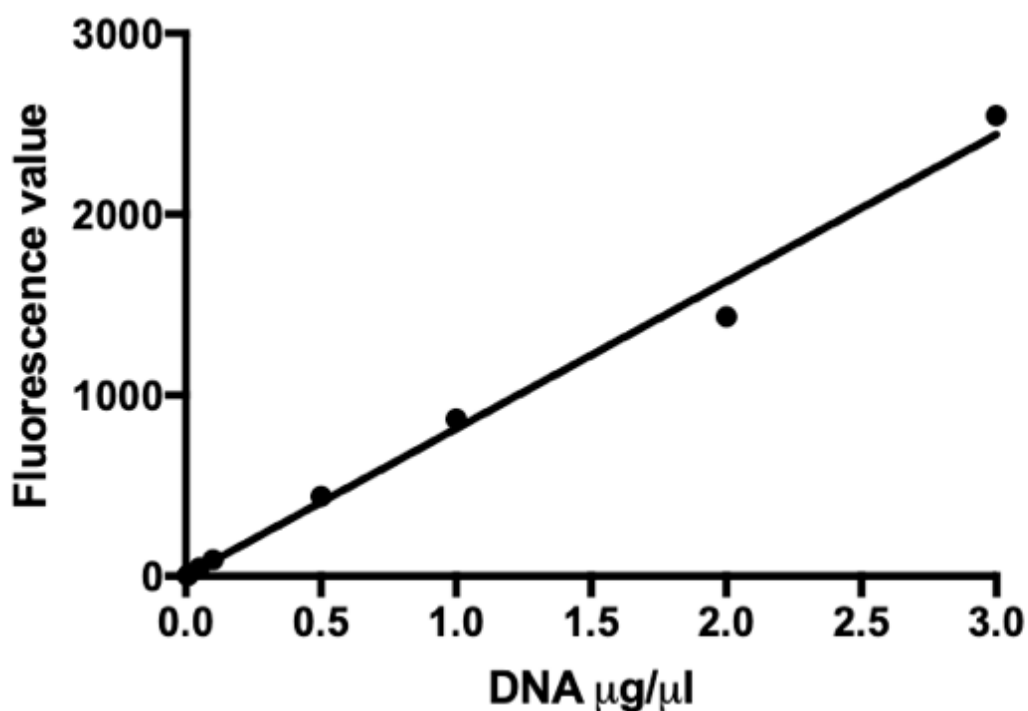
Figure 2.11 PicoGreen ds DNA assay standard curve

2.14 TEER analysis

Transepithelial electrical resistance (TEER) analysis examines the integrity of epithelial monolayers. TEER analysis was carried out on A549 cells cultured in monolayer on well inserts using the Millipore® RS2 as illustrated in Figure 2.12. Culture medium was aspirated from samples and replaced with PBS within the well and well insert. The longer electrode (E1) was inserted to the bottom of the well plate and the shorter electrode (E2) was placed within the well insert (close to but not disturbing the cells) and held horizontally at 90° for a few seconds whilst a reading was recorded. Following the measurement, the PBS was aspirated and replaced with culture media. To calculate the electrical resistance the following equation was used:

$$Unit\ area\ resistance\ (\Omega cm^2) = resistance\ (\Omega) \times membrane\ area\ (cm^2)$$
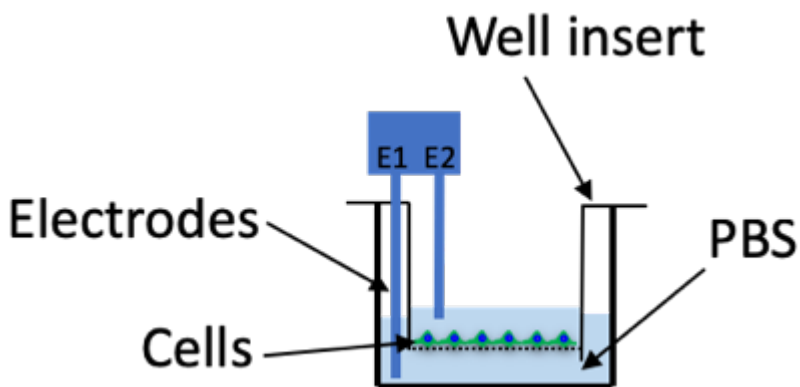
Figure 2.12 Illustration showing the set-up to measure transepithelial electrical resistance of cells cultured in monolayer in a well insert. The longer electrode (E1) is placed with the well plate and the shorter electrode (E2) is placed in the well insert. The electrodes are held at 90° whilst an electrical resistance reading is taken.

2.15 AlamarBlue® Assay

The alamarBlue® assay is designed to measure the metabolic activity of cells by exploiting the reduction of resazurin to resorufin. The AlamarBlue reagent was added to culture media at a 1:10 dilution. The AlamarBlue solution was added directly to the cells

and left in culture at 37°C for 2 hours protected from light. 100μl of the alamarBlue solution was removed from each sample in duplicate and pipetted directly into a 96 well plate. Fluorescence was measured on a plate reader at excitation wavelength of 530nm. Following measurements, the remaining alamarBlue solution was removed from all samples and replaced with fresh culture media.

2.16 Culturing cells at hyperoxia

Cells were exposed to a hyperoxia environment using a previously described method[177,178]. Tissue culture plates were placed into polycarbonate containers with sealed lids (using petroleum jelly to make them air-tight). The containers were flushed with pre-mixed gas of 40% O_2, 5% CO2, and 65% N_2 (sourced from BOC) by pumping the gas into one of the holes of the container (Figure 2.13). After one minute the empty hole was sealed using a bung. After another 2 minutes the gas source was removed, and a bung was swiftly placed into the hole to seal the container. Containers were re-gassed following media changes or gel measuring.
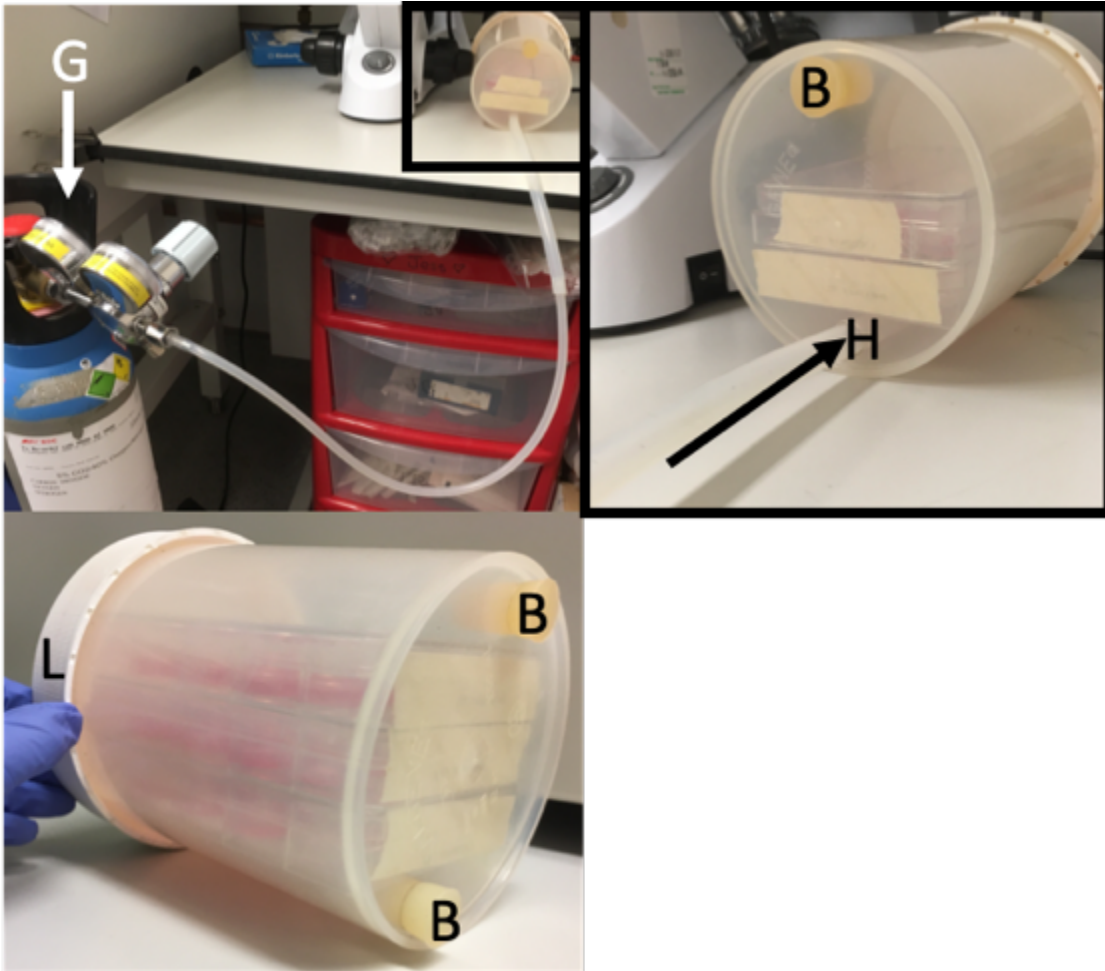
Figure 2.13 Exposing cells to hyperoxia. Cell culture well plates stacked within a sealed polycarbonate air-tight container. The plates were inserted into the container and the lid (L) was sealed using petroleum jelly to make it air-tight. A tube leading from a gas cylinder container pre-mixed 40% oxygen gas (G) was fed into one of the holes (H). Gas was pumped into the container (arrow) and after 1 minute the top hole was sealed using a bung (B). After a further 2 minutes the tube was removed, and the second bung was put into the hole to seal the container

.

Chapter 3

Designing an *in vitro* model

to represent the lung

alveolus

3.1 Introduction

BPD can be a life-threatening condition for premature neonates. Our current knowledge of the disease has relied heavily on animal models which do not accurately represent the disease pathogenesis in humans[60]. This has led to a limit in our understanding of BPD. Advances in regenerative medical methodologies has provided new ways to investigate diseases *in vitro*. Collagen hydrogels provide a 3D biocompatible scaffold which can mimic native tissue. Collagen and elastin are key molecules found in the lung mesenchyme. Both molecules provide mechanical capabilities to allow expansion and recoil of the alveoli during breathing. Collagen and elastin provide the lung architecture and are thought to be the driving force of lung maturation. It has been demonstrated in BPD, where lung maturation is distorted, that there is an abnormal collagen-elastin architecture. It is therefore appropriate that collagen-elastin hydrogels form the basis of an *in vitro* model to represent BPD. Previous work from our lab compared the Young's modules of collagen-elastin hydrogels to the expected Young's modules of a human lung alveolus (Figure 3.1)[97]. It was found that the addition of lung fibroblasts and elastin increased the theoretical Young's modules value for a single alveolar wall ($\approx$5 kPa). Due to the advantageous mechanical properties of collagen-elastin hydrogels, this was used as the starting point to develop a more complex alveolar model.
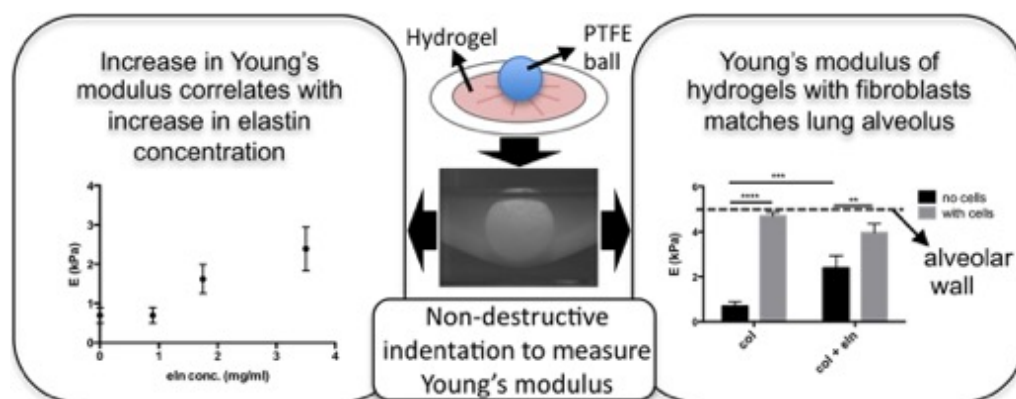
Figure 3.1 Young's modules of collagen hydrogels. The Young's modulus is improved with the addition of soluble elastin and lung fibroblasts (Image sourced from Dunphy *et al.*[97]).

The human lung alveoli are a complex multicellular tissue. The alveolus wall comprises of AEC1 and AEC2 which are exposed to an air interface to allow gas exchange. Surrounding the lung alveoli is the pulmonary mesenchyme containing the lung fibroblasts which are thought to drive the collagen and elastin architecture. Based on this design we proposed an *in vitro* model which would represent the multicellular lung alveolus whilst providing an air interface (Figure 3.2).
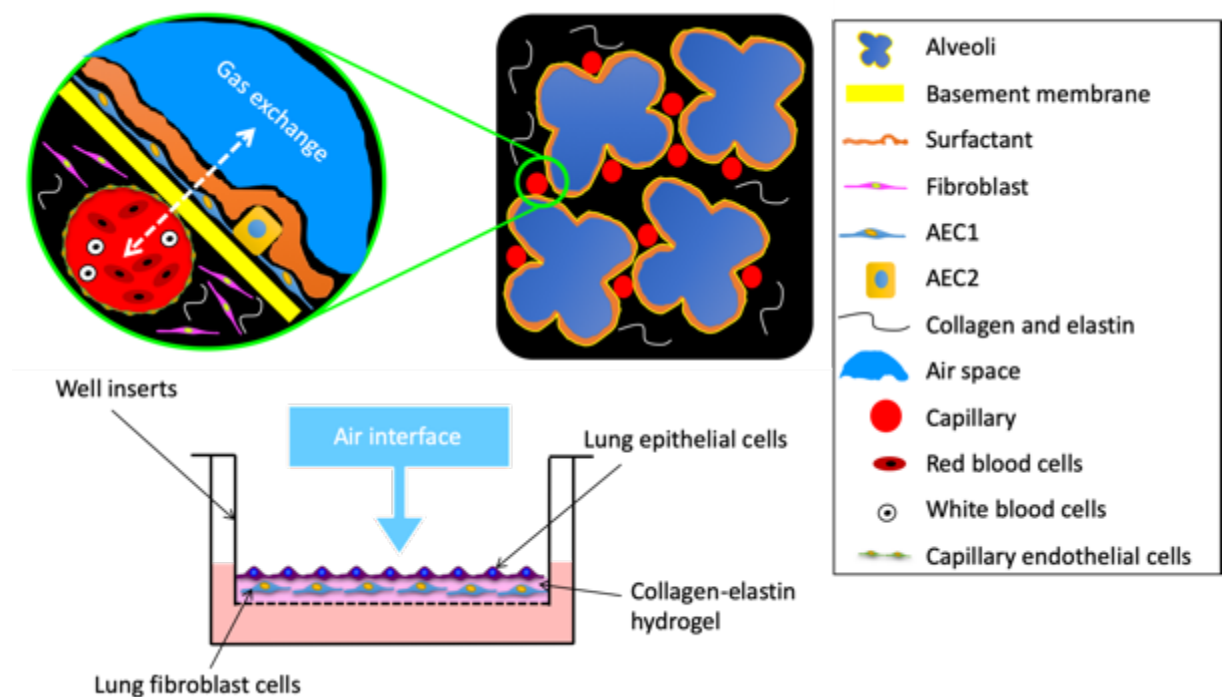
Figure 3.2 Designing an *in vitro* model to represent the human lung alveolus. The alveolus is a multicellular tissue which allows gas exchange during breathing. It is composed of AEC1 and AEC2 which form the alveolus wall. Surrounding the alveolus is the lung mesenchyme which consists mostly of collagen and elastin produced by lung fibroblasts. The proposed *in vitro* model is composed of a collagen-elastin hydrogel seeded with lung fibroblasts and lung epithelial cells. The construct is set within a well insert to provide an air interface. The model aims to represent the human alveolus.

The suggested model consists of a collagen-elastin hydrogel seeded with lung fibroblasts. Lung epithelial cells can be seeded on the hydrogel surface. The cell seeded hydrogel is

set within a well insert which provides the ability to expose the epithelial cells to an air interface. This is a vital part of the model since BPD is thought to be exacerbated by mechanical ventilation at high oxygen levels >21% (hyperoxia) [78,132].

3.2 Aims

This study aims to develop a lung alveolus model consisting of a collagen-elastin hydrogel that would allow the co-culture of human lung epithelial and human lung fibroblast cells. The model will be designed to allow for hyperoxygen exposure and mechanical stimulus to represent the clinical ventilation of BPD patients.

3.3 Study design

Initially we examined the contractibility and viability of adult and foetal lung fibroblasts (35FL and IMR90 respectively) when seeded within collagen hydrogels and how the addition of elastin affected cell and hydrogel performance. Next, we established if lung epithelial cells could be successfully cultured as a monolayer on the hydrogel surface and whether they could be removed for single-cell molecular analysis. The lung epithelial hydrogels were exposed to hydrostatic stimulation to evaluate the effect on cell viability, cell migration and compression of hydrogels. We assessed the effect of 80% oxygen on human lung cells IMR90, 35FL and A549 cell viability. A diagram of the study design is shown in Schematic 3.1.

Schematic 3.1 A schematic to show the flow of experimental design for chapter 3.

3.4 Methods

3.4.1 Examining the effect lung fibroblast seeding density has on

hydrogel contraction and cell viability

To investigate cell contraction and viability, lung fibroblasts were seeded within collagen

hydrogels of varying collagen concentrations and seeding densities. Collagen hydrogels of

concentration 1.5mg/ml and 3.5mg/ml were made as described previously (section 2.9).

Before gelation, IMR90 cells or 35FL cells were resuspended into the collagen solution at

a density of $1x10^5$ cell/gel or $2.5x10^5$ cells/gel. 500µl collagen solution per hydrogel was

set into the well of a 12 well plate and incubated at 37°C for 30 minutes. Following

gelation 1.5ml growth medium was added to the samples and they were incubated at 37°C

for up to 25 days with media changes every 2-3 days. At day 0 and day 20 hydrogels were

digested with proteinase K (section 2.12) and DNA was quantified (section 2.13).

Hydrogel diameter was measured every 5 days and depth was measured at day 0 and day

20 to calculate percentage change (section 2.10). At day 2 phase contrast light

microscopic images were taken and at day 25 the LiveDead assay was performed (section

2.7).

3.4.2 Investigating IMR90 DNA content in collagen hydrogels

To assess how DNA content changed through a 20-day experiment, collagen hydrogels of

concentration 3.5mg/ml were made as previously described (section 2.9) with IMR90

cells at a concentration of $1x10^5$ cells/gel. On day 1, day 10 and day 20 hydrogels were

digested with proteinase K digestion (section 2.12) and DNA quantified (section 2.13).

Hydrogel depth and diameter were measured (section 2.10) every couple of days and

phase contrast microscope images were taken to observe cell morphology.

3.4.3 Establishing cell seeding density, cell viability and cell migration for A549 on collagen hydrogels

Collagen hydrogels of concentration 3.5mg/ml were cast in a 12 well plate (section 2.9) and incubated at 37°C for 30 minutes to allow for gelation. Once the hydrogels had set A549 cells were trypsinised, counted and (section 2.2.3) gently seeded onto the hydrogel surface at a concentration of 10,000, 100,000 or 250,000 cells/gel. Cells were cultured at 37°C with 1.5ml growth medium per gel for 6 days. Phase contrast images were taken at day 3 and at day 6 the LiveDead assay was performed (section 2.7).

3.4.3.1 A549 removal from hydrogels

Following on from the culture of A549 on hydrogel surface we looked at the removal of the epithelial cells for future analysis. Trypsin was initially trialled using techniques already described (section 2.2.1). Briefly, growth medium was aspirated and the samples were washed carefully with PBS. Trypsin was added in varying concentrations (1x, 2x, 5x and 10x concentration). The cells were observed under phase contrast microscopy for rounding. Cell removal using TrypLE (recombinant enzyme) was tested by aspirating growth media and adding 1ml of TrypLE to the samples. The samples were incubated for an hour at 37°C cells. Cells were imaged under phase contrast microscopy every 10 minutes to check for cell detachment. After 60 minutes of incubation cells had become rounded and the Tryp-LE was aspirated to remove detached cells and centrifuged at 3500 rpm for 5 minutes to form a cell pellet. Hydrogel samples were observed under phase contrast microscopy to establish if all A549 cells had been removed. Physical cell removal using a cell scraper was tested by aspirating growth media, adding 1ml PBS and gently scraping the hydrogel surface.

3.4.4 Exposing collagen hydrogels seeded with A549 to hydrostatic stimulation

A549 cells were cultured as described (section 2.2). 3.5mg/ml collagen hydrogels were prepared using the protocol described (section 2.9). 3 sample types were included as shown in Figure 3.3: A549 seeded on collagen hydrogels in tissue culture plastic (TC), A549 seeded on collagen hydrogels in well plate insert, and A549 seeded within collagen hydrogels in well plate inserts. For the samples which had cells seeded on the hydrogel surface, once the hydrogels had set $2.5x10^5$ cells/gel were seeded as a monolayer on hydrogel surface. For cellular hydrogels, $2.5x10^5$ cells/gel were resuspended in the collagen solution before gelation. Once all hydrogels had set, growth medium was pipetted onto the cells and into the well where a well insert was used. The cells were cultured at 37°C for 24 hours to allow cell attachment at which point the cell culture medium was aspirated from within the well insert. Cells were cultured for 10 days to achieve a confluent monolayer. Every 24 hours the samples were exposed to intermittent hydrostatic stimulation utilized using a DynaGen® Hydrostatic Pressure Tissue Culture Plate Bioreactor Chamber (Instron) at a frequency of 1Hz, with a pressure level of 1.5 KPa in a sinusoidal wave for 1 hour. 1.5KPa is the expected pressure ventilated babies would be exposed to (based on information provided by NICU clinicians). Samples that were not exposed to hydrostatic pressure were used as static controls. The static controls under-went the same media changes as the stimulated samples. Immediately following stimulation samples were stained using the LiveDead kit (section 2.7). Cells were imaged using a phase contrast microscope and a confocal microscope to observe cell morphology, cell alignment and cell migration.
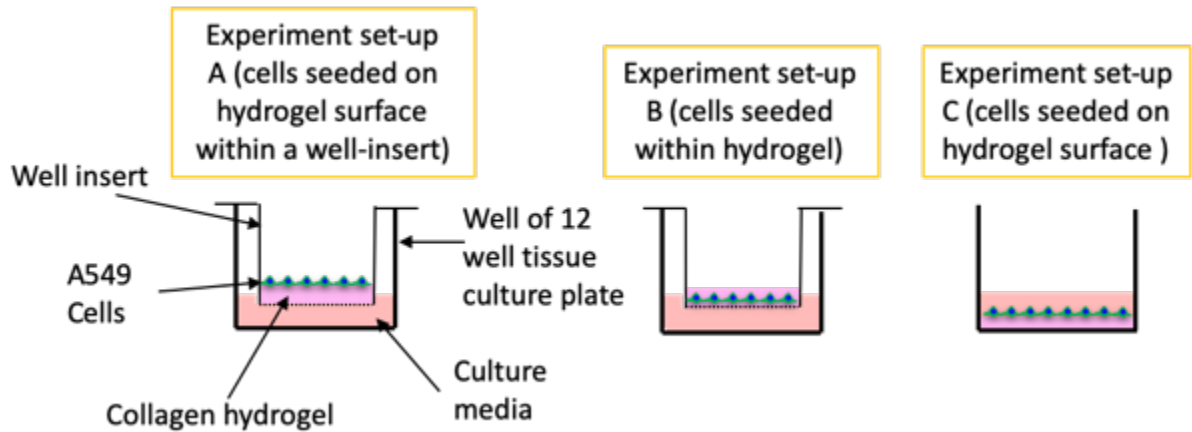
Figure 3.3 Experimental set-up to examine the effect of hydrostatic stimulation on A549 cells culture on or within collagen hydrogels. A549 were seeded on collagen hydrogel in a well insert (A) or in a well plate (C), A549 cells were seeded within a collagen hydrogel and set in a well insert (B).

3.4.5 Examining the effect elastin has on human lung fibroblasts cell viability and contraction

To assess the effect elastin had on cell viability and contraction lung fibroblast seeded collagen-elastin hydrogels were cultured. Collagen-elastin hydrogels were made as described previously (section 2.9). The hydrogels consisted of varying concentrations of elastin whilst the collagen concentration remained the same at 3.5mg/ml. The concentration ratio consisted of 1:1 (collagen:elastin), 2:1 and 1:0 (Table 3.1).

Table 3.1 Concentrations of collagen and elastin in hydrogels

	Collagen concentration	Elastin concentration
1:1	3.5mg/ml	3.5mg/ml
2:1	3.5mg/ml	1.75mg/ml
1:0	3.5mg/ml	0mg/ml

Before gelation 1×10^5 cells/gel lung fibroblasts IMR90 or 35FL were resuspended into the hydrogel solution and 500µl of the solution was set in a well of a 12 well plate. 1.5mg/ml collagen only hydrogels seeded with 1×10^5 cells/gel were also made as an internal control. On day 1 and 20 hydrogels were digested with Proteinase K solution (section 2.12) and DNA quantified (section 2.13). Every 5 days hydrogel depth and diameter were measured (section 2.10) and phase contrast images were taken. The LiveDead imaging using confocal microscopy was achieved on day 20 (section 2.7).

3.4.6 Assessing lung fibroblasts seeding density for collagen-elastin hydrogels

Collagen-elastin hydrogels were made as described previously (section 2.9). Collagen hydrogels consisting of 3.5mg/ml collagen with varying concentrations of elastin (1:1, 2:1 and 1:0) were seeded with lung fibroblasts 35FL at a seeding density of 1×10^5, 7.5×10^4, 5×10^4, 1×10^4 cells/gel were set in a 12 well plate and cultured for 20 days. Hydrogel depth and diameter were measured every 5 days (section 2.9). Hydrogels were digested using proteinase K and DNA was quantified (2.12 and 2.13) on day 20. Phase contrast microscope images were taken on day 7 and day 20.

3.4.7 Exposing cells in monolayer to hyperoxia

Cells were exposed to hyperoxia to assess the effect of cell viability. IMR90, 35FL and A549 cells were expanded and trypsinised ready for seeding as described previously (section 2.2). All cells were seeded in a 24 well plate at a density of 4×10^4 cells/well. Cells were cultured at 21% oxygen or 80% oxygen, achieved using an O_2 controlled incubator (PHCBI IncuSafe MCO-5M) for 7 days at 37°C. Phase contrast microscopy images were taken on day 1 and day 10. Alamar blue assay was performed on day 2, 5 and 10 as described (section 2.15). On day 10 cells were trypsinised and counted (section 2.2.1).

3.4.8 Statistical analysis

Hydrogel measurements and DNA quantification were all statistically compared using two-way ANOVA with Tukey's multiple comparisons test to determine the statistical significance, $p \leq 0.05$ was considered significant. Analysis was performed using GraphPad Prism version 7.01. All values quoted in the results are mean ± standard deviation.

3.5 Results

3.5.1 Assessment of human lung fibroblast seeding density into collagen hydrogels

Human lung fibroblasts 35FL and IMR90 were seeded within collagen hydrogels of concentration 1.5mg/ml and 3.5mg/ml at a seeding density of 1×10^5 and 2.5×10^5 cells/gel. The hydrogels were cultured for 20 days at 21% oxygen, 37°C. As the hydrogels began to contract the diameter was measured every 5 days. Hydrogel depth was measured on day 1 and day 20 and DNA was quantified. All hydrogels contracted over the 20-day period as shown in Figure 3.5. Hydrogels of a lower collagen concentration and a higher cell seeding density contracted the most. There was no contraction in the hydrogel diameter of 3.5mg/ml collagen concentration with 1×10^5 cells/gel. There was an increase in DNA quantity in 35FL hydrogels but a decrease in DNA quantity for IMR90 hydrogels. Cell viability was assessed using the LiveDead cell viability kit after 25 days of culture. Cell viability is suggested to be good since the cells show green-fluorescence for all samples and displayed a fibroblastic morphology consisting of elongated spindly-shape which is illustrated in Figure 3.4.
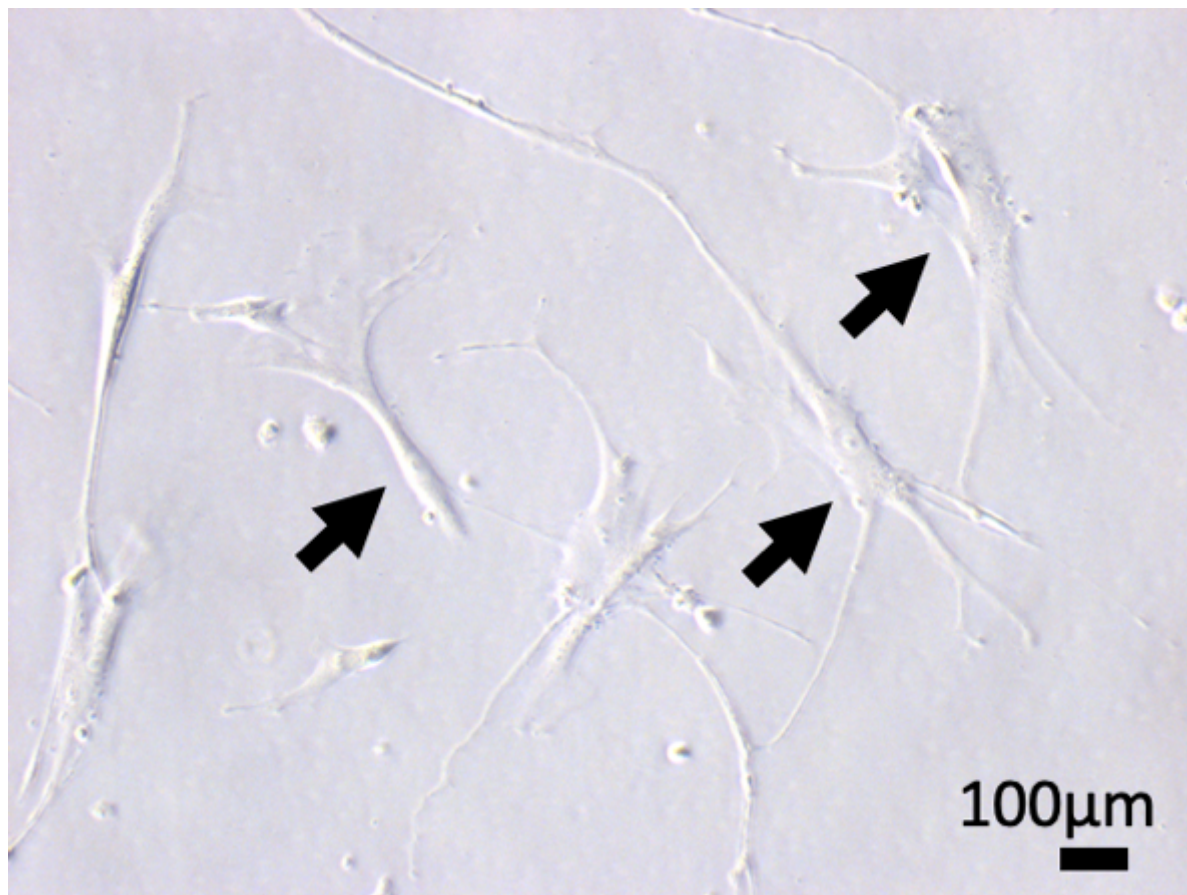
Figure 3.4 Lung fibroblast morphology. Phase contrast microscope image of lung fibroblasts in culture (indicated by arrows). The typical fibroblast morphology consists of a large, flat, elongated spindle-shape. Processes extend outwards from the cell body.
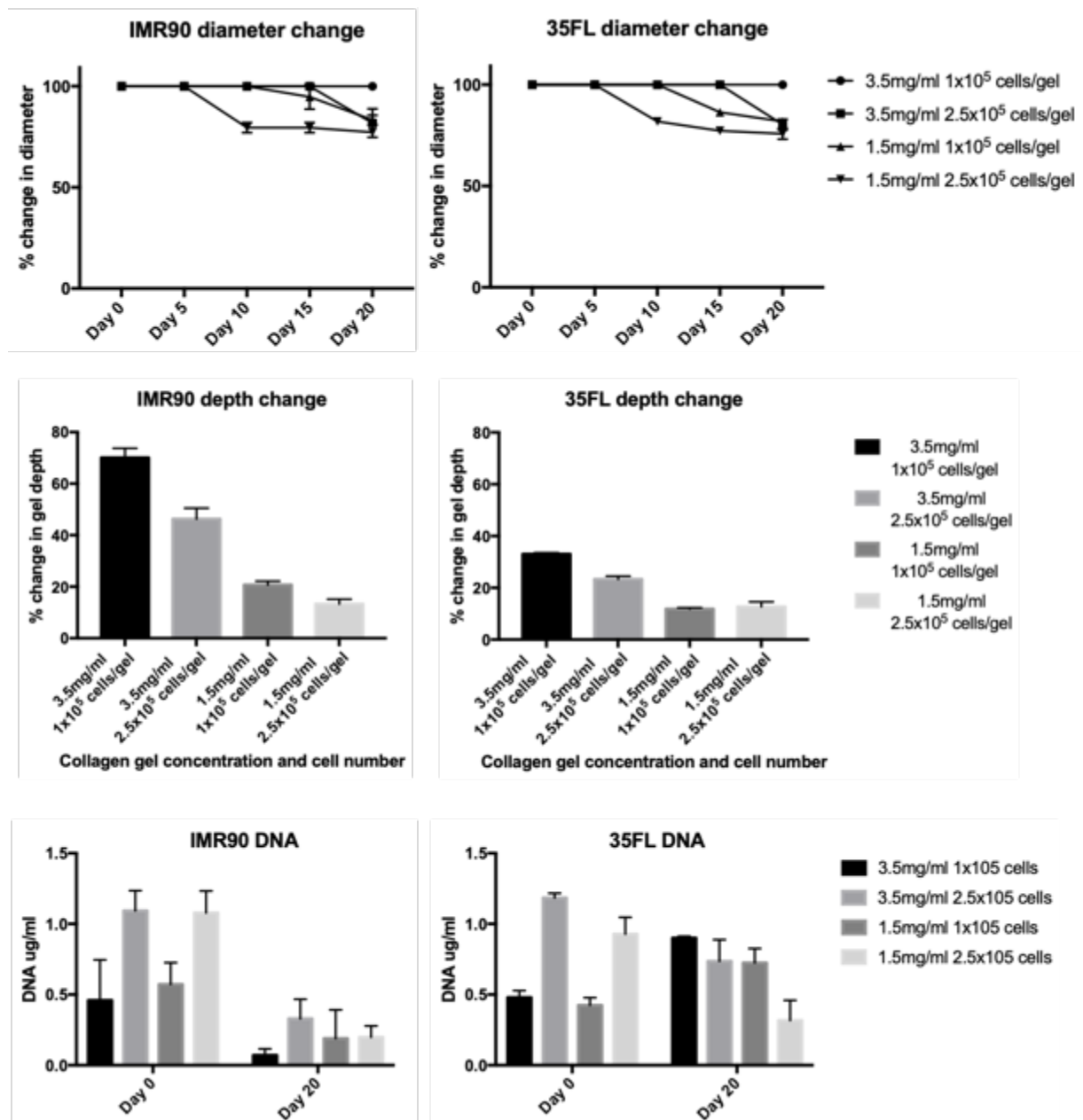
Figure 3.5 Collagen hydrogels seeded with human lung fibroblasts. Collagen hydrogels 3.5mg/ml were seeded with 35FL or IMR90 cells. Hydrogel contraction was monitored by measuring hydrogel diameter and depth over a 20 day period. Hydrogels with a higher cell number and a lower collagen concentration contracted more rapidly. DNA was quantified on day 0 and day 20. IMR90 hydrogels reduced in DNA by day 20. All 35FL hydrogels had a similar DNA quantity by day 20. Data is expressed as mean ± standard deviation, n=9.
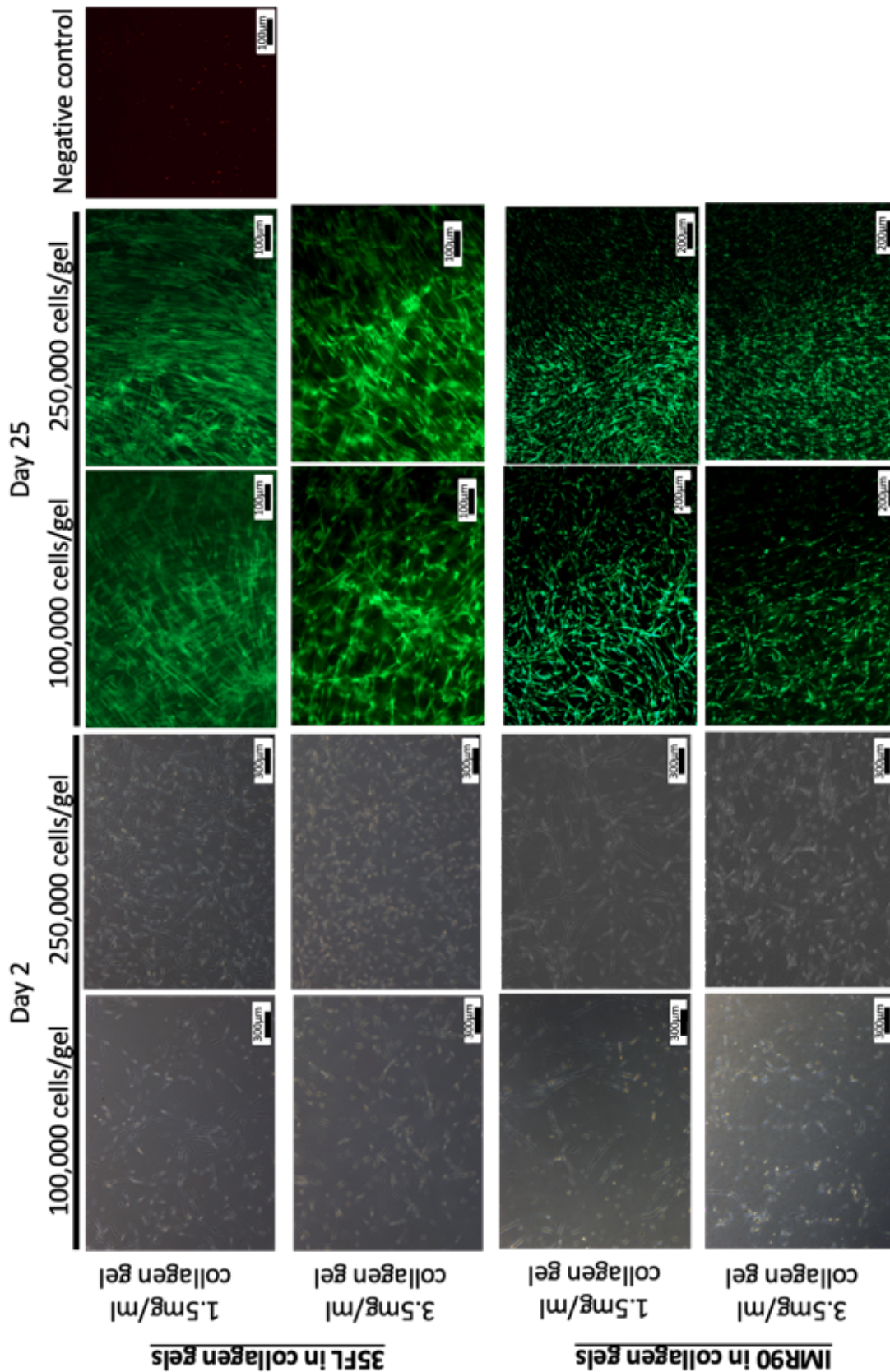
Figure 3.6 Microscopic images of collagen hydrogels seeded with human lung fibroblasts. Cell viability was checked using the LiveDead cell viability kit after culture for 25 days. Cells with compromised membranes exhibit red-fluorescence from the nucleic acid stain ethidium homodimer. Cells with intact cell membranes exhibit green-fluorescence by calcein.

3.5.2 A549 cells form monolayer of collagen hydrogel surface

A549 of varying seeding densities were seeded on 3.5mg/ml collagen hydrogels. Cell morphology, confluence and viability was assessed by imaging the samples on day 3 and day 6. Cells seeded at 2.5×10^5 cells/gel were observed to form a confluent monolayer by day 6 (Figure 3.7). Cell viability was good as shown by the LiveDead cell viability stain (Figure 3.7). Cell migration was checked by imaging the whole hydrogel, but cells could only be observed on the hydrogel surface. For future investigatory purposes we examined the possibility of removing the A549 cells from the hydrogel surface. The use of trypsin in high concentrations was unsuccessful. This is thought to be due to FBS from the growth media remaining in the hydrogels preventing the action of trypsin. The cell scraper proved ineffective because the hydrogels were too delicate for manual handling. Tryp-LE was the most successful cell removal technique. Cells were observed to become rounded after a long incubation time however some cells remained attached to the collagen hydrogel surface and couldn't be aspirated.
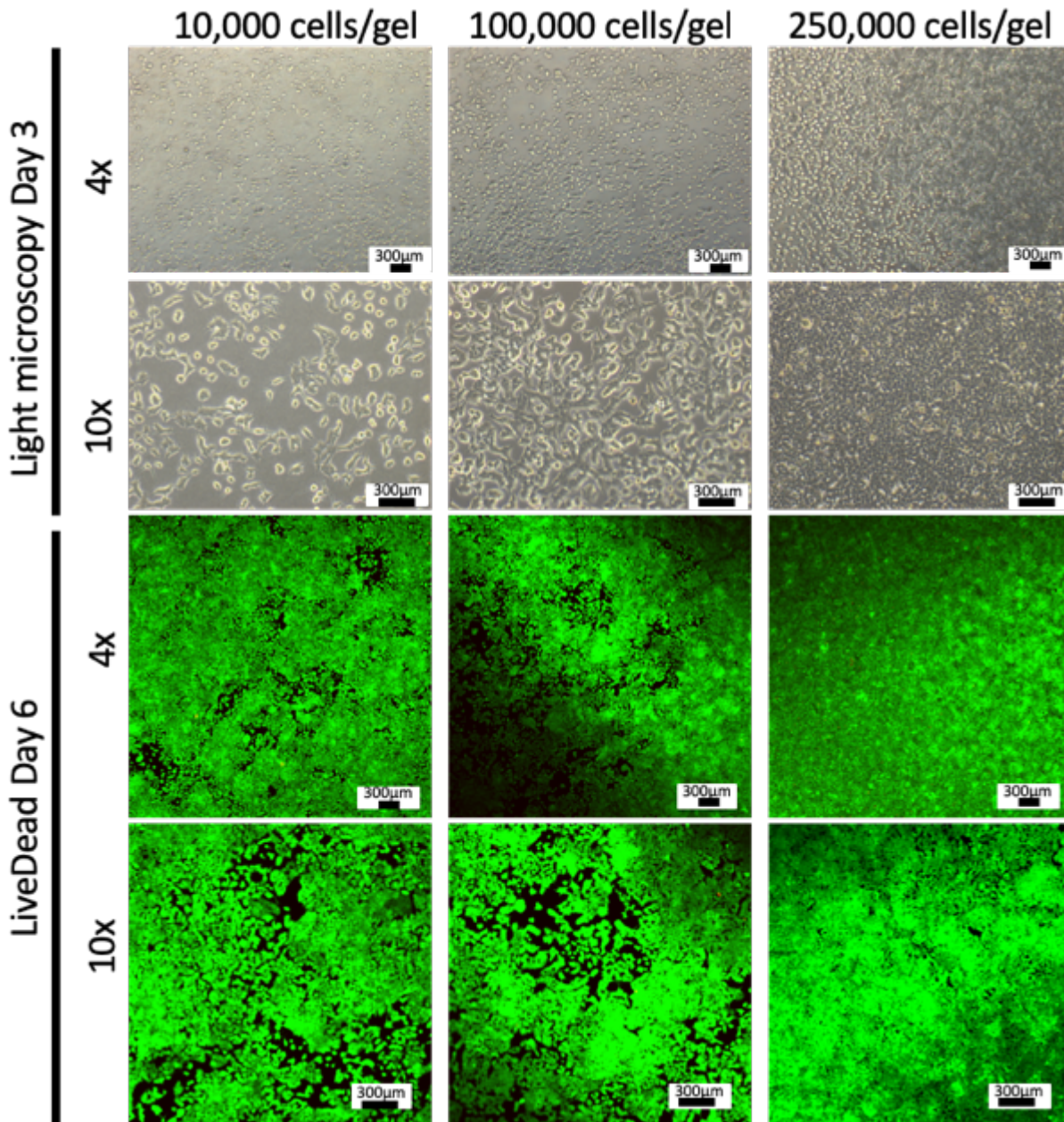
Figure 3.7 A549 cells cultured on collagen hydrogels. Cells were imaged using phase contrast light microscopy and confocal flourecence imaging after staining with LiveDead staining kit. Cells formed a monolayer on the hydrogel surface. Cells are more tightly compact when seeding density of 250,000 cells/gel

3.5.3 Elastin in collagen hydrogels does not affect cell viability

Collagen-elastin hydrogels of varying concentrations of elastin (collagen:elastin 1:1, 2:1, 1:0) were seeded with 250,000 cells/gel human lung fibroblasts 35FL or IMR90. Hydrogel contraction was monitored, and DNA quantified (Figure 3.8). For 35FL seeded hydrogels

the addition of elastin had a significant effect on hydrogel contraction. Hydrogels containing elastin contracted in diameter and hydrogel depth initially decreased but increased again by day 20. 35FL DNA increased by day 20 and was not statistically affected by the addition of elastin. The IMR90 hydrogels did not contract in hydrogel diameter but did contract in hydrogel depth. The 1.5mg/ml collagen hydrogel seeded with $1x10^5$ cells/gel acted as an internal control and had the expected results in terms of hydrogel contraction and DNA quantity. Phase contrast images were taken every 5 days and confocal images on day 20 (Figure 3.9 and Figure 3.10). Initially IMR90 cell morphology was more rounded and did not become elongated until day 20. The 35FL cells become elongated by day 5 and continued to have this morphology until day 20. Cell number visually increases over the 20 days and hydrogels were very confluent by day 20. The presence of green fluorescence indicates cell viability was good and unaffected by the addition of elastin for both cell types.
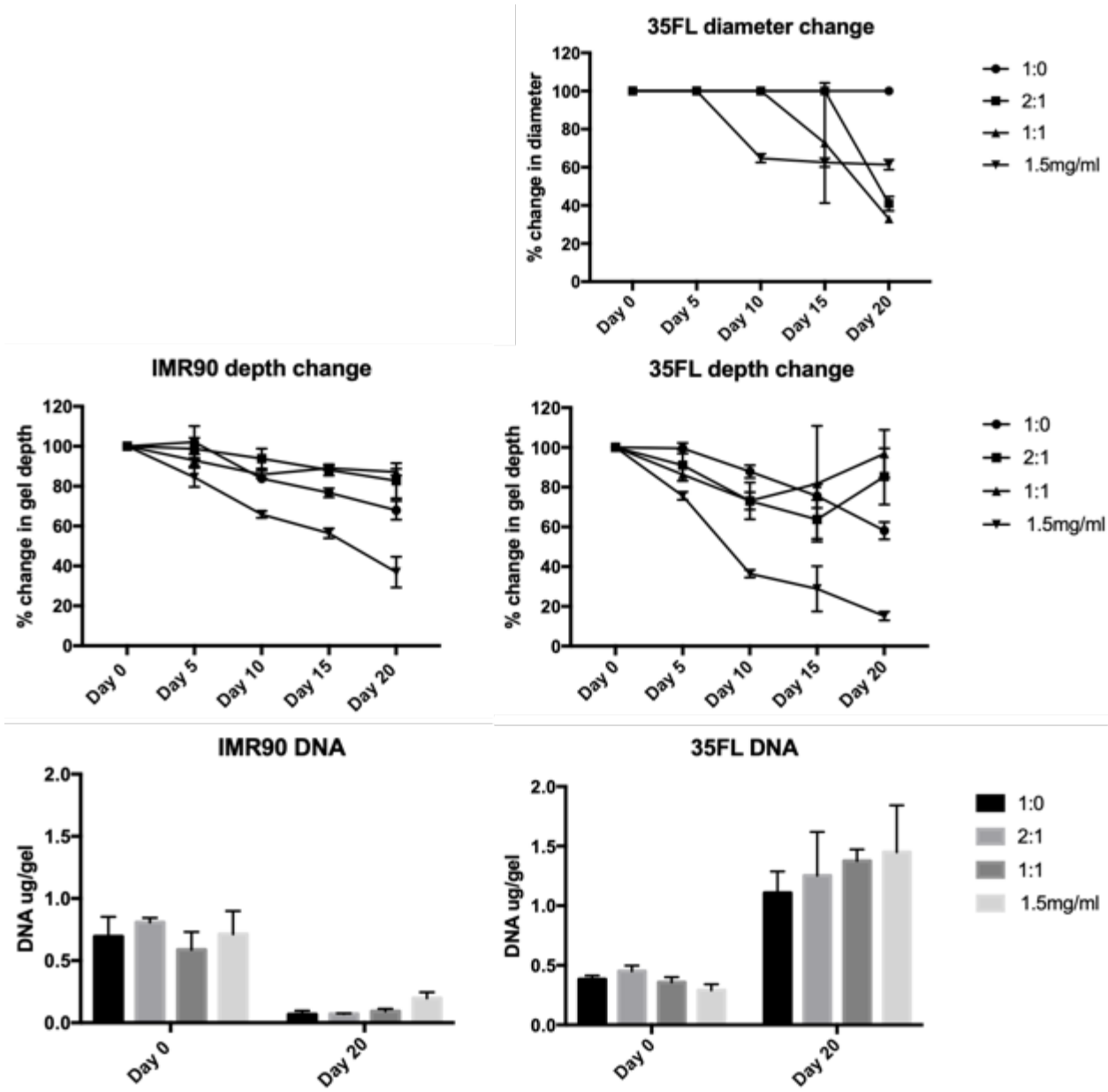
Figure 3.8 Human lung fibroblasts (IMR90 and 35FL) collagen-elastin hydrogels.
Hydrogel contraction was measured and DNA quantified over 20 days in culture. IMR90
hydrogels did not contract so have been omitted from the figure. The addition of elastin
caused hydrogels to contract more rapidly. DNA increased for 35FL hydrogels indicating
elastin had no effect on cell proliferation. DNA decreased for IMR90 hydrogels indicating
there was cell death. Data is expressed as mean ± standard deviation, N=6.
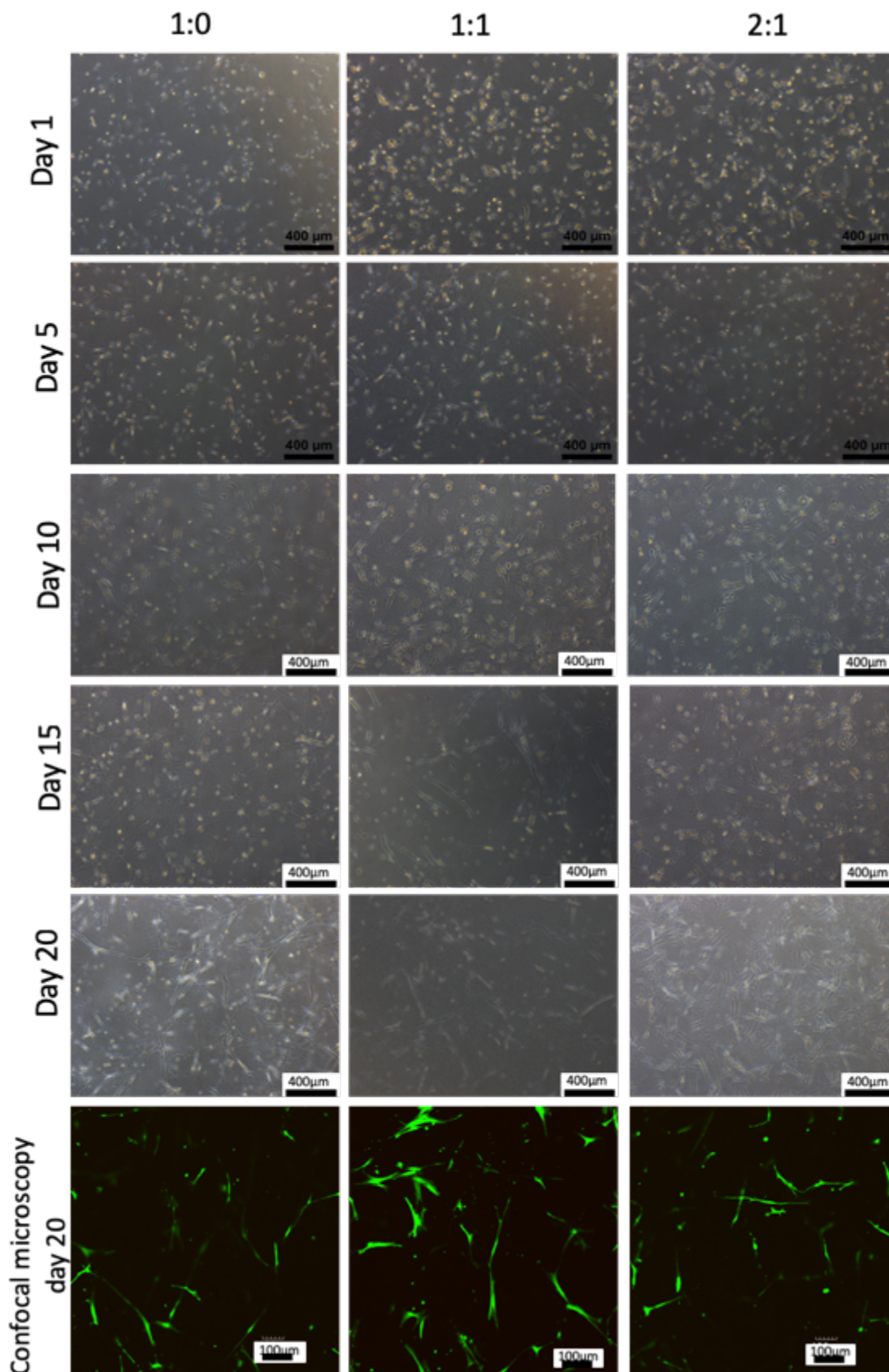
Figure 3.9 Human lung fibroblast IMR90 collagen-elastin hydrogels. Hydrogels were imaged every 5 days in culture with phase contrast microscopy. On day 20 cell were stained with the LiveDead kit and imaged using confocal microscopy. Cell viability and cell morphology was not observed to be affected by the addition of elastin.
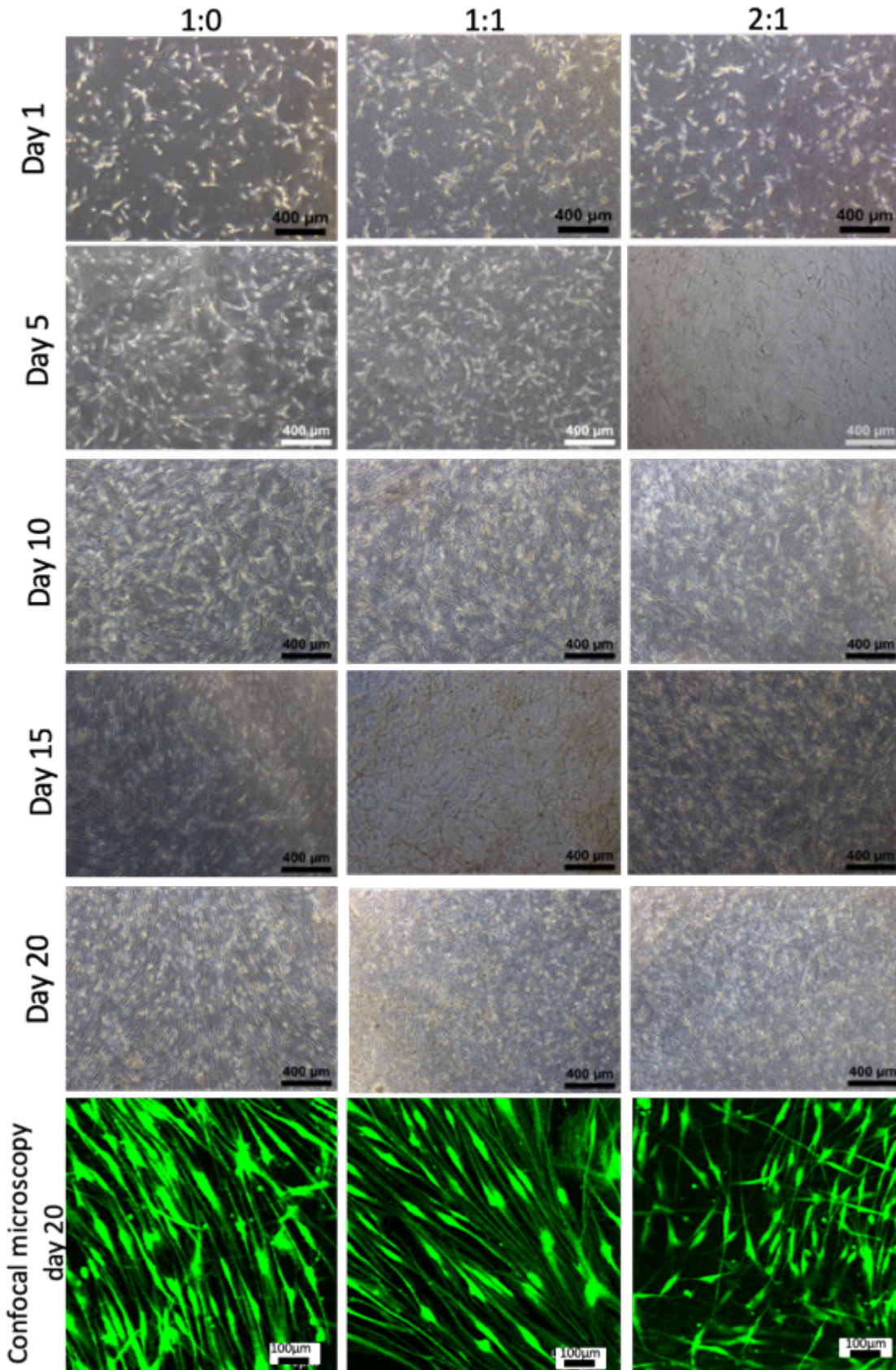
Figure 3.10 Human lung fibroblasts 35FL cultured in collagen-elastin hydrogels.
Hydrogels were imaged every 5 days in culture with phase contrast microscopy. On day
20 cell were stained with the LiveDead kit and imaged using confocal microscopy. Cell
viability and cell morphology was not observed to be affected by the addition of elastin

3.5.4 Monitoring DNA quantity of IMR90 seeded collagen hydrogels

To examine the change in DNA quantification of IMR90 collagen hydrogels, collagen hydrogels of 3.5mg/ml collagen concentration were seeded with 1×10^5cells/gel and set in the wells of a 12 well plate. Hydrogel depth and DNA were measured, and phase contrast images were taken (Figure 3.11). Hydrogel depth decreased at a similar rate as in previous experiments. Phase contrast images show cell morphology was elongated and fibroblasts-like throughout the 20 days of culture and cell number increases. DNA quantification significantly increases by day 10 but significantly decreases by day 20.
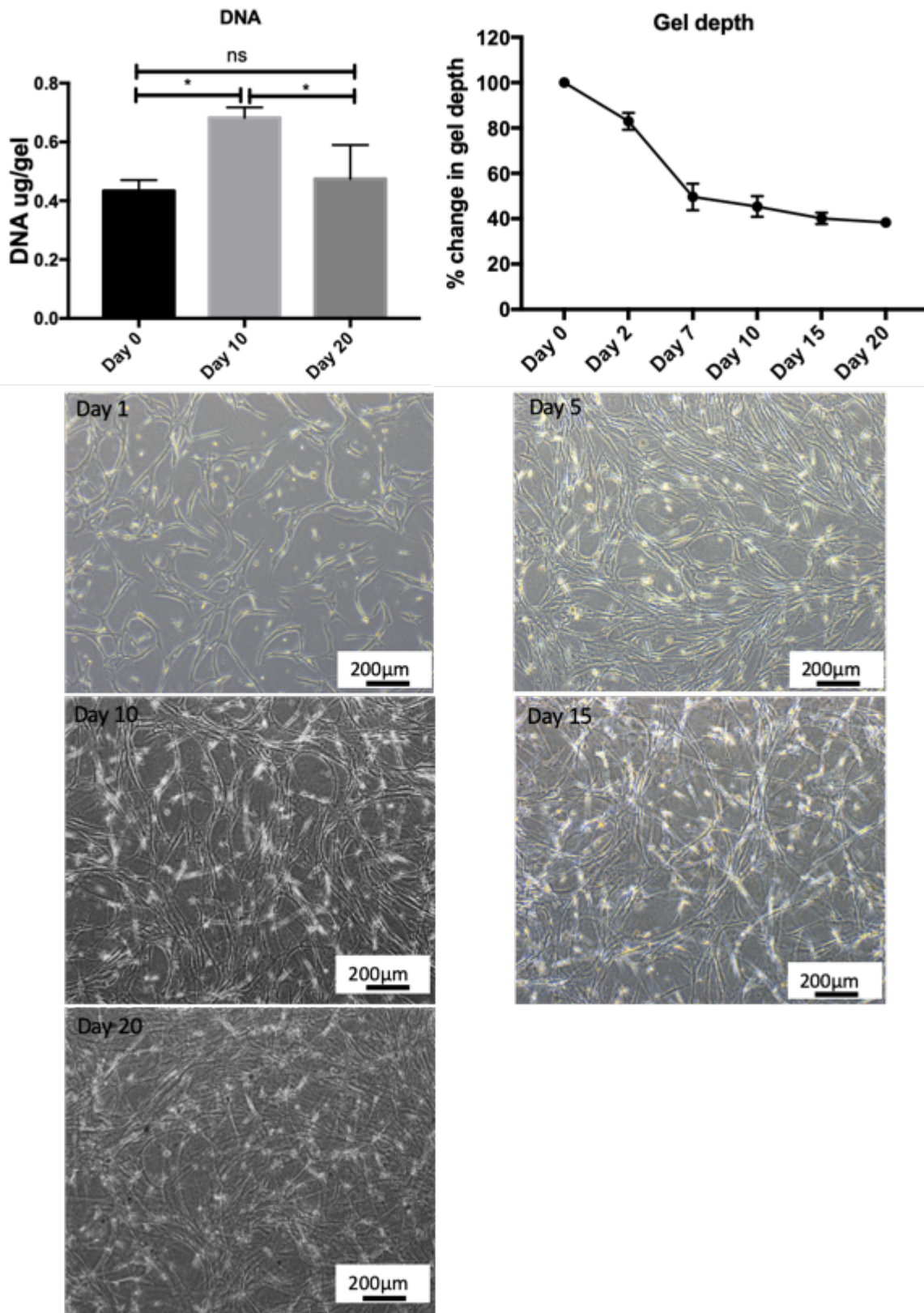
Figure 3.11 Collagen hydrogels seeded with human lung neonatal fibrobalsts IMR90. Hydrogel contraction was monitored over 20 days in culture. DNA was quantified every 10 days and phase contrast images were taken every 5 days. DNA increased by day 10 but decreased by day 20 and which point contraction levels out. Images show cells with a fibroblastic morphology. Data are expressed as mean ± standard deviation, n=3 (*p≤0.05).

3.5.5 Decreasing cell-seeding density for 35FL collagen-hydrogels prevents contraction of hydrogel diameter

Human lung fibroblasts 35FL were cultured at varying seeding densities (100,000, 75,000, 50,000, 10,000 and 1,000 cells/gel) in collagen-elastin hydrogels and cultured for 20 days. Hydrogel contraction was monitored, and DNA quantified. Hydrogels did not contract in diameter when the seeding density was reduced to 7.5×10^5 cells/gel or below (Figure 3.12). Elastin had no significant effect on DNA quantification.
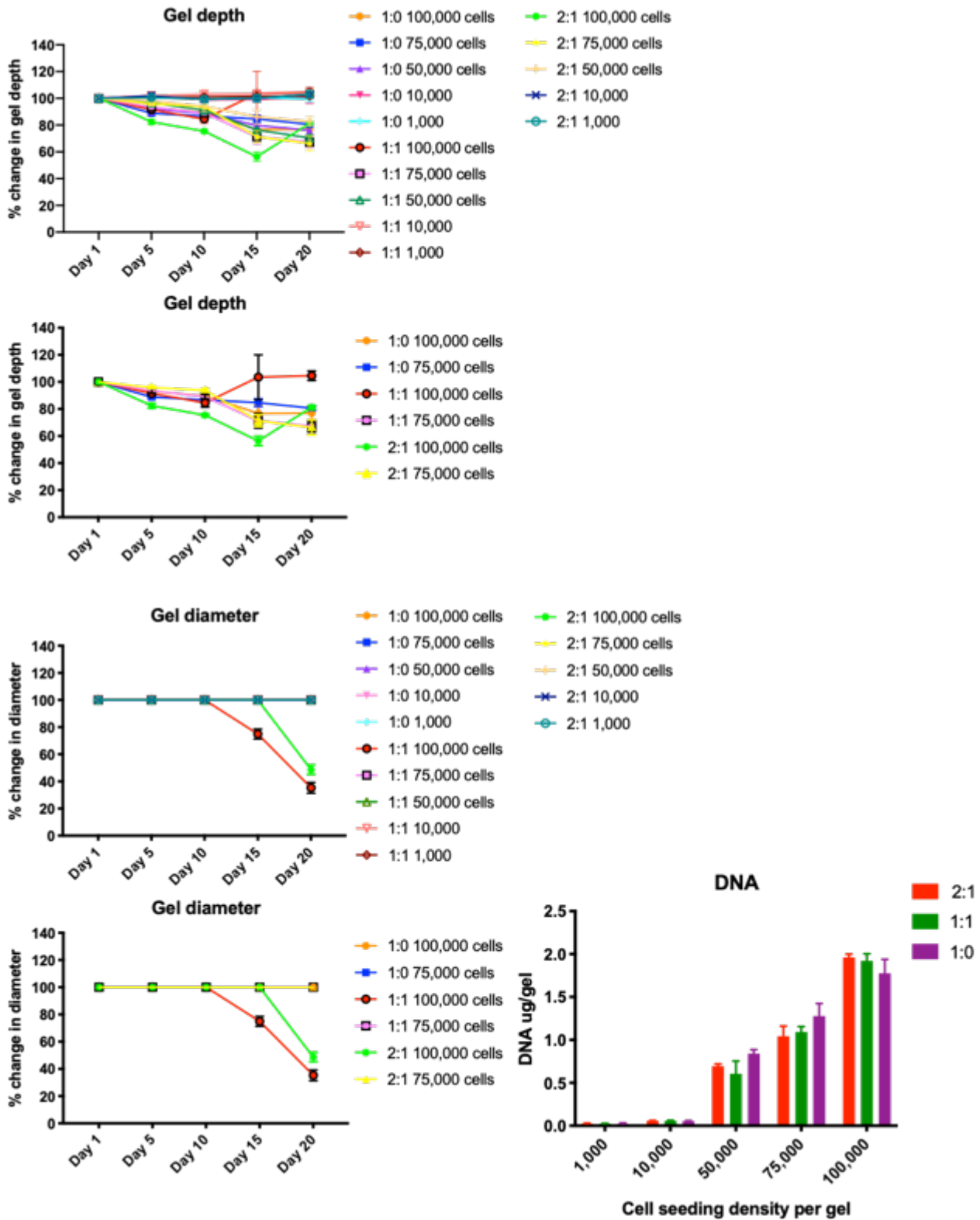
Figure 3.12 The effect of cell seeding density on the contraction of collagen-elastin hydrogels. Collagen-elatsin hydrogels (collagen:elastin rato 1:1, 2:1, 1:0) were seeded with human adult lung fibroblasts 35FL. Contraction was monitored for 20 days in culture and DNA quantified. Graphs will only the high seeding densty have been included for clarity. Collagen-elastin hydrogels with a seeding density of 75,000 cells/gel did not contract in diameter but still displayed contraction in gel depth. Data are expressed as mean ± standard deviation, N=6

3.5.6 Hydrostatic stimulation does not compress collagen hydrogels and does not affect cell viability

Human lung epithelial cells A549 were cultured on the surface of collagen hydrogels (in well inserts or directly in a well of a 12-well plate) or within collagen hydrogels. Samples were subjected to hydrostatic pressure at a frequency of 1Hz, with a pressure level of 1.5KPa in a sinusoidal wave for 1 hour each day for 10 days. Phase contrast and confocal images were taken of all samples (Figure 3.13). The bioreactor stimulation had no effect on cell morphology or viability when visualised with phase contrast microscopy and LiveDead staining kit. There was no sign of migration of cells seeded as a monolayer of the collagen hydrogel surface. Hydrogel depth was measured using OCT (Figure 3.14). Hydrostatic stimulation had no statistically significant effect on hydrogel depth after stimulation. These results also demonstrate that A549 can be cultured successfully as a monolayer on a hydrogel without growth medium directly on the cells (growth medium only surrounded the well insert).
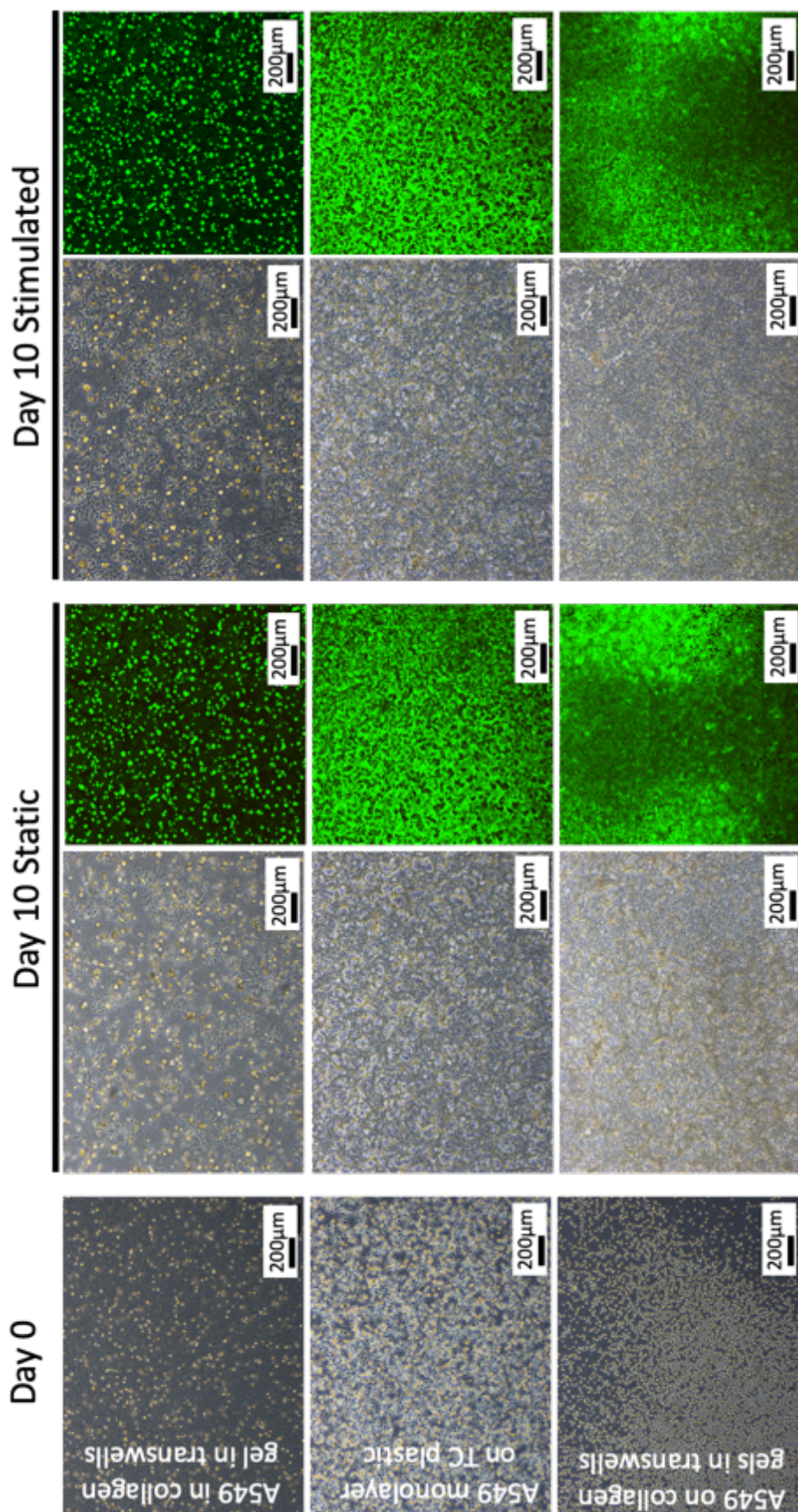
Figure 3.13 Human lung epithelial cells A549 cultured within or on-top of collagen hydrogels and subjected to hydrostatic conditions. The cells were imaged using a phase contrast microscope or confocal microscope using the LiveDead staining kit on day 10. The hydrostatic stimulation had no observed effect on cell viability or morphology.
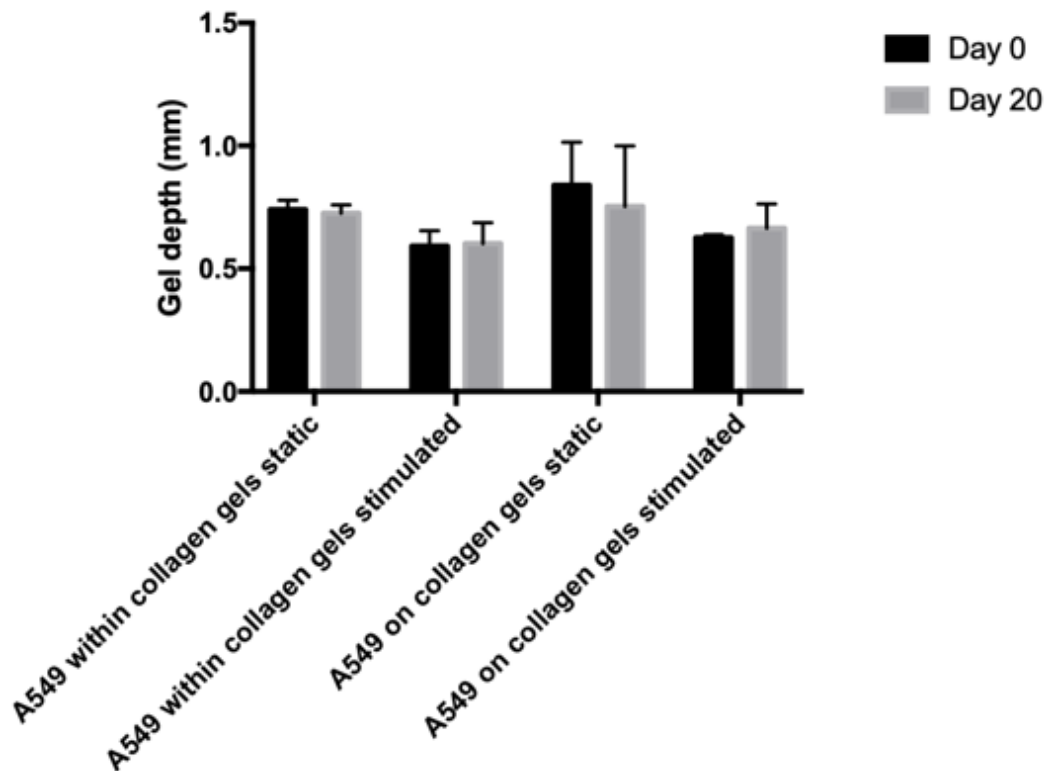
Figure 3.14 Human lung epithelial cells A549 cultured within or on-top of collagen hydrogels and subjected to hydrostatic conditions. The hydrogel depth was measured using OCT and compared on day 0 and day 20 in either static or hydrostatic conditions. The hydrogel depth did not change when subjected to hydrostatic stimulation. Data are expressed as mean ± standard deviation, N=3

3.5.7 Culturing cells at 80% oxygen affects cell proliferation

Cells 35FL, IMR90 and A549 were cultured in a monolayer at 80% oxygen for 10 days after which cell counts and Alamar blue assay were performed to assess the effect hyperoxia has on cell proliferation. Examining the effect hyperoxia has on cells is important when investigating BPD since patients are placed on ventilation of up to 100% oxygen. Figure 3.15 shows phase contrast images of the cells A549, 35FL and IMR90 cultured over a 10-day period at 21% and 80% oxygen. With all three cell types there are fewer cells visualised at day 10 when cultured 80% oxygen. When cell counts are performed on day 10 (Figure 3.16) there are statistically fewer cells at 80% oxygen. Alamar Blue assay was performed on the cells at day 2, 5 and 7. There was a significantly

lower fluorescence value for all cells cultured at 80% oxygen when compared to 21% oxygen. This indicates there was reduced metabolic activity likely due to the presence of fewer cells.
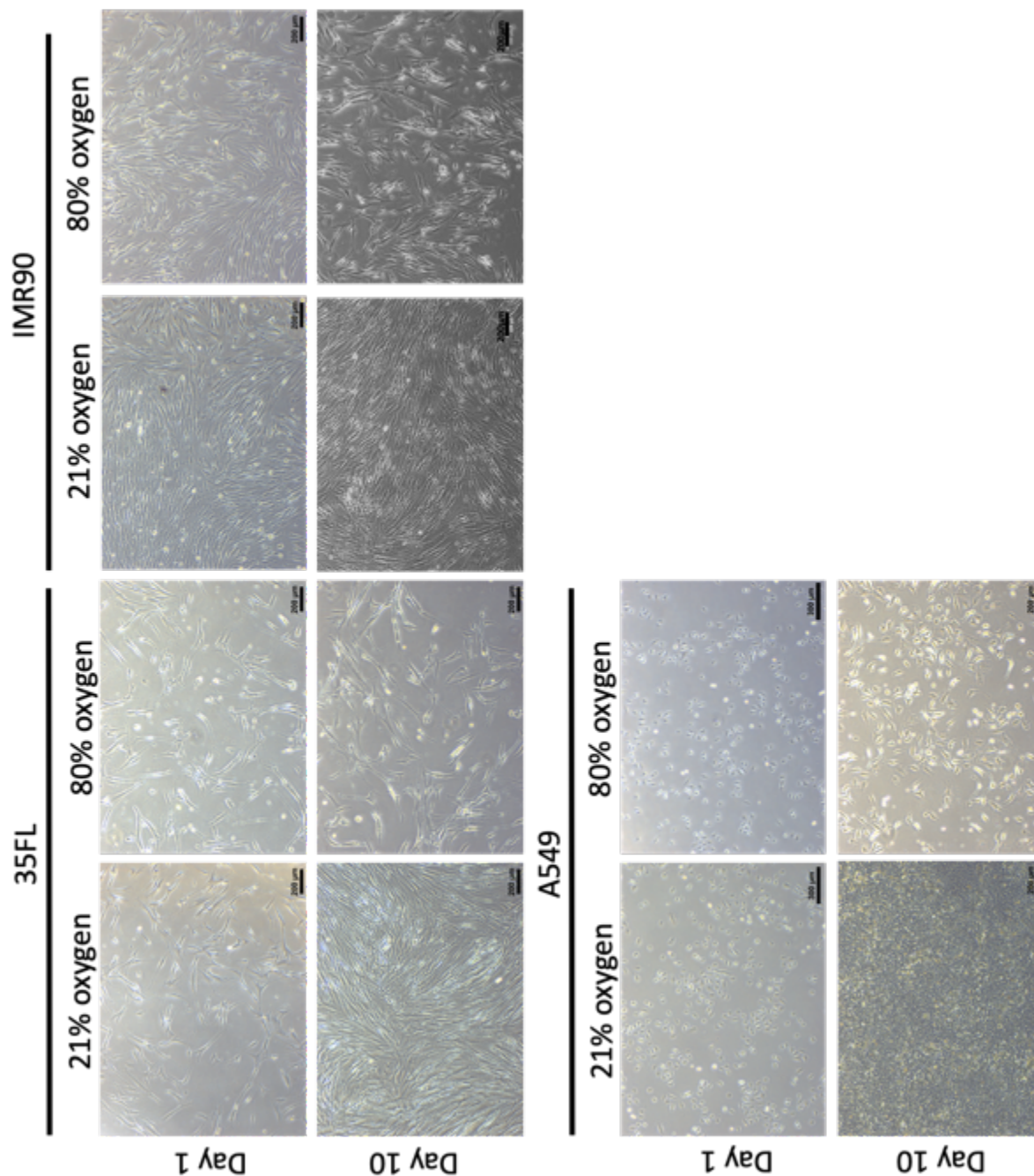
Figure 3.15 Human lung cells IMR90, 35FL and A549 cultured for 10 days at 21% oxygen and 80% oxygen. Phase contrast images were taken at day 1 and day 10 of culture. Fewer cells can be visualised on day 10 at 80% oxygen when compared to 21% oxygen for all cell types.
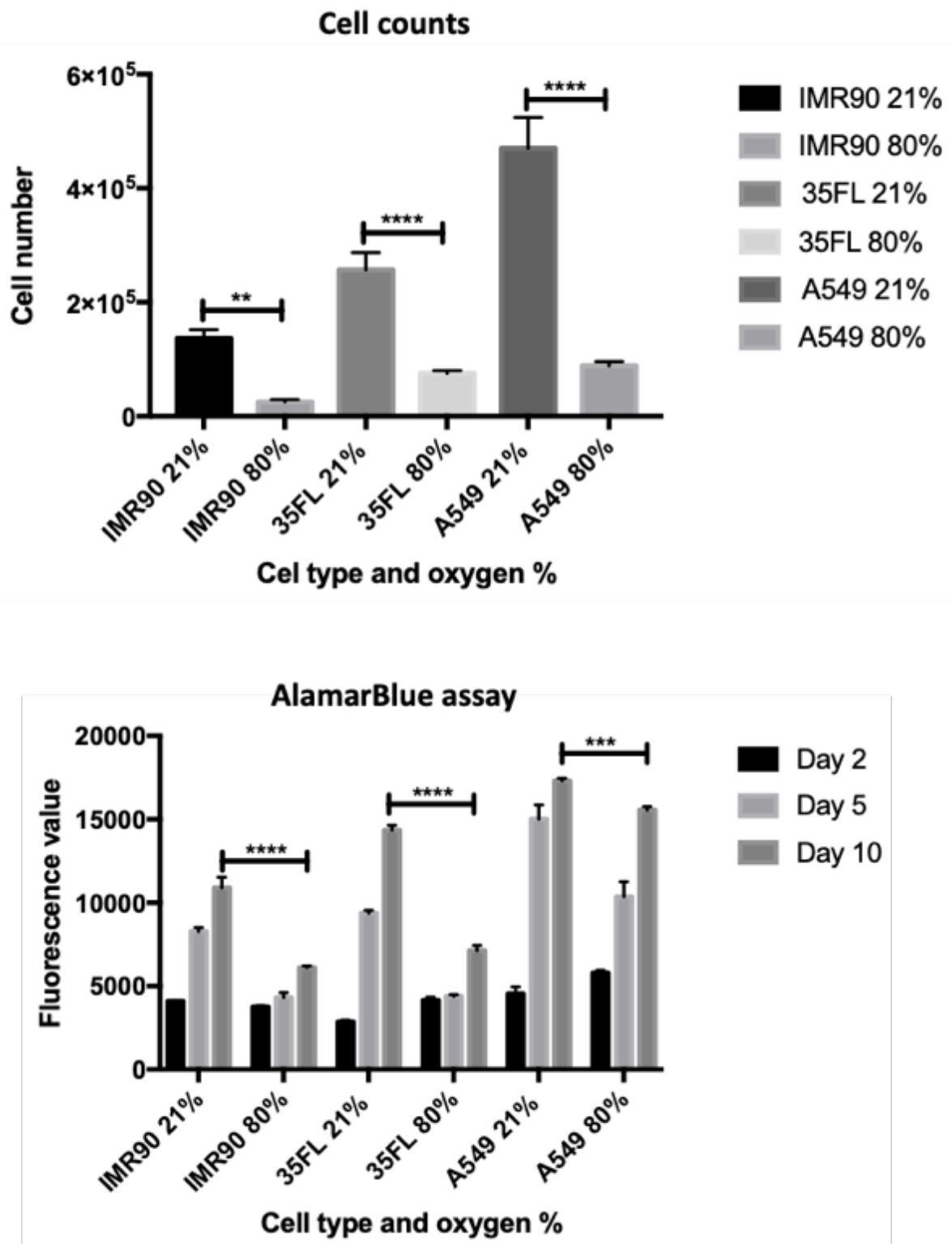
Figure 3.16 Human lung cells IMR90, 35FL and A549 cultured for 10 days at 21% oxygen and 80% oxygen. Cell counts were performed on day 10 and AlamarBlue assay was performed on day 2, 5 and 10 of culture. 80% oxygen significantly reduced cell number and metabolic activity. Data are expressed as mean ± standard deviation, N=3 (**p≤0.005, ***p≤0.001, ****p≤0.0001).

3.6 Discussion

Knowledge of BPD has relied heavily on the use of animal models[60]. Whilst they have contributed to our current knowledge and understanding of the disease pathogenesis, they lack biological relevance and can be expensive. In terms of BPD the most common animal model are rodents which lack biological significance since they do not follow the same developmental pathway as humans[61]. Animal models that are developmentally relevant, such as primates, are associated with high cost, logistical and ethical issues[65]. 3D *in vitro* models have come at the forefront of regenerative medicine due to their biological relevance and accurate representation of tissue architecture. The development of *in vitro* lung models has focused mainly on the conducting airway since it is a more simple structure to mimic[87]. Current lung alveolar models rarely offer the ideal combination of multicellular, 3D, hyperoxygen exposure and mechanical stimulus. In this study we have begun to investigate the possibility of designing such a model. The following describes in detail aspects of the model this chapter has considered.

3.6.1.1 Collagen hydrogel concentration and cell seeding density

Collagen hydrogels are the ideal material for a lung alveolar model and BPD. Collagen is one of the key components in the human lung mesenchyme. It provides structural, mechanical and biological support[90,92] and is thought to be a driving force for alveologenesis during development[66]. Aberrant collagen has consistently been associated with BPD[66,95]. Our initial investigatory work looked at collagen construct fabrication and the encapsulation of human fibroblastic cells.

Collagen hydrogels of concentration 1.5mg/ml and 3.5mg/ml were prepared seeded with human lung cells IMR90 and 35FL. These two cell types were chosen since they derive from a developing human foetus lung and a human adult lung respectively. The cells were encapsulated in the hydrogel solution before gelation. The hydrogel contraction was

measured, DNA quantified, and microscopic images taken to examine the following questions:- do the cells contract; to what extent do the cells contract; is cell viability affected; do the cells proliferate. Measuring the contraction of the hydrogel diameter was important since we did not want the hydrogel contracting along the diameter. This is because when an epithelial monolayer is eventually seeded on the hydrogel surface, contraction could cause the epithelial monolayer to peel off. Hydrogel contraction has previously been used as a measure of fibroblast function and ECM production[179,180]. Hydrogels of a higher collagen concentration and lower cell number contracted less, a recurring observation in the literature[181]. We found that collagen hydrogels of 3.5mg/ml with $1x10^5$ cells/500µl gel did not contract in diameter and were therefore the appropriate sample type to take forward in future experiments.

Cell viability was unaffected by culture conditions as demonstrated by the LiveDead viability staining. 35FL DNA quantity increased for all sample conditions further supporting that culture conditions were favoured by the human lung fibroblasts. However, a decrease in DNA was observed for IM90 samples suggesting cell number was decreasing. This was a consistent observation and lead to DNA quantification on day 10. DNA significantly increased on day 10 but significantly decreased by day 20. It is hypothesised that the hydrogels were not favoured by the IMR90 cells since phase contrast microscopic images show the IMR90 cells to be more rounded and fewer cells could be observed with confocal imaging. Phase contrast imaging is not an ideal technique to image 3D constructs since images can only target one section of the hydrogel and therefore may not represent the hydrogel as a whole. The working distance (distance between the objective's front lens and the closest surface and the specimen to allow the specimen to be in sharp focus) was also a limiting factor when imaging hydrogels which were thick and therefore couldn't be imaged in focus. Confocal imaging provides the

option to produce z-stacks that are capable of imaging the hydrogel as a whole. Confocal imaging also mitigates the issue of autofluorescence from the collagen fibres.

3.6.1.2 A549 cells can be cultured in monolayers on hydrogel surface

After successfully identifying a stable collagen hydrogel and fibroblast seeding density, we investigated the possibility of seeding lung epithelial cell line A549 on the hydrogel surface which has previously been achieved for lung cancer modelling[182]. The A549 cells formed a cell monolayer on the hydrogel surface with good cell attachment and cell viability as shown by the LiveDead staining and confocal imaging. There was no cell migration observed. This is important because we want to maintain a confluent monolayer on the hydrogel surface to accurately represent the alveolus cell wall. Cells seeded at 2.5×10^5 were observed to be confluent by day 6, 1×10^5 were confluent by day 15 and 1×10^4 were confluent by day 35. Since the future aim is to have long-term culture, a culture period of 20 days at a seeding density of 1×10^5 is appropriate.

For end-of-experiment analysis we looked at removing the A549 cells using various techniques; cell scraper and trypsin were unsuccessful with only Tryp-LE capable of removing some cells after long incubation times. Although the removal of some A549 cells meant some analysis could be achieved on A549 cells, the inefficiency of this this technique means the hydrogels remain in a co-culture state so future molecular analysis would be contaminated with epithelial cells and not purely fibroblasts cells. The long incubation period for Tryp-LE may have a detrimental effect on cells so molecular analysis would not be representative of experiment conditions. Research by Tsuji *et al.* examined the effect of Tryp-LE and antigen expression after 30 minutes exposure and found it did not affect surface marker expression[183] however our exposure time reached 60 minutes.

3.6.1.3 The addition of elastin causes a higher rate of hydrogel contraction but doesn't affect cell viability

An important feature found in the lung tissue samples of BPD patients and animal models has been an abnormal elastin network[32,94]. Along with collagen, elastin provides structural and mechanical support for respiration and is thought to influence alveologenesis[49]. Previous work from our lab demonstrated the cell seeded collagen hydrogel has the same Young's modulus of the theoretical Young's modulus of the lung alveolus[97]. We can therefore be confident that the hydrogel provides the appropriate mechanical properties as well as biological relevance. Elastin was included into collagen hydrogels at 2 collagen:elastin ratios: 1:1 and 2:1. Collagen only hydrogels were also included (1:0). The elastin had no effect on cell viability in terms of cell morphology, cell proliferation (assessed by DNA quantification) or cell viability. However, the elastin caused the hydrogel diameter to contract at a faster rate which is not appropriate for epithelial cell culture. We went on to investigate an appropriate cell number to avoid contraction of hydrogel diameter which was achieved with a seeding density of 7.5×10^5 cells/gel. We seeded varying A549 cell seeding densities onto collagen-elastin hydrogels to establish an appropriate seeding density of 7.5×10^4 cells/gel.

3.6.1.4 Hydrogels can be exposed to hydrostatic bioreactor stimulation and hyperoxia

BPD patients can fall into 2 categories: ventilator dependant or those that require non-invasive support. Which group they fall into depends on gestational age or weight; those under 27 weeks GA or under 1Kg falling into the ventilator dependant group and older/bigger babies needing less support. It is thought that it is a combination of high oxygen and mechanical strain which exacerbates the disease[66,116]. In this study we wanted to examine severe BPD so exposed the model to an environment consistent with

the ventilator dependant group. This included culture at >40% oxygen and mechanical stress typical of invasive ventilation. Although predominately used for bone research, the hydrostatic bioreactor[129] possess attributes which may bode well for lung research. It can provide cyclic hydrostatic pressure that mimics the mechanical ventilators used to aid neonatal respiration in the clinical environment. The hydrostatic bioreactor can provide simulation of 1.5kPA, the expected mean airway pressure ventilated babies would experience. Preliminary experiments confirmed that incorporating hydrostatic stimulation could be achieved and this did not have a detrimental effect of epithelial cell viability, collagen compression or cell migration. This study also demonstrated that A549 cells were capable of maintaining a cell monolayer on the surface of a hydrogel without growth media directly on top of the cells. All the necessary nutrients for cell growth sufficiently diffused through the hydrogel. This allows the model to be maintained at an air interface therefore mimicking *in vivo* oxygen exposure*.* Hyperoxia of 80% oxygen was achieved using an incubator IncuSafe MCO-5M capable of achieving high oxygen culture. 80% oxygen had a detrimental effect on all lung cells exposed (A549, 35FL and IMR90) which is representative of previous published work in which very high oxygen levels cause growth arrest[184,185].

3.7 Conclusion

We have established an *in vitro* 3D co-culture alveolar model that can be used to represent the complex lung alveolus. The model is biologically relevant to human disease and capable of being exposed to numerous environmental factors to make it applicable to a variety of lung diseases or used as a drug testing tool. Out-put measures can be easily achieved by assessing hydrogel contraction using measuring techniques, molecular analysis and imaging with phase contrast microscopy and confocal fluorescent imaging.

We were unable to establish an efficient method to separate the two cell populations.

Future work would examine the potential use of FACS to isolate the cell populations.

Chapter 4

The extraction and characterisation of placenta mesenchymal stem cells and neonatal lung cells

4.1 Introduction

This chapter looks at extracting and characterising primary cells. Firstly, primary lung cells were isolated and expanded for future culture in the *in vitro* model previously designed in Chapter 3. The addition of these cells adds novelty and biological relevance for further experimental investigations into BPD. Secondly, we sourced, cultured and characterised placenta derived MSCs to assess their potential as a cell therapy for BPD.

4.1.1 Human neonatal lung cells

The previously proposed *in vitro* model has been designed to represent the human lung alveolus by providing a collagen-elastin substrate which can support lung cell co-culture. Cells from numerous tissue sources could be incorporated into the model to provide biological or disease relevance. In the case of a BPD model we sought to incorporate lung fibroblastic and epithelial cells that represent the immature lung of a premature ventilated neonate. This would provide a more accurate representation of cellular behaviour and interaction when examining the effects of hyperoxygen or mechanical stress which BPD patients are exposed to. In this chapter we firstly examine the ability to extract and culture lung fibroblast cells and epithelial cells from tracheal suctionings of ventilated babies from the NICU. We looked at two approaches to isolate the appropriate cells: Endotracheal suctionings and nasal scrapings.

4.1.1.1 Tracheal suctionings

Tracheal suctionings are routine practice for endotracheal intubated patients to maintain airway patency[186]. They are performed following clinical observations indicating excess mucus or fluid obstructing ventilation. Occasionally the sample may be required for microbiological assessment but typically the sample is immediately disposed of making it an ideal source for research purposes. The procedure involves introducing a suctioning catheter into the patients trachea and applying negative pressure[187]. Assessment of

cytokines and fibrinolysis in tracheal suctions has been previously achieved[188,189]. Ahn and Hwang reported on the cytological component of tracheal suctionings demonstrating the potential of tracheal suctionings as a research tool[190].

4.1.1.2 Nasal scrapings

The collection of nasal scrapings or brushings is an established method for isolating respiratory cells[191–197], studying ciliary ultrastructure and evaluating inflammation[198,199]. The technique benefits from being easy to collect, minimally invasive, possessing few ethical concerns and is associated with a low site morbidity. However, the procedure is not routine practice and can be accompanied with some discomfit for the patient. The disease relevance of nasal cells for BPD is questionable since BPD is a disease of the respiratory zone not the conducting airway (upper respiratory tract). However nasal epithelial cells have been shown to be a potential surrogate for bronchial epithelial cells for paediatric asthma studies in that they have a similar response to IL-13 (interleukin-13)[200]. Since BPD is also a paediatric disease nasal epithelial cells may be a suitable candidate for BPD investigation.

4.1.2 MSCs for BPD

In the last decade MSCs have become one the most widely researched cell type in regenerative medicine. First described by Friedenstein *et al.*[201] MSCs possess certain attributes which make them an ideal candidate for cell therapies including immunomodulatory properties, differentiation capacity and proliferative capacity[165,202]. Bone marrow was the first established source of MSCs and has since become the most widely investigated stem cell which is now easily attainable commercially[203]. More recently alternative sources of MSCs have been investigated which are arguably better in terms of acquisition, cell proliferation and immunoregulation. In this instance we are particularly interested in the human term placenta. The placenta is a recognised source

of MSCs which can be extracted from both the chorion membrane (maternal side) and the amnion membrane (foetus side). The placenta is a waste material normally disposed of after birth which makes it an attractive MSC source since it avoids issues of acquisition, morbidity and ethical dilemmas. Studies suggest that placental MSCs (pMSCs) possess better immunoregulatory properties than other sources [77,161], they also have a high capacity for self-renewal, adhere to plastic, possess stromal markers (CD166, CD105, CD73, CD90), are negative for haematopoietic markers (CD14, CD34 and CD45) and have differentiation potential[167,204,205]. The placenta is an underutilised source of MSCs possibly due to the lack of availability for research facilities. Sourcing placentas in the UK requires the participation of busy NHS medical personnel who often lack the facilities and knowhow to acquire and store placentas for research purposes. Despite this, in recent years placenta derived MSCs have come at the forefront for cell therapies for a variety of diseases because they have the potential to restore normal function. For BPD in particular there is extensive evidence to suggest that MSCs could help alleviate the detrimental effect of oxygen ventilation and promote normal lung development[158,159]. It has now become evident that the lung possess its own endogenous MSCs suggesting they are a key modulator in normal lung maturation and function[206].

4.2 Aims

We aimed to develop a method to isolate and culture human lung fibroblasts and epithelial cells from the tracheal suctioning of ventilated neonates and nasal scrapings. We also investigated the isolation of placenta derived mesenchymal stem cell (chorion and amnion membrane) and the effect hyperoxia has on their characteristics. Results in the previous chapter demonstrated 80% oxygen had a detrimental effect on lung cells. Therefore hyperoxia experiments utilised 40% oxygen which is representative of oxygen levels for endotracheal ventilated severe BPD infants.

4.2.1 Study design
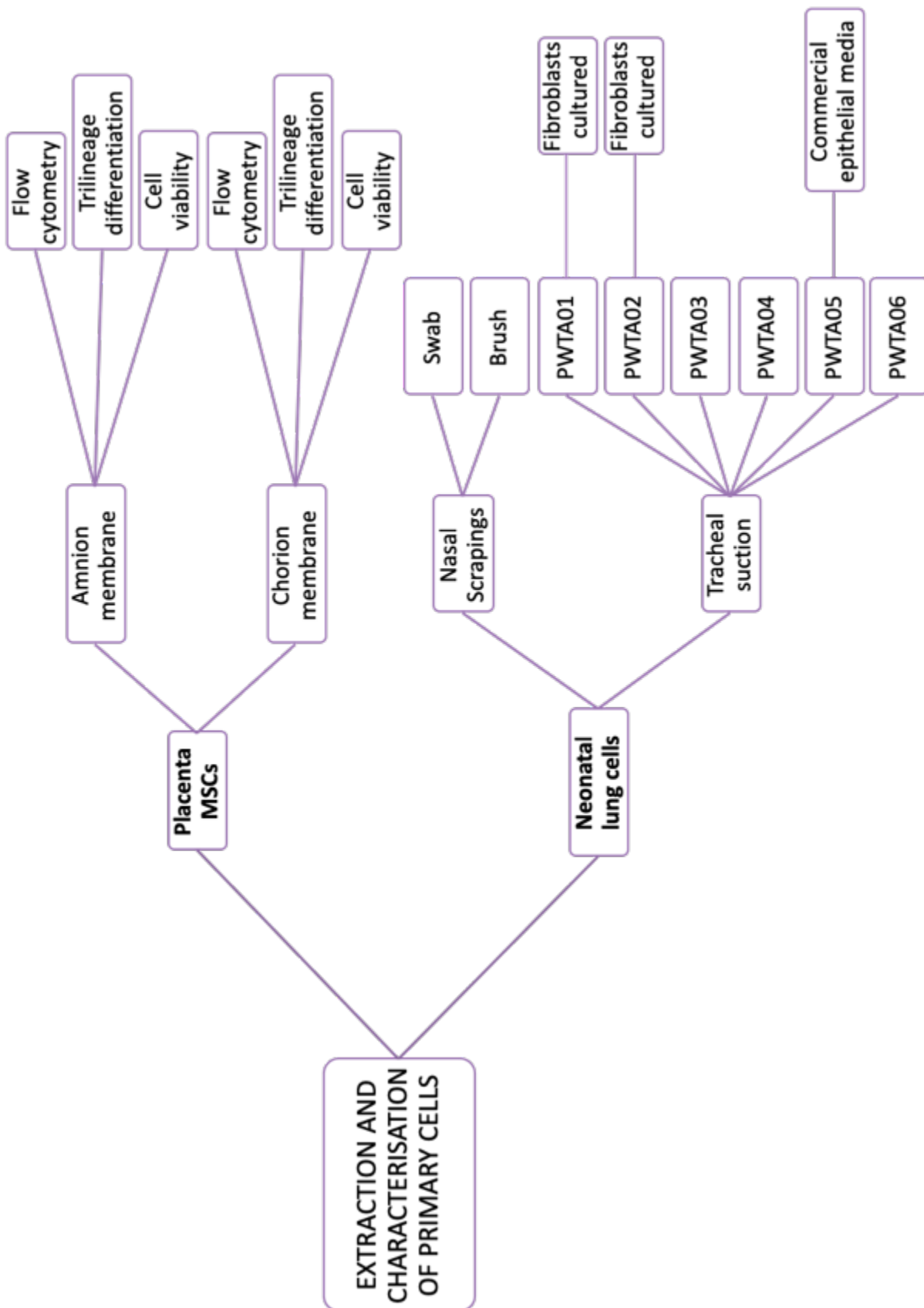
Schematic 4.1 A schematic to show the flow of experimental design for chapter 4.

4.3 Methods

4.3.1 Tracheal suctioning sample processing, cell extraction and cell culture

Patient recruitment and consent was sought in accordance with the study protocol. Tracheal suctionings were collected from neonates on ventilation and processed as described in (section 2.3). When collecting the suctionings, clinical staff may have used saline to loosen thick mucus or to wash endotracheal tubes. Consent was sought for all samples prior to collection and the relevant patient medical details were provided. Cell counts were performed using the trypan blue exclusion assay (section 2.2.3) to provide a live/dead cell count. Cells which were isolated and expanded, hence forth referred to as neonatal lung fibroblasts (NLF), were imaged every 5-7 days with phase contrast microscopy. Once confluency was achieved cells were passaged and cell counts recorded.

4.3.2 Culturing lung tracheal cells in collagen hydrogels

To aid in the characterisation of the NLF cells, cells were cultured in collagen hydrogels to assess contraction and cell viability. NLF cells were resuspended in 1.5mg/ml collagen solution (section 2.9) at a seeding density of $1x10^5$ cells per 500µl collagen hydrogel solution and cultured in 12 well plates. Hydrogels were cultured at 37°C for 30 minutes to allow gelation at which point growth medium was gently added to samples. 35FL seeded hydrogels were prepared under the same conditions. Percentage change in hydrogel depth and diameter were calculated (section 2.10). Hydrogels were stained using the LiveDead cell viability kit and imaged using confocal microscopy (section 2.7).

4.3.3 Extracting epithelial cells from tracheal suctionings

Tracheal suctioning sample PWTA05 was processed and cultured as described (section 2.3.4). Cells were seeded at a seeding density of 4×10^4 cells/cm^2 and cultured with various commercially available lung epithelial media types: BEGM, LHC-9 and CA media (Table 2.4) at 37°C for 30 days. Phase contrast microscopic images were taken at day 10.

4.3.4 Nasal scrapings sample processing and cell isolation

Nasal scrapings were taken from the lower edge of the inferior turbinate of the nasal cavity. This is an easily accessible area associated with a low risk of bleeding. Two methods of specimen collection were used due to their small size: a cervical cytology brush and a sterile swab. Each method was used for one nostril of the same patient and was performed by a consultant obstetrician. Both swab and cytology brush were inserted and gently rotated with the aim of collecting epithelial cells from the nasal mucosa. The implements were removed and inserted into separate collection tubes containing sterile PBS and agitated. The samples were taken to the laboratory where they were labelled as PWNB01B (for the brush sample) and PWNS01S (for the swab sample) and processed using sterile techniques.

4.3.4.1 Nasal scrapings cell isolation

The sample collection implement was removed from the sterile PBS and a cell count was performed using the trypan blue exclusion assay (section 2.2.3). The PBS was centrifuged at 400G for 20 minutes. The supernatant was aspirated and the pellet resuspended in the appropriate culture media. Cells were seeded at 2×10^5 cells/well in a collagen coated 24 well plate. Samples were cultured at 37°C for 20 days with media changes every 2-3 days.

4.3.5 Placenta derived MSC

4.3.5.1 Cell extraction and culture in 21% oxygen and 40% oxygen

MSC extraction for the chorion and amnion membrane was achieved as described in section 0. To assess the effect of hyperoxia on derived cells, cells were trypsinised (section 2.2.1) and plated at $2x10^4$ cells/well of a 12 well plate and cultured for 25 days at 37°C at 21% oxygen or 40% oxygen (40% oxygen achieved using polycarbonate containers, section 2.16). The AlamarBlue assay was performed (section 2.15) every few days and DNA was quantified (section 2.13) at day 25. Samples were stained using the LiveDead cell viability assay (section 2.7) and imaged using phase contrast and fluorescence microscopy.

4.3.5.2 MSC characterisation

To validate MSC identity of extracted cells tri-lineage differentiation and marker expression (using flow cytometry) was used as described in section 2.8. Cells previously isolated in 4.3.5.1 were cultured at 21% oxygen and 40% oxygen until 100% confluency was achieved. Cells were trypsinised and underwent the protocol described in section 2.5 for tri-lineage analysis and section 2.8 for marker expression. Results were analysed using Flowing Software 2.5.1.

4.3.6 Statistical analysis

Hydrogel measurements, DNA quantification and Alamar blue results were all statistically compared using two-way ANOVA with Tukey's multiple comparisons test to determine the statistical significance, $p \leq 0.05$ was considered significant. Analysis was performed using GraphPad Prism version 7.01. All values quoted in the results are mean average ± standard deviation.

4.4 Results

4.4.1 Sample collection and cell isolation

Tracheal suctionings were collected from recruited patients as described. Details of each sample and patient were collected as shown in Table 4.1. Three of the patients were consented but samples were not processed in the laboratory due to patient death or logistical disturbances.

Samples were successfully collected from 6 infants; each sample underwent a live and dead cell count (Figure 4.1 **A**); of those samples cells were successfully isolated and cultured from 60% (Figure 4.1 **B**). Cells from the samples were cultured on tissue culture plastic or collagen coated tissue culture plastic until 90-100% confluency was achieved. Cells were passaged up to 10 times and cell doubling times were determined (Figure 4.1 **C** and **D**). Most of the isolated cells maintain a constant doubling time except samples PWTA013C and PWTA021P which dramatically increased their doubling time at passage 6 and 3 respectively indicating the cells senesced (cells ceasing to divide). Cells were imaged every few days with phase contrast light microscope (Figure 4.2-Figure 4.4). Cells from samples PWTA011, PWTA013 and PWTA021 exhibited a fibroblast morphology which was maintained through further passaging and hence forth referred to as NLF cells. Images for the other samples consistently show rounded detached cells which were indirectly aspirated during media changes.

Table 4.1 Information from patients who have given their consent to their samples being collected

Patient ID	HTA ID	Sample collected	Gender	DOB	GA at birth	Birth weight (g)	Steriods	Mode of delivery	Other notes
1	PWTA011	02/08/2017	Male	11/07/2017	28 +2	880	Yes	C/S	
	PWTA012								
	PWTA013								
	PWTA014	03/08/2017							
2	PWTA021	23/08/2018	Male	22/08/2017	26/40,	580	Yes pre-delivery	C/S	Eclampsia, apyrexial, Current medication: magnesium sulphate, benzylpenecillian, fluconazole
	PWTA022	23/08/2018							
3	PWTA031	23/08/2018	Female	22/08/2017	33 +5/40	2180	Yes	Breech C/S	Apyrexial, PPROM >24/40, Current medication: benzylpenecillian, gentamicin
	PWTA032	23/08/2018							
4	Deceased								
5	Didn't receive sample	-	Male	12/09/2017	25 +4	830	Yes	NVD breech	
6	PWTA041	06/12/2017	Male	13/11/2017		780	Yes	C/S	Current medication: phosphate, abidec, caffeine citrate, chlorochiazine, spironolaxane
	PWTA042	07/12/2017							
7	PWTA051	20/03/2018	Male	12/03/2018	26+0	935	Unknown	C/S	Current medication: caffein citrate and sodium chloride
	PWTA052	20/03/2018							
	PWTA053	20/03/2018							
	PWTA054	28/03/2018							
8	Didn't receive sample	-	Male	08/04/2018	24+4 weeks	670	no		Current medication: insuline, morphine, caffein, fluconazole, vancomycin, meropenem
9	PWTA061	30/04/2018	Female	20/04/2018	39+3 weeks	2960		C/S	Sample was a light brown colour. Current medication: benzylpenecilin, hydrocortisone, gentamycin, morphine
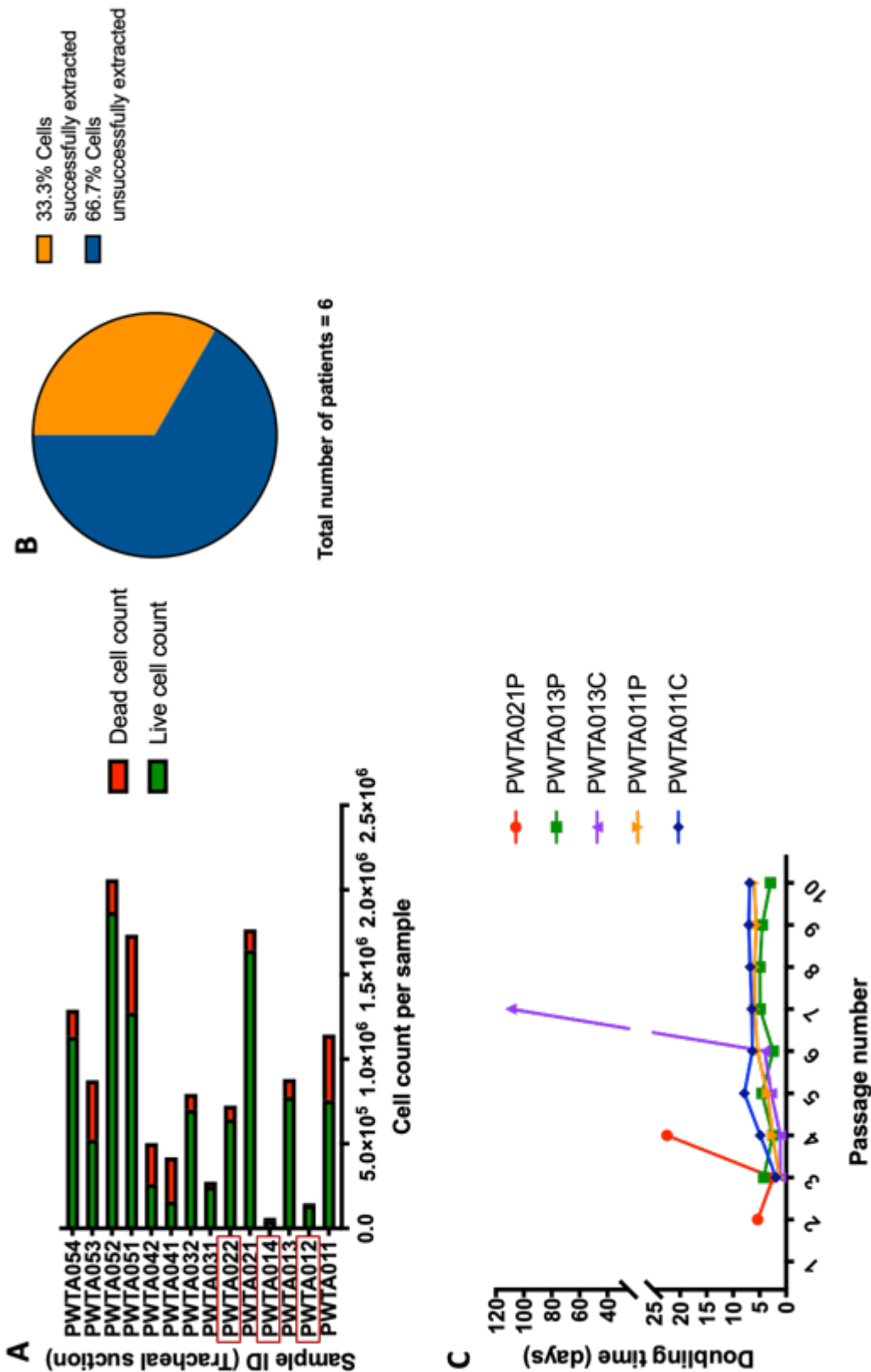
Figure 4.1 Cell counts of tracheal suctionings collected from ventilated babies on the NICU. Cells extracted from tracheal suctionings were counted using the trypan blue exclusion assay (A). The number of patients in which samples were sourced and how successful cell extraction was in shown (B). Samples which cells were successfully cultured from are highlighted with a red box (A). The cell doubling time for each passage was calculated and recorded (C).
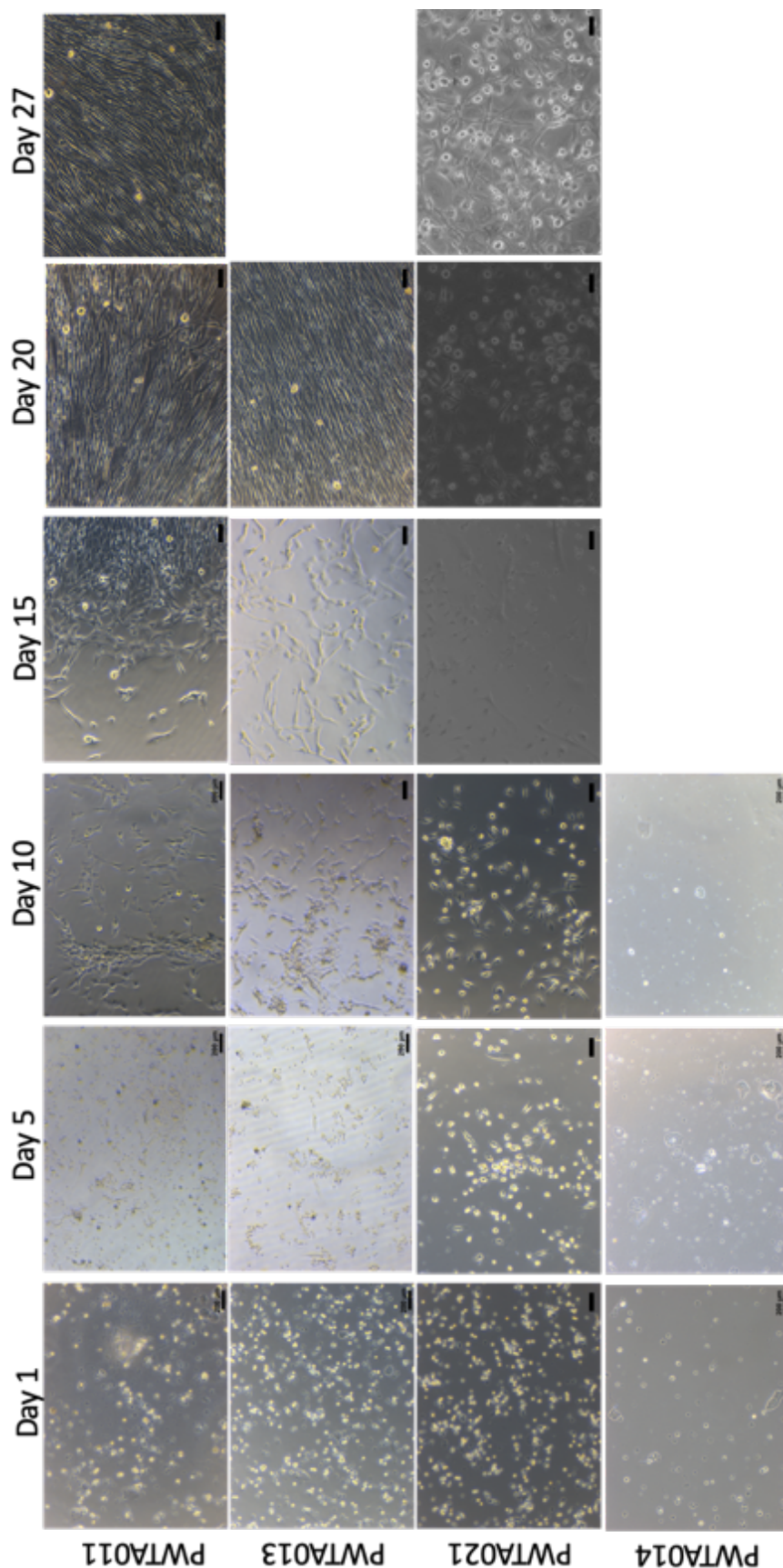
Figure 4.2 Phase contrast light microscopic images of cells extracted from tracheal suctionings of ventilated babies at passage 0. Representative images of sample PWTA011, PWTA013, PWTA021 and PWTA014 were taken every 5 days in culture for each sample.
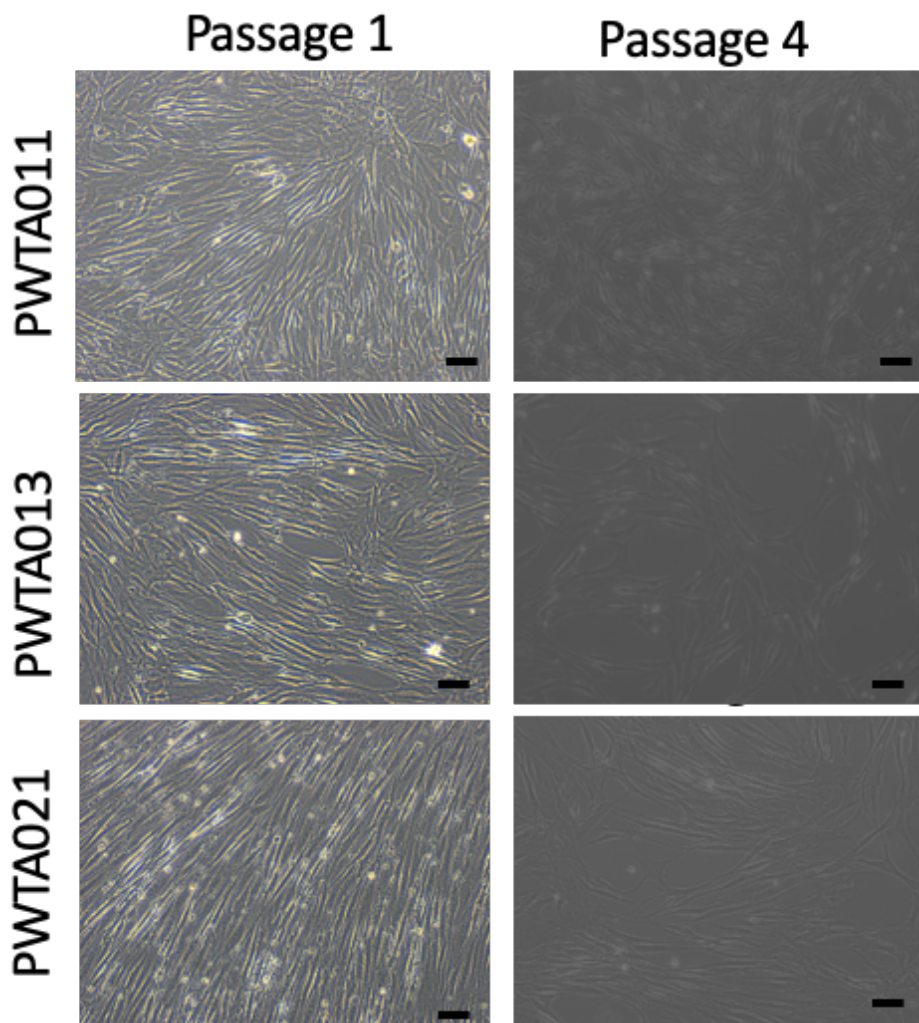
Figure 4.3 Phase contrast light microscopic images of cells extracted from tracheal suctionings of ventilated babies at passage 1 and 4. Representative images of samples PWTA011, PWTA013, PWTA021 and PWTA014 were taken at passage 1 and 4. Scale bar represent 200μm.
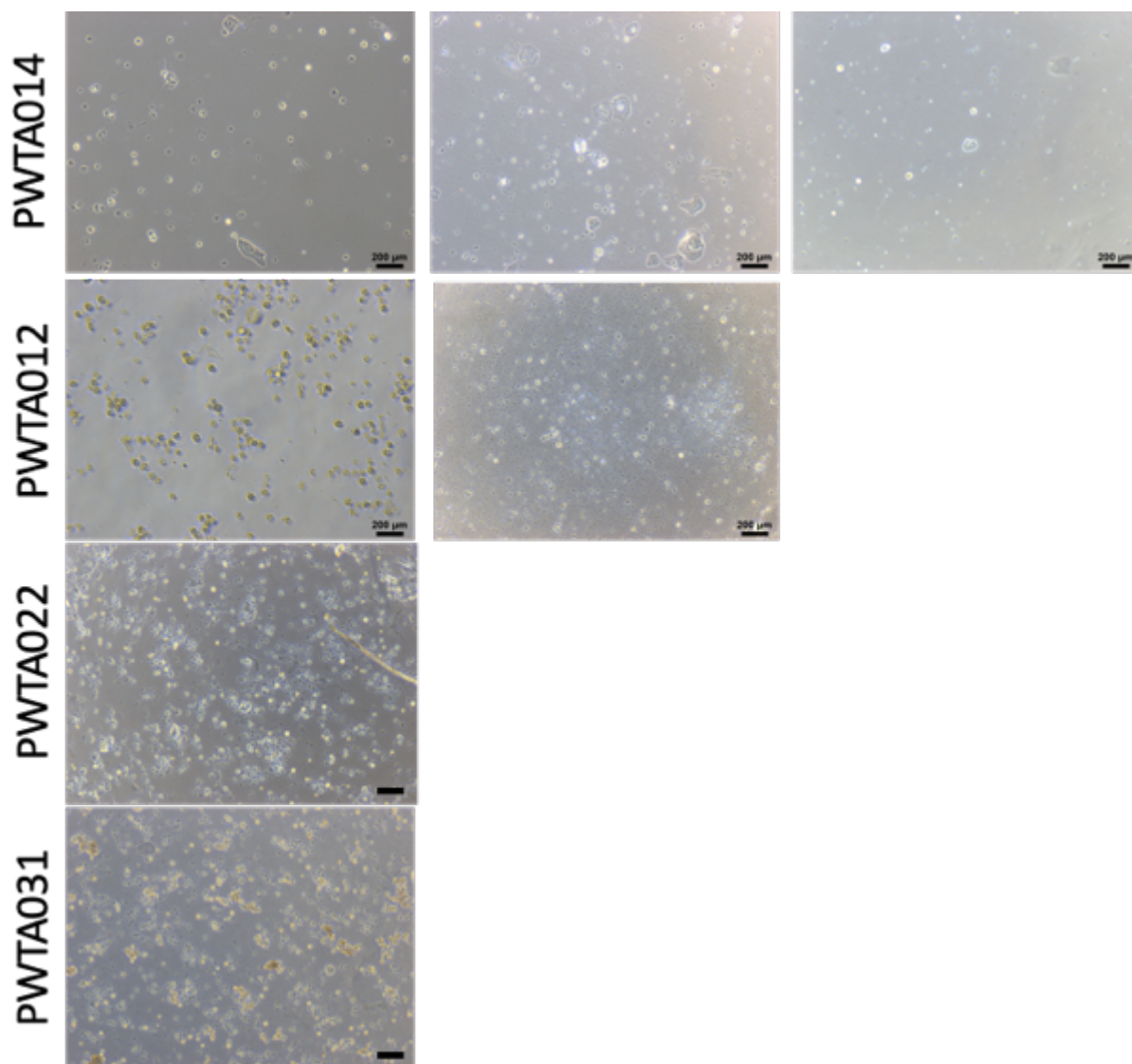
Figure 4.4 Phase contrast light microscopic images of cells extracted from tracheal suctionings of ventilated babies. Representative images of samples PWTA014, PWTA012, PWTA022 and PWTA031 were taken every 5 days in culture for each sample. Scale bar represent 200μm.

4.4.2 Extracted cells from neonatal tracheal aspirates contract collagen hydrogels

Extracted and cultured NLF cells (sample PWTA013P) were seeded in 1.5mg/ml collagen hydrogels at a density of 100,000 cells/gel and cultured for 20 days to assess contractibility. Percentage change in hydrogel depth and diameter was calculated (Figure 4.5). 35FL hydrogels were prepared in the same manner as an internal control. Confocal z-stacks were collated to assess cell morphology and viability (Figure 4.6). 35FL seeded hydrogels contracted in the same manner as previously shown. The NLF seeded hydrogels contracted at a significantly higher rate in comparison. Z-stack images show the cells fluorescing green indicating good cell viability. The NLF cells are more highly compact with smaller cells that the 35FL cells. The z-stack images indicate NLF and 35FL cells migrated to the bottom of the hydrogel (Figure 4.6).
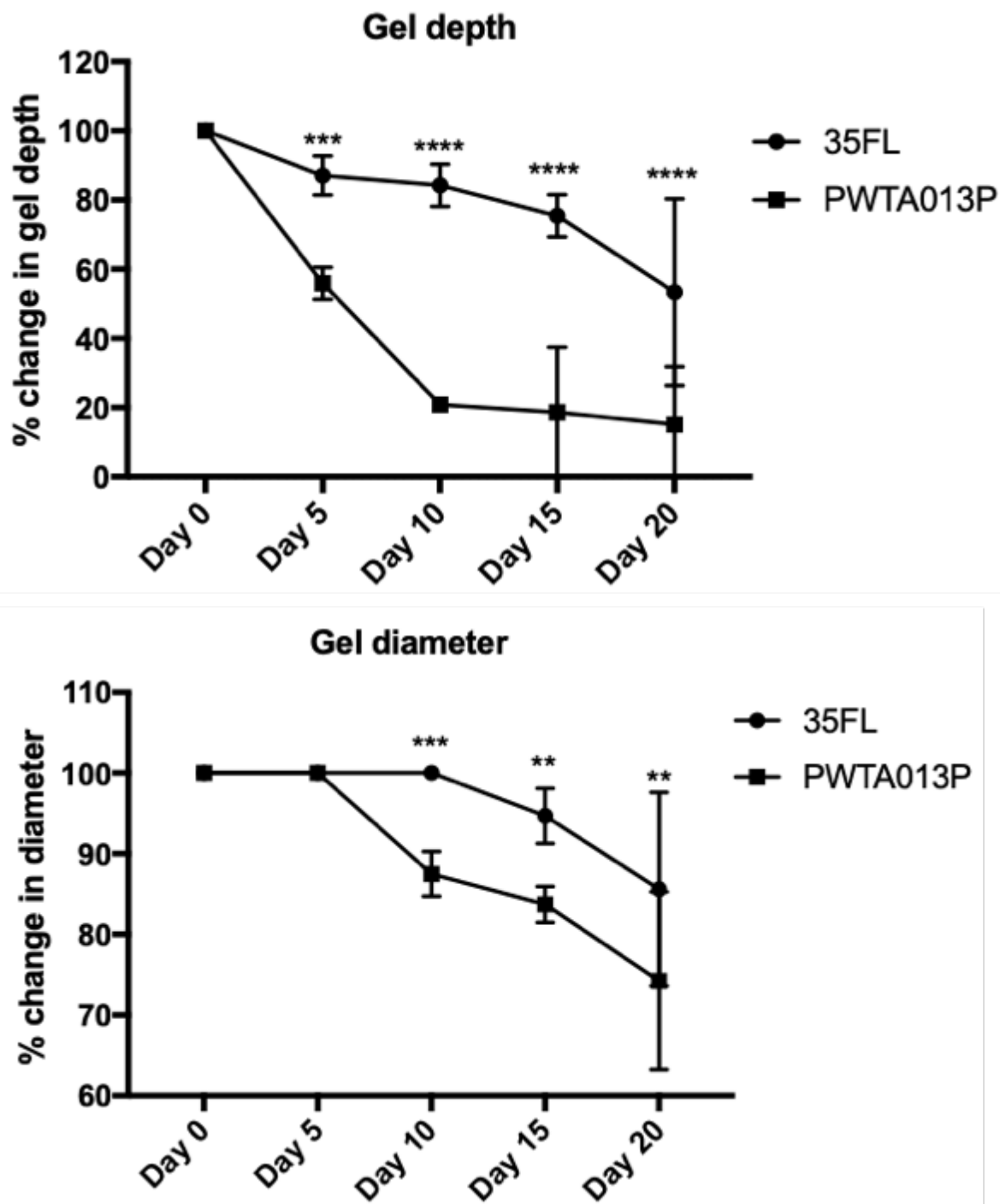
Figure 4.5 Adult lung cells 35FL and NLF cells cultured in collagen hydrogels. Change in hydrogel depth and diameter was measured over 20 days in culture to assess cell function. Data is expressed as mean ± standard deviation, n=4 (**p≤0.05, ***p≤0.001, ****p≤0.0001)
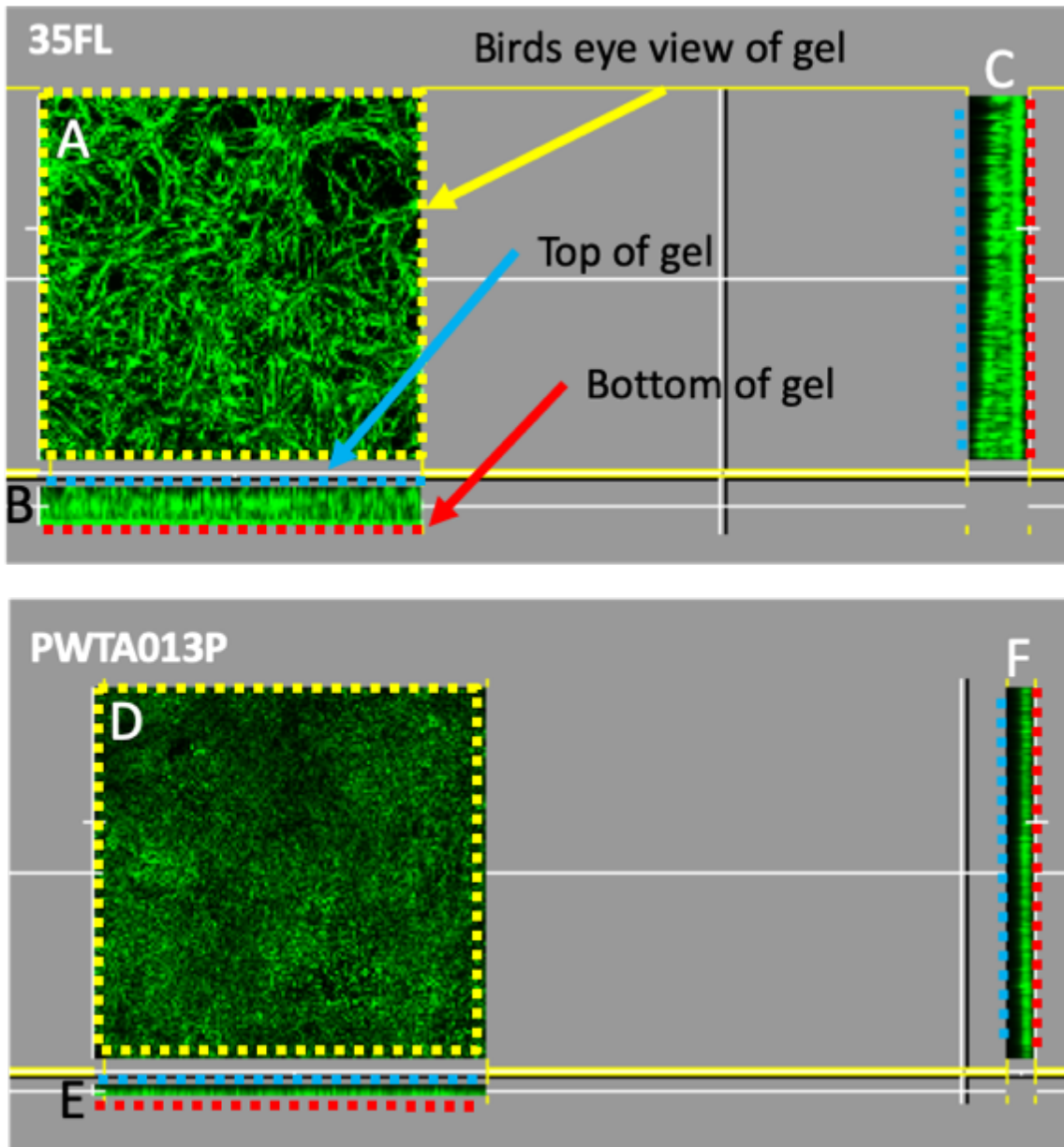
Figure 4.6 Adult lung cells 35FL and NLF cells cultured in collagen hydrogels. Confocal z stack images were taken of hydrogels stained with LiveDead staining kit. Images shows hydrogels from on top through the z-axis (A and D) and in the x and y axis (B, C, E and F). Green fluorescence indicates cell viability is good.

4.4.3 Extracting epithelial cells from tracheal aspirates was

unsuccessful

To encourage the culture of epithelial cells from neonatal lung tracheal aspirates sample PWTA051 was immediately cultured in commercially available lung epithelial media. Samples were imaged with phase contrast microscopy at day 7 of culture (Figure 4.7).

Cells were rounded, clumped and appeared detached (due to rounded, free-floating cells) from the plate. Observed cells reduced in number over the 30 days in culture.
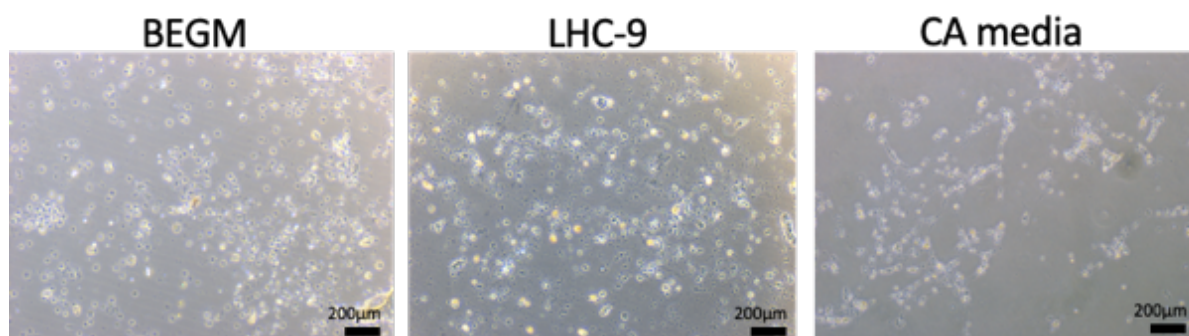
Figure 4.7 Tracheal suctioning sample (PWTA05) cultured in commercial lung epithelial medias BEGM, LHC-9 and CA media day 7. Cells displayed a rounded morphology, clumping and detached from the culture plate. Through media changes the detached cells were aspirated away.

4.4.4 Cell extraction from infant nasal scrapings

Samples were taken from the inferior turbinate of the nasal cavity of a healthy infant using either a swab or a brush. A cell count was performed on each sample and phase contrast microscope images taken (Figure 4.8). The brush technique had a cell count of over 3 times larger than the swab technique and possessed a lower percentage of dead cells. Observations with phase contrast microscopic imaging showed small rounded cells clustering together for both extraction techniques. Cells did not demonstrate attachment to the tissue culture plastic which were washed away through medium chages. During the culture period fewer cells could be observed.
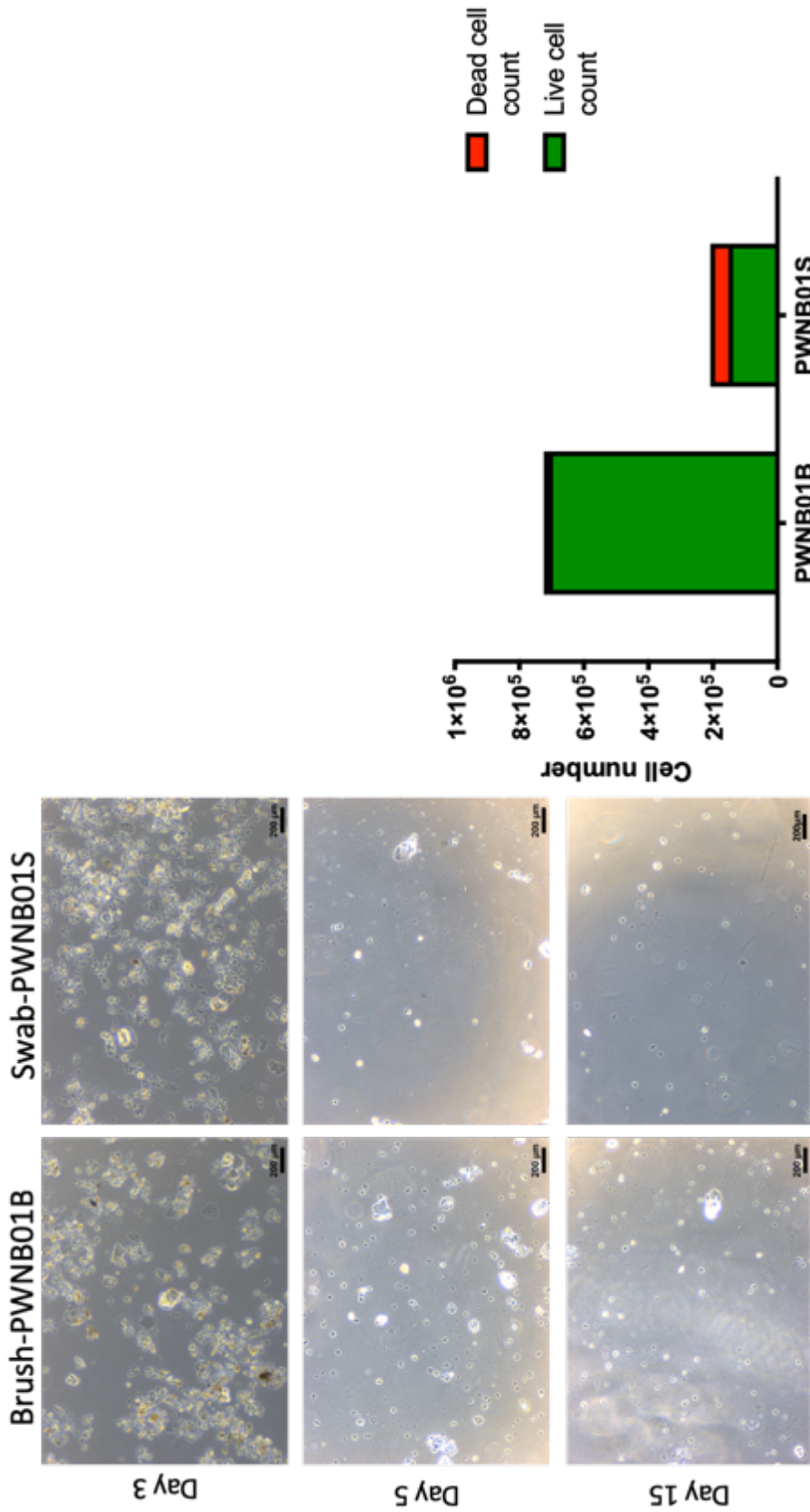
Figure 4.8 Cultured nasal scrapings. Samples were taken using a brush technique (PWNB01B) or a swab (PWNB01S). Cells counts were achieved using the trypan blue exclusion method. Phase contrast light microscopic images were captured of samples in culture. The brush technique removed more cells and had a lower percentage of dead cells.

4.4.5 Hyperoxia affects placenta derived MSCs proliferation

Extracted amnion and chorion MSCs were cultured for 25 days at 21% and 40% oxygen. Cells were imaged with light microscopy and confocal fluorescence microscopy with the LiveDead cell viability kit (Figure 4.9). Both amnion and chorion cells were 100% confluent at 21% oxygen, but cell density was much lower at 40% oxygen. The LiveDead staining showed the cells were viable in all conditions as shown by the green fluorescence. No red fluorescence was observed. The cells at 21% oxygen have a more elongated cell morphology than cells at 40% oxygen. For the AlamarBlue assay a statistically lower fluorescence value was measured at later time points for cells cultured at 40% oxygen. This trend was the same for both amnion MSCs and chorion MSCs. Quantified DNA was statically lower at day 25 for both cell types when cultured at 40% oxygen. The effect was more evident for chorion MSCs (Figure 4.9).
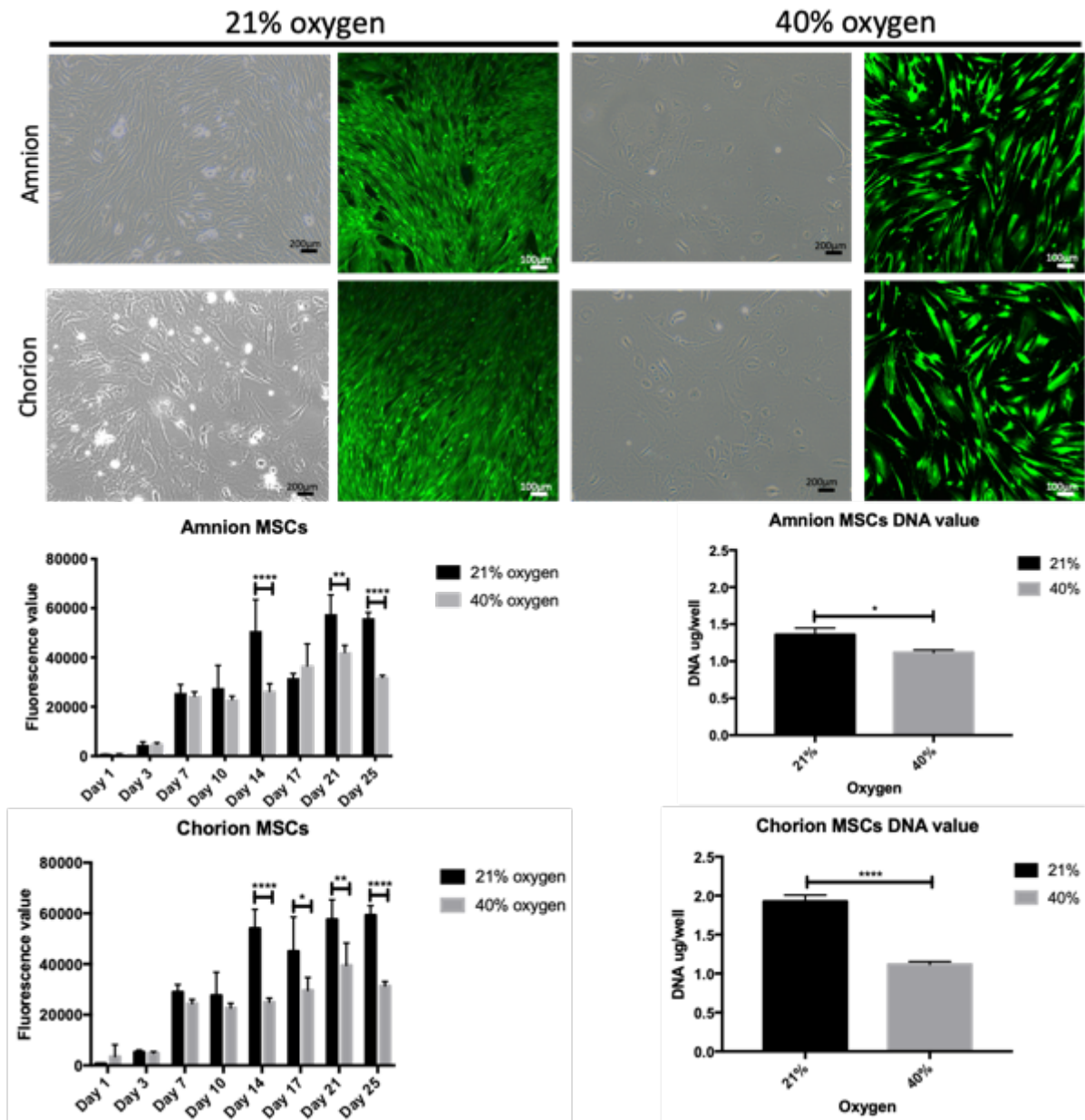
Figure 4.9 MSCs extracted from placentas cultured at 21% oxygen and 40% oxygen.
Cells from the amnion membrane and chorion membrane were imaged after 20 days in culture with phase contrast microscopy and confocal imaging using the LiveDead staining kit. The AlamarBlue assay was performed every few days and DNA quantified day 25. 40% oxygen significantly affects placenta MSCs proliferation and metabolic activity. Data are expressed as mean ± standard deviation, n=6 (*p≤0.05, **p≤0.05, ****p≤0.0001).

4.4.6 Hyperoxia affects placental MSC characterisation.

Cells extracted from the amnion and chorion placenta membranes were cultured at 21% and 40% oxygen with two aims:

- to characterise isolated MSCs

- to assess the effect hyperoxia has on placenta derived MSCs characterisation and proliferation

Characterisation was achieved using flow cytometry to measured marker expression and tri-lineage differentiation capacity. Both chorion and amnion MSCs expressed the expected stromal markers associated with MSCs when cultured at 21% oxygen (Figure 4.10 and Figure 4.11). However, chorion MSCs at 40% oxygen marker expression indicates 2 populations of cells. Two peaks are seen for markers CD73, CD90 and CD105. For markers CD34, CD45 and HLADR there is a shift in peak to the right suggesting some cells expressed these markers. Marker expression seems less affected by hyperoxygen for the amnion MSCs which is as expected for MSCs with the exception of CD90 which is shifted to the right.

Tri-lineage differentiation was positive for all sample conditions and was unaffected by hyperoxygen (Figure 4.12 and Figure 4.13). There is a marked difference in staining levels comparing amnion and chorion MSCs. More intense staining levels can be seen for amnion MSCs. Staining for lipid accumulation for amnion MSCs at 40% oxygen was slightly reduced compared with amnion MSCs at 21% oxygen. Control samples cultured with growth media only were negative for all staining.
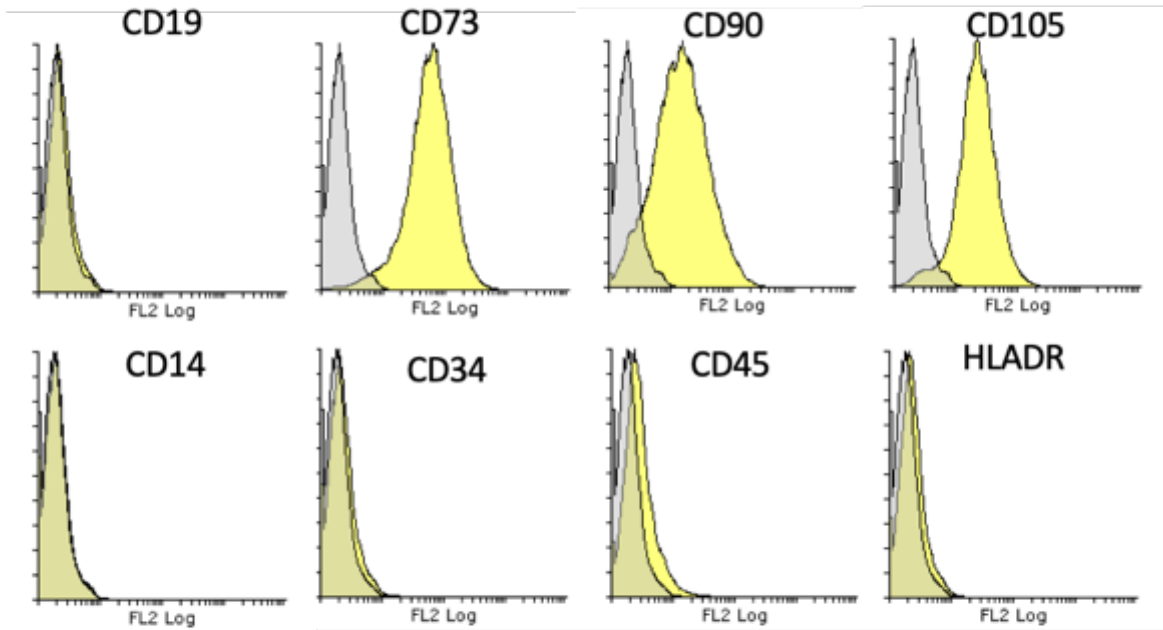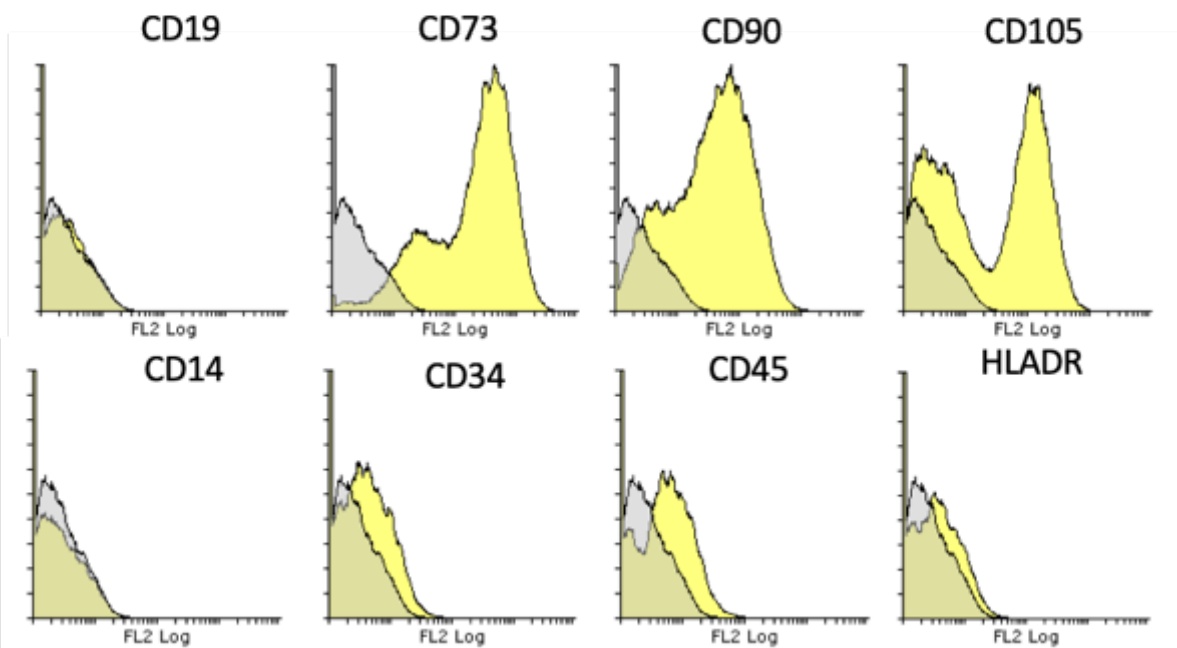
Figure 4.10 Flow cytometry results for chorion placenta derived MSCs. Expression of MSC related markers was analysed for MSC extracted from chorion placenta membrane and cultured in 21% oxygen and 40% oxygen. MSC markers typically negative: CD19, CD14, CD34, CD45 and HLADR. MSC markers typically positive: CD73, CD90 and CD105. Grey fill represents isotype control IgG1 or IgG2a, yellow fill represents antibody marker. Cells cultured at 40% affects the expression of markers CD73, CD90 and CD105.
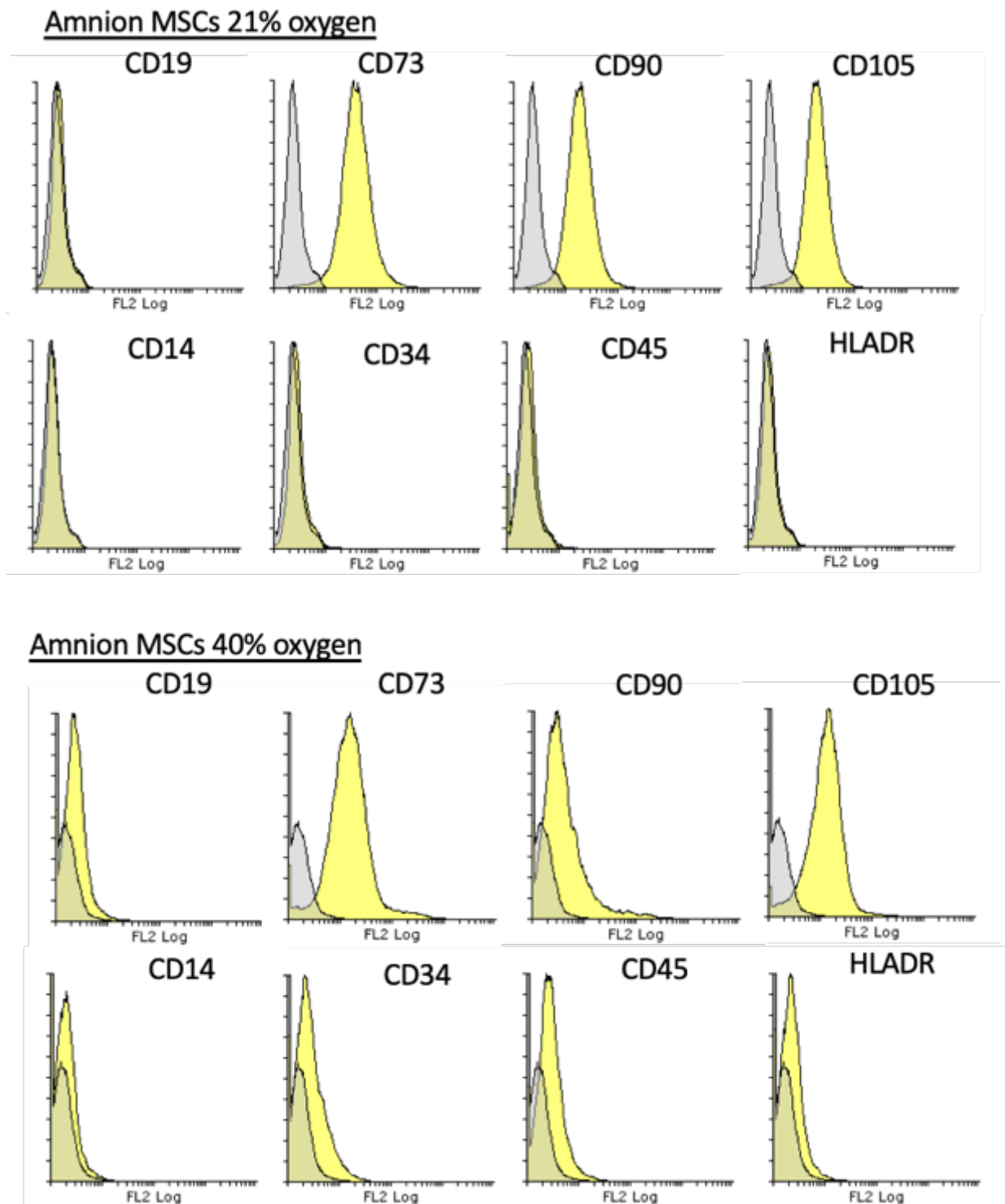
Figure 4.11 Flow cytometry results for amnion placenta derived MSCs. Expression of MSC related markers was analysed for MSC extracted from amnion placenta membrane and cultured in 21% oxygen and 40% oxygen. MSC markers typically negative: CD19, CD14, CD34, CD45 and HLADR. MSC markers typically positive: CD73, CD90 and CD105. Grey fill represents isotype control IgG1 or IgG2a, yellow fill represents antibody marker. Cells cultured at 40% affects the expression of marker CD90.
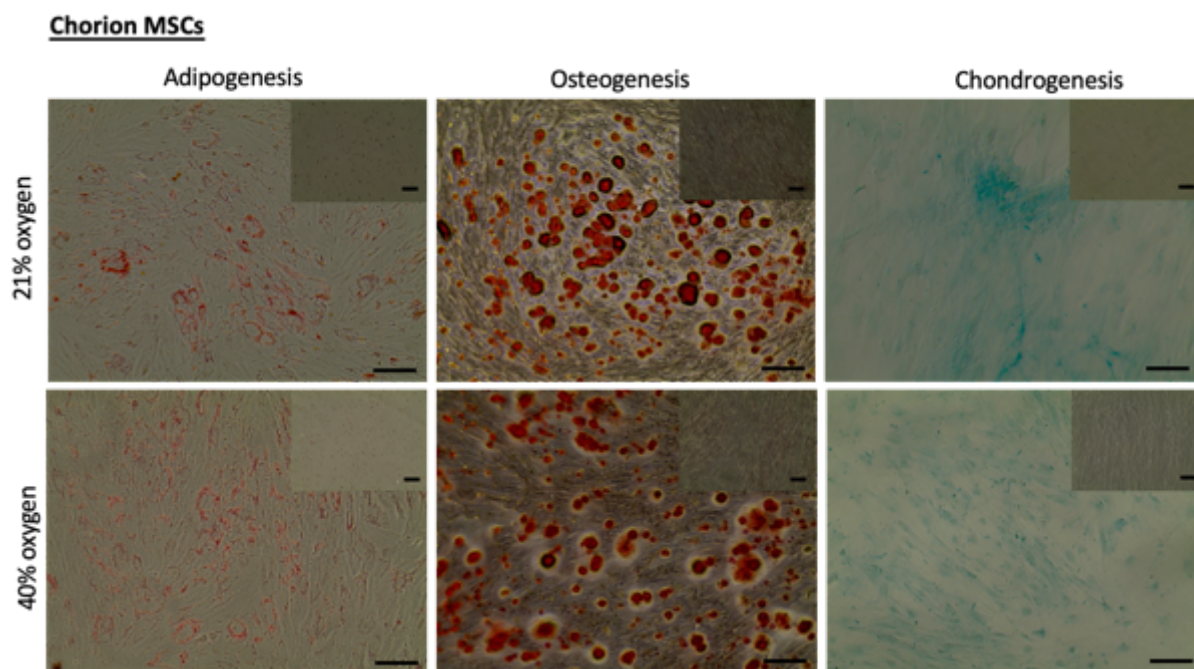
Chorion MSCs

Figure 4.12 Tri-lineage differentiation staining for chorion placenta MSCs. Images of cells cultured under the appropriate conditions to encourage MSC differentiation into adipocytes, osteocytes and chondrocytes. Cells cultured in either 21% or 40% oxygen and were fixed and stained: Osteogenic samples were stained with alizarin red S for calcium deposits, chondrogenic samples were stained with alcian blue for SGAGs, Adipogenic samples are stained with oil red O for lipid droplets. Images of control cells cultured in standard culture media and stained as appropriate are inset for comparison. Scale bars represent 200μm.
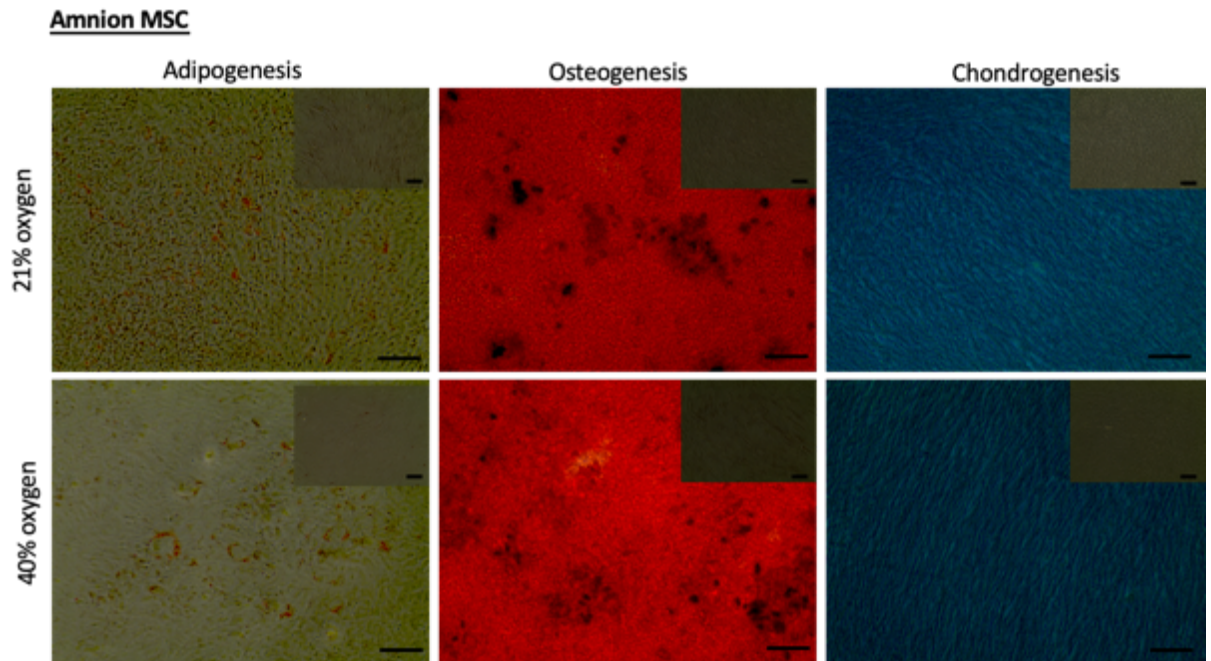
Figure 4.13 Tri-lineage differentiation staining for amnion placenta MSCs. Images of cells cultured at the appropriate conditions to encourage MSC differentiation into adipocytes, osteocytes and chondrocytes. Cells cultured at either 21% or 40% oxygen and were fixed and stained: Osteogenic samples were stained with alizarin red S for calcium deposits, chondrogenic samples were stained with alcian blue for SGAGs, Adipogenic samples are stained with oil red O for lipid droplets. Images of controls cells cultured in standard culture media and stained as appropriate are inset for comparison

4.5 Discussion

4.5.1 Tracheal suctioning for isolation and expansion of neonatal lung cells

Cell counts, cytokine analysis and RNA expression have all been previously achieved from tracheal suctionings from adult and neonates [207–209]. However, there are few examples of the isolation of cells for long-term culture. Here we investigated whether cells could be isolated and expanded for use in an *in vitro* model of BPD. Tracheal suctioning is a routine procedure to maintain patency of the airways of artificially ventilated infants. The aspirated secretions are usually disposed of and offer an advantage for research purposes since there are no additional risk factors to the infant. Recruitment and seeking consent

were relatively straight forward procedures with parent/guardians overall being willing to participate in the study since there was no additional risk to the infant. Definite BPD diagnosis is made 28 days after birth so during the time of sample collection diagnosis of BPD had not been confirmed. However, clinicians have a strong idea based of gestational age and birth weight. Tracheal suctioning collection is an unplanned procedure based on clinical indications. This proved difficult for laboratory purposes since equipment preparation time is limited. It is also not possible to foresee how many tracheal suctions each infant will need to have during their time in NICU. Sample collection from the hospital was straightforward with no major issues arising. However due to the nature of the NHS, samples may have been left waiting at room temperature for various time periods, it wasn't possible to document this or to store samples in a temperature-controlled unit.

Cells were successfully isolated from 40% of patients. Multiple samples were collected from each patient, but cells were not always isolated from samples of the same patient. This indicates cell culture success is not necessarily based on the patient themselves but possibly external factors such as the procedure, personnel performing the procedure or time of sample collection. Tracheal suctionings can be deep, or shallow determined by how far the catheter is inserted. With deep tracheal suctionings the catheter is inserted until respiratory wall or the tracheal bifurcation is met. With shallow insertion the catheter only goes as deep as the trachea. The technique used was not recorded and may have affected sample quality. However reports have indicated there is no difference between cellular component of deep versus shallow tracheal suctionings [190].

Cell counts varied considerably between samples and there was no observed correlation between cell counts and the isolation of cells. Cultured cells possessed a morphology indicative of fibroblasts in terms of their spindle-like, elongated morphology, adhesion to

tissue culture plastic, high proliferation and contractibility of collagen hydrogels. Their ability to maintain good cell viability, proliferative function and contraction in collagen-elastin hydrogels makes them an ideal candidate for use in our previously developed alveolus model. Further investigation is required to state with confidence that the extracted cells are fibroblasts in origin. Staining for a mesenchymal marker such as vimentin along with the absence of non-fibroblast markers such as epithelial or haemopoietic markers would provide a more detailed understanding of cell type. The identification of antibody TE-7 and smooth muscle actin have also been acknowledge as a lung fibroblast marker [210]. The isolation of fibroblast-like cells is further supported by work done by Hennrick *et al.* They isolated cells from the tracheal aspirate fluid of premature, ventilated neonates that possessed characteristics typical of mesenchymal stem cells [157]. They observed a trend relating the isolation of cells and more severe ventilation suggesting that MSCs home in to the site of injury. This postulates the idea that the cells we isolated could demonstrate MSC characteristics. Further analysis into cell markers and differentiation potential would be required to further evaluate cell type. Unlike Hennrick *et al*. we did not find any trend between cell isolation and patient type. However, we had a much smaller sample size of only 6 patients with a success rate of 33% which is under the 55% success rate observed by Hennrick *et al.*

We further investigated whether epithelial cells could be isolated from tracheal suctionings. In initial experiments we used attachment time and collagen coating to select the attachment of fibroblasts and epithelial cells (fibroblasts attach quicker than epithelial cells and collagen coating encourages epithelial attachment[211]). This time-dependant and substrate-dependant technique failed to isolated both fibroblasts and epithelial cells with only fibroblast-like cells being cultured. To promote epithelial isolation, we sourced three types of commercially available lung epithelial media which were used to culture cells from sample PWTA05 but again this was unsuccessful. It is

likely that epithelial cells are present in tracheal suctions due to accidental damage to the tracheal mucosa during the procedure, however these cells may not be viable[190]. To evaluate the cell populations, present in tracheal suctionings, flow cytometry could be performed. Cells would be fluorescently labelled for cell membrane markers typically associated with certain cell types. Flow cytometry, previously used for bronchoalveolar lavage analysis [212], could also be used to assess cell heath and be used for cell sorting.

Nasal scrapings were investigated as an alternative source of cells. Nasal biopsies or lavage are a common tool to monitor inflammation and isolating respiratory cells [191–197]. Two samples were collected using a brush and a swab. Both techniques delivered cell numbers comparable to those seen in previous published work[191]. The brush technique has been found to have better diagnostic accuracy when used for paediatric disease diagnosis[213] and we found the technique extracted 72,000 cells compared with only 21,000 cells for the swab technique. Both extraction techniques proved futile for cell expansion. Further investigation is required to optimise culture techniques and conditions such as plating substrate, media composition and seeding density. Sample collection was logistically more difficult since the procedure isn't current routine practice and can cause mild discomfort to the child. Our attention moved away from using nasal scrapings for cell isolation and we focused on the tracheal suctionings as a cell source.

4.5.2 Placenta derived MSCs

MSCs are a well-established cell type for their regenerative capacity and function in development. Multiple studies have identified their presence in the developing lung [157,214]. Work by Popova *et al.* suggested MSC isolation from tracheal aspirates can be used a prediction of BPD and suggests that lung MSCs have a role in BPD progression. This indicates that MSCs may provide an ideal candidate for a cell therapy for the treatment of

BPD. There have been many experimental studies examining the effect MSCs have on animal models of BPD. A meta-analysis by Augustine *et al.* showed that administration of MSCs significantly improved lung injury in rodents [215]. A phase I dose-escalated clinical trial was conducted to assess the intratracheal transplantation of human umbilical cord blood (UCB)-derived MSCs in preterm infants at high risk of BPD [171]. The study concluded the cell therapy was a safe and feasible treatment for BPD. The group now hopes to conduct a phase 2 clinical trial (ClinicalTrials.gov Identifier NCT03392467). UCB MSCs possess similar attributes to placenta derived MSCs in that they are both sourced from gestational tissue, they are waste materials associated with no additional morbidities and therefore provides an ideal source of stem cells. Protocols have been established for MSC isolation from the chorion and the amnion placenta membranes.

In this chapter we have successfully isolated amnion and chorion membrane placenta MSCs sourced from routine caesarean sections of healthy term births. We did not face any logistical issues when collecting placentas for processing. The only difficulty for researchers is timing; routine caesarean sections are planned procedures so scheduling can be estimated, however, emergency cases will take priority and push back routine procedures. This therefore disrupts timing and can cause issues for laboratory planning. The MSC isolation procedure we used was based on a previous established protocol [165] and further developed in our laboratory. The isolated cells from both the chorion and the amnion were compliant with the differentiation potential and marker expression associated with MSCs as recommended by the Mesenchymal and Tissue Stem Cell Committee of the International Society for Cellular Therapy (Table 4.2). To further develop this, we wanted to understand the effect hyperoxia had on MSC markers since this cell therapy would be used for BPD infants likely to be undergoing hyperoxygen ventilation (ranging from >21%-100% oxygen). We exposed the isolated aMSCs and cMSCs to 40% oxygen during culture and compared this with culture at 21% oxygen. Both

sets of cells had a similar response with those cells at 21% oxygen possessing all the expected characteristics of MSCs however cells at 40% oxygen had reduced proliferative capacity, senescent-like morphology (larger, flattened cells)[216] and distorted marker expression. The marker expression suggests there are two populations of cells.

The effect of cultivated oxygen level has been well documented when comparing atmospheric oxygen (21%) with physiological (<5%) oxygen. Atmospheric oxygen impedes cell proliferation and affects marker expression due to oxidative stress [217,218]. aMSCs and cMSCs possessed similar responses and displayed morphological similarities as has been previously demonstrated[219]. There is very little evidence available which looks at the effect of hyperoxia of >21% on MSCs, emphasising the novelty of this work. A couple of reports have demonstrated oxidative stress impedes cellular proliferation and leads to senescence[163,220]. A recent publication by Popova *et al.* [221] showed that resident foetal lung mesenchymal cells cultured at 60% oxygen alters surface markers and production of extracellular matrix. However, in contrast umbilical cord blood derived MSCS cultured at 60% oxygen dramatically increased antioxidant and anti-inflammatory factors[221]. This suggests hyperoxia exposure may impede endogenous MSCs which leads to BPD phenotype. Umbilical cord blood MSCs on the other hand could provide beneficiary effects to protect the organ.

The importance of considering the effect of hyperoxia on cell therapies depends on the administered route. In animal models MSCs have been delivered systemically, intratracheally and intraperitoneally[222]. The most obvious delivery route for the lung is intratracheal because this is a similar method to surfactant delivery, a current routine procedure and would deliver cells directly to the diseased tissue. Intratracheal delivery has been found to be a more efficient delivery route when compared with IV[163]. The cell therapy would be exposed to atmospheric oxygen (21%) or hyperoxygen (>21%) if the

patient is requiring oxygen ventilation. A current discussion point surrounding MSCs as a cell therapy is the mode of action. Evidence suggests that MSC cell engraftment is not necessary for these stem cells to influence native tissue. MSCs may stimulate native cells through paracrine mechanisms[223] meaning that the hyperoxygen environment a cell therapy is exposed to would not matter; or that pre-conditioned media could be as advantageous as administering the cells. Previous work has demonstrated both aMSCs and cMSCs excrete large amounts of soluble factors; however some differences have been noted for example aMSCs have an enhanced secretion of PGE2 leading to reduced T-lymphocyte proliferation [224]. So, although aMSCs and cMSCs possess similar characteristics in terms of proliferative capacity and marker expression, one cell type may perform better as a cell therapy for certain diseases. At this point it is difficult to establish which MSC source would provide a better outcome for BPD since the disease mechanism is still uncertain.

Table 4.2 Mesenchymal and Tissue Stem Cell Committee of the International Society for Cellular Therapy recommended MSC markers

	Characteristic		
1	Adherence to plastic in culture		
2	Marker expression	**Positive**	**Negative**
		CD105	CD45
		CD73	CD34
		CD90	CD14 or CD11b
			CD79 or CD19
			HLA-DR
3	*In vitro* differentiation to osteoblasts, adipocytes and chondrocytes		

4.6 Conclusion

We have demonstrated that tracheal suctionings from ventilated neonates can be used for the isolation and expansion of human lung neonatal cells. These cells (NLF) were fibroblastic in nature and are a suitable candidate for use in an *in vitro* model of BPD since they can be cultured long-term in collagen-elastin hydrogels. Further cell characteristic analysis is necessary to identify cell type. Previous published work has isolated cells in a similar manner and identified them as possessing MSC characteristics. The cells we isolated could indeed also possess similar characteristics and we therefore hypothesise that MSCs are recruited in lung injury and are necessary for normal lung maturation and healing.

MSCs were successfully isolated and expanded from chorion and amnion placenta membranes. Characterisation using the tri-lineage differentiation technique and marker expression indicated these cells possess the necessary attributes of MSCs as described by Mesenchymal and Tissue Stem Cell Committee of the International Society for Cellular Therapy recommended MSC markers[225]. Both aMSCs and cMSCs marker expression and proliferation were affected by hyperoxia exposure. This could have detrimental impacts if MSC cell therapy could ever potentially be used as a cell therapy for BPD infants who require hyperoxygen ventilation.

Chapter 5

Examining the therapeutic capabilities of placenta MSCs when exposing lung cells to hyperoxia

5.1 Introduction

In recent years the regenerative and repair capabilities of MSCs have been the focus of regenerative medicine. For the lung in particular stem cells have been of interest for a variety of chronic conditions including idiopathic pulmonary fibrosis, emphysema, asthma and chronic obstructive pulmonary disease (COPD). Data gathered from BPD animal models suggests stem cells could play a significant role in alleviating the effects of lung injury found in BPD through their immunomodulatory properties, antifibrotic effects, and antioxidative properties. In the early days of stem cell research it was suggested that administered MSCs function through migration and engraftment. However, emerging evidence indicates therapeutic MSCs may function through paracrine mechanisms. The paracrine effect of MSCs has been investigated for a variety of diseases including cardiovascular disease, acute kidney disease, liver fibrosis, neurological disease and wound healing[226]. For BPD in particular MSCs have been shown to release anti-inflammatory cytokines and exosomes to ameliorate the parenchymal injury found in preclinical BPD models[158,159,227,228]. This offers a viable alternative to cell therapies since the use of pre-conditioned media or purified exosomes would avoid the inherent risks of cell therapies such as tumorigenesis, autoimmune reaction and disease transmission[229,230].

The limiting factor of many reports on BPD is the use of rodent models. As previously explained rodent models arguably do not accurately represent the human pre-term lung[231]. In previous chapters we have established a human relevant 3D alveolus model in which we incorporated human lung cells isolated from the lung of ventilated neonates. In this chapter we expose human lung adult and neonatal cells in a 2D and 3D state to hyperoxia representative of clinical ventilation experienced by BPD patients. We initially assessed the cellular response when the cells are exposed to hyperoxia. We then co-

culture the adult and neonatal lung cells with placenta derived MSCs to assess the potential alleviation of oxidative stress. Since emerging evidence suggests MSCs act in a paracrine manner an indirect co-culture method using well-inserts has been incorporated.

5.2 Aims

The aim of this chapter was to integrate aspects developed from the previous two experimental chapters. Firstly, we exposed adult lung cells (35FL and A549) and neonatal lung cells (isolated NLF) to 40% oxygen in both a 2D state and the 3D model previously established. The effects of hyperoxygen compared to atmospheric oxygen was assessed through examining cell proliferation, function and DNA expression. Secondly, we co-cultured the lung cells with placenta MSCs to evaluate the potential protective value MSCs house to cells undergoing oxidative stress. A diagram of the experimental design is shown in Schematic 5.1.

5.3 Study design
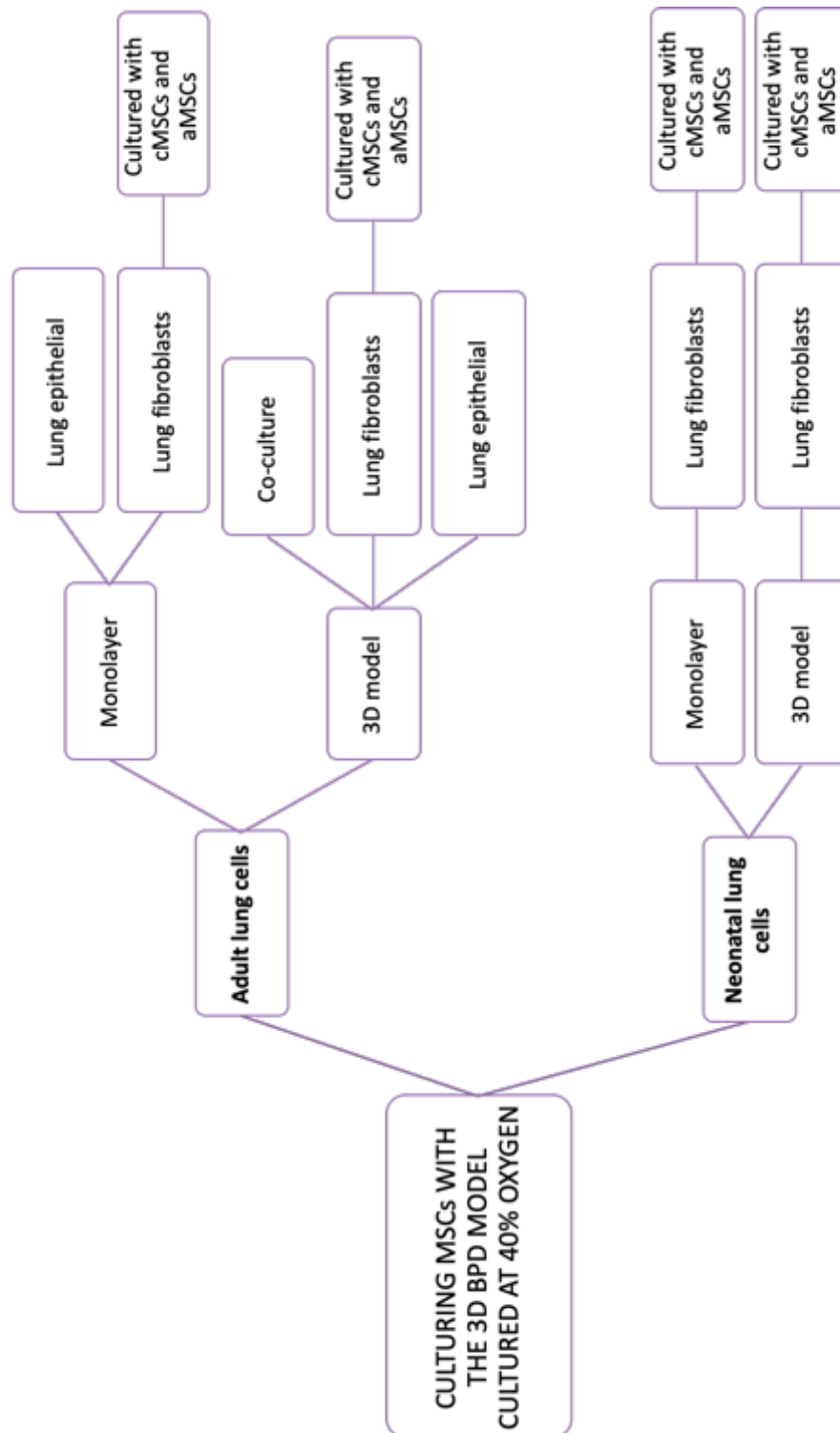
Schematic 5.1 A schematic to show the flow of experimental design for chapter 5.
Adult lung cells and neonatal lung cells were cultured in 3D hydrogels or in 2D monolayer
and exposed to hyperoxia. The adult lung cells 35FL and A549 were cultured in the 3D
model as single cell cultures or co-culture. Both the neonatal and adult lung fibroblasts
were exposed to placenta derived MSCs to assess therapeutic effect when exposed to
hyperoxia. Culture at atmospheric oxygen was included as a control.

5.4 Methods

In Chapter 3 we developed an *in vitro* model to represent the lung alveolus. We concluded elastin did not affect cell viability and therefore we employed a collagen-elastin hydrogel of ratio 1:1. Previously, no contraction in hydrogel diameter was observed when collagen-elastin hydrogels were seeded with 75,000 cells per 500μl gel. In this study hydrogels were set within a well insert to provide an air interface. The well inserts have a smaller surface area than the wells of a 12 well plate hydrogels were previous set into. To maintain consistency a hydrogel volume of 145μl was included which requires a seeding density of 21,750 cells/gel.

5.4.1 Exposing adult lung cells to hyperoxia cultured in monolayer and 3D culture

Lung cells A549 and 35FL were cultured as previously described (section 2.2). Cells were trypsinised and seeded as a monolayer in a 12 well plate well insert at a density of 21,750 cells/well (section 2.2.1). Cell-seeded collagen-elastin hydrogels (1:1) were made (section 2.9). Before gelation 35FL were resuspended in the hydrogel solution. 145μl of solution was pipetted into 12 well plate well inserts and incubated at 37°C for 30 minutes to allow gelation. A549 cells were trypsinised, counted and seeded on the hydrogel surface at a density of 21,750 cells/gel. Hydrogels were cultured with culture media at 21% oxygen for 24 hours after which medium was aspirated from inside the well insert. All samples were incubated at 37°C at 21% oxygen or 40% oxygen (section 2.16) for 20 days. Every 5 days cell-seeded hydrogels were measured using the OCT (section 2.10). The LiveDead assay was performed (section 2.7) on day 20 and imaged with confocal microscopy and phase contrast light microscopy. On day 20 DNA was quantified using the PicoGreen DNA assay (section 2.13) and RNA was extracted for RT-PCR analysis (section 2.11).

5.4.2 The effect of 40% on A549 cell monolayer integrity using TEER analysis

To assess if hyperoxia affects cell monolayer integrity, the TEER (Transepithelial Electrical Resistance) method was used. A549 cells were trypsinised, counted and seeded at a density of 21,750 cells/well in 12 well plate well inserts (section 2.2.1) or on the surface of collagen-elastin hydrogel (1:1) made in 12 well plate inserts (section 2.9). Collagen-elastin hydrogels were either acellular or seeded with 35FL cells at a density of 21,750 cells/gel. Samples were cultured at 37°C at 21% oxygen or 40% oxygen (section 2.16) for up to 28 days. TEER analysis was performed as previously described (section 2.14). Images were taken with phase contrast microscopy.

5.4.3 Exposing neonatal lung cells to hyperoxia in monolayer and 3D culture

Lung cells NLF were cultured as previously described (section 2.3.3). Cells were trypsinised and seeded in monolayer in a 12 well plate well insert at a density of 21,750 cells/well (section 2.3.3). Cell-seeded collagen-elastin hydrogels (1:1) were made (section 2.9). Before gelation NLF were resuspended in the hydrogel solution. 145μl of solution was pipetted into 12 well plate inserts and incubated at 37°C for 30 minutes to allow gelation. Hydrogels were cultured with culture media for 24 hours at 21% oxygen after which medium was aspirated from inside the well insert. All samples were then incubated at 37°C at 21% oxygen or 40% oxygen (section 2.16) for 20 days. Every 5 days cell-seeded hydrogels were measured using the OCT (section 2.10). The LiveDead assay was performed (section 2.7) on day 20 and imaged with confocal microscopy and phase contrast light microscopy. On day 20 DNA was quantified using the PicoGreen DNA assay (section 2.13) and RNA was extracted for RT-PCR analysis (section 2.11).

5.4.4 Assessing the protective effect of placenta MSCs when lung cells are exposed to hyperoxia

To assess if the co-culture of placenta derived MSCs (aMSCs and cMSCs) could alleviate the effect hyperoxygen has on lung cells we examined the contraction, DNA quantity, cell morphology and cell viability of lung cells 35FL and NLF when cultured at 40% oxygen in 2D and 3D.

5.4.4.1 Experimental set-up

Cells 35FL and NLF were cultured and trypsinised as previously described (section 2.2 and 2.3.3). Cells were plated either in 3D (3.5mg/ml collagen-elastin hydrogels) or in monolayer. For the monolayer culture cells were directly plated in 12 well plate well inserts at a seeding density of 21,750 cells/well and cultured in media at 21% oxygen for 24 hours. For the 3D constructs, 3.5mg/ml collagen-elastin hydrogel solution (1:1) was made as described (section 2.9). Before gelation 35FL or NLF cells were resuspended in the solution. The hydrogel solution was then pipetted into 12 well plate well inserts and allowed to set for 30 minutes. Culture medium was then added on top of the hydrogels and cultured for 24 hours at 21% oxygen. Chorion derived MSCs and amnion derived MSCs were cultured, trypsinised and counted (section 0). Cells were plated at a density of 20,000 cells/well in 12 well plates and cultured in culture media for 24 hours at 21% oxygen. Using sterile technique, tweezers were used to remove the well inserts and place them in the appropriate well containing either aMSCs or cMSCs (illustrated in Figure 5.1). Culture medium was gently aspirated from the hydrogels surface and cells in monolayer. Control samples were included which were cultured without any MSCs but underwent the same conditions. Samples were cultured for 20 days at either 21% oxygen or 40% oxygen at 37°C. Medium was changed every 2-3 days.
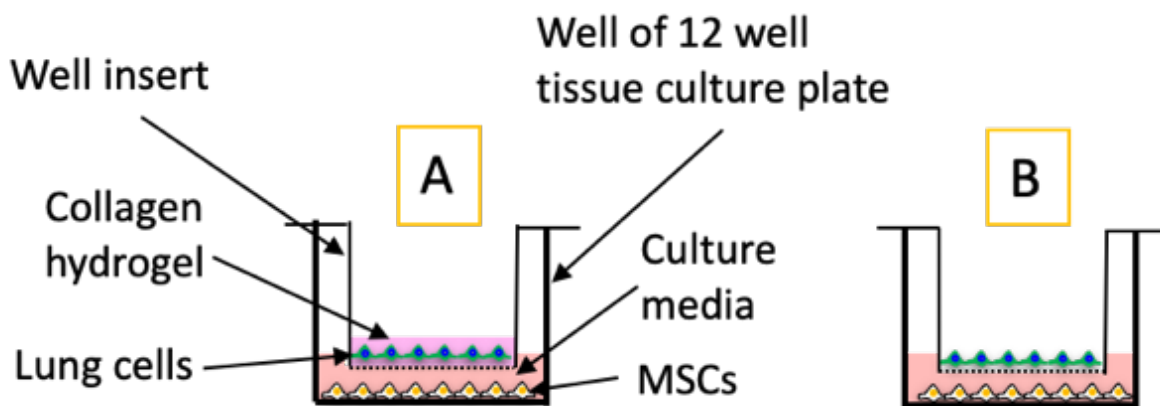
Figure 5.1 Experimental set-up of human lung cells co-cultured with placenta derived MSCS and exposed to 21% or 40%. Lung cells (35FL or NLF) were cultured on porous well plate inserts in 3D collagen-elastin hydrogels (image A) or as 2D monolayer (image B). Placenta derived MSCs (amnion MSCs or chorion MSCs) were co-cultured with the lung cells at the bottom of the well plate. All cells were cultured at 21% oxygen or 40% oxygen for 20 days.

5.4.4.2 Experimental analysis

To examine if the effect of MSCs co-cultured with lung cells at hyperoxygen the same output measures as before were used to examine hydrogel contraction, DNA quantification and cell imaging. On day 20 hydrogels were digested (section 2.12) and DNA quantified (section 2.13). Samples were stained with LiveDead staining assay (section 2.7) and imaged using confocal microscopy, including z-stacks to produce a 3D representative image. All cells (35Fl, NLF, aMSCs and cMSCs) were also imaged using phase contrast microscopy. Every 5 days of culture hydrogel depth was measured using OCT (section 2.10) and percentage change in gel depth calculated.

5.4.5 Statistical analysis

Hydrogel measurements, DNA quantification, gene analysis and TEER results were all statistically compared using two- way ANOVA with Tukey's multiple comparisons test to

determine the statistical significance, $p \leq 0.05$ was considered significant. Analysis was performed using GraphPad Prism version 7.01. All values quoted in the results are mean average ± standard deviation.

5.5 Results

5.5.1 Adult lung cells

5.5.1.1 The effect of hyperoxia on adult lung cells cultured in 2D and 3D at 21% oxygen and 40% oxygen

Adult lung fibroblasts cells (35FL) and epithelial cells (A549) were cultured in monolayer or 3D collagen-elastin hydrogels (1:1) for 20 days at 21% or 40% oxygen. Cells were co-cultured with placenta derived MSCs or single cell culture. Hyperoxia caused a decrease in hydrogel contraction for 35FL seeded hydrogels suggesting high oxygen culture affects the contraction of adult lung fibroblasts (Figure 5.2). However, this effect was not shown to be significant. Co-culture hydrogels also contracted more rapidly at 21%. It is likely this contraction was due to the 35FL cells because there was negligible contraction of A549 only gels. DNA quantity significantly (P<0.0001) increased for all sample types except for 35FL samples cultured at 40% oxygen, these cells whether in monolayer or hydrogels did not significantly increase DNA quantity. This indicates cell proliferation of 35FL cells is affected by 40% oxygen culture. This is further supported by microscopic images in which fewer 35FL cells could be observed at 40% oxygen than 21% oxygen (Figure 5.3). The LiveDead staining assay indicated cell viability was good with only green fluorescently stained cells observed in all samples. The stained 35FL in monolayer have a less elongated morphology at 40% than 21% oxygen. The z-stacks (Figure 5.4) demonstrates A549 cells remain as a monolayer on the hydrogel surface. The 35FL are dispersed throughout the gel and have migrated towards the bottom of the hydrogel where medium is. No difference between the dispersion of cells can be observed at 21% or 40% oxygen.
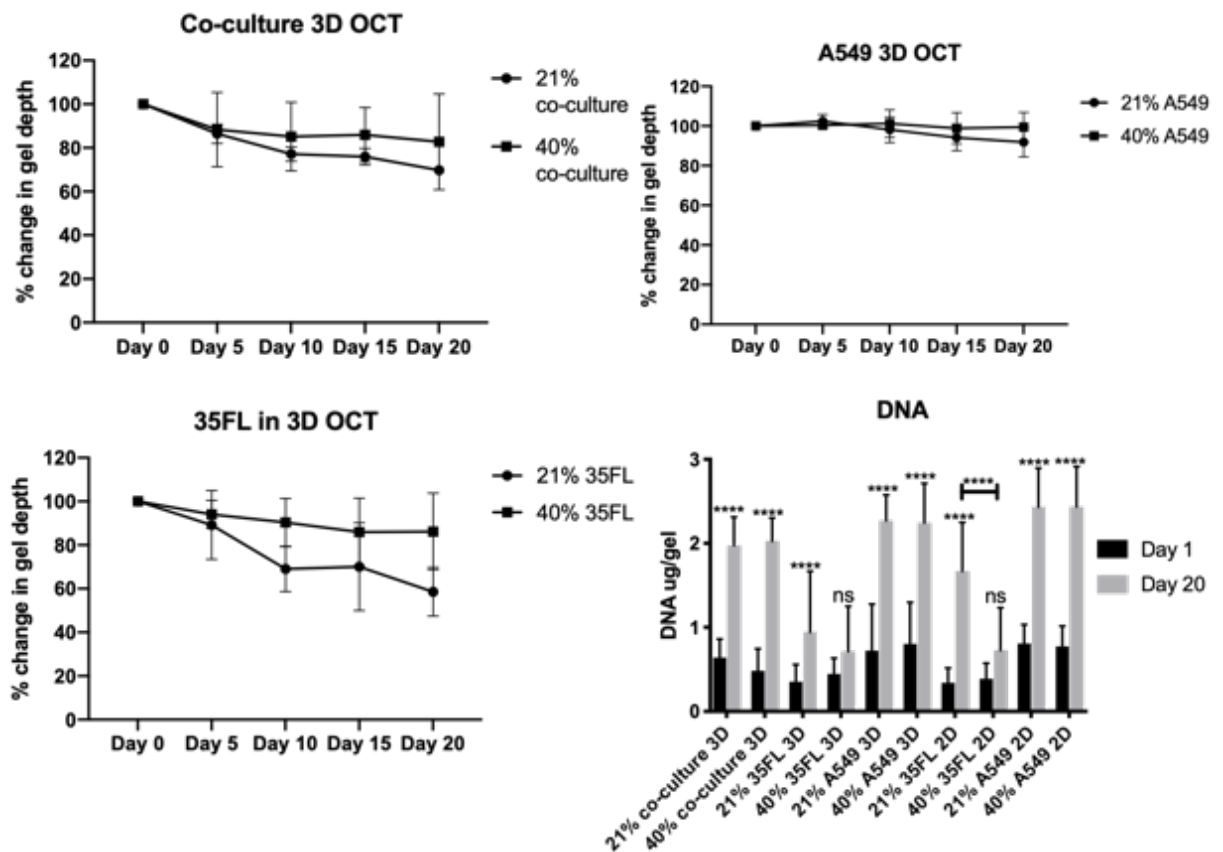
Figure 5.2 Human adult lung cells cultured in 3D collagen-elastin hydrogel or 2D monolayer at 21% or 40% oxygen. Lung fibroblast cells 35FL were cultured in 3D collagen-elastin (1:1) hydrogels and lung epithelial cells A549 cultured on the hydrogel surface. The cells were cultured as a single cell culture or in co-culture. The same cells were also cultured in 2D monolayer. All samples were cultured at 40% oxygen or 21% oxygen for 20 days. Percentage change in hydrogel depth was measured every 5 days and DNA quantified using the PicoGreen quantification assay. Contraction of hydrogel was observed to be more rapid for co-culture 3D and 35FL 3D at 21% oxygen. This contraction is likely due to the 35FL cells since there was negligible contraction observed for A549 3D. There was no statistically significant change in 3D hydrogel contraction in any of the groups. At 40% oxygen DNA quantity for 35FL cells in 3D and 2D does not significantly increase suggesting hyperoxia affects cell proliferation. A549 cell DNA is no different at 21% and 40% oxygen. The co-culture hydrogels DNA was also not affected by 40% oxygen, the predominant cell in these samples are the A549. Data are expressed as mean ± standard deviation, n=6 (****p≤0.0001).
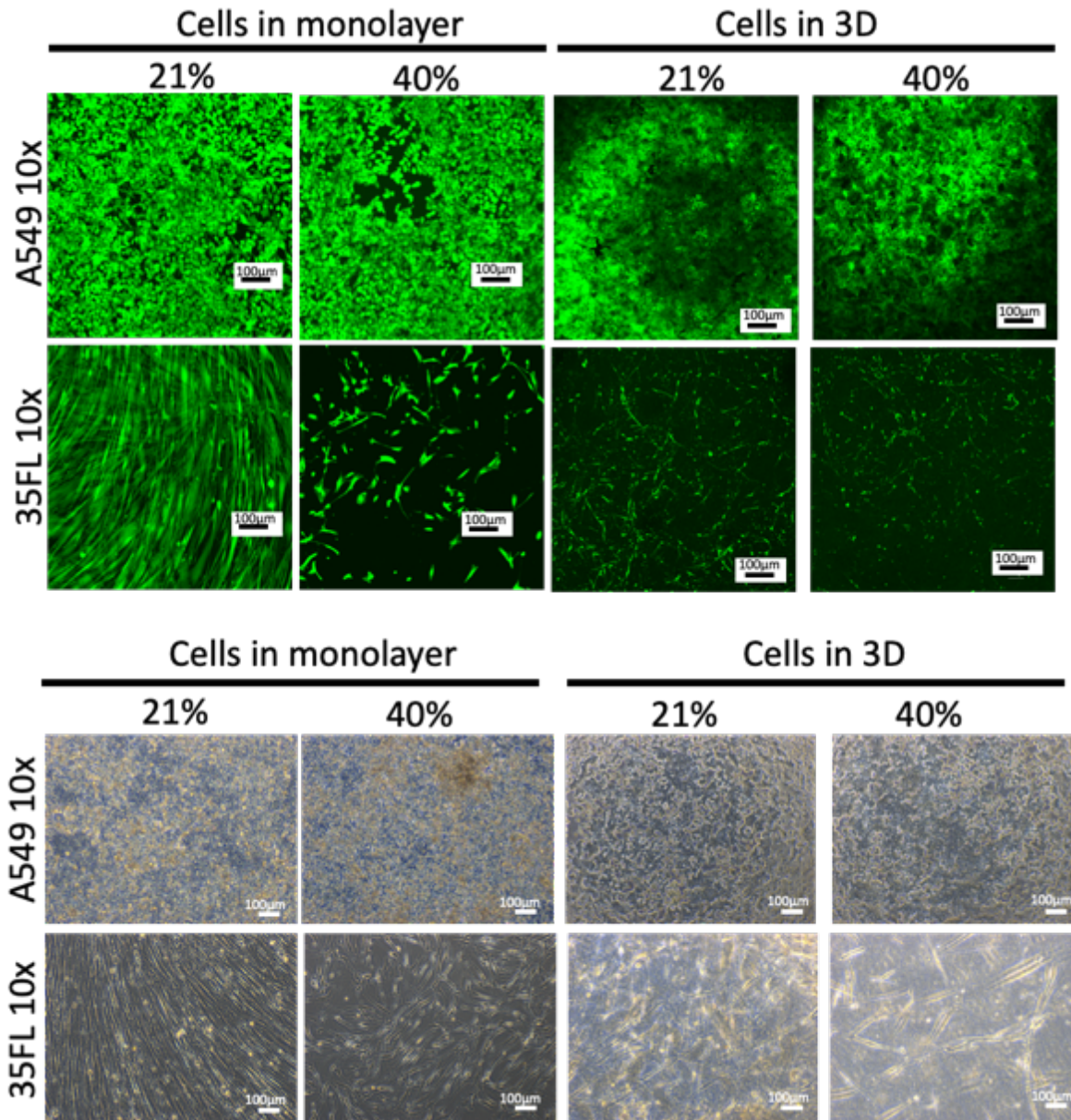
Figure 5.3 Adult lung cells cultured in monolayer or 3D collagen-elastin hydrogels at 21% and 40% oxygen and imaged by fluorescence and phase contrast microscopy. Adult lung fibroblasts 35FL and epithelial cells A549 were seeded in monolayer or collagen-elastin (1:1) hydrogels and cultured at 21% or 40% oxygen. The cells were stained with the LiveDead staining assay and imaged with confocal microscopy and phase contrast microscopy. The presence of green fluorescence indicates cell viability was uncompromised by the hyperoxia. Fewer cells can be seen in both the phase contrast and confocal images of 35FL in monolayer at 40% oxygen suggesting hyperoxia slows down 35FL cell proliferation.
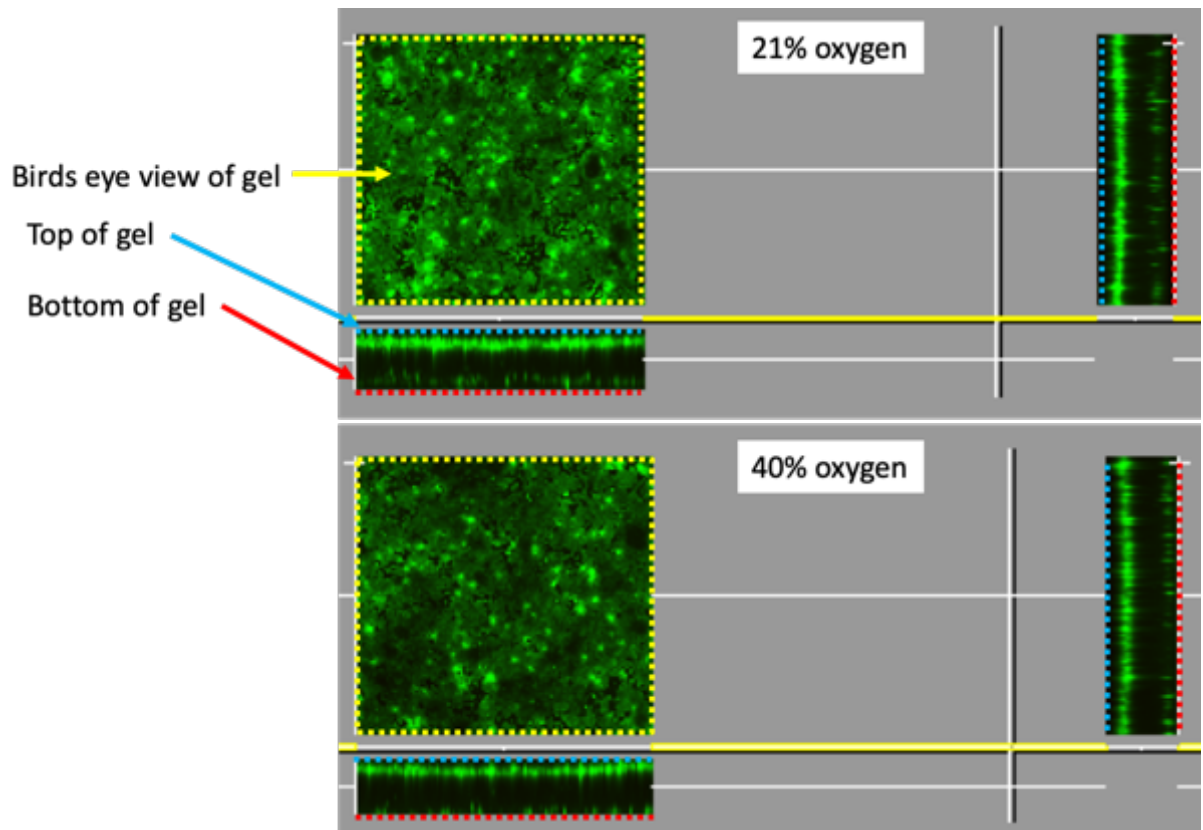
Figure 5.4 Orientation of adult lung cell populations in 3D collagen-elastin hydrogel at 21% and 40% oxygen. Adult lung fibroblasts 35FL and epithelial cells A549 were co-cultured in collagen-elastin (1:1) hydrogels and cultured at 21% or 40% oxygen. The cells were stained with the LiveDead staining assay and imaged by confocal microscopy. Z-stacks were taken of the samples to create a 3D image. The A549 cells form a monolayer on the hydrogel surface and do not migrate through the hydrogel. The 35FL are dispersed throughout the hydrogels and migrate towards the bottom of the hydrogel likely towards the medium containing nutrients. The dispersion and migration of 35FL are unaffected by hyperoxia.

5.5.1.2 Adult lung cells expression of BPD related genes

The gene expression of BPD related markers relative to the housekeeping gene GAPDH is shown in Figure 5.5-Figure 5.9. The genes of interest included TGFβ, Collagen type 1, Elastin, NQO1 and smooth muscle actin (SMA). We analysed all sample types and compared cultures at 21% and 40% oxygen, 2D versus 3D after 20 days in culture. The only significant result observed was a raised expression level of NQO1 for A549 cells

cultured in monolayer at 40% oxygen (P<0.05) and co-culture collagen-elastin hydrogels

cultured at 40% oxygen (P<0.01).

We compared gene expression levels in 2D versus 3D culture to assess variations in

expression of ECM related markers (collage, elastin and smooth muscle actin). COL1A was

upregulated in A549 cells cultured in 3D. Elastin and SMA for 35FL in 3D culture were

both downregulated.   When cells were in co-culture TGFβ, COL1A, SMA were all

downregulated compared to single cell cultures; however none were found to be

statistically significant (P>0.05).
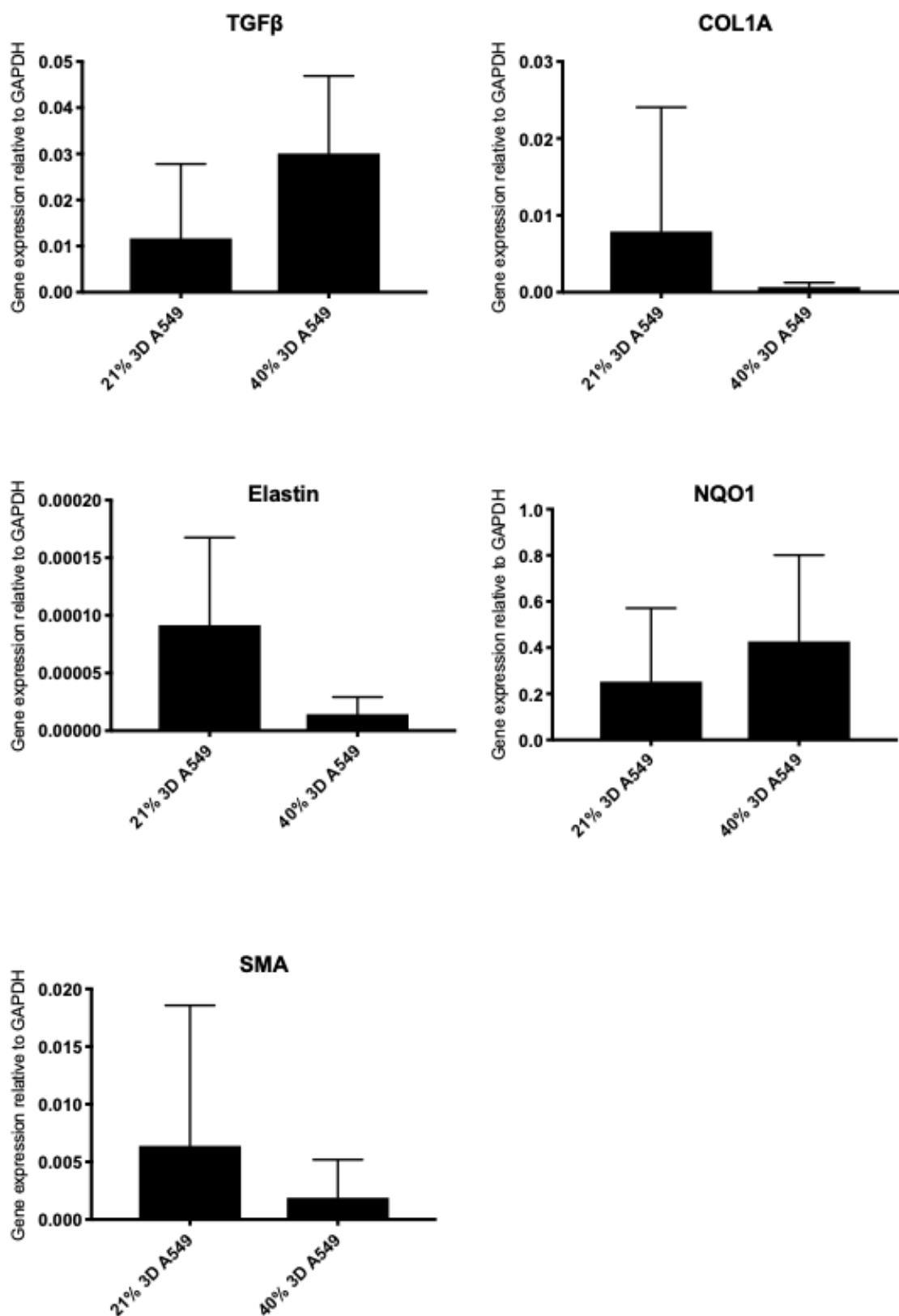
Figure 5.5 Gene expression of lung cells A549 cultured on collagen-elastin hydrogels at 40% or 21% oxygen. RT-PCR was used to analyse the expression of BPD related genes TGFβ, Collagen, Elastin, NQO1 and SMA relative to GAPDH expression of A549 cells cultured on the surface of collagen-elastin (1:1) hydrogels cultured at 21% of 40% oxygen. Data are expressed as mean ± standard deviation, n=4.
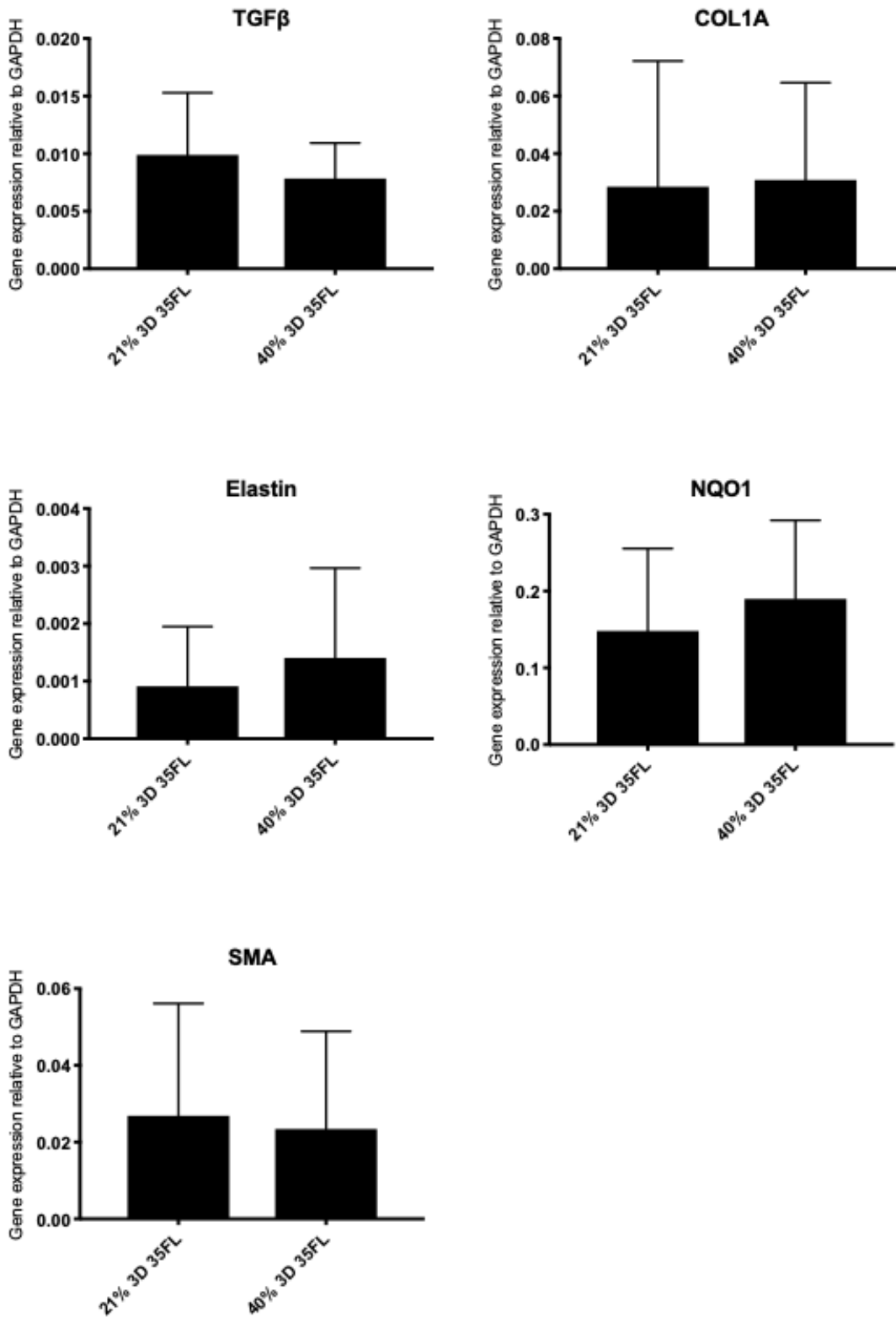
Figure 5.6 Gene expression of lung cells 35FL cultured in collagen-elastin hydrogels at 40% or 21% oxygen. RT-PCR was used to analyse the expression of BPD related genes TGFβ, Collagen, Elastin, NQO1 and SMA relative to GAPDH expression of 35FL cells cultured in the collagen-elastin (1:1) hydrogels cultured at 21% of 40% oxygen. Data are expressed as mean ± standard deviation, n=4.
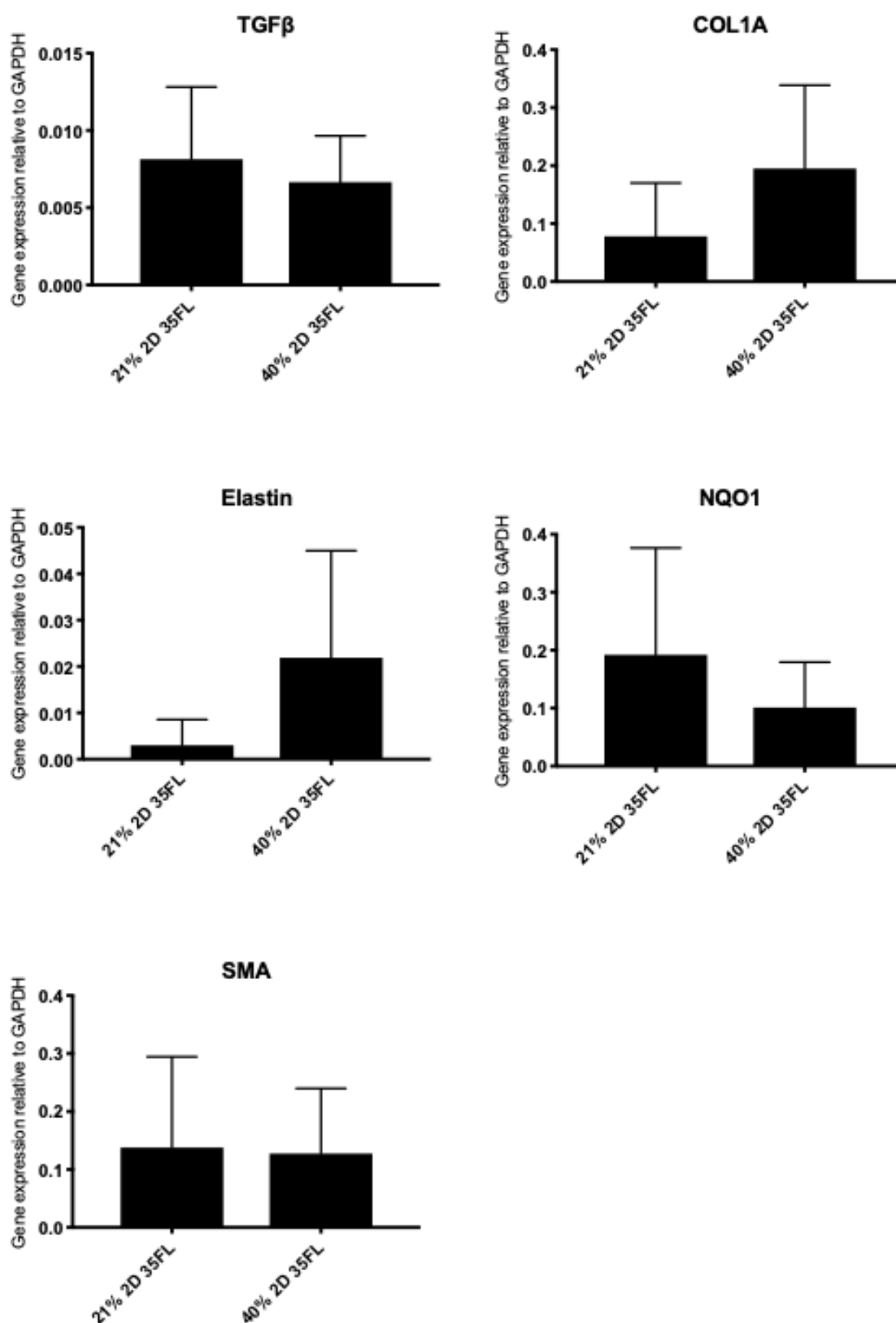
Figure 5.7 Gene expression of lung cells 35FL cultured in monolayer at 40% or 21% oxygen. RT-PCR was used to analyse the expression of BPD related genes TGFβ, Collagen, Elastin, NQO1 and SMA relative to GAPDH expression of 35FL cells cultured in monolayer at 21% of 40% oxygen. Data are expressed as mean ± standard deviation, n=4.
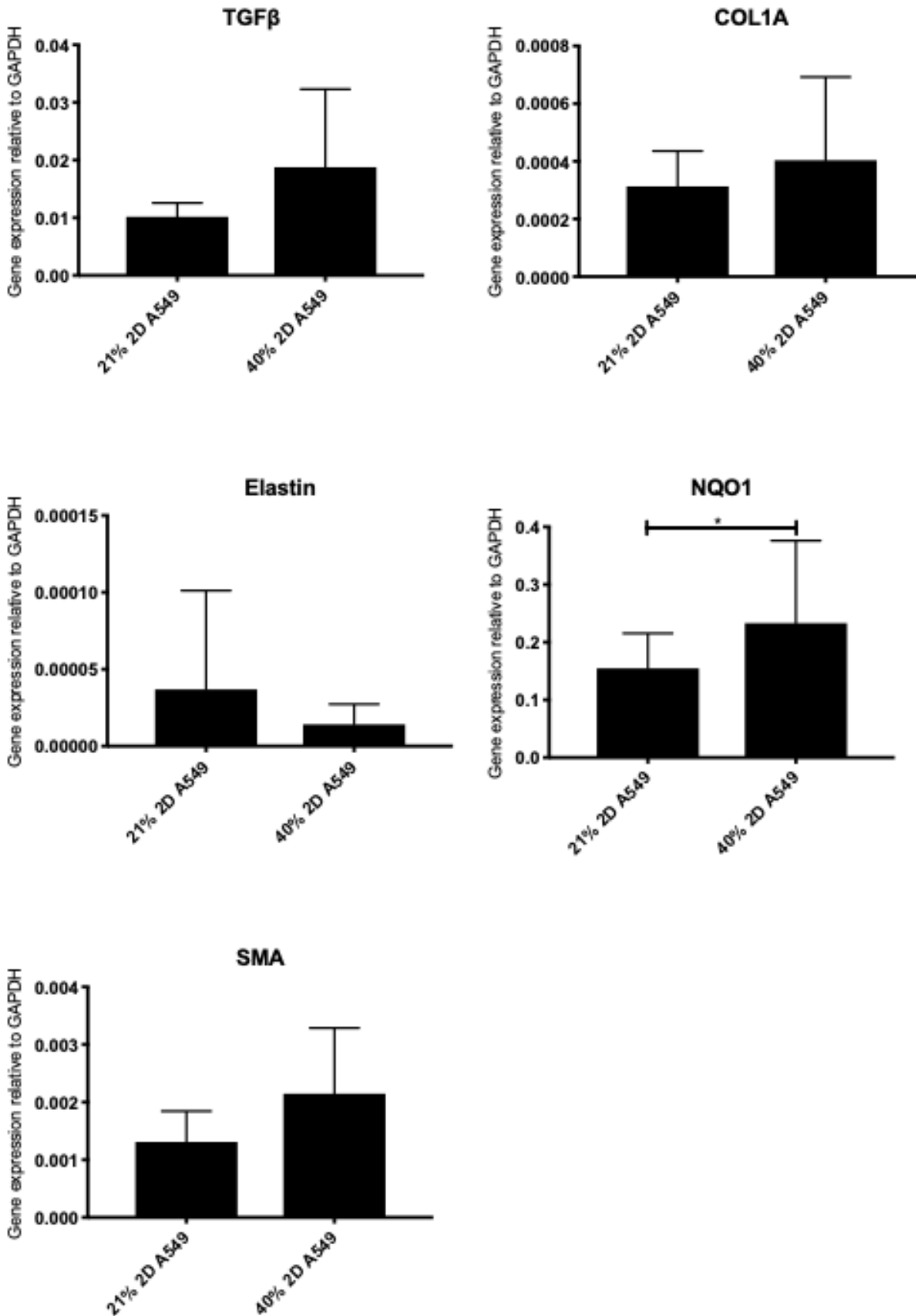
Figure 5.8 Gene expression of lung cells A549 cultured in monolayer at 40% or 21% oxygen. RT-PCR was used to analyse the expression of BPD related genes TGFβ, Collagen, Elastin, NQO1 and SMA relative to GAPDH expression of A549 cells cultured in monolayer at 21% of 40% oxygen. Data are expressed as mean ± standard deviation, n=4 (*p≤0.05).
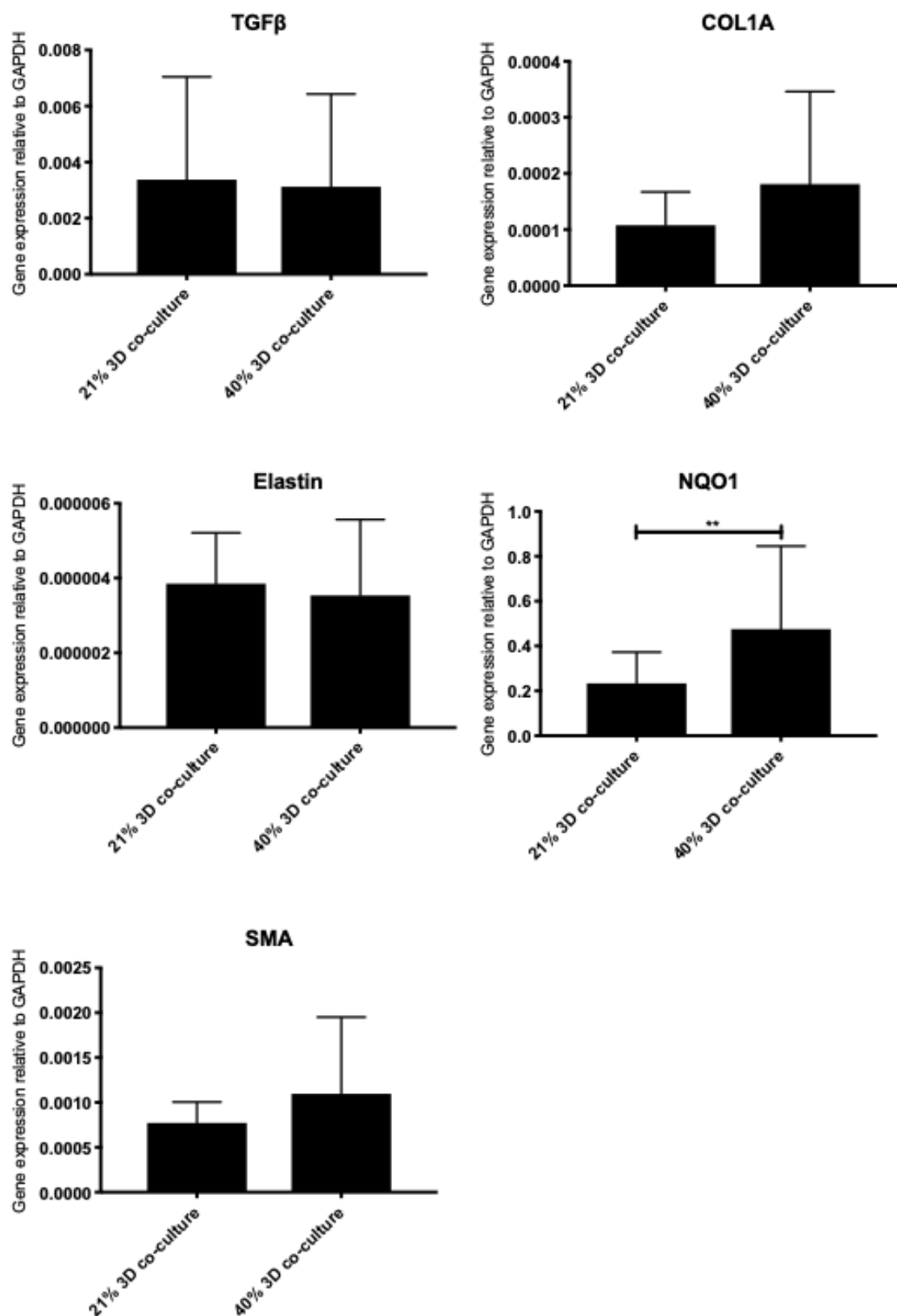
Figure 5.9 Gene expression of lung cells 35FL and A549 cultured in co-culture in 3D constructs at 40% or 21% oxygen. RT-PCR was used to analyse the expression of BPD related genes TGFβ, Collagen, Elastin, NQO1 and SMA relative to GAPDH expression of cells cultured in the collagen-elastin (1:1) hydrogels cultured at 21% of 40% oxygen. Data are expressed as mean ± standard deviation, n=4 (**p≤0.05).

5.5.1.3 TEER of A549 cells cultured at 21% and 40% oxygen.

To assess the integrity of lung epithelial cell monolayer cultured at 21% and 40% oxygen A549 cells were seeded in 12 well plate well inserts and allowed to form a confluent monolayer or were seeded on the surface of collagen-elastin hydrogels (acellular or seeded with 35FL). For the 2D culture TEER was assessed every 7 days for up to 28 days and phase contrast images taken. For the 3D culture TEER was assessed at day 28 (Figure 5.10). At day 7 TEER was significantly reduced (P<0.001) for A549 in 2D monolayer at 40% oxygen. From day 14 onwards TEER was the same in both oxygen conditions. For 3D culture TEER was significantly improved for co-culture samples. Phase contrast images show A549 in 2D monolayer at 10x and 20x magnification. No differences in cell morphology or monolayer formation can be observed in the different oxygen conditions.
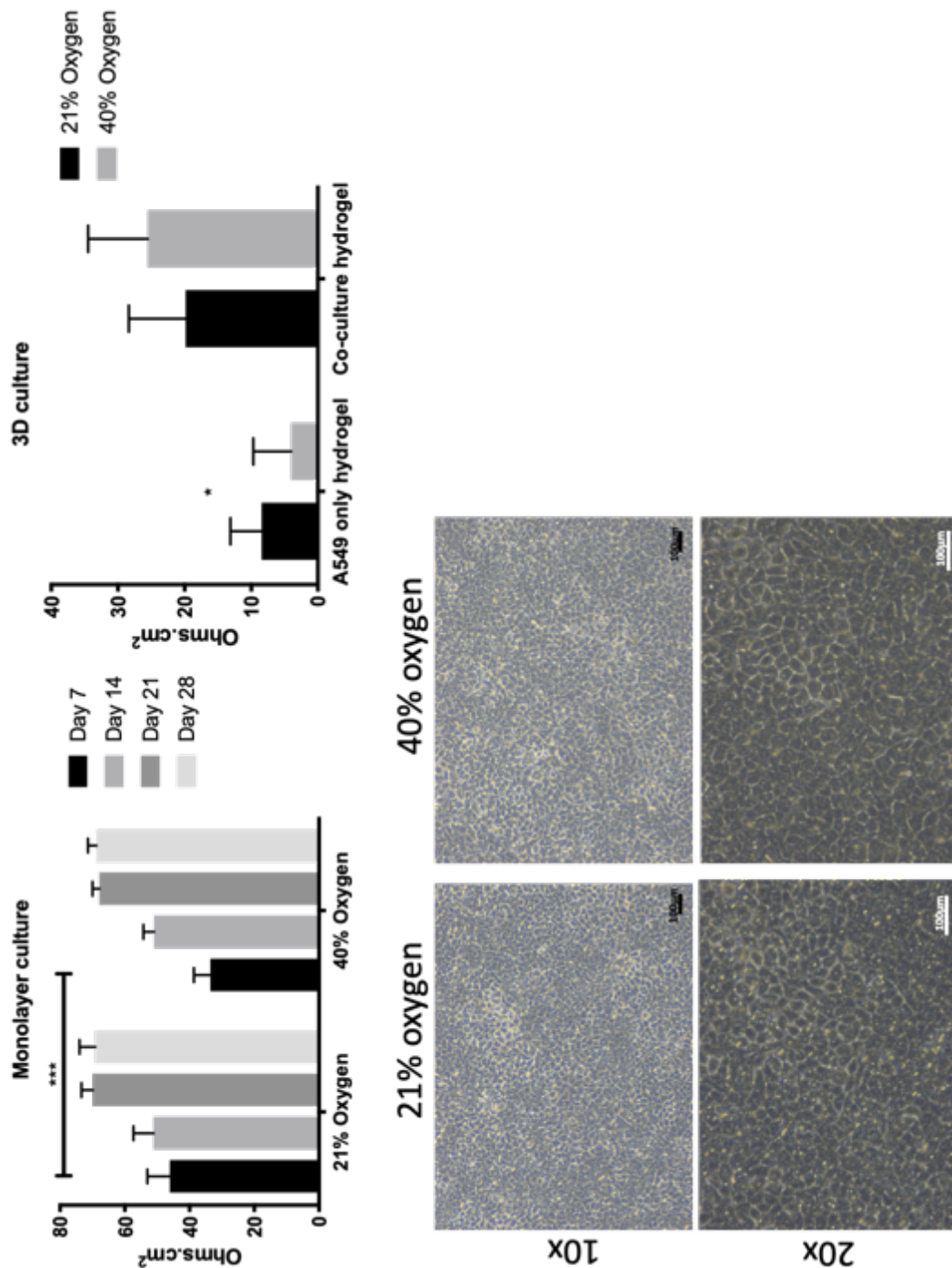
Figure 5.10 TEER analysis of human lung cells A549 cultured in monolayer on culture well plate inserts or on 3D collagen-elastin hydrogels cultured at 21% or 40% oxygen. Lung cells A549 well culture at 21% or 40% oxygen in monolayer directly on well plate inserts or on collagen-elastin hydrogels (acellular or seeded with lung fibroblasts 35FL). Samples were cultured up to 28 days and TEER measurements taken. The co-culture of A549 and 35FL significantly increased the TEER. Hyperoxia affects the TEER of A549 cultured at 40% oxygen by day 7. By day 14 the cells recover since there is no significant difference between oxygen concentrations. Cells were imaged using phase contrast microscopy showing a confluent monolayer. Data were normalised with acellular hydrogels and are expressed as mean ± standard deviation, n=6 (*p≤0.05, ***p≤0.001).

5.5.2 Neonatal cells

5.5.2.1 The effect of hyperoxia on neonatal lung cells cultured in 2D and 3D at

21% oxygen and 40% oxygen

Isolated neonatal cells from tracheal suctionings of ventilated neonates (NLF) were

seeded in monolayer or in collagen-elastin hydrogels and cultured at 21% or 40% oxygen.

All samples significantly increased in DNA over 20 days in culture. There was no

significant difference in quantified DNA after 20 days in culture when cultured at 40%

oxygen compared with 21% oxygen (Figure 5.11). Hydrogels cultured at 21% and 40%

oxygen both contract at a similar rate with hydrogels cultured at 21% oxygen culturing

slightly more, but this was not statistically significant (Figure 5.11). Phase contrast images

of the cells after 20 days in culture so no variation in cell numbers or morphology (Figure

5.12).
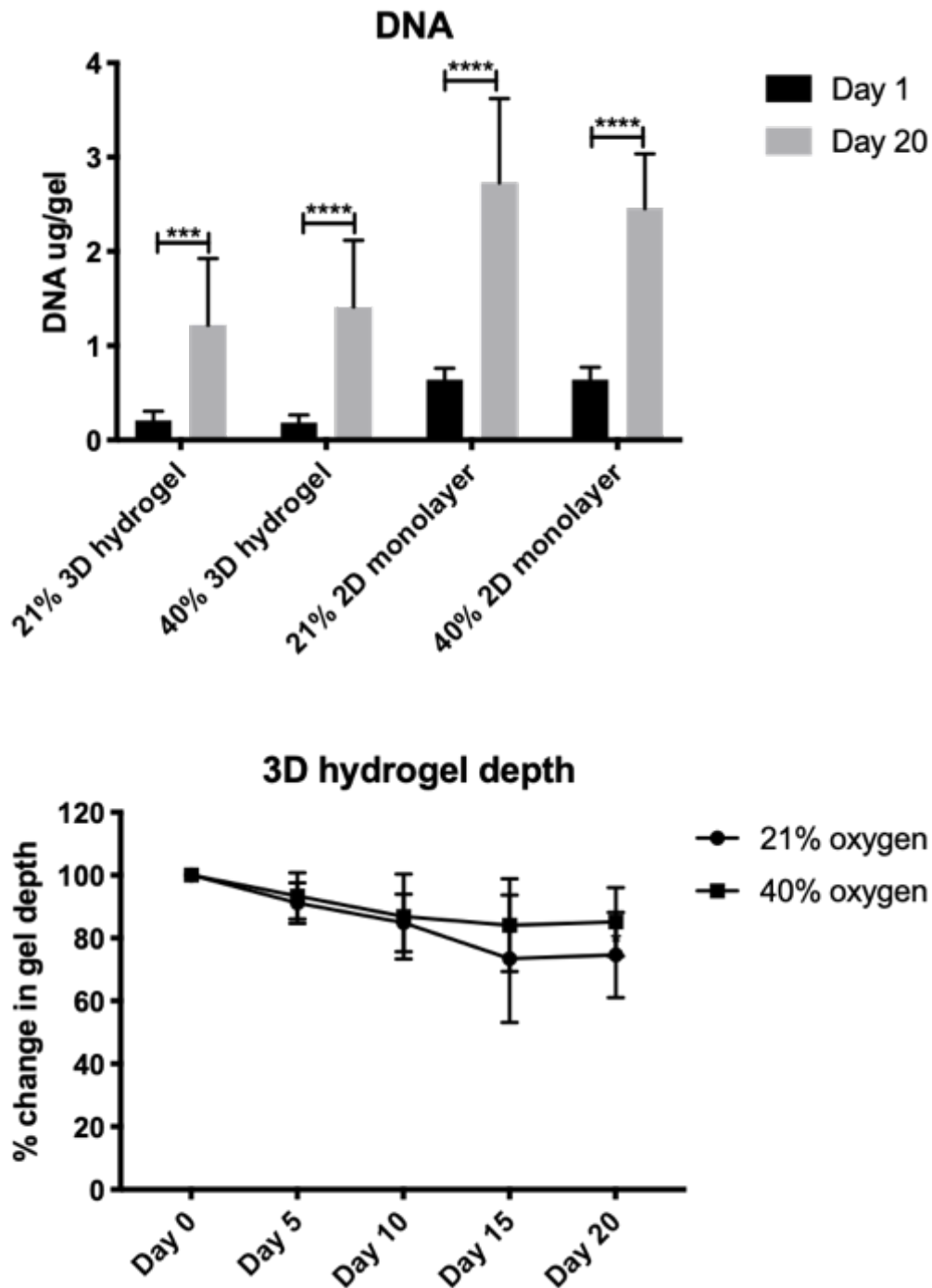
Figure 5.11 Human neonatal lung cells cultured in collagen-elastin hydrogels or in monolayer at 21% or 40% oxygen. Lung cells isolated from the tracheal aspirates of ventilated neonates were cultured in well plate inserts in monolayer or seeded within collagen-elastin hydrogels (1:1) and cultured at 21% or 40% oxygen for 20 days. After this, DNA was quantified using the PicoGreen DNA quantification kit and compared to day 1. Change in hydrogel depth was calculated using the OCT to measure hydrogel depth every 5 days. DNA significantly increased for all groups indicating cell proliferation was not affected by 40% oxygen. Hydrogel contraction was observed to be reduced at 40% oxygen however this is not statistically significantly. Data are expressed as mean ± standard deviation, n=9 (*** p≤0.001).
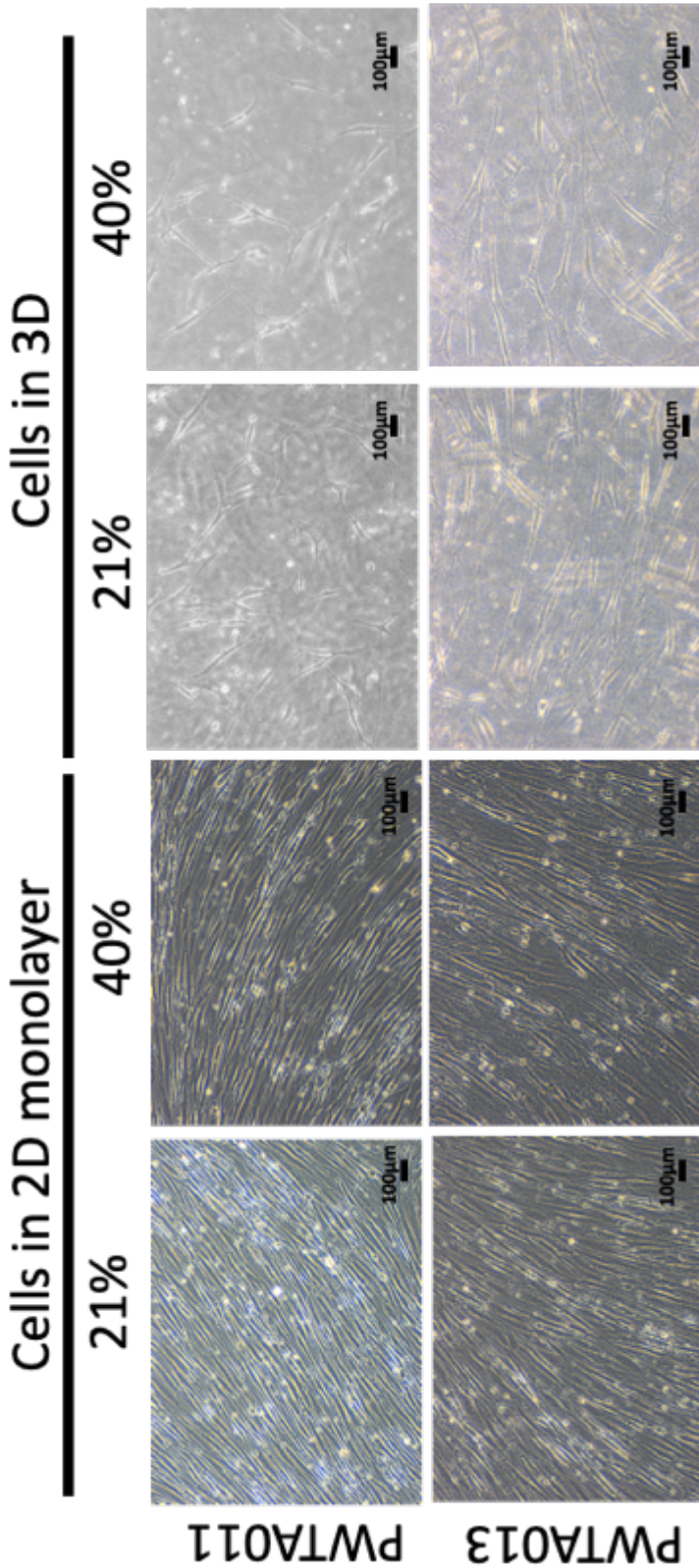
Figure 5.12 Human neonatal lung cells cultured in collagen-elastin hydrogels or in monolayer at 21% or 40% oxygen. Cells isolated from tracheal suctions of ventilated neonates were cultured in monolayer on well plate inserts or in collagen-elastin hydrogels (1:1) and imaged after 20 days of culture using phase contrast microscopy. Cells isolated from 2 samples (PWTA011 and PETA013) were cultured. There are no observed differences in cell number or cell morphology at 21% or 40% oxygen.

5.5.2.2 Neonatal lung cells gene expression of BPD related markers

The gene expression of BPD related markers relative to the housekeeping gene GAPDH is shown in Figure 5.13. The genes of interest included TGFβ, Collagen type 1, Elastin, NQO1 and smooth muscle actin (SMA). We analysed neonatal cells cultured in 2D and 3D hydrogels and compared culture at 21% and 40% after 20 days. There was no significant change in gene expression when cultured in 3D or under hyperoxia.
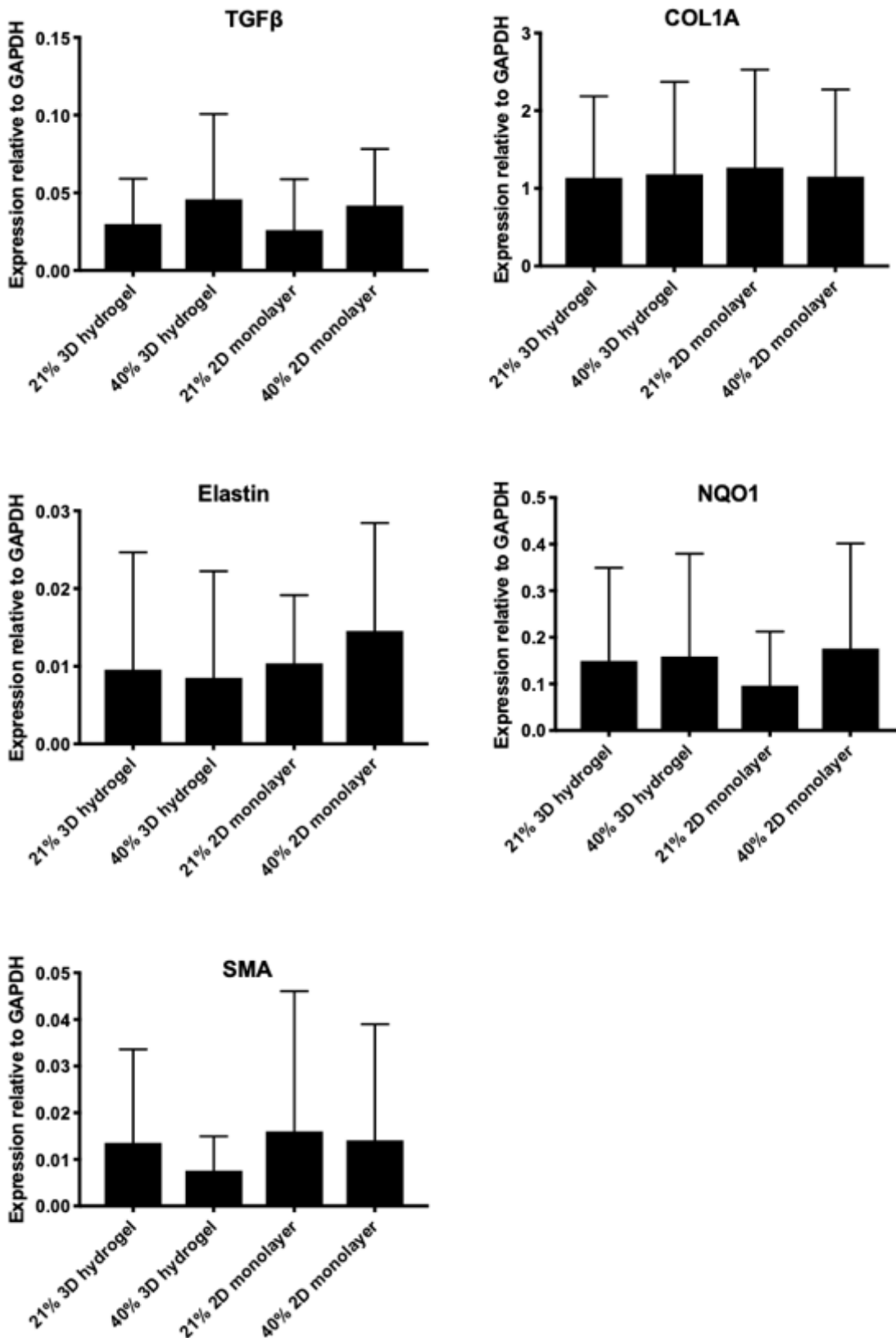
Figure 5.13 Gene expression of neonatal lung cells cultured in 2D monolayer or in 3D collagen-elastin hydrogels at 40% or 21% oxygen. RT-PCR was used to analyse the expression of BPD related genes TGF beta, Collagen, Elastin, NQO1 and SMA relative to GAPDH expression of cells isolated from the tracheal suctions of ventilated neonates and cultured at 21% or 40% oxygen. Data are expressed as mean ± standard deviation, n=4.

5.5.3 Adult human lung cells co-cultured with placenta MSCs

To assess if MSCs could protect lung cells from the effect of hyperoxia, human adult lung cells 35FL were co-cultured with cMSCs and aMSCs in monolayer or 3D. Well inserts were used for co-cultures, so any effect seen was due to paracrine signalling. Single cell type cultures were included as controls.

5.5.3.1 Monolayer cultures

As previously shown in monolayer cultures of aMSCs, cMSCs and 35FL, DNA quantity was all reduced when cultured at 40% oxygen. When the lung cells 35FL were co-cultured with MSCs, both aMSCs and cMSCs significantly increased (*) the DNA quantity of 35FL cells (Figure 5.14). This is representative in phase contrast images in which more 35FL cells can be observed when co-cultured with MSCs (Figure 5.15).

5.5.3.2 3D cultures

As well as monolayer cultures, lung cells 35FL were also cultured in 3D collagen-elastin (1:1) hydrogels in well inserts. Placenta MSCs (aMSCs and cMSCs) were cultured on the bottom of the well so cells were indirectly co-cultured. 40% oxygen had a detrimental effect on DNA quantification for 35FL hydrogels. The co-culture of aMSCs or cMSCs statistically increased DNA quantification when cultured in monolayer 40% oxygen. The same effect was not seen for cells in 3D. At 21% oxygen the co-culture of MSCs with 35FL hydrogels caused a significant decrease in DNA quantity compared to 35FL hydrogels alone (****). Hydrogel contraction was slightly reduced at 40% oxygen and the addition of MSCs had no statistical influence on this. Confocal microscopy imaging (Figure 5.16) showed green fluorescent staining of cells indicating cells had a good viability at both 21% and 40% oxygen when co-cultured with MSCs. However, cells can be observed to have migrated less at 40% oxygen
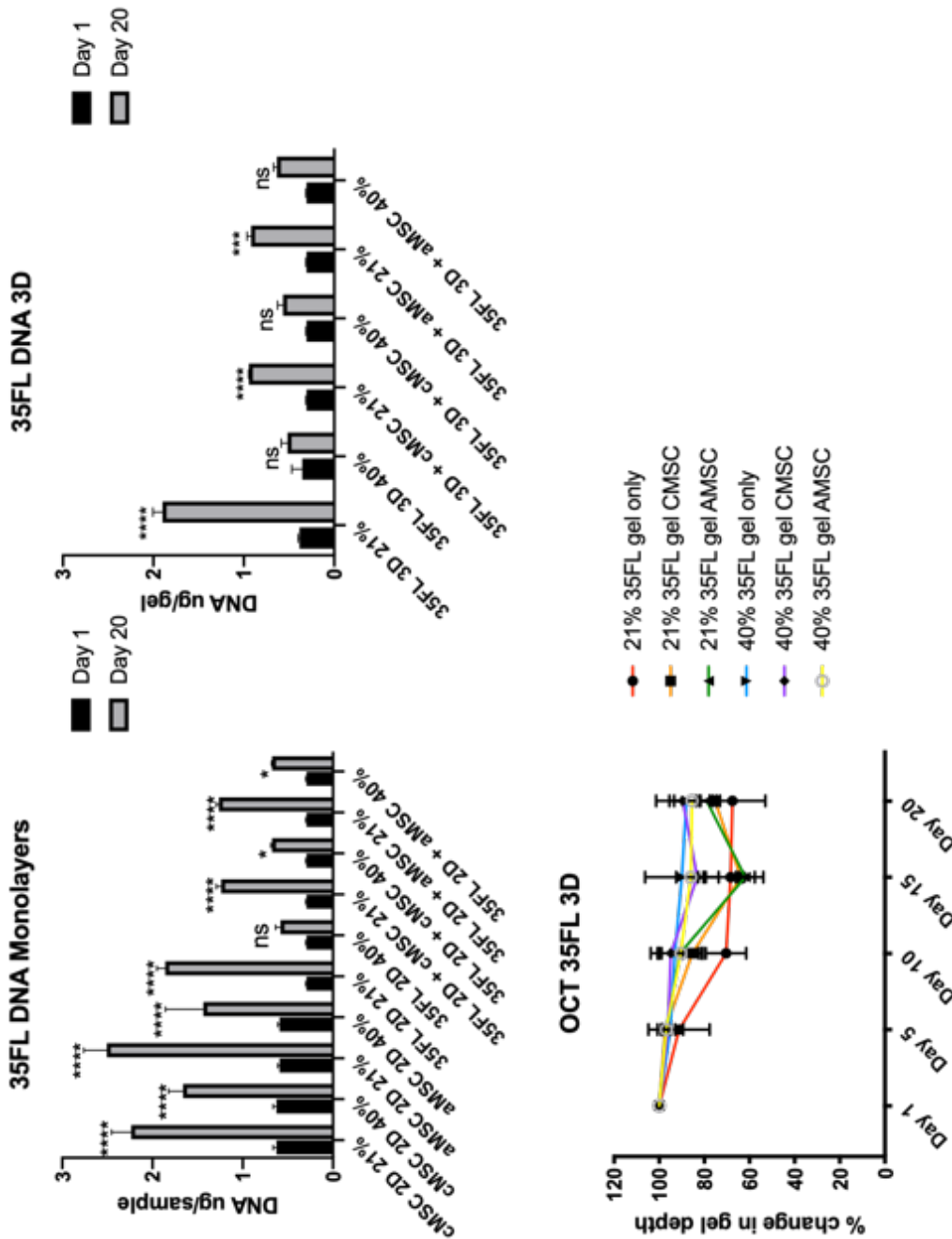
Figure 5.14 Human adult lung cells co-cultured with placenta MSCs in 3D hydrogels or 2D monolayer at 21% or 40% oxygen. Human adult lung cells 35FL were cultured in 3D collagen-elastin hydrogels and were co-culture with placenta MSCs (cMSCs or aMSCs). Samples were exposed to either 21% or 40% oxygen for 20 days. DNA was quantified using the PicoGreen DNA quantification assay on day 1 and day 20. Hydrogel depth was measured using OCT every 5 days and change in depth was calculated. 40% oxygen prevents 35FL DNA increasing but when they are in monolayer and co-cultured with MSCs a statistically significant increase is observed. The rate of hydrogel contraction is reduced at 40% oxygen however this is not significant. Data is expressed as mean ± standard deviation, n=4 (* p≤0.1, *** p≤0.001, **** p≤0.0001, ns not significant).
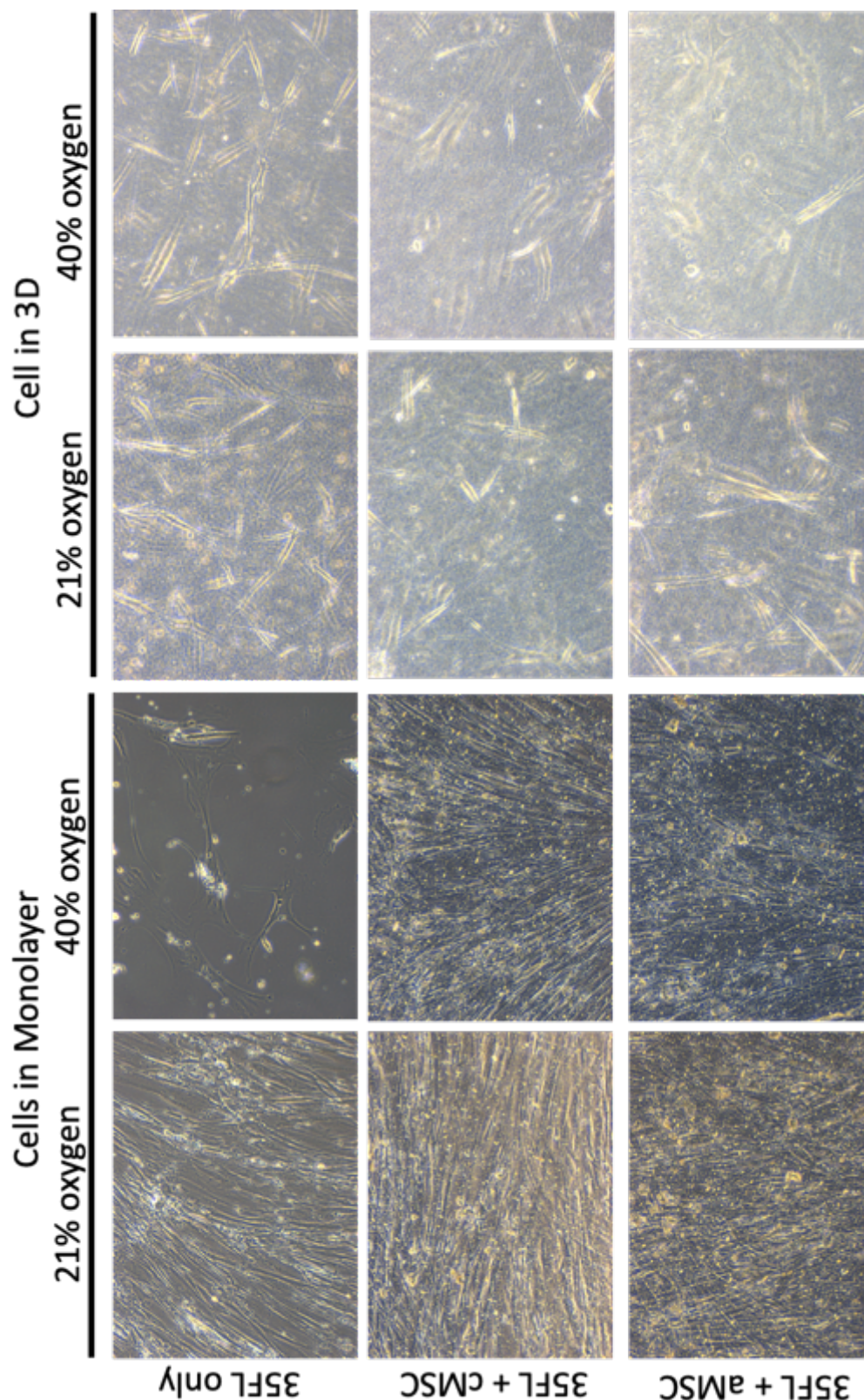
Figure 5.15 Human adult lung cells co-cultured with placenta MSCs in monolayer and 3D hydrogels at 21% or 40% oxygen. Human adult lung cells (35FL) were cultured in 3D collagen-elastin hydrogels and were co-cultured with placenta MSCs (cMSCs or aMSCs). Samples were exposed to either 21% or 40% oxygen for 20 days. Phase contrast images were taken on day 20. Fewer cells can be observed for 35FL cultured at 40% oxygen but when they are co-cultured with MSCs, more cells can be observed.
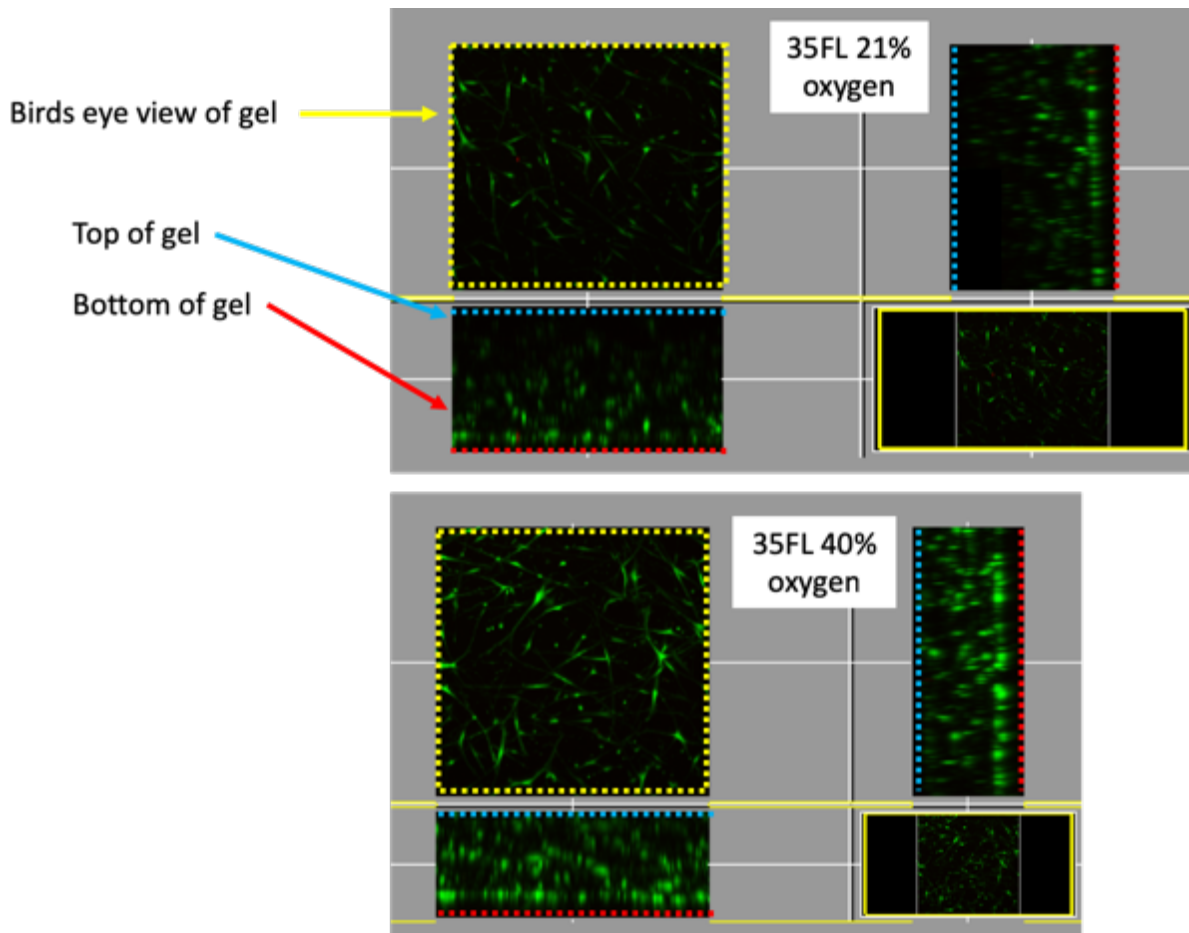
Figure 5.16 Human adult lung cells co-cultured with placenta MSCs in 3D hydrogels at 21% or 40% oxygen. Human adult lung cells (35FL) were cultured in 3D collagen-elastin hydrogels and were co-cultured with placenta MSCs (cMSCs or aMSCs). Samples were exposed to either 21% or 40% oxygen for 20 days after which they were stained with the LiveDead staining kit and imaged with confocal microscopy. Z-stacks were compiled to produce 3D images of the hydrogels. The presence of green fluorescently stained cells shows that cell viability was good at 21% and 40% oxygen. Cell are dispersed throughout the gels. At 40% oxygen there seems to be less migration of cells.

5.5.4 Neonatal human lung cells co-cultured with placenta MSCs

Previous results have indicated 40% oxygen has no detrimental effect on NLF cells. We repeated these experiments with the addition of placenta derived MSCs (cMSCs and aMSCs) to assess if there was any impact on cell performance. As with the adult lung cells previously, NLF cells were co-cultured with cMSCs and aMSCs in monolayer or 3D. Well inserts were used for co-cultures, so any effect seen was due to paracrine signalling. Single cell cultures were included as controls.

5.5.4.1 Monolayer cultures

NLF monolayer cultures were unaffected by hyperoxia in terms of DNA quantification (Figure 5.17). However, the DNA quantity of NLF cells was significantly reduced (*) when co-cultured with MSCs, independent of oxygen type and MSC type. Phase contrast images display NLF cells densely packed in all monolayer cell culture conditions (Figure 5.18).

5.5.4.2 3D cultures

Unlike the monolayer cultures, culture of NLF cells in 3D at 40% oxygen or the co-culture with MSCs had no significant effect of DNA quantity (Figure 5.17). The co-culture of NLF cells and MSCs did have a significant effect of hydrogel contraction at 40% oxygen (P<0.001) with no significant difference observed between cMSCs and aMSCs (Figure 5.17, change in gel depth). At 21% oxygen the co-culture with aMSCs significantly increased hydrogel contraction (P<0.01). 40% oxygen significantly (P<0.001) reduced the contraction of adult lung cells 35FL when cultured alone. As was observed for the adult lung cells, the LiveDead z-stack confocal images (Figure 5.19) demonstrated the migration of cells was less. The presence of green fluorescence demonstrates cell viability was good and unaffected by the co-culture of MSCs.
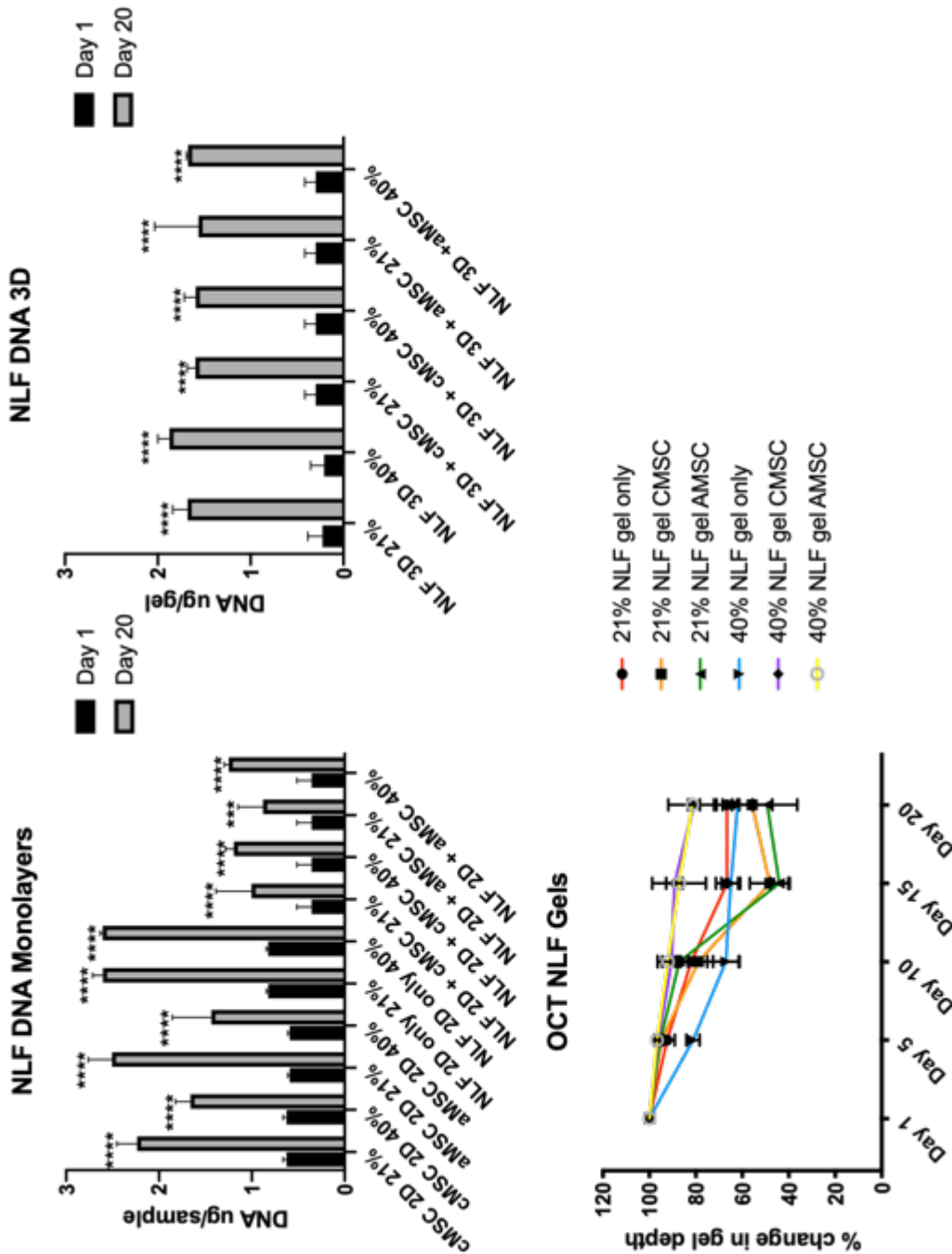
Figure 5.17 Human neonatal lung cells co-cultured with placenta MSCs in 3D hydrogels or 2D monolayers at 21% or 40% oxygen. Human neonatal lung cells NLF were cultured in 3D collagen-elastin hydrogels or in monolayer and were co-culture with placenta MSCs (cMSCs or aMSCs). Samples were exposed to either 21% or 40% oxygen for 20 days. Hydrogel depth was measured using OCT every 5 days and change in depth was calculated. DNA was quantified at day 1 and day 20 using the PicoGreen DNA quantification. The co-culture of NLF cells in monolayer with MSCs caused a significantly reduced DNA quantity at day 20 (****). 40% oxygen had no effect on DNA quantification of NLF cells in monolayer or 3D. 40% oxygen reduced hydrogel contraction, but the effect was not statistically significant. Data are expressed as mean ± standard deviation, n=4 (*** p≤0.001, **** p≤0.0001).
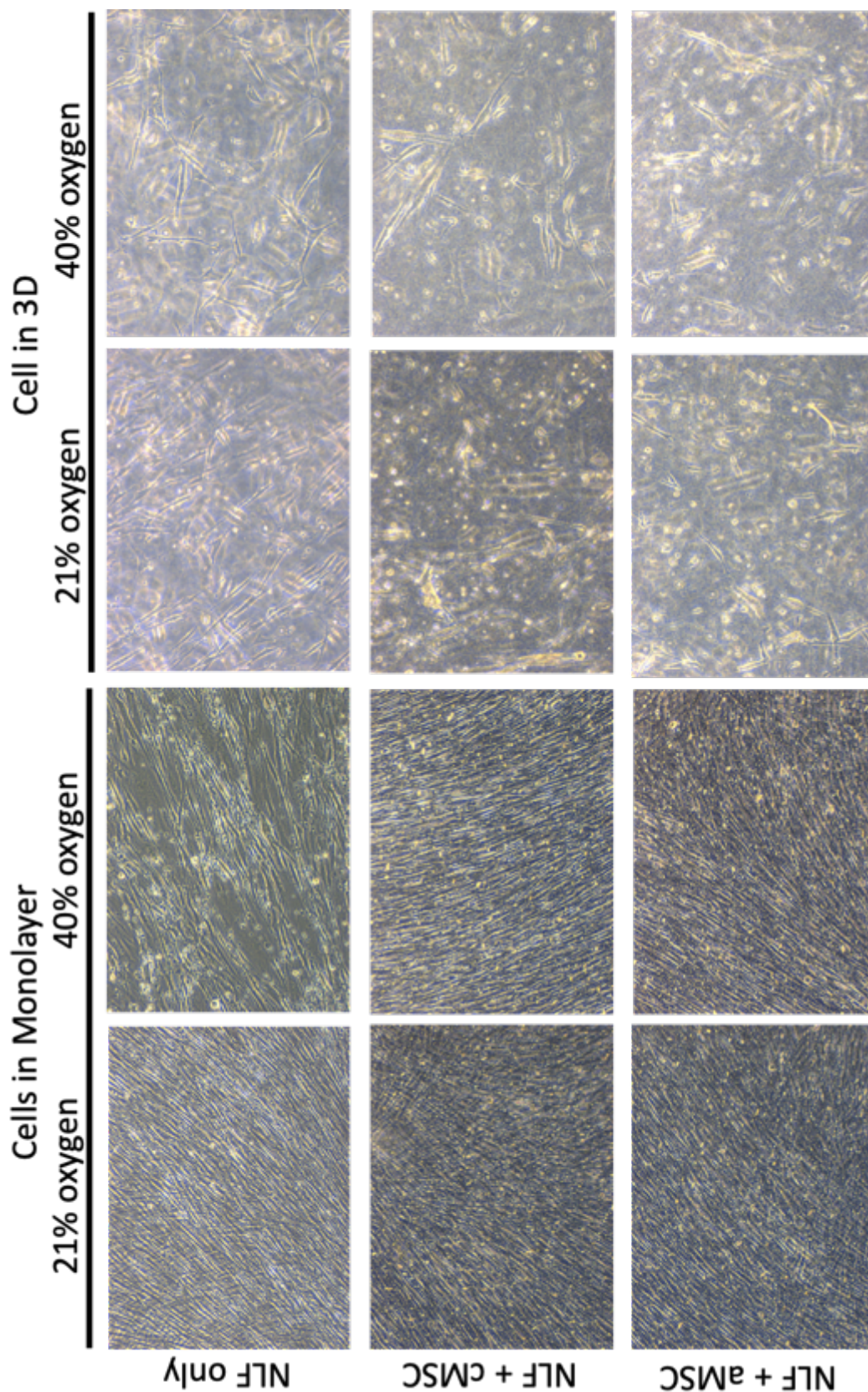
Figure 5.18 Neonatal lung cells co-cultured with placenta MSCs in monolayer and 3D hydrogels at 21% or 40% oxygen. Human neonatal lung cells (NLF) were cultured in 3D collagen-elastin hydrogels and were co-culture with placenta MSCs (cMSCs or aMSCs). Samples were exposed to either 21% or 40% oxygen for 20 days. Phase contrast images were taken on day 20.
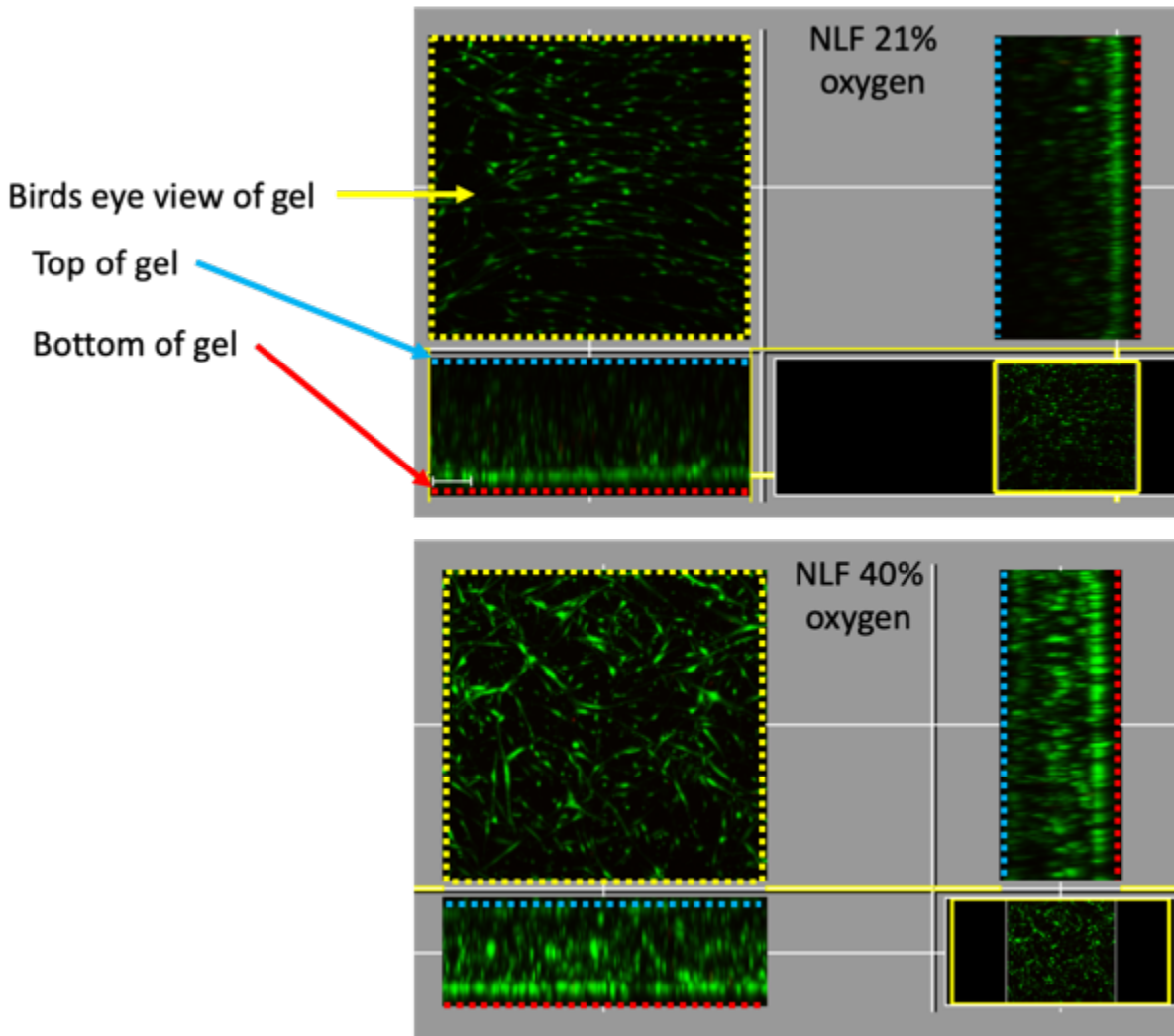
Figure 5.19 Human neonatal lung cells co-cultured with placenta MSCs in 3D hydrogels at 21% or 40% oxygen. Human neonatal lung cells (NLF) were cultured in 3D collagen-elastin hydrogels and were co-cultured with placenta MSCs (cMSCs or aMSCs). Samples were exposed to either 21% or 40% oxygen for 20 days. Z-stacks were compiled to produce 3D images of the hydrogels. The presence of green fluorescently stained cells shows that cell viability was good at 21% and 40% oxygen. Cell are dispersed throughout the gels. At 40% oxygen there seems to be less migration of cells.

5.6 Discussion

In this chapter we brought together aspects developed in the previous 2 chapters. Firstly, we cultured human adult lung fibroblasts (35FL) and human neonatal lung cell (NLF) in the developed 3D model and cultured at 40% oxygen to represent the high oxygen severe BPD neonates receive through endotracheal ventilation. The most severe BPD neonates

will commonly receive ventilation of 40% oxygen or above. It's these infants that require the most clinical intervention and therefore need to be targeted.

5.6.1 The effect of hyperoxia

5.6.1.1 Adult lung cells

We have shown that *in vitro* culture at 40% oxygen has a detrimental effect on adult lung fibroblast cells. Collagen contraction assay is a key tool used widely to characterise fibroblasts and assess wound healing[232,233]. At 40% oxygen 35FL cells cultured in collagen-elastin hydrogels did not contract the hydrogels as rapidly as at 21% oxygen. A reduced ability for cells to contract has been associated with cigarette smoke exposure[234] and chronic lung conditions, correlating with disease severity[235]. In BPD there is a disruption in ECM protein network, a process which is thought to be reliant on the ability of myofibroblasts to deposit and remodel collagen and elastin[236,237]. Our results indicate that this cell mechanism could be disrupted during oxidative stress. To further assess the link between hydrogel contraction and protein modelling it would be interesting to use protein analysis techniques such as Sircol Collagen Assay[238] and Fastin Elastin assay[239] to quantify collagen and elastin and immunofluorescent techniques to stain and visualise protein alignment[240] .

Hyperoxia culture prevented an increase in DNA quantity between day 1 and day 20 indicating cell proliferation was prevented. This is supported by phase contrast microscopic images and Live Dead stained confocal images which show live cells present but many fewer and with a less elongated appearance than at 21% oxygen suggesting the cells were senescent due to the oxidative stress[216,241]. This phenomenon has been previously reported in numerous publications[184,242–244]. Balin *et al.* observed high oxygen disrupted DNA synthesis during mitosis of WI-38 (human lung fibroblast from a 3 month

GA foetus)[245], preventing cells from proliferating. Davies *et al.* suggested that rather than this observed growth arrest being due to toxic outcomes, it is a protective mechanism to conserve resources and protect DNA[244]. The lack of cell proliferation may account for the reduced rate in contraction since we have shown in Chapter 3 that contraction rate is dependent on cell number, or the cells were conserving cellular functions as a protective outcome.

Confocal microscopy allows z-stacks to be taken to provide a 3D image of the whole construct. From these images we could see the 35FL had migrated towards the bottom of the hydrogel, towards the medium. It is likely the cells are migrating towards high concentrations of nutrients. This migration was also observed when 35FL and A549 were in co-culture which differs from observation made by Chetty *et al.* and Infeld *et al.* who found fibroblasts sandwiched between collagen gels migrated towards epithelial cells located on the collagen gel surface [112,246]. However their co-culture model included culture medium directly on top on the hydrogels suggesting the migration was not favoured by nutrient availability. The movement of cells under hyperoxia suggests that even though cells were not proliferating they were still responsive and able to migrate. Senescing cells have been shown to lose the ability to migrate[247,248] contradicting the theory that our cells are senescing. To examine this further senescence could be analysed β-Galactosidase activity; a biomarker expressed by cells senescing [249].

The A549 cells seeded on the hydrogel surface did not migrate through the hydrogel and provided a monolayer as expected. Initial results indicated 40% oxygen had no bearing on DNA quantity (proliferation), cell morphology or monolayer. To investigate this further we examined the TEER of A549 cells cultured in monolayer on well inserts or on the surface of acellular or cell-seeded hydrogels at 21% and 40% oxygen. We found the TEER to be significantly lower at day 7 of culture for cells cultured at 40% oxygen. This

suggests hyperoxia initially affects monolayer formation either through cell proliferation or through cell adhesion. We also saw resistance significantly increase when A549 cells were cultured on cell seeded hydrogels. This is supported by work previously published by Harrington *et al.* who found the co-culture of epithelial and fibroblasts cells in a 3D model enhanced the TEER[250] suggesting cell-cell interaction is necessary to enhance tissue integrity and encourage cell adhesion. Therefore the inclusion of multiple cell types is a vital parameter when designing *in vitro* models. The resistance of the hydrogels over-all was less than the cells cultured in 2D and represents observations which indicate the A549 cells do not form a confluent monolayer on hydrogel surface at the edges. When the hydrogels set, they are concave due to the meniscus of the hydrogel solution. The A549 cells do not migrate towards the edges of the hydrogel possibly due to this shape.

We looked at gene expression using RT-PCR. Altered expression of genes *α-SMA, TGFβ, ELN and COL1A* have all been notably associated with BPD. *NQO1* is associated with oxidative stress and was included as an indicator of hyperoxygen exposure[236]. Table 5.1 describes gene expression alterations in BPD. There were no significant changes in gene expressions noted at 40% oxygen compared with 21% except for *NQO1* expression which significantly increased for A549 cells cultured in co-culture with 35FL at 40% oxygen. A549 culture in monolayer at 40% oxygen also showed a significant increase in expression indicating the A549 cells are responding to the hyperoxia. Since the A549 cells in other aspects seem unaffected by the hyperoxia it is hypothesised they are producing antioxidant qualities in response to oxidative stress.

Table 5.1 Genes associated with BPD

Gene	Protein	Expression in BPD
αSMA	Alpha smooth muscle actin	Actin isoform predominantly found in myofibroblasts and associated with cell contraction. Increased αSMA positive cells and over expression has been found in animal models of BPD and hyperoxia exposure[236,251]
TGFβ1	Transforming growth factor beta	Over expression found in animal models of BPD and in the BALF fluid of preterm infants [57,252–254]. TGFβ is a secreted cytokine shown to regulate cell proliferation, fibroblast contraction, wound healing and fibrosis[255,256] and is responsible for the expression of αSMA in lung parenchymal fibroblasts [257]. Mechanical forces generated through the cytoskeleton can stimulate the expression of TGFβ[258,259].
ELN	Elastin	Elastin is an important protein in lung ECM providing mechanical stability. Abnormal elastin structure is associated in BPD. Upregulation of *ELN* in ventilated infants and lamb models of BPD has been noted[260,261].
COL1A1	Collagen type 1	Another protein found in the lung ECM to provided mechanical capabilities. Irregular collagen deposition/network is associated with clinical BPD. *COL1A1* overexpression has been associated BPD in both animal models and premature ventilated infants[236,237]
NQO1	NAD(P)H dehydrogenase [quinone] 1	A phase II enzyme activated by Nrf2 in response to oxidative stress[236,262,263].

5.6.1.2 Neonatal lung cells

Despite attempts we were not able to isolate epithelial cells from tracheal aspirates. For this study we included only the NLF cells previously established in Chapter 4. Since these cells demonstrate a fibroblastic nature, we cultured them within the collagen-elastin hydrogel to represent the lung mesenchyme. Culture at hyperoxia had no significant effect on cell presentation. Hydrogel contraction, DNA, gene expression and cell morphology remained unchanged when cultured at 21% or 40% oxygen. This observation is of clinical importance because it is not consistent with adult lung cells indicating neonatal cells may possess protective properties against oxygen toxicity which allows the cells to continue to proliferate and re-organise lung ECM during maturation. Similar to the 35FL NLF cells also migrated towards the bottom of the hydrogel surface.

5.6.2 Placenta MSC co-culture

Reports have indicated that MSCs have a role in mitigating oxygen-induced lung injury[158]. Results in this chapter have indicated hyperoxia causes damaging effects to adult lung fibroblasts in terms of proliferation, morphology and contraction. To assess if placenta derived MSCs could alleviate such effects we co-cultured placenta-derived MSCs with 35FL and NLF cells independently in 2D monolayer or 3D collagen-elastin hydrogels at 40% oxygen. MSCs can be sourced from both the amniotic membrane and the chorionic membrane which surround the foetus in the womb providing protection and segregation from the mother (Figure 5.20). The chorion is the outer maternal membrane whereas the amnion is the inner membrane which is in direct contact with the developing foetus. As shown in numerous publications both membranes are an abundant source of stem cells which possess mesenchymal related markers, tri-lineage differentiation potential and are immune-privileged cells[264–267]. As such, we examined the potential therapeutic effect of both sources of stem cells as a comparison.
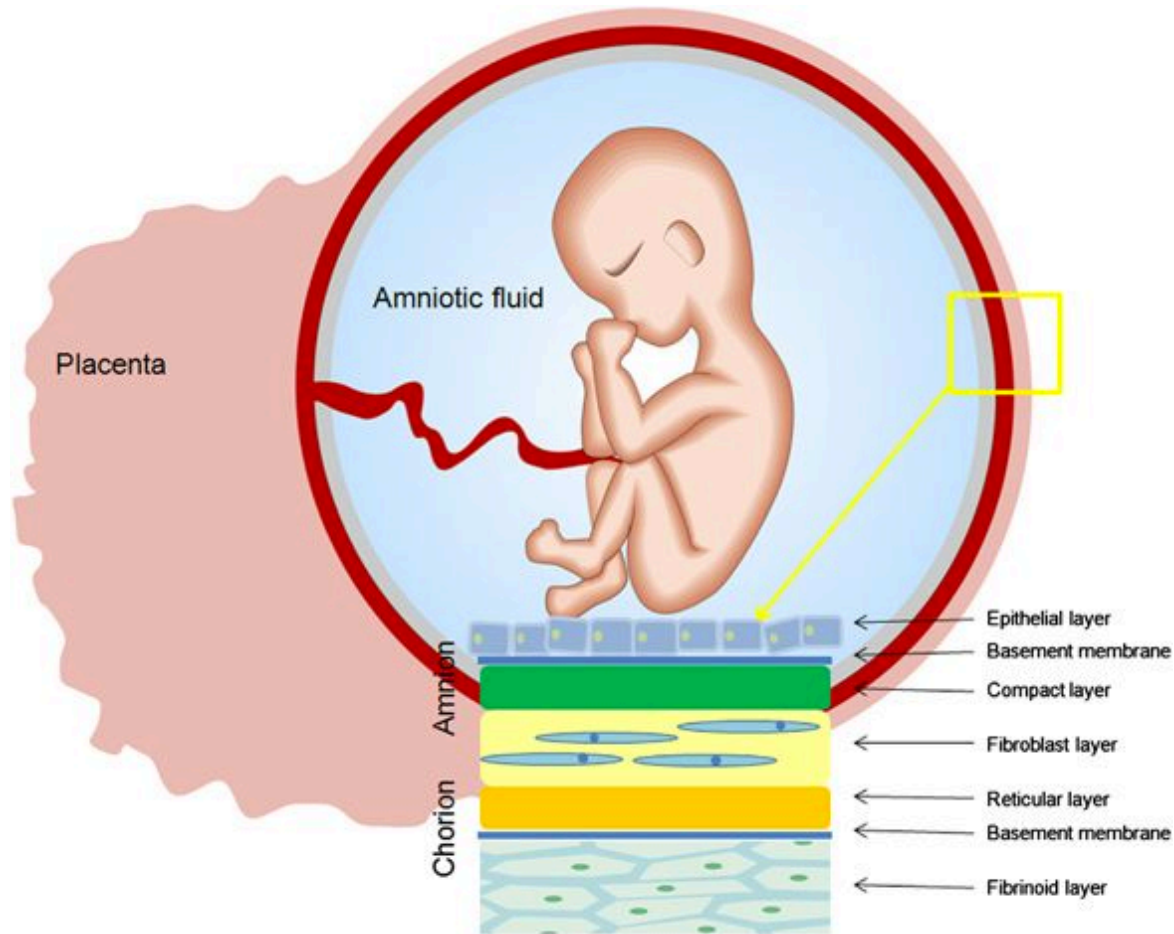
Figure 5.20 The amniotic sac. Image demonstrates the various structures of the amniotic sac and where the anion and chorion lie. Image sourced from Kang *et al.* [268].

Interestingly, we found that 35FL cells in monolayer culture at hyperoxia significantly increased DNA by day 20 when co-cultured with placenta MSCs. The effect was independent of MSC type (aMSCs or cMSCs) and was not observed for cells in hydrogels. This increase in DNA is likely due to an increase in cell number from cell proliferation as suggested by the appearance of more cells in microscopic images. These results suggest placenta MSCs could mitigate oxygen stress that adult lung fibroblasts experience through a paracrine mechanism and corresponds to preclinical hyperoxia animal models[215]. When cultured at 21% oxygen DNA was significantly lowered for cells in co-culture for 35FL and NLF. This may be due to the lack of available nutrients from the large number of cells in culture. Although media changes were achieved regularly there was no assessment of

nutrient availability. Taking this model forward the availability of nutrients within the culture media will be an important consideration and requires optimisation.

5.7 Conclusion

This chapter expanded on the previous two chapters. Human adult and neonatal lung cells (A549, 35FL and NLF) were successfully cultured in 3D collagen-elastin hydrogels at hyperoxia. Hyperoxia had a detrimental effect of adult lung fibroblasts, preventing proliferation and hydrogel contraction. It is hypothesized hyperoxia causes the cells to senesce, an effect also observed in Chapter 4 with placenta derived MSCs. Interestingly, the co-culture of these cells with placenta MSCs significantly increased DNA content and cell number when cells were cultured at hyperoxia. This suggests the MSCs did alleviate the oxygen stress cells were experiencing however there was no improvement in hydrogel contraction. The NLF cells were not notably affected by hyperoxia suggesting they possess protective features against oxygen stress. We did not highlight any significant alterations if BPD related gene expression. The A549 adult lung epithelial cell line was not affected by hyperoxia over long-term culture, however the formation of a monolayer was delayed as shown by reduced TEER at day 7 of culture. The increased NQO1 expression for A549 cells suggests these cells were under oxygen stress.

Chapter 6

Summative discussion, conclusion and future directions

6.1 Discussion

Bronchopulmonary disease is a chronic lung disorder affecting premature infants. Despite advances in neonatal care BPD remains a significant clinical challenge instigating financial, emotional and physical drain on those affected. BPD develops as a consequence of premature birth which interrupts the later stages of lung development, principally alveologenesis[10]. As a consequence, BPD infants rely on artificial respiratory support which, for the most severe cases delivers high oxygen concentrations under pressure[116]. This is thought to exacerbate the disease due to mechanical strain and oxidative damage[269].

Advances in BPD research have been restricted by a lack of appropriate disease models[60]. The field of regenerative medicine now allows us to develop complex *in vitro* models that can provide a platform for understanding disease mechanisms and evaluate potential treatments such as stem cell therapy. Stem cell therapy is at the forefront of regenerative medicine and published work has suggested it holds a great potential for BPD, a disease which is predominately caused by an interruption of lung generation[158,159]. The potential for stem cell therapy as a BPD treatment is supported not only by the presence of stem cells in the normal developing lung but also by the promising effect of administration of stem cells in BPD preclinical and clinical studies[33,171,206,270]. However, many questions still remain unanswered such as the optimal route of administration, MSC source, timing of the therapy, dosing for MSC delivery and mechanism of action. Accumulating evidence suggests that stem cells function through a paracrine mechanism indicating a cell-free approach may provide a safer, cheaper and more efficient therapy[223].

The objective of this work was to assess the potential therapeutic value of placenta derived MSCs, an underutilised waste material. To achieve this, we established and

optimised an *in vitro* model to represent the lung alveolus in BPD. Secondly, we isolated and cultured primary cells from the suctionings of premature neonates on ventilation. These cells were seeded within the alveolus model to provide BPD relevance. Finally, we exposed the model to hyperoxygen to recreate the oxygen stress BPD infants experience during clinical ventilation. Placenta derived MSCs were co-cultured with the model to assess the potential therapeutic value.

6.1.1 Developing an *in vitro* model for BPD research

As previously described, there is a lack of appropriate *in vitro* models for BPD research. The ideal alveolus model encompasses 4 key properties: a 3D structure, human lung cells in co-culture, mechanical stimulation and opportunity for high oxygen exposure (these factors have been described in detail in section 1.2.2). Published work from our lab has previously demonstrated that collagen-elastin hydrogels provide a biologically and mechanically relevant alveolus model[97]. Collagen and elastin are significant proteins present in the lung mesenchyme providing the lung with its mechanical properties and are thought to be the key driving forces in alveoli maturation[45,90,91]. Disruption to their deposition and alignment are hallmarks of clinical BPD[32,94] so their inclusion in a hydrogel provides physiological, mechanical and disease relevance mimicking the 3D *in vivo* lung environment.

In this study we developed and optimised collagen-elastin hydrogels capable of supporting the co-culture of lung epithelial and fibroblast cells. We showed that the addition of elastin into collagen hydrogels did not affect cell viability however increased hydrogel contraction. This led us to optimise an ideal fibroblast seeding density which prevented hydrogel contraction along the diameter allowing an epithelial monolayer to be cultured on the hydrogel surface. The hydrogels can be analysed in a number of ways:

calculating change in hydrogel contraction, DNA quantification, RNA extraction and microscopic imaging. The broad availability of out-put measures means the model could be utilised for a number of lung diseases. The main difficulty we encountered was being unable to isolate epithelial cells from the fibroblast-seeded hydrogel. However, FACS could be utilised for this application. Table 6.1 describes the many advantages that our alveolus *in vitro* model possesses and the associated limitations.

Table 6.1 The advantages and drawbacks of the *in vitro* alveolus model.

Advantages	Drawbacks
Provides a 3D matrix consisting of proteins (collagen and elastin) relevant to the alveolus and to BPD	Specialised technology is required for isolation of co-culture cells (FACS)
The inclusions of an air-liquid interface which is tissue relevant and allows for hyperoxia exposure	The model does not incorporate a pulmonary capillary component
The model provides the ability to co-culture multiple cell types	The model is not representative of an organoid
Collagen hydrogel is transparent to allow imaging, possesses mechanical properties relevant to the lung alveoli and is relatively straightforward to manufacture	The high concentration of collagen for hydrogels and use of well inserts increases costs
Hydrostatic stimulation can be incorporated for mechanical stress	
The model is simple to produce only requiring standard cell culture technique/equipment	

Overall our model is a suitable candidate for BPD research and could be exploited for other lung conditions such as emphysema and COPD. It successfully meets three out of the four properties we identified that an alveolus *in vitro* model should possess. The missing property, mechanical stress, is discussed later in this chapter (section 6.1.5). The

model is simple to produce and requires only basic cell culture techniques. It can be exposed to various stimuli (oxygen stress, hydrostatic pressure, drugs, stem cell therapy) and allows culture of a variety of cells making it easily adaptable.

6.1.2 The extraction and culture of human lung cells from the suctionings of ventilated infants

Tracheal suctioning is a routine procedure for endotracheal ventilated infants to remove and dispose excess fluid and mucus from the lungs[186]. It is an ideal material for utilisation in respiratory research since it avoids any additional morbidity to the patient and provides human/disease relevance. We obtained ethical approval to collect and process tracheal suctionings in the laboratory. We developed a simple, cheap protocol to extract and culture lung cells from the suctionings. The extracted cells (referred to as NLF) expressed attributes associated with fibroblastic cells and could be cultured in the alveolus model. The addition of NLF cells adds human, gestational age and disease relevance. We attempted to extract and culture epithelial cells from the suctionings using collagen coating to encourage cell attachment; adhesion time to differentiate between epithelial and fibroblast cells and; incorporating commercially available epithelial media to encourage cell culture. These procedures were unsuccessful at isolating epithelial cells and this requires further investigation as discussed later in this chapter.

6.1.3 The effect of hyperoxia on cell function

Hyperoxia is a key modulator of BPD and is commonly used to induce BPD in pre-clinical models[231]. We employed 40% oxygen to represent clinical ventilation and exposed both adult and neonatal lung cells to oxygen stress.

Hyperoxia had a pronounced effect on adult lung fibroblasts. Hydrogel contraction and cell proliferation were both reduced. This represents observations made in other published work. A549 epithelial cell proliferation was not affected by 40% oxygen however TEER demonstrates cell monolayer adhesion was compromised initially (day 7) but the cells recovered by day 20. Interestingly, the neonatal cells were unaffected by 40% oxygen suggesting they possess a prominent antioxidant stress mechanism which is potentially lost into adulthood. Further assessment is necessary to determine if other factors were affected such as cell marker expression.

6.1.4 Placenta MSCs as a cell therapy

Pre-clinical models and clinical trials have demonstrated that MSCs offer a promising tool for the treatment of BPD[158,159]. We assessed if placenta derived MSCs could offer an advantageous source for mediating oxygen stress. Hyperoxygen had a detrimental effect of MSC cell marker expression but not differentiation potential. This causes us to question the suitability of MSCs for BPD treatment which would require exposure to hyperoxygen. However, when placental MSCs were co-cultured with adult lung cells, proliferation was improved through a paracrine mechanism; independent of which placenta membrane the MSCs originated. This has important consequence since it indicates MSCs alleviate oxidative stress through a paracrine mechanism suggesting pre-conditioned media may provide a viable treatment option.

6.1.5 Limitations of the study

This study successfully applied both adult and neonatal lung cells to a 3D alveolus model, applied hyperoxygen and exposed the model to placenta derived MSCs. However, there are a number of limiting factors to consider when interpreting this data.

1. **Choice of adult lung cells**

In this study we used cells 35FL and A549 to represent the adult lung. These cells were carefully chosen due to their biological and age relevance. However, they do possess limitations. A549 is a cell line commonly used to model AEC2 cells and is used as a surrogate to study the alveolar epithelia[271] but these cells do not transition to or represent the AEC1 cells found *in vivo.* A more accurate representation of the alveolus wall would be to include both AEC1 and AEC2.

As previously described cells 35FL are fibroblast cells extracted from a 35 year old female lung[177] and therefore represent fibroblasts found in an adult lung. To support our findings of the effects of hyperoxia it would be beneficial to repeat the hyperoxia work with alternative adult cell types. Commercially available human lung fibroblasts or cells extracted from the suctions of endotracheal ventilated adult patients would be appropriate alternative cell types.

2. **Donor cell variability**

Cells were successfully extracted from endotracheal suctions of BPD infants which provided biological/disease relevance to the model. We experienced sample variation which possess difficulties when using these cells for research purposes. Further investigation into this might reveal protocol optimising could alleviate this problem.

3. **Mechanical stimulation**

Due to unavoidable technical issues we were unable to continue using the hydrostatic bioreactor to provide mechanical stimulus. Although advances in medical practice has provided less invasive ventilation systems, severe BPD infants will normally require endotracheal mechanical intubation which, along with high oxygen, is thought to exacerbate the disease[272]. Until strategies are developed to avoid high pressured

ventilation it is necessary to include mechanical stimulation in any BPD model. The withdrawal of the hydrostatic bioreactor meant in this study we could focus on the effects of hyperoxia, one factor of a multifactorial disease.

4. **Isolating cells cultured in hydrogel model**

For analysis purposes it is necessary to separate and assess cell types in isolation. We were unable to efficiently remove epithelial cells from the hydrogel. This meant co-cultured hydrogels (A549 and 35FL) could only be assessed as a mixed population of cells. To overcome this, we assessed the cells when cultured as a co-culture and when cultured individually. This prevented us from accurately assessing cell-cell interaction. This issue could be avoided by using fluorescence activated cell sorting (FACS).

5. **Oxygen exposure**

In initial experiments in Chapter 3 high oxygen exposure was achieved using an automated incubator capable of providing a controlled culture environment in-line with a pre-programmed oxygen percentage. Due to technical problems we had to revert to achieving hyperoxia using a sealed container filled with pre-mixed gas. Although a well-established technique this system does not allow constant monitoring of oxygen percentage. To achieve media changes or daily analysis (such as imaging) samples were removed from the sealed container and exposed to atmospheric oxygen. This meant samples were experiencing a daily hyperoxia-normoxia transition. It has been well characterised in BPD that infants experience episodes of hypoxia[270,271] suggesting the change in oxygen levels may provide a more accurate representation of clinical BPD.

6.2 Future directions

The work described has raised alternative directions which could strengthen and expand on the conclusions already drawn.

Characterising the extracted NLF cells was achieved through cell imaging and contraction assays. This could be expanded by assessing the expression of alpha smooth muscle actin and vimentin, commonly used fibroblastic markers; and by assessing the absence of epithelial marker e-cadherin and MSC markers (as previously listed in Chapter 4).

To further improve the efficiency of the cell extraction from tracheal suctionings we would look at optimising the protocol further. This could include a mucus digestion step which may improve cell isolation. We would also look at collecting many more samples from neonates of varying ages to investigate correlation between GA and cell isolation. Future work could include developing techniques to successfully isolate lung epithelial cells form the suctionings. Epithelial cells have previously been identified in similar sample types[275] but require population identification through cell labelling and flow cytometry techniques. Culturing these cells may entail culture at an air-liquid interface[276]. Sourcing epithelial cells from tracheal suctionings would contribute greatly to our model and BPD research.

The collagen and elastin network are of great importance in clinical BPD. Further evaluation of the collagen-elastin hydrogels structure would provide information regarding protein deposition and ECM remodelling. This could provide new evidence into the disruption of collagen and elastin distribution during hyperoxia exposure. Polarized light microscopy to highlight collagen alignment[277], fluorescent dye SRB for elastin

staining[278] and histological staining with Verhoeff's van Gieson to highlight collagen and elastin fibres are potential techniques to assess protein alterations.

We have shown that the co-culture of placenta MSCs alleviated the effects of oxygen stress on adult lung cells through a paracrine communication. The mechanism of this effect was not investigated here but previous work has already demonstrated the immunomodulatory and regenerative properties of MSCs are mediated through the production of extracellular vesicles[215,279]. By examining the factors released by MSCs cultured in our model we could begin to understand the mechanism of action.

6.3 Conclusion

BPD is a multifactorial disease requiring the investigation of many interacting factors including oxygen exposure, mechanical stress, cell-cell interaction and cell-matrix interaction. While *in vivo* models provide an insight into disease mechanism, they lack human relevance and are unable to recapitulate the alveoli of a preterm infant. Curren*t in vitro* lung research has focused on the conduction airway and there is a lack of sophisticated alveolus models. This project has successfully developed a novel *in vitro* alveolus model capable of accommodating multiple cell types including lung fibroblasts and lung epithelial cells in a 3D environment. The model creates an air-liquid interface capable of achieving clinically relevant hyperoxygen exposure and allows the study of cell-cell and cell-ECM interactions that occur *in vivo.* The unique inclusion of primary cells derived from BPD infants provides a disease relevant representation of cellular behaviour and allows the assessment of prospective treatment options.

We have shown that hyperoxia has a detrimental effect on adult lung cells however neonatal lung cells may possess defence mechanisms which alleviate oxygen stress. The

co-culture of placenta MSCs with adult lung cells alleviated oxygen stress, independent of membrane MSC source. These results support pre-clinical evidence of the promising regenerative potential MSCs possess for the treatment of BPD.

References

1. World Health Organization. Born too soon. The global action report on preterm birth. *J Perinatol*. 2012;13(5):393-396. doi:http://whqlibdoc.who.int/publications/2012/9789241503433_eng.pdf

2. National Academy of Science. Preterm Birth: Causes, Consequences, and Prevention - PubMed - NCBI. *IOM Reports*. 2006:1-4.

3. Jacob J, Kamitsuka M, Clark RH, Kelleher AS, Spitzer AR. Etiologies of NICU deaths. *Pediatrics*. 2015;135(1):e59-65. doi:10.1542/peds.2014-2967

4. Northway WH, Rosan RC, D.Y. P. Pulmonary disease following respiratory therapy of hyaline-membrane disease. *J Pediatr Surg*. 1967;2(3):271-272. doi:10.1016/0022-3468(67)90014-0

5. Baraldi E, Filippone M. Chronic Lung Disease after Premature Birth. *N Engl J Med*. 2007;357:1946-1955.

6. WHO. *Model Lists of Essential Medicines 3rd List*. World Health Organization; 2011.

7. Greenough A, Peacock J, Zivanovic S, et al. United Kingdom Oscillation Study: long-term outcomes of a randomised trial of two modes of neonatal ventilation. *Health Technol Assess (Rockv)*. 2014;18(41). doi:10.3310/hta18410

8. Costeloe KL, Hennessy EM, Haider S, Stacey F, Marlow N, Draper ES. Short term outcomes after extreme preterm birth in England: comparison of two birth cohorts in 1995 and 2006 (the EPICure studies). *BMJ*. 2012;345(dec04 3):e7976-e7976. doi:10.1136/bmj.e7976

9. Tommy's - for pregnancy information and research - Tommy's. http://www.tommys.org/. Accessed March 7, 2016.

10. Stoll BJ, Hansen NI, Bell EF, et al. Neonatal outcomes of extremely preterm infants from the NICHD Neonatal Research Network. *Pediatrics*. 2010;126(3):443-456. doi:10.1542/peds.2009-2959

11. Farstad T, Bratlid D, Medbø S, Markestad T. Bronchopulmonary dysplasia - prevalence, severity and predictive factors in a national cohort of extremely premature infants. *Acta Paediatr*. 2011;100(1):53-58. doi:10.1111/j.1651-2227.2010.01959.x

12. Jobe AH, Bancalari E. Bronchopulmonary dysplasia. *Am J Respir Crit Care Med*. 2001;163(7):1723-1729. doi:10.1164/ajrccm.163.7.2011060

13. Ehrenkranz RA. Validation of the National Institutes of Health Consensus Definition of Bronchopulmonary Dysplasia. *Pediatrics*. 2005;116(6):1353-1360. doi:10.1542/peds.2005-0249

14. Bhandari V, Bizzarro MJ, Shetty A, et al. Familial and genetic susceptibility to major neonatal morbidities in preterm twins. *Pediatrics*. 2006;117(6):1901-1906. doi:10.1542/peds.2005-1414

15. Greenough A, Cox S, Alexander J, et al. Health care utilisation of infants with chronic lung disease, related to hospitalisation for RSV infection. *Arch Dis Child*. 2001;85(6):463-468.

16. Jobe AH. Antenatal factors and the development of bronchopulmonary dysplasia. *Semin Neonatol*. 2003;8(1):9-17. doi:10.1016/S1084-2756(02)00188-4

17. Fanos V, Pintus MC, Lussu M, et al. Urinary metabolomics of bronchopulmonary dysplasia (BPD): preliminary data at birth suggest it is a congenital disease. *J Matern Fetal Neonatal Med*. 2014;27 Suppl 2:39-45. doi:10.3109/14767058.2014.955966

18. Torchin H, Ancel P-Y, Goffinet F, et al. Placental Complications and Bronchopulmonary Dysplasia: EPIPAGE-2 Cohort Study. *Pediatrics*. 2016;137(3):1-10. doi:10.1542/peds.2015-2163

19. Lal CV, Ambalavanan N. Genetic predisposition to bronchopulmonary dysplasia. *Semin Perinatol*. 2015;39(8):584-591. doi:10.1053/j.semperi.2015.09.004

20. Greenough A. Long term respiratory outcomes of very premature birth (<32

weeks). *Semin Fetal Neonatal Med.* 2012;17(2):73-76. doi:10.1016/j.siny.2012.01.009

21. Greenough A, Alexander J, Boorman J, et al. Respiratory morbidity, healthcare utilisation and cost of care at school age related to home oxygen status. *Eur J Pediatr.* 2011;170(8):969-975. doi:10.1007/s00431-010-1381-6

22. O'Reilly M, Thébaud B. Using cell-based strategies to break the link between bronchopulmonary dysplasia and the development of chronic lung disease in later life. *Pulm Med.* 2013;2013. doi:10.1155/2013/874161

23. Álvarez-Fuente M, Arruza L, Muro M, et al. The economic impact of prematurity and bronchopulmonary dysplasia. *Eur J Pediatr.* 2017;176(12):1587-1593. doi:10.1007/s00431-017-3009-6

24. Polin RA, Carlo WA. Surfactant replacement therapy for preterm and term neonates with respiratory distress. *Pediatrics.* 2014;133(1):156-163. doi:10.1542/peds.2013-3443

25. Brown MK, DiBlasi RM. Mechanical Ventilation of the Premature Neonate. *Respir Care.* 2011;56(9):1298-1313. doi:10.4187/respcare.01429

26. The Royal College of Obstetricians and Gynaecologists. Antenatal Corticosteroids to Reduce Neonatal Morbidity. 2010;(7).

27. Onland W, Offringa M, van Kaam A. Late (≥ 7 days) inhalation corticosteroids to reduce bronchopulmonary dysplasia in preterm infants. *Cochrane database Syst Rev.* 2012;4:CD002311. doi:10.1002/14651858.CD002311.pub3

28. Yeh TF, Lin YJ, Lin HC, et al. Outcomes at School Age after Postnatal Dexamethasone Therapy for Lung Disease of Prematurity. *N Engl J Med.* 2004;350(13):1304-1313. doi:10.1056/NEJMoa032089

29. Li F, He J, Wei J, Cho WC, Liu X. Diversity of epithelial stem cell types in adult lung. *Stem Cells Int.* 2015;2015(Aec Ii):17-21. doi:10.1155/2015/728307

30. Deutsch G, Pinar H. Prenatal Lung Development. In: *Chronic Obstructive Lung*

Diseases. ; 2002:7-20.

31. Mascaretti RS, Mataloun MMGB, Dolhnikoff M, Rebello CM. Lung morphometry, collagen and elastin content: changes after hyperoxic exposure in preterm rabbits. *Clin (São Paulo, Brazil).* 2009;64(11):1099-1104. doi:10.1590/S1807-59322009001100010

32. Margraf LR, Tomashefski JF, Bruce MC, Dahms BB. Morphometric analysis of the lung in bronchopulmonary dysplasia. *Am Rev Respir Dis.* 1991;143(2):391-400. doi:10.1164/ajrccm/143.2.391

33. Mobius MA, Thebaud B. Bronchopulmonary Dysplasia: Where Have All the Stem Cells Gone? Origin and (Potential) Function of Resident Lung Stem Cells. *Phys Lett A.* 2017;152(5):1043-1052. doi:10.1016/j.chest.2017.04.173

34. Carraro S, Filippone M, Da Dalt L, et al. Bronchopulmonary dysplasia: The earliest and perhaps the longest lasting obstructive lung disease in humans. *Early Hum Dev.* 2013;89:S3-S5. doi:10.1016/j.earlhumdev.2013.07.015

35. McEvoy CT, Jain L, Schmidt B, Abman S, Bancalari E, Aschner JL. Bronchopulmonary dysplasia: NHLBI Workshop on the Primary Prevention of Chronic Lung Diseases. *Ann Am Thorac Soc.* 2014;11 Suppl 3:S146-53. doi:10.1513/AnnalsATS.201312-424LD

36. Jobe AH. Pharmacology Review: Why Surfactant Works for Respiratory Distress Syndrome. *Neoreviews.* 2006;7(2):e95-e106. doi:10.1542/neo.7-2-e95

37. Crapo JD, Barry BE, Gehr P, Bachofen M, Weibel ER. Cell Number and Cell Characteristics of the Normal Human Lung1–3. *Am Rev Respir Dis.* May 2015.

38. Lopez-Rodriguez E, Pérez-Gil J. Structure-function relationships in pulmonary surfactant membranes: from biophysics to therapy. *Biochim Biophys Acta.* 2014;1838(6):1568-1585. doi:10.1016/j.bbamem.2014.01.028

39. Evans MJ, Cabral LJ, Stephens RJ, Freeman G. Transformation of alveolar Type 2 cells to Type 1 cells following exposure to NO2. *Exp Mol Pathol.* 1975;22(1):142-

150. doi:10.1016/0014-4800(75)90059-3

40. Barkauskas CE, Cronce MJ, Rackley CR, et al. Type 2 alveolar cells are stem cells in adult lung. *J Clin Invest*. 2013;123(7):3025-3036. doi:10.1172/JCI68782

41. Desai TJ, Brownfield DG, Krasnow MA. Alveolar progenitor and stem cells in lung development, renewal and cancer. *Nature*. 2014;507(7491):190-194. doi:10.1038/nature12930

42. Kim CFB, Jackson EL, Woolfenden AE, et al. Identification of bronchioalveolar stem cells in normal lung and lung cancer. *Cell*. 2005;121(6):823-835. doi:10.1016/j.cell.2005.03.032

43. Fehrenbach H. Alveolar epithelial type II cell: defender of the alveolus revisited. *Respir Res*. 2001;2(1):33-46. doi:10.1186/rr36

44. Dunsmore SE, Rannels DE. Extracellular matrix biology in the lung. *Am J Physiol*. 1996;270(1 Pt 1):L3-L27.

45. Davidson JM. Biochemistry and turnover of lung interstitium. *Eur Respir J Off J Eur Soc Clin Respir Physiol*. 1990;3(9):1048-1063.

46. Rehan VK, Sugano S, Wang Y, et al. EVIDENCE FOR THE PRESENCE OF LIPOFIBROBLASTS IN HUMAN LUNG. *Exp Lung Res*. 2006;32(8):379-393. doi:10.1080/01902140600880257

47. Torday J, Hua J, Slavin R. Metabolism and fate of neutral lipids of fetal lung fibroblast origin. *Biochim Biophys Acta - Lipids Lipid Metab*. 1995;1254(2):198-206. doi:10.1016/0005-2760(94)00184-Z

48. McGowan SE, Grossmann RE, Kimani PW, Holmes AJ. Platelet-Derived Growth Factor Receptor-Alpha-Expressing Cells Localize to the Alveolar Entry Ring and Have Characteristics of Myofibroblasts During Pulmonary Alveolar Septal Formation. *Anat Rec Adv Integr Anat Evol Biol*. 2008;291(12):1649-1661. doi:10.1002/ar.20764

49. Branchfield K, Li R, Lungova V, Verheyden JM, McCulley D, Sun X. A three-

dimensional study of alveologenesis in mouse lung. *Dev Biol*. 2016;409(2):429-441. doi:10.1016/J.YDBIO.2015.11.017

50.   Danan C, Franco M-L, Jarreau P-H, et al. High Concentrations of Keratinocyte Growth Factor in Airways of Premature Infants Predicted Absence of Bronchopulmonary Dysplasia. *Am J Respir Crit Care Med*. 2002;165(10):1384-1387. doi:10.1164/rccm.200112-134BC

51.   Gesche J, Fehrenbach H, Koslowski R, et al. rhKGF stimulates lung surfactant production in neonatal rats in vivo. *Pediatr Pulmonol*. 2011;46(9):882-895. doi:10.1002/ppul.21443

52.   Bourbon J, Boucherat O, Chailley-Heu B, Delacourt C. Control Mechanisms of Lung Alveolar Development and Their Disorders in Bronchopulmonary Dysplasia. *Pediatr Res*. 2005;57(5):38R-46R. doi:10.1203/01.PDR.0000159630.35883.BE

53.   Wang J, Bao L, Yu B, et al. Interleukin-1β Promotes Epithelial-Derived Alveolar Elastogenesis via αvβ6 Integrin-Dependent TGF-β Activation. *Cell Physiol Biochem*. 2015;36(6):2198-2216. doi:10.1159/000430185

54.   Hawwa R, Hokenson M, Wang Y, Huang Z, Sharma S. IL-10 inhibits inflammatory cytokines released by fetal mouse lung fibroblasts exposed to mechanical stretch. *Pediatr Pulmonol*. 2011;46(7):1640-1649. doi:10.1038/nature13314.A

55.   Kambas K, Chrysanthopoulou a., Kourtzelis I, et al. Endothelin-1 Signaling Promotes Fibrosis In Vitro in a Bronchopulmonary Dysplasia Model by Activating the Extrinsic Coagulation Cascade. *J Immunol*. 2011;186(11):6568-6575. doi:10.4049/jimmunol.1003756

56.   Brya K, Lappalainen U. Pathogenesis of bronchopulmonary dysplasia : the role of interleukin 1beta in the regulation of inflammation-mediated pulmonary retinoic acid pathways in transgenic mice . *Semin Perinatol*. 2006;30(3):121-128.

57.   Been J V., Debeer A, Van Iwaarden JF, et al. Early alterations of growth factor patterns in bronchoalveolar lavage fluid from preterm infants developing

bronchopulmonary dysplasia. *Pediatr Res*. 2010;67(1):83-89. doi:10.1203/PDR.0b013e3181c13276

58.   Morrisey EE, Hogan BLM. Preparing for the first breath: genetic and cellular mechanisms in lung development. *Dev Cell*. 2010;18(1):8-23. doi:10.1016/j.devcel.2009.12.010

59.   Chao C-M, Moiseenko A, Zimmer K-P, Bellusci S. Alveologenesis: key cellular players and fibroblast growth factor 10 signaling. *Mol Cell Pediatr*. 2016;3(1):17. doi:10.1186/s40348-016-0045-7

60.   Hilgendorff A, Reiss I, Ehrhardt H, Eickelberg O, Alvira CM. Chronic Lung Disease in the Preterm Infant: Lessons Learned From Animal Models. *Am J Respir Cell Mol Biol*. 2013;50(2):130911135746008. doi:10.1165/rcmb.2013-0014TR

61.   Berger J, Bhandari V. Animal models of bronchopulmonary dysplasia. The term mouse models. *Am J Physiol Lung Cell Mol Physiol*. 2014;307(12):L948-58. doi:10.1152/ajplung.00160.2014

62.   Smith FJC. Morphological Changes in the Lungs of rats Living Under Compressed Air Conditions. *J Exp Med*. 1932;56(1):79-89. doi:10.1084/jem.56.1.79

63.   Albertine KH. Utility of large-animal models of BPD: chronically ventilated preterm lambs. *Am J Physiol Lung Cell Mol Physiol*. 2015;308(10):L983-L1001. doi:10.1152/ajplung.00178.2014

64.   Brew N, Hooper SB, Zahra V, et al. Mechanical Ventilation Injury and Repair in Extremely and Very Preterm Lungs. Morty RE, ed. *PLoS One*. 2013;8(5):e63905. doi:10.1371/journal.pone.0063905

65.   Coalson JJ, Winter VT, Siler-Khodr T, Yoder BA. Neonatal chronic lung disease in extremely immature baboons. *Am J Respir Crit Care Med*. 1999;160(4):1333-1346. doi:10.1164/ajrccm.160.4.9810071

66.   Mižíková I, Ruiz-Camp J, Steenbock H, et al. Collagen and elastin cross-linking is altered during aberrant late lung development associated with hyperoxia. *Am J*

Physiol - *Lung Cell Mol Physiol*. 2015:ajplung.00039.2015. doi:10.1152/ajplung.00039.2015

67.   Benjamin JT, Gaston DC, Halloran BA, Schnapp LM, Zent R, Prince LS. The role of integrin α8β1 in fetal lung morphogenesis and injury. *Dev Biol*. 2009;335(2):407-417. doi:10.1016/j.ydbio.2009.09.021

68.   Alapati D, Rong M, Chen S, Hehre D, Hummler SC, Wu S. Inhibition of β-Catenin Signaling Improves Alveolarization and Reduces Pulmonary Hypertension in Experimental Bronchopulmonary Dysplasia. *Am J Respir Cell Mol Biol*. 2014;51(1):104-113. doi:10.1165/rcmb.2013-0346OC

69.   Alphonse RS, Vadivel A, Fung M, et al. Existence, functional impairment, and lung repair potential of endothelial colony-forming cells in oxygen-induced arrested alveolar growth. *Circ Res*. 2014;129(21):2144-2157. doi:10.1161/CIRCULATIONAHA.114.009124

70.   Silva DMGG, Nardiello C, Pozarska A, Morty RE. Recent advances in the mechanisms of lung alveolarization and the pathogenesis of bronchopulmonary dysplasia. *Am J Physiol* - *Lung Cell Mol Physiol*. 2015;309(11):ajplung.00268.2015. doi:10.1152/ajplung.00268.2015

71.   Irvin CG, Bates JHT. Measuring the lung function in the mouse: the challenge of size. *Respir Res*. 2003;4:4.

72.   Coalson JJ, Kuehl TJ, Escobedo MB, et al. A baboon model of bronchopulmonary dysplasia. *Exp Mol Pathol*. 1982;37(3):335-350. doi:10.1016/0014-4800(82)90046-6

73.   Maniscalco WM, Watkins RH, Pryhuber GS, Bhatt A, Shea C, Huyck H. Angiogenic factors and alveolar vasculature: development and alterations by injury in very premature baboons. *Am J Physiol Lung Cell Mol Physiol*. 2002;282(4):L811-23. doi:10.1152/ajplung.00325.2001

74.   Lee MK, Pryhuber GS, Schwarz MA, Smith SM, Pavlova Z, Sunday ME. Developmental

regulation of p66Shc is altered by bronchopulmonary dysplasia in baboons and humans. *Am J Respir Crit Care Med*. 2005;171(12):1384-1394. doi:10.1164/rccm.200406-776OC

75. Berger TM, Frei B, Rifai N, et al. Early high dose antioxidant vitamins do not prevent bronchopulmonary dysplasia in premature baboons exposed to prolonged hyperoxia: a pilot study. *Pediatr Res*. 1998;43(6):719-726. doi:10.1203/00006450-199806000-00002

76. Awasthi S, Coalson JJ, Crouch E, Yang F, King RJ. Surfactant proteins A and D in premature baboons with chronic lung injury (Bronchopulmonary dysplasia). Evidence for an inhibition of secretion. *Am J Respir Crit Care Med*. 1999;160(3):942-949. doi:10.1164/ajrccm.160.3.9806061

77. Talwadekar MD, Kale VP, Limaye LS, et al. Placenta-derived mesenchymal stem cells possess better immunoregulatory properties compared to their cord-derived counterparts–a paired sample study. *Sci Rep*. 2015;5:15784. doi:10.1038/srep15784

78. Frank L, Bucher JR, Roberts RJ. Oxygen toxicity in neonatal and adult animals of various species. *J Appl Physiol*. 1978;45(5):699-704.

79. Bérubé K, Prytherch Z, Job C, Hughes T. Human primary bronchial lung cell constructs: the new respiratory models. *Toxicology*. 2010;278(3):311-318. doi:10.1016/j.tox.2010.04.004

80. RUSSELL, W. M. S., & BURCH RL. *The Principles of Humane Experimental Technique*. London; 1959.

81. National Centre for the Replacement Refinement & Reduction of Animals in Research. The 3Rs. https://www.nc3rs.org.uk/the-3rs. Accessed January 22, 2016.

82. Bridge JC, Aylott JW, Brightling CE, et al. Adapting the Electrospinning Process to Provide Three Unique Environments for a Tri-layered In Vitro Model of the Airway Wall. *J Vis Exp*. 2015;(101):e52986. doi:10.3791/52986

83. Haydon P, Bolmarcich J, Wilbert S, et al. Mechanisms Of Goblet Cell Hyperplasia Induced By Simulated Viral Exposure Or TH2 Cytokines In The EpiAirway-FT™ In Vitro Human Airway Model. *Am Thorac Soc Int Conf Meet Abstr*. 2011.

84. Douglas WH, Moorman GW, Teel RW. The formation of histotypic structures from monodisperse fetal rat lung cells cultured on a three-dimensional substrate. *In Vitro*. 1976;12(5):373-381.

85. Cortiella J, Nichols JE, Kojima K, et al. Tissue-engineered lung: an in vivo and in vitro comparison of polyglycolic acid and pluronic F-127 hydrogel/somatic lung progenitor cell constructs to support tissue growth. *Tissue Eng*. 2006;12(5):1213-1225. doi:10.1089/ten.2006.12.1213

86. Andrade CF, Wong AP, Waddell TK, Keshavjee S, Liu M. Cell-based tissue engineering for lung regeneration. *Am J Physiol Lung Cell Mol Physiol*. 2007;292(2):L510-8. doi:10.1152/ajplung.00175.2006

87. Harrington H, Cato P, Salazar F, et al. Immunocompetent 3D Model of Human Upper Airway for Disease Modeling and In Vitro Drug Evaluation. *Mol Pharm*. 2014;11(7):2082-2091. doi:10.1021/mp5000295

88. Mondrinos MJ, Koutzaki S, Lelkes PI, Finck CM. A tissue-engineered model of fetal distal lung tissue. *Am J Physiol Lung Cell Mol Physiol*. 2007;293(3):L639-50. doi:10.1152/ajplung.00403.2006

89. Baiguera S, Jungebluth P, Burns A, et al. Tissue engineered human tracheas for in vivo implantation. *Biomaterials*. 2010;31(34):8931-8938. doi:10.1016/j.biomaterials.2010.08.005

90. Karlinsky JB, Snider GL, Franzblau C, Stone PJ, Hoppin FG. In vitro effects of elastase and collagenase on mechanical properties of hamster lungs. *Am Rev Respir Dis*. 1976;113(6):769-777. doi:10.1164/arrd.1976.113.6.769

91. Suki B, Ito S, Stamenovic D, Lutchen KR, Ingenito EP. Biomechanics of the lung parenchyma : critical roles of collagen and mechanical forces Be. *Am Physiol Soc*.

2005;98:1892-1899. doi:10.1152/japplphysiol.01087.2004.

92.   Yuan H, Ingenito EP, Suki B. Dynamic properties of lung parenchyma: mechanical contributions of fiber network and interstitial cells. *J Appl Physiol*. 1997;83(5):1420-1431; discussion 1418-1419.

93.   Abraham T, Hirota J a., Wadsworth S, Knight D a. Minimally invasive multiphoton and harmonic generation imaging of extracellular matrix structures in lung airway and related diseases. *Pulm Pharmacol Ther*. 2011;24(5):487-496. doi:10.1016/j.pupt.2011.03.008

94.   Bland RD, Ertsey R, Mokres LM, et al. Mechanical ventilation uncouples synthesis and assembly of elastin and increases apoptosis in lungs of newborn mice. Prelude to defective alveolar septation during lung development? *Am J Physiol Lung Cell Mol Physiol*. 2008;294(1):L3-14. doi:10.1152/ajplung.00362.2007

95.   Witsch TJ, Turowski P, Sakkas E, et al. Deregulation of the lysyl hydroxylase matrix cross-linking system in experimental and clinical bronchopulmonary dysplasia. *Am J Physiol Lung Cell Mol Physiol*. 2014;306(3):L246-59. doi:10.1152/ajplung.00109.2013

96.   Thibeault DW, Mabry SM, Ekekezie II, Zhang X, Truog WE. Collagen scaffolding during development and its deformation with chronic lung disease. *Pediatrics*. 2003;111(4 Pt 1):766-776. doi:10.1159/000192718

97.   Dunphy SE, Bratt JAJ, Akram KM, Forsyth NR, El Haj AJ. Hydrogels for lung tissue engineering: Biomechanical properties of thin collagen–elastin constructs. *J Mech Behav Biomed Mater*. 2014;38:251-259. doi:10.1016/j.jmbbm.2014.04.005

98.   Petersen TH, Calle EA, Zhao L, et al. Tissue-engineered lungs for in vivo implantation. *Science.* 2010;329(5991):538-541. doi:10.1126/science.1189345

99.   Macchiarini P, Jungebluth P, Go T, et al. Clinical transplantation of a tissue-engineered airway. *Lancet*. 2008;372(9655):2023-2030. doi:10.1016/S0140-6736(08)61598-6

100. Engler AJ, Griffin MA, Sen S, Bönnemann CG, Sweeney HL, Discher DE. Myotubes differentiate optimally on substrates with tissue-like stiffness. *J Cell Biol*. 2004;166(6):877-887. doi:10.1083/jcb.200405004

101. Falconnet D, Csucs G, Grandin HM, Textor M. Surface engineering approaches to micropattern surfaces for cell-based assays. *Biomaterials*. 2006;27(16):3044-3063. doi:10.1016/j.biomaterials.2005.12.024

102. Saha K, Keung AJ, Irwin EF, et al. Substrate Modulus Directs Neural Stem Cell Behavior. *Biophys J*. 2008;95(9):4426-4438. doi:10.1529/biophysj.108.132217

103. Yim EKF, Pang SW, Leong KW. Synthetic nanostructures inducing differentiation of human mesenchymal stem cells into neuronal lineage. *Exp Cell Res*. 2007;313(9):1820-1829. doi:10.1016/j.yexcr.2007.02.031

104. Ott HC, Clippinger B, Conrad C, et al. Regeneration and orthotopic transplantation of a bioartificial lung. *Nat Med*. 2010;16(8):927-933. doi:10.1038/nm.2193

105. O'Neill JD, Anfang R, Anandappa A, et al. Decellularization of Human and Porcine Lung Tissues for Pulmonary Tissue Engineering. *Ann Thorac Surg*. 2013;96(3):1046-1056. doi:10.1016/j.athoracsur.2013.04.022

106. Ochs M, Nyengaard JR, Jung A, et al. The Number of Alveoli in the Human Lung. *Am J Respir Crit Care Med*. 2004;169(1):120-124. doi:10.1164/rccm.200308-1107OC

107. Ahn SY, Chang YS, Sung DK, et al. Cell type–dependent variation in paracrine potency determines therapeutic efficacy against neonatal hyperoxic lung injury. *Cytotherapy*. 2015;17(8):1025-1035. doi:10.1016/j.jcyt.2015.03.008

108. Giard DJ, Aaronson SA, Todaro GJ, et al. In Vitro Cultivation of Human Tumors: Establishment of Cell Lines Derived From a Series of Solid Tumors. *J Natl Cancer Inst*. 1973;51(5):1417-1423. doi:10.1093/jnci/51.5.1417

109. Mason RJ, Williams MC. Phospholipid composition and ultrastructure of A549 cells and other cultured pulmonary epithelial cells of presumed type II cell origin. *Biochim Biophys Acta - Lipids Lipid Metab*. 1980;617(1):36-50. doi:10.1016/0005-

2760(80)90222-2

110. Swain RJ, Kemp SJ, Goldstraw P, Tetley TD, Stevens MM. Assessment of cell line models of primary human cells by Raman spectral phenotyping. *Biophys J*. 2010;98(8):1703-1711. doi:10.1016/j.bpj.2009.12.4289

111. Kemp SJ, Thorley AJ, Gorelik J, et al. Immortalization of human alveolar epithelial cells to investigate nanoparticle uptake. *Am J Respir Cell Mol Biol*. 2008;39(5):591-597. doi:10.1165/rcmb.2007-0334OC

112. Anne Chetty, Steven Faber, Heber C., Chetty A, Faber S, Nielsen HC. Epithelial-Mesenchymal Interaction and Insulin-Like Growth Factors in Hyperoxic Lung Injury. *Exp Lung Res*. 1999;25(8):701-718. doi:10.1080/019021499270015

113. Greer RM, Miller JD, Okoh VO, Halloran BA, Prince LS. Epithelial-mesenchymal co-culture model for studying alveolar morphogenesis. *Organogenesis*. 2014;10(4):340-349. doi:10.4161/org.29198

114. Huh D (Dan). A Human Breathing Lung-on-a-Chip. *Ann Am Thorac Soc*. 2015;12(Supplement 1):S42-S44. doi:10.1513/AnnalsATS.201410-442MG

115. Moreno L, Perez-Vizcaino F, Harrington L, et al. Pharmacology of airways and vessels in lung slices in situ: role of endogenous dilator hormones. *Respir Res*. 2006;7(1):111. doi:10.1186/1465-9921-7-111

116. Keszler M, Sant'Anna G. Mechanical Ventilation and Bronchopulmonary Dysplasia. *Clin Perinatol*. 2015;42(4):781-796. doi:10.1016/j.clp.2015.08.006

117. Kitterman JA. Physiological factors in fetal lung growth. *Can J Physiol Pharmacol*. 1988;66(8):1122-1128.

118. Kitterman JA. The effects of mechanical forces on fetal lung growth. *Clin Perinatol*. 1996;23(4):727-740.

119. Hooper SB, Han VK, Harding R. Changes in lung expansion alter pulmonary DNA synthesis and IGF-II gene expression in fetal sheep. *Am J Physiol Cell Mol Physiol*. 1993;265(4):L403-L409. doi:10.1152/ajplung.1993.265.4.L403

120. Chernick V. Fetal Breathing Movements and the Onset of Breathing at Birth. *Clin Perinatol*. 1978;5(2):257-268. doi:10.1016/S0095-5108(18)31178-3

121. Keeley FW, Bellingham CM, Woodhouse KA. Elastin as a self-organizing biomaterial: use of recombinantly expressed human elastin polypeptides as a model for investigations of structure and self-assembly of elastin. *Philos Trans R Soc Lond B Biol Sci*. 2002;357(1418):185-189. doi:10.1098/rstb.2001.1027

122. Liu M, Post M. Invited review: mechanochemical signal transduction in the fetal lung. *J Appl Physiol*. 2000;89(5):2078-2084.

123. Wendt D, Riboldi SA. Bioreactors in Tissue Engineering: From Basic Research to Automated Product Manufacturing. In: *Fundamentals of Tissue Engineering and Regenerative Medicine*. Berlin, Heidelberg: Springer Berlin Heidelberg; 2009:595-611. doi:10.1007/978-3-540-77755-7_42

124. Liu M, Montazeri S, Jedlovsky T, et al. Bio-stretch, a computerized cell strain apparatus for three-dimensional organotypic cultures. *In Vitro Cell Dev Biol Anim*. 1999;35(2):87-93. doi:10.1007/s11626-999-0006-8

125. Mourgeon E, Isowa N, Keshavjee S, Zhang X, Slutsky a S, Liu M. Mechanical stretch stimulates macrophage inflammatory protein-2 secretion from fetal rat lung cells. *Am J Physiol Lung Cell Mol Physiol*. 2000;279(4):L699-L706.

126. Hawwa RL, Hokenson MA, Wang Y, Huang Z, Sharma S, Sanchez-Esteban J. Differential expression of MMP-2 and -9 and their inhibitors in fetal lung cells exposed to mechanical stretch: Regulation by IL-10. *Lung*. 2011;189(4):341-349. doi:10.1007/s00408-011-9310-7

127. Smith PG, Garcia R, Kogerman L. Mechanical strain increases protein tyrosine phosphorylation in airway smooth muscle cells. *Exp Cell Res*. 1998;239(0014-4827; 2):353-360.

128. Wirtz H, Dobbs L. Calcium mobilization and exocytosis after one mechanical stretch of lung epithelial cells. *Science (80-)*. 1990;250(4985):1266-1269.

doi:10.1126/science.2173861

129. Henstock JRR, Rotherham M, Rose JBB, El Haj AJJ. Cyclic hydrostatic pressure stimulates enhanced bone development in the foetal chick femur in vitro. *Bone*. 2013;53(2):468-477. doi:10.1016/j.bone.2013.01.010

130. Carroll SF, Buckley CT, Kelly DJ. Cyclic hydrostatic pressure promotes a stable cartilage phenotype and enhances the functional development of cartilaginous grafts engineered using multipotent stromal cells isolated from bone marrow and infrapatellar fat pad. *J Biomech*. 2014;47(9):2115-2121. doi:10.1016/j.jbiomech.2013.12.006

131. Reinwald Y, Leonard KHL, Henstock JR, et al. Evaluation of the growth environment of a hydrostatic force bioreactor for preconditioning of tissue-engineered constructs. *Tissue Eng Part C Methods*. 2015;21(1):1-14. doi:10.1089/ten.tec.2013.0476

132. deLemos RA, Coalson JJ, Gerstmann DR, Kuehl TJ, Null DM. Oxygen Toxicity in the Premature Baboon with Hyaline Membrane Disease. *Am Rev Respir Dis*. 1987;136(3):677-682. doi:10.1164/ajrccm/136.3.677

133. Kaneko S, Takamatsu K. Cell Handling and Culture Under Controlled Oxygen Concentration. In: *Biomedical Tissue Culture*. InTech; 2012. doi:10.5772/52112

134. Huh D, Matthews BD, Mammoto A, Montoya-Zavala M, Hsin HY, Ingber DE. Reconstituting organ-level lung functions on a chip. *Science*. 2010;328(5986):1662-1668. doi:10.1126/science.1188302

135. Umino T, Wang H, Zhu Y, et al. Modification of type I collagenous gels by alveolar epithelial cells. *Am J Respir Cell Mol Biol*. 2000;22(6):702-707. doi:10.1165/ajrcmb.22.6.3806

136. Phinney DG, Prockop DJ. Concise review: mesenchymal stem/multipotent stromal cells: the state of transdifferentiation and modes of tissue repair--current views. *Stem Cells*. 2007;25(11):2896-2902. doi:10.1634/stemcells.2007-0637

137. O'Reilly M, Thébaud B. The promise of stem cells in bronchopulmonary dysplasia. *Semin Perinatol*. 2013;37(2):79-84. doi:10.1053/j.semperi.2013.01.003

138. Baker CD, Seedorf GJ, Wisniewski BL, et al. Endothelial colony-forming cell conditioned media promote angiogenesis in vitro and prevent pulmonary hypertension in experimental bronchopulmonary dysplasia. *Am J Physiol Lung Cell Mol Physiol*. 2013;305(1):L73-81. doi:10.1152/ajplung.00400.2012

139. Alvarez DF, Huang L, King JA, ElZarrad MK, Yoder MC, Stevens T. Lung microvascular endothelium is enriched with progenitor cells that exhibit vasculogenic capacity. *Am J Physiol Lung Cell Mol Physiol*. 2008;294(3):L419-30. doi:10.1152/ajplung.00314.2007

140. Balasubramaniam V, Mervis CF, Maxey AM, Markham NE, Abman SH. Hyperoxia reduces bone marrow, circulating, and lung endothelial progenitor cells in the developing lung: implications for the pathogenesis of bronchopulmonary dysplasia. *Am J Physiol Lung Cell Mol Physiol*. 2007;292(5):L1073-84. doi:10.1152/ajplung.00347.2006

141. Qi Y, Jiang Q, Chen C, Cao Y, Qian L. Circulating endothelial progenitor cells decrease in infants with bronchopulmonary dysplasia and increase after inhaled nitric oxide. *PLoS One*. 2013;8(11):e79060. doi:10.1371/journal.pone.0079060

142. Borghesi A, Massa M, Campanelli R, et al. Circulating endothelial progenitor cells in preterm infants with bronchopulmonary dysplasia. *Am J Respir Crit Care Med*. 2009;180(6):540-546. doi:10.1164/rccm.200812-1949OC

143. Ilancheran S, Michalska A, Peh G, Wallace EM, Pera M, Manuelpillai U. Stem cells derived from human fetal membranes display multilineage differentiation potential. *Biol Reprod*. 2007;77(3):577-588. doi:10.1095/biolreprod.106.055244

144. Miki T, Lehmann T, Cai H, Stolz DB, Strom SC. Stem cell characteristics of amniotic epithelial cells. *Stem Cells*. 23(10):1549-1559. doi:10.1634/stemcells.2004-0357

145. Hodges RJ, Jenkin G, Hooper SB, et al. Human amnion epithelial cells reduce

ventilation-induced preterm lung injury in fetal sheep. *Am J Obstet Gynecol*. 2012;206(5):448.e8-15. doi:10.1016/j.ajog.2012.02.038

146. Lim R, Malhotra A, Tan J, et al. First-In-Human Administration of Allogeneic Amnion Cells in Premature Infants With Bronchopulmonary Dysplasia: A Safety Study. *Stem Cells Transl Med*. 2018;7(9):628-635. doi:10.1002/sctm.18-0079

147. Takahashi K, Yamanaka S. Induction of pluripotent stem cells from mouse embryonic and adult fibroblast cultures by defined factors. *Cell*. 2006;126(4):663-676. doi:10.1016/j.cell.2006.07.024

148. Keller GM. In vitro differentiation of embryonic stem cells. *Curr Opin Cell Biol*. 1995;7(6):862-869. doi:10.1016/0955-0674(95)80071-9

149. Van Haute L, De Block G, Liebaers I, Sermon K, De Rycke M. Generation of lung epithelial-like tissue from human embryonic stem cells. *Respir Res*. 2009;10(1):105. doi:10.1186/1465-9921-10-105

150. Denham M, Cole TJ, Mollard R. Embryonic stem cells form glandular structures and express surfactant protein C following culture with dissociated fetal respiratory tissue. *Am J Physiol Lung Cell Mol Physiol*. 2006;290(6):L1210-5. doi:10.1152/ajplung.00427.2005

151. Vosdoganes P, Lim R, Moss TJM, Wallace EM. Cell therapy: a novel treatment approach for bronchopulmonary dysplasia. *Pediatrics*. 2012;130(4):727-737. doi:10.1542/peds.2011-2576

152. Akram K, Patel N, Spiteri M, Forsyth N. Lung Regeneration: Endogenous and Exogenous Stem Cell Mediated Therapeutic Approaches. *Int J Mol Sci*. 2016;17(1):128. doi:10.3390/ijms17010128

153. Chamberlain G, Fox J, Ashton B, Middleton J. Concise review: mesenchymal stem cells: their phenotype, differentiation capacity, immunological features, and potential for homing. *Stem Cells*. 2007;25(11):2739-2749. doi:10.1634/stemcells.2007-0197

154. Ghannam S, Bouffi C, Djouad F, Jorgensen C, Noël D. Immunosuppression by mesenchymal stem cells: mechanisms and clinical applications. *Stem Cell Res Ther*. 2010;1(1):2. doi:10.1186/scrt2

155. Jarvinen L, Badri L, Wettlaufer S, et al. Lung resident mesenchymal stem cells isolated from human lung allografts inhibit T cell proliferation via a soluble mediator. *J Immunol*. 2008;181(6):4389-4396.

156. Lama VN, Smith L, Badri L, et al. Evidence for tissue-resident mesenchymal stem cells in human adult lung from studies of transplanted allografts. *J Clin Invest*. 2007;117(4):989-996. doi:10.1172/JCI29713

157. Hennrick KT, Keeton AG, Nanua S, et al. Lung cells from neonates show a mesenchymal stem cell phenotype. *Am J Respir Crit Care Med*. 2007;175(11):1158-1164. doi:10.1164/rccm.200607-941OC

158. Van Haaften T, Byrne R, Bonnet S, et al. Airway delivery of mesenchymal stem cells prevents arrested alveolar growth in neonatal lung injury in rats. *Am J Respir Crit Care Med*. 2009;180(11):1131-1142. doi:10.1164/rccm.200902-0179OC

159. Aslam M, Baveja R, Liang OD, et al. Bone marrow stromal cells attenuate lung injury in a murine model of neonatal chronic lung disease. *Am J Respir Crit Care Med*. 2009;180(11):1122-1130. doi:10.1164/rccm.200902-0242OC

160. Amable PR, Teixeira MVT, Carias RBV, Granjeiro JM, Borojevic R. Protein synthesis and secretion in human mesenchymal cells derived from bone marrow, adipose tissue and Wharton's jelly. *Stem Cell Res Ther*. 2014;5(2):53. doi:10.1186/scrt442

161. in 't Anker PS, Scherjon SA, Kleijburg-van der Keur C, et al. Isolation of mesenchymal stem cells of fetal or maternal origin from human placenta. *Stem Cells*. 2004;22(7):1338-1345. doi:10.1634/stemcells.2004-0058

162. Le Blanc K. Immunomodulatory effects of fetal and adult mesenchymal stem cells. *Cytotherapy*. 2003;5(6):485-489. doi:10.1080/14653240310003611

163. Chang YS, Oh W, Choi SJ, et al. Human umbilical cord blood-derived mesenchymal

stem cells attenuate hyperoxia-induced lung injury in neonatal rats. *Cell Transplant*. 2009;18(8):869-886. doi:10.3727/096368909X471189

164. Pipino C, Shangaris P, Resca E, et al. Placenta as a reservoir of stem cells: An underutilized resource? *Br Med Bull*. 2013;105(1):43-67. doi:10.1093/bmb/lds033

165. Marongiu F, Gramignoli R, Sun Q, et al. Isolation of Amniotic Mesenchymal Stem Cells. *Curr Protoc Stem Biol*. 2010;Chapter 1:1-11. doi:10.1002/9780470151808

166. Bieback K, Brinkmann I. Mesenchymal stromal cells from human perinatal tissues: From biology to cell therapy. *World J Stem Cells*. 2010;2(4):81-92. doi:10.4252/wjsc.v2.i4.81

167. Pasquinelli G, Tazzari P, Ricci F, et al. Ultrastructural characteristics of human mesenchymal stromal (stem) cells derived from bone marrow and term placenta. *Ultrastruct Pathol*. 2007;31(1):23-31. doi:10.1080/01913120601169477

168. Yen BL, Huang H-I, Chien C-C, et al. Isolation of multipotent cells from human term placenta. *Stem Cells*. 2005;23(1):3-9. doi:10.1634/stemcells.2004-0098

169. Kong P, Xie X, Li F, Liu Y, Lu Y. Placenta mesenchymal stem cell accelerates wound healing by enhancing angiogenesis in diabetic Goto-Kakizaki (GK) rats. *Biochem Biophys Res Commun*. 2013;438(2):410-419. doi:10.1016/J.BBRC.2013.07.088

170. Medipost. PNEUMOSTEM. http://www.medi-post.com/pneumostem/. Accessed February 29, 2016.

171. Chang YS, Ahn SY, Yoo HS, et al. Mesenchymal stem cells for bronchopulmonary dysplasia: phase 1 dose-escalation clinical trial. *J Pediatr*. 2014;164(5):966-972.e6. doi:10.1016/j.jpeds.2013.12.011

172. Chang YS, Ahn SY, Jeon HB, et al. Critical Role of Vascular Endothelial Growth Factor Secreted by Mesenchymal Stem Cells in Hyperoxic Lung Injury. *Am J Respir Cell Mol Biol*. 2014;51(3):391-399. doi:10.1165/rcmb.2013-0385OC

173. Knoll A, Brockmeyer T, Chevalier R, Zscheppang K, Nielsen H, Dammann C. Adult Rat Bone Marrow-Derived Stem Cells Promote Late Fetal Type II Cell

Differentiation in a Co-Culture Model. *Open Respir Med J.* 2013;7:46-53. doi:10.2174/1874306401307010046

174. Fung M, Thébaud B. Stem cell-based therapy for neonatal lung disease-it's in the juice. *Pediatr res.* 2014;75(0):2-7. doi:10.1038/pr.2013.176.Stem

175. McAleese KA, Knapp MA, Rhodes TT. Financial and Emotional Cost Of Bronchopulmonary Dysplasia. *Clin Pediatr (Phila).* 1993;32(7):393-400. doi:10.1177/000992289303200702

176. Kotton DN, Morrisey EE. Lung regeneration: mechanisms, applications and emerging stem cell populations. *Nat Med.* 2014;141(4). doi:10.1016/j.surg.2006.10.010.Use

177. Forsyth NR, Evans AP, Shay JW, Wright WE. Developmental differences in the immortalization of lung fibroblasts by telomerase. *Aging Cell.* 2003;2(5):235-243. doi:10.1046/j.1474-9728.2003.00057.x

178. Forsyth NR, Vezzoni P, Simpson H. Physiologic Oxygen Enhances Human Embryonic Stem Cell Clonal Recovery and Reduces Chromosomal Abnormalities Article in Cloning and Stem Cells ·. 2006. doi:10.1089/clo.2006.8.16

179. Bell E, Ivarsson B, Merrill C. Production of a tissue-like structure by contraction of collagen lattices by human fibroblasts of different proliferative potential in vitro. *Proc Natl Acad Sci U S A.* 1979;76(3):1274-1278.

180. Yang T-H, Thoreson AR, Gingery A, et al. Collagen gel contraction as a measure of fibroblast function in carpal tunnel syndrome. *J Biomed Mater Res A.* 2015;103(2):574-580. doi:10.1002/jbm.a.35200

181. Chieh H-F, Sun Y, Liao J-D, et al. Effects of cell concentration and collagen concentration on contraction kinetics and mechanical properties in a bone marrow stromal cell-collagen construct. *J Biomed Mater Res A.* 2010;93(3):1132-1139. doi:10.1002/jbm.a.32606

182. Wang D-D, Liu W, Chang J-J, et al. Bioengineering three-dimensional culture model

of human lung cancer cells: an improved tool for screening EGFR targeted inhibitors. *RSC Adv.* 2016;6(29):24083-24090. doi:10.1039/C6RA00229C

183. Tsuji K, Ojima M, Otabe K, et al. Effects of Different Cell-Detaching Methods on the Viability and Cell Surface Antigen Expression of Synovial Mesenchymal Stem Cells. *Cell Transplant.* 2017;26(6):1089-1102. doi:10.3727/096368917X694831

184. Tzaki MG, Byrne PJ, Tanswell AK. Cellular interactions in pulmonary oxygen toxicity in vitro: II. Hyperoxia causes adult rat lung fibroblast cultures to produce apparently autocrine growth factors. *Exp Lung Res.* 1988;14(3):403-419.

185. Balin AK, Goodman DBP, Rasmussen H, Cristofalo VJ. The effect of oxygen tension on the growth and metabolism of WI-38 cells. *J Cell Physiol.* 1976;89(2):235-249. doi:10.1002/jcp.1040890207

186. Leddy R, Wilkinson JM. Endotracheal suctioning practices of nurses and respiratory therapists: How well do they align with clinical practice guidelines? *Can J Respir Ther CJRT = Rev Can la Ther Respir RCTR.* 2015;51(3):60-64.

187. Restrepo RD et al. AARC Clinical Practice Guidelines. Endotracheal suctioning of mechanically ventilated patients with artificial airways 2010. *Respir Care.* 2010;55(6):758-764. doi:10.4037/ajcc2014424

188. Shimotake TK, Izhar FM, Rumilla K, et al. Interleukin (IL)-1β in Tracheal Aspirates from Premature Infants Induces Airway Epithelial Cell IL-8 Expression via an NF-κB Dependent Pathway. *Pediatr Res.* 2004;56(6):907-913. doi:10.1203/01.PDR.0000145274.47221.10

189. Singhal KK, Parton LA. Plasminogen Activator Activity in Preterm Infants with Respiratory Distress Syndrome: Relationship to the Development of Bronchopulmonary Dysplasia. *Pediatr Res.* 1996;39(2):229-235. doi:10.1203/00006450-199602000-00007

190. Ahn Y, Hwang T. The effects of shallow versus deep endotracheal suctioning on the cytological components of respiratory aspirates in high-risk infants. *Respiration.*

2003;70(2):172-178. doi:10.1159/000070065

191. Bridges MA, Walker DC, Davidson AGF. Cystic Fibrosis and Control Nasal Epithelial Cells Harvested by a Brushing Procedure. *Vitr Cell Dev Biol*. 27:684-686. doi:10.2307/4296730

192. LOPEZ-SOUZA N, AVILA PC, WIDDICOMBE JH. POLARIZED CULTURES OF HUMAN AIRWAY EPITHELIUM FROM NASAL SCRAPINGS AND BRONCHIAL BRUSHINGS. *Vitr Cell Dev Biol - Anim*. 2003;39(7):266. doi:10.1290/1543-706X(2003)039<0266:PCOHAE>2.0.CO;2

193. Diekman BO, Christoforou N, Willard VP, et al. Cartilage tissue engineering using differentiated and purified induced pluripotent stem cells. *Proc Natl Acad Sci U S A*. 2012;109(47):19172-19177. doi:10.1073/pnas.1210422109

194. Pipkorn U, Karlsson G, Enerbäck L. A brush method to harvest cells from the nasal mucosa for microscopic and biochemical analysis. *J Immunol Methods*. 1988;112(1):37-42.

195. Thavagnanam S, Parker JC, McBrien ME, Skibinski G, Shields MD, Heaney LG. Nasal Epithelial Cells Can Act as a Physiological Surrogate for Paediatric Asthma Studies. Knoll B, ed. *PLoS One*. 2014;9(1):e85802. doi:10.1371/journal.pone.0085802

196. Merkle, Ditzinger, Lang, Peter, Schmidt. In vitro cell models to study nasal mucosal permeability and metabolism. *Adv Drug Deliv Rev*. 1998;29(1-2):51-79.

197. Howarth PH, Persson CGA, Meltzer EO, Jacobson MR, Durham SR, Silkoff PE. Objective monitoring of nasal airway inflammation in rhinitis. doi:10.1016/j.jaci.2004.12.1134

198. Gelardi M, Iannuzzi L, Quaranta N, Landi M, Passalacqua G. NASAL cytology: practical aspects and clinical relevance. *Clin Exp Allergy*. 2016;46(6):785-792. doi:10.1111/cea.12730

199. Meltzer EO, Orgel HA, Rogenes PR, Field EA. Nasal cytology in patients with allergic rhinitis: effects of intranasal fluticasone propionate. *J Allergy Clin Immunol*.

1994;94(4):708-715.

200. Mcdougall CM, Blaylock MG, Douglas JG, Brooker RJ, Helms PJ, Walsh GM. Nasal Epithelial Cells as Surrogates for Bronchial Epithelial Cells in Airway Inflammation Studies. doi:10.1165/rcmb.2007-0325OC

201. Friedenstein AJ, Chailakhyan RK, Latsinik N V, Panasyuk AF, Keiliss-Borok I V. Stromal cells responsible for transferring the microenvironment of the hemopoietic tissues. Cloning in vitro and retransplantation in vivo. *Transplantation*. 1974;17(4):331-340.

202. Stewart MC, Stewart AA. Mesenchymal Stem Cells: Characteristics, Sources, and Mechanisms of Action. *Vet Clin North Am Equine Pract*. 2011;27(2):243-261. doi:10.1016/j.cveq.2011.06.004

203. Baksh D, Song L, Tuan RS. Adult mesenchymal stem cells: characterization, differentiation, and application in cell and gene therapy. *J Cell Mol Med*. 8(3):301-316.

204. Sudo K, Kanno M, Miharada K, et al. Mesenchymal Progenitors Able to Differentiate into Osteogenic, Chondrogenic, and/or Adipogenic Cells In Vitro Are Present in Most Primary Fibroblast-Like Cell Populations. *Stem Cells*. 2007;25(7):1610-1617. doi:10.1634/stemcells.2006-0504

205. Igura K, Zhang X, Takahashi K, Mitsuru A, Yamaguchi S, Takashi TA. Isolation and characterization of mesenchymal progenitor cells from chorionic villi of human placenta. *Cytotherapy*. 2004;6(6):543-553.

206. Collins JJP, Thébaud B. Lung Mesenchymal Stromal Cells in Development and Disease: To Serve and Protect? *Antioxid Redox Signal*. 2014;21(13):1849-1862. doi:10.1089/ars.2013.5781

207. Arnon S, Grigg J, Silverman M, Shmuel Arnon Jonathan Grigg Michael Silverman O. Pulmonary inflammatory cells in ventilated preterm infants: effect of surfactant treatment. *Arch Dis Child*. 1993;69:44-48. doi:10.1136/adc.69.1_Spec_No.44

208. LoMonaco MB, Barber CM, Sinkin RA. Differential Cytokine mRNA Expression by Neonatal Pulmonary Cells. *Pediatr Res*. 1996;39(2):248-252. doi:10.1203/00006450-199602000-00010

209. Aghai ZH, Kode A, Saslow JG, et al. Azithromycin Suppresses Activation of Nuclear Factor-kappa B and Synthesis of Pro-inflammatory Cytokines in Tracheal Aspirate Cells From Premature Infants. *Pediatr Res*. 2007;62(4):483-488. doi:10.1203/PDR.0b013e318142582d

210. Goodpaster T, Legesse-Miller A, Hameed MR, Aisner SC, Randolph-Habecker J, Coller HA. An immunohistochemical method for identifying fibroblasts in formalin-fixed, paraffin-embedded tissue. *J Histochem Cytochem*. 2008;56(4):347-358. doi:10.1369/jhc.7A7287.2007

211. Liberio MS, Sadowski MC, Soekmadji C, Davis RA, Nelson CC. Differential effects of tissue culture coating substrates on prostate cancer cell adherence, morphology and behavior. *PLoS One*. 2014;9(11):e112122. doi:10.1371/journal.pone.0112122

212. Maestre-Batlle D, Pena OM, Hirota JA, et al. Novel flow cytometry approach to identify bronchial epithelial cells from healthy human airways. *Sci Rep*. 2017;7(February):42214. doi:10.1038/srep42214

213. Pipolo C, Bianchini S, Barberi S, et al. Nasal cytology in children: scraping or swabbing? *Rhinol J*. 2017;55(3):242250. doi:10.4193/Rhin16.287

214. Popova AP, Bozyk PD, Bentley JK, et al. Isolation of Tracheal Aspirate Mesenchymal Stromal Cells Predicts Bronchopulmonary Dysplasia. *Pediatrics*. 2010;126(5):e1127-e1133. doi:10.1542/peds.2009-3445

215. Augustine S, Avey MT, Harrison B, et al. Mesenchymal Stromal Cell Therapy in Bronchopulmonary Dysplasia: Systematic Review and Meta-Analysis of Preclinical Studies. *Stem Cells Transl Med*. October 2017. doi:10.1002/sctm.17-0126

216. Nishio K, Inoue A, Qiao S, Kondo H, Mimura A. Senescence and cytoskeleton: overproduction of vimentin induces senescent-like morphology in human

fibroblasts. *Histochem Cell Biol*. 2001;116(4):321-327. doi:10.1007/s004180100325

217. Bahsoun S, Coopman K, Forsyth NR, Akam EC. The Role of Dissolved Oxygen Levels on Human Mesenchymal Stem Cell Culture Success, Regulatory Compliance, and Therapeutic Potential. *Stem Cells Dev*. 2018;27(19):1303-1321. doi:10.1089/scd.2017.0291

218. Rosová I, Dao M, Capoccia B, Link D, Nolta JA. Hypoxic Preconditioning Results in Increased Motility and Improved Therapeutic Potential of Human Mesenchymal Stem Cells. *Stem Cells*. 2008;26(8):2173-2182. doi:10.1634/stemcells.2007-1104

219. Araújo AB, Salton GD, Furlan JM, et al. Comparison of human mesenchymal stromal cells from four neonatal tissues: Amniotic membrane, chorionic membrane, placental decidua and umbilical cord. *Cytotherapy*. 2017;19(5):577-585. doi:10.1016/j.jcyt.2017.03.001

220. Choo KB, Tai L, Hymavathee KS, et al. Oxidative Stress-Induced Premature Senescence in Wharton's Jelly-Derived Mesenchymal Stem Cells. *Int J Med Sci*. 2014;11(11):1201-1207. doi:10.7150/ijms.8356

221. Popova AP. Mesenchymal cells and bronchopulmonary dysplasia: new insights about the dark side of oxygen. *AJRCMB Artic Press Publ*. 2019;15. doi:10.1165/rcmb.2019-0010ED

222. Urbanek K, De Angelis A, Spaziano G, et al. Intratracheal Administration of Mesenchymal Stem Cells Modulates Tachykinin System, Suppresses Airway Remodeling and Reduces Airway Hyperresponsiveness in an Animal Model. *PLoS One*. 2016;11(7):e0158746. doi:10.1371/journal.pone.0158746

223. Kay AG, Long G, Tyler G, et al. Mesenchymal Stem Cell-Conditioned Medium Reduces Disease Severity and Immune Responses in Inflammatory Arthritis. *Sci Rep*. 2017;7(1):18019. doi:10.1038/s41598-017-18144-w

224. Yamahara K, Harada K, Ohshima M, et al. Comparison of Angiogenic, Cytoprotective,

and Immunosuppressive Properties of Human Amnion- and Chorion-Derived Mesenchymal Stem Cells. Asakura A, ed. *PLoS One*. 2014;9(2):e88319. doi:10.1371/journal.pone.0088319

225. Dominici M, Le Blanc K, Mueller I, et al. Minimal criteria for defining multipotent mesenchymal stromal cells. The International Society for Cellular Therapy position statement. *Cytotherapy*. 2006;8(4):315-317. doi:10.1080/14653240600855905

226. Merino-González C, Zuñiga FA, Escudero C, et al. Mesenchymal Stem Cell-Derived Extracellular Vesicles Promote Angiogenesis: Potencial Clinical Application. *Front Physiol*. 2016;7:24. doi:10.3389/fphys.2016.00024

227. Ionescu L, Byrne RN, van Haaften T, et al. Stem cell conditioned medium improves acute lung injury in mice: in vivo evidence for stem cell paracrine action. *Am J Physiol Cell Mol Physiol*. 2012;303(11):L967-L977. doi:10.1152/ajplung.00144.2011

228. Pierro M, Ionescu L, Montemurro T, et al. Short-term, long-term and paracrine effect of human umbilical cord-derived stem cells in lung injury prevention and repair in experimental bronchopulmonary dysplasia. *Thorax*. 2013;68(5):475-484. doi:10.1136/thoraxjnl-2012-202323

229. Yu B, Zhang X, Li X, Yu B, Zhang X, Li X. Exosomes Derived from Mesenchymal Stem Cells. *Int J Mol Sci*. 2014;15(3):4142-4157. doi:10.3390/ijms15034142

230. Herberts CA, Kwa MSG, Hermsen HPH. Risk factors in the development of stem cell therapy. *J Transl Med*. 2011;9:29. doi:10.1186/1479-5876-9-29

231. Nardiello C, Mižíková I, Morty RE. Looking ahead: where to next for animal models of bronchopulmonary dysplasia? *Cell Tissue Res*. 2017;367(3):457-468. doi:10.1007/s00441-016-2534-3

232. Grinnell F. Fibroblasts, myofibroblasts, and wound contraction. *J Cell Biol*. 1994;124(4):401-404.

233. Mio T, Adachi Y, Romberger DJ, Ertl RF, Rennard SI. Regulation of fibroblast

proliferation in three-dimensional collagen gel matrix. *In Vitro Cell Dev Biol Anim*. 32(7):427-433.

234. Wang H, Liu X, Umino T, et al. Effect of cigarette smoke on fibroblast-mediated gel contraction is dependent on cell density. *Am J Physiol Cell Mol Physiol*. 2003;284(1):L205-L213. doi:10.1152/ajplung.00042.2002

235. Togo S, Holz O, Liu X, et al. Lung Fibroblast Repair Functions in Patients with Chronic Obstructive Pulmonary Disease Are Altered by Multiple Mechanisms. *Am J Respir Crit Care Med*. 2008;178(3):248. doi:10.1164/RCCM.200706-929OC

236. Sucre JMS, Wilkinson D, Vijayaraj P, et al. A 3-Dimensional Human Model of the Fibroblast Activation that Accompanies Bronchopulmonary Dysplasia Identifies Notch-Mediated Pathophysiology. *Am J Physiol - Lung Cell Mol Physiol*. 2016;310(33):ajplung.00446.2015. doi:10.1152/ajplung.00446.2015

237. Kaarteenaho-Wiik R, Pääkkö P, Herva R, Risteli J, Soini Y. Type I and III collagen protein precursors and mRNA in the developing human lung. *J Pathol*. 2004;203(1):567-574. doi:10.1002/path.1547

238. Lareu RR, Zeugolis DI, Abu-Rub M, Pandit A, Raghunath M. Essential modification of the Sircol Collagen Assay for the accurate quantification of collagen content in complex protein solutions. *Acta Biomater*. 2010;6(8):3146-3151. doi:10.1016/J.ACTBIO.2010.02.004

239. Lescan M, Perl RM, Golombek S, et al. De Novo Synthesis of Elastin by Exogenous Delivery of Synthetic Modified mRNA into Skin and Elastin-Deficient Cells. *Mol Ther Nucleic Acids*. 2018;11:475-484. doi:10.1016/j.omtn.2018.03.013

240. Manova-Todorova K, Fujisawa S, Yarilin D, et al. Understanding the three-dimensional world from two-dimensional immunofluorescent adjacent sections. *J Pathol Inform*. 2015;6(1):27. doi:10.4103/2153-3539.158052

241. Wang Z, Wei D, Xiao H. Methods of cellular senescence induction using oxidative stress. *Methods Mol Biol*. 2013;1048:135-144. doi:10.1007/978-1-62703-556-9_11

242. Oh S, Lee E, Lee J, Lim Y, Kim J, Woo S. Comparison of the effects of 40% oxygen and two atmospheric absolute air pressure conditions on stress-induced premature senescence of normal human diploid fibroblasts. *Cell Stress Chaperones*. 2008;13(4):447. doi:10.1007/S12192-008-0041-5

243. von Zglinicki T, Saretzki G, Döcke W, Lotze C. Mild Hyperoxia Shortens Telomeres and Inhibits Proliferation of Fibroblasts: A Model for Senescence? *Exp Cell Res*. 1995;220(1):186-193. doi:10.1006/excr.1995.1305

244. Davies K. The Broad Spectrum of Responses to Oxidants in Proliferating Cells: A New Paradigm for Oxidative Stress. *IUBMB Life*. 1999;48(1):41-47. doi:10.1080/713803463

245. Balin AK, Goodman DB, Rasmussen H, Cristofalo VJ. Oxygen-sensitive stages of the cell cycle of human diploid cells. *J Cell Biol*. 1978;78(2):390-400. doi:10.1083/JCB.78.2.390

246. Infeld MD, Brennan JA, Davis PB. Human tracheobronchial epithelial cells direct migration of lung fibroblasts in three-dimensional collagen gels. *Am J Physiol Cell Mol Physiol*. 1992;262(5):L535-L541. doi:10.1152/ajplung.1992.262.5.L535

247. Schneider EL, Mitsui Y. The relationship between in vitro cellular aging and in vivo human age. *Proc Natl Acad Sci U S A*. 1976;73(10):3584-3588.

248. Nishio K, Inoue A. Senescence-associated alterations of cytoskeleton: extraordinary production of vimentin that anchors cytoplasmic p53 in senescent human fibroblasts. *Histochem Cell Biol*. 2005;123(3):263-273. doi:10.1007/s00418-005-0766-5

249. Debacq-Chainiaux F, Erusalimsky JD, Campisi J, Toussaint O. Protocols to detect senescence-associated beta-galactosidase (SA-βgal) activity, a biomarker of senescent cells in culture and in vivo. *Nat Protoc*. 2009;4(12):1798-1806. doi:10.1038/nprot.2009.191

250. Harrington H, Cato P, Salazar F, et al. Immunocompetent 3D model of human upper

airway for disease modeling and in vitro drug evaluation. *Mol Pharm*. 2014;11(7):2082-2091. doi:10.1021/mp5000295

251. Vicencio AG, Lee CG, Cho SJ, et al. Conditional Overexpression of Bioactive Transforming Growth Factor–β1 in Neonatal Mouse Lung. *Am J Respir Cell Mol Biol*. 2004;31(6):650-656. doi:10.1165/rcmb.2004-0092OC

252. Hilgendorff A, Parai K, Ertsey R, et al. *Neonatal Mice Genetically Modified to Express the Elastase Inhibitor Elafin Are Protected against the Adverse Effects of Mechanical Ventilation on Lung Growth*. Vol 303. American Physiological Society Bethesda, MD; 2012:L215-L227. doi:10.1152/ajplung.00405.2011

253. Mokres LM, Parai K, Hilgendorff A, et al. Prolonged mechanical ventilation with air induces apoptosis and causes failure of alveolar septation and angiogenesis in lungs of newborn mice. *Am J Physiol Lung Cell Mol Physiol*. 2010;298(1):L23-35. doi:10.1152/ajplung.00251.2009

254. Zhang Z-Q, Huang X-M, Lu H. Early biomarkers as predictors for bronchopulmonary dysplasia in preterm infants: a systematic review. *Eur J Pediatr*. 2014;173(1):15-23. doi:10.1007/s00431-013-2148-7

255. Montesano R, Orci L. Transforming growth factor beta stimulates collagen-matrix contraction by fibroblasts: Implications for wound healing. *Proc Natd Acad Sci USA*. 1988;85(July):4894-4897.

256. LIU XD, UMINO T, ERTL R, et al. PERSISTENCE OF TGF-β1 INDUCTION OF INCREASED FIBROBLAST CONTRACTILITY. *Vitr Cell Dev Biol - Anim*. 2001;37(3):193. doi:10.1290/1071-2690(2001)037<0193:POTIOI>2.0.CO;2

257. Pechkovsky D V., Hackett TL, An SS, Shaheen F, Murray LA, Knight DA. Human Lung Parenchyma but Not Proximal Bronchi Produces Fibroblasts with Enhanced TGF-β Signaling and α-SMA Expression. *Am J Respir Cell Mol Biol*. 2010;43(6):641-651. doi:10.1165/rcmb.2009-0318OC

258. Wipff P-J, Rifkin DB, Meister J-J, Hinz B. Myofibroblast contraction activates latent

TGF-β1 from the extracellular matrix. *J Cell Biol*. 2007;179(6):1311-1323. doi:10.1083/jcb.200704042

259. Tomasek JJ, Gabbiani G, Hinz B, Chaponnier C, Brown RA. Myofibroblasts and mechano-regulation of connective tissue remodelling. *Nat Rev Mol Cell Biol*. 2002;3(5):349-363. doi:10.1038/nrm809

260. Thibeault DW, Mabry SM, Ekekezie II, Truog WE. Lung elastic tissue maturation and perturbations during the evolution of chronic lung disease. *Pediatrics*. 2000;106(6):1452-1459.

261. Pierce RA, Albertine KH, Starcher BC, Bohnsack JF, Carlton DP, Bland RD. Chronic lung injury in preterm lambs: disordered pulmonary elastin deposition. *Am J Physiol Cell Mol Physiol*. 1997;272(3):L452-L460. doi:10.1152/ajplung.1997.272.3.L452

262. Cho HY, Jedlicka AE, Reddy SPM, et al. Role of NRF2 in protection against hyperoxic lung injury in mice. *Am J Respir Cell Mol Biol*. 2002;26(2):175-182. doi:10.1165/ajrcmb.26.2.4501

263. Fahey JW, Talalay P. *Antioxidant Functions of Sulforaphane: A Potent Inducer of Phase II Detoxication Enzymes*.

264. Bailo M, Soncini M, Vertua E, et al. Engraftment potential of human amnion and chorion cells derived from term placenta. *Transplantation*. 2004;78(10):1439-1448.

265. Soncini M, Vertua E, Gibelli L, et al. Isolation and characterization of mesenchymal cells from human fetal membranes. *J Tissue Eng Regen Med*. 2007;1(4):296-305. doi:10.1002/term.40

266. Alviano F, Fossati V, Marchionni C, et al. Term Amniotic membrane is a high throughput source for multipotent Mesenchymal Stem Cells with the ability to differentiate into endothelial cells in vitro. *BMC Dev Biol*. 2007;7(1):11. doi:10.1186/1471-213X-7-11

267. Kim SS, Song CK, Shon SK, et al. Effects of human amniotic membrane grafts combined with marrow mesenchymal stem cells on healing of full-thickness skin defects in rabbits. *Cell Tissue Res*. 2009;336(1):59-66. doi:10.1007/s00441-009-0766-1

268. Kang N-H, Hwang K-A, Kim SU, et al. Potential antitumor therapeutic strategies of human amniotic membrane and amniotic fluid-derived stem cells. *Cancer Gene Ther*. 2012;19(8):517-522. doi:10.1038/cgt.2012.30

269. Perrone S, Tataranno ML, Buonocore G. Oxidative stress and bronchopulmonary dysplasia. *J Clin Neonatol*. 2012;1(3):109-114. doi:10.4103/2249-4847.101683

270. Simones AA, Beisang DJ, Panoskaltsis-Mortari A, Roberts KD. Mesenchymal stem cells in the pathogenesis and treatment of bronchopulmonary dysplasia: a clinical review. *Pediatr Res*. 2018;83(1-2):308-317. doi:10.1038/pr.2017.237

271. Wu J, Wang Y, Liu G, et al. Characterization of air-liquid interface culture of A549 alveolar epithelial cells. *Brazilian J Med Biol Res*. 2018;51(2). doi:10.1590/1414-431X20176950

272. Fischer HS, Schmölzer GM, Cheung P-Y, Bührer C. Sustained inflations and avoiding mechanical ventilation to prevent death or bronchopulmonary dysplasia: a meta-analysis. *Eur Respir Rev*. 2018;27(150):180083. doi:10.1183/16000617.0083-2018

273. Ratner V, Slinko S, Utkina-Sosunova I, Starkov A, Polin RA, Ten VS. Hypoxic stress exacerbates hyperoxia-induced lung injury in a neonatal mouse model of bronchopulmonary dysplasia. *Neonatology*. 2009;95(4):299-305. doi:10.1159/000178798

274. Martin RJ, Di Fiore JM, Walsh MC. Hypoxic Episodes in Bronchopulmonary Dysplasia. *Clin Perinatol*. 2015;42(4):825-838. doi:10.1016/j.clp.2015.08.009

275. Walkty A, Lagace-Wiens PRS, Manickam K, et al. Re-evaluation of rejection criteria for endotracheal tube (ETT) specimens from adult patients. *J Med Microbiol*.

2012;61(Pt_9):1306-1310. doi:10.1099/jmm.0.042333-0

276. Lam HC, Choi AMK, Ryter SW. Isolation of Mouse Respiratory Epithelial Cells and Exposure to Experimental Cigarette Smoke at Air Liquid Interface. *J Vis Exp*. 2011;(48). doi:10.3791/2513

277. Whittaker P, Boughner DR, Kloner RA. *Analysis of Healing After Myocardial Infarction Using Polarized Light Microscopy*. Vol 134.; 1989.

278. Ricard C, Vial J-C, Douady J, van der Sanden B. In vivo imaging of elastic fibers using sulforhodamine B. *J Biomed Opt*. 2007;12(6):064017. doi:10.1117/1.2821421

279. Del Fattore A, Luciano R, Pascucci L, et al. Immunoregulatory Effects of Mesenchymal Stem Cell-Derived Extracellular Vesicles on T Lymphocytes. *Cell Transplant*. 2015;24(12):2615-2627. doi:10.3727/096368915X687543

Appendices

Appendix A: Ethical approval for the use of tracheal suctionings and nasal scrapings

Ymchwil Iechyd a Gofal Cymru
Health and Care Research Wales

Gwasanaeth Moeseg Ymchwil
Research Ethics Service

Ariennir gan
Lywodraeth Cymru
Funded by
Welsh Government

WALES REC 7
PO Box 108
Building 1
St David's Park
Jobswell Road
Carmarthen
SA31 3WY

Tel: 01267 225045
Email: sue.byng@wales.nhs.uk

Miss Jessica Bratt
Guy Hilton Research Centre,
Thornburrow Drive,
Stoke-on-Trent
ST4 7QB

23 August 2016

Dear Miss Bratt

Study title:	Regenerative medicine therapy of Bronchopulmonary dysplasia
REC reference:	16/WA/0265
Protocol number:	1.1
IRAS project ID:	210337

Thank you for your application for ethical review, which was received on 18 August 2016. I can confirm that the application is valid and will be reviewed by the Sub-Committee.

One of the REC members is appointed as the lead reviewer for each application reviewed by the Sub-Committee. The lead reviewer for your application is Dr Raymond Jones.

Please note that the lead reviewer may wish to contact you by phone or email between 30 August and 7 September 2016 to clarify any points that might be raised by members and assist the Sub-Committee in reaching a decision.

If you will not be available between these dates, you are welcome to nominate another key investigator or a representative of the study sponsor who would be able to respond to the lead reviewer's queries on your behalf. If this is your preferred option, please identify this person to us and ensure we have their contact details.

You are not required to attend a meeting of the Proportionate Review Sub-Committee.

Please do not send any further documentation or revised documentation prior to the review unless requested.

Documents received

The documents to be reviewed are as follows:

Document	Version	Date
Evidence of Sponsor insurance or indemnity (non NHS Sponsors only) [Insurance]		1/8/16 to 31/7/17
IRAS Application Form [IRAS_Form_18082016]		18 August 2016
IRAS Checklist XML [Checklist_18082016]		18 August 2016
Letter from funder		10 June 2014
Participant consent form	1	10 June 2016
Participant information sheet (PIS) [PIS group A]	1	10 June 2016
Participant information sheet (PIS) [PIS group B]	1	10 June 2016
Participant information sheet (PIS) [PIS group C]	1	10 June 2016

Research protocol or project proposal	1.1	15 July 2016
Summary CV for Chief Investigator (CI) [Jessica Bratt]		
Summary CV for supervisor (student research) [Dr Pensee Wu]		

No changes may be made to the application before the meeting. If you envisage that changes might be required, you are advised to withdraw the application and re-submit it.

Notification of the Sub-Committee's decision

We aim to notify the outcome of the Sub-Committee review to you in writing within 10 working days from the date of receipt of a valid application.

If the Sub-Committee is unable to give an opinion because the application raises material ethical issues requiring further discussion at a full meeting of a Research Ethics Committee, your application will be referred for review to the next available meeting. We will contact you to explain the arrangements for further review and check they are convenient for you. You will be notified of the final decision within 60 days of the date on which we originally received your application. If the first available meeting date offered to you is not suitable, you may request review by another REC. In this case the 60 day clock would be stopped and restarted from the closing date for applications submitted to that REC.

Setting up sites in the NHS

All researchers and local research collaborators who intend to participate in this study at sites in the National Health Service (NHS) or Health and Social Care (HSC) in Northern Ireland should work with the relevant care organisation to ensure management permission is confirmed before the study begins. Guidance on how to work with sites is provided in the IRAS help section at https://www.myresearchproject.org.uk/help/hlpnhshscr.aspx

Final management permission will not be confirmed until after a favourable opinion has been given by this Committee, and all other relevant approvals for the research to begin are in place. Please contact the NHS R&D office at the lead site in the first instance for further guidance.

Communication with other bodies

All correspondence from the REC about the application will be copied to the research sponsor and to the R&D office for University Hospitals of North Midlands NHS Trust. It will be your responsibility to ensure that other investigators, research collaborators and NHS care organisation(s) involved in the study are kept informed of the progress of the review, as necessary.

HRA Training

We are pleased to welcome researchers and R&D staff at our training days – see details at http://www.hra.nhs.uk/hra-training/

16/WA/0265	Please quote this number on all correspondence

Yours sincerely

SueByg

Ms Sue Byng
REC Manager

Copy to: Dr Tracy Nevatte
               Dr Darren Clement, University Hospitals of North Midlands NHS Trust

218

Appendix B: Letter of Access

University Hospitals of North Midlands **NHS**

NHS Trust

RESEARCH AND DEVELOPMENT DEPARTMENT
Academic Research Unit
Courtyard Annexe – C Block
Newcastle Road
Stoke-on-Trent
ST4 6QG
Tel: 01782 675398
Fax: 01782 675399

23rd March 2017

Miss Jessica Bratt
6 Thornhill Drive,
Madeley,
Crewe,
Cheshire
CW3 9UE

Dear Jessica

Letter of access for research – RegenBro (Regenerative medicine therapy of Bronchopulmonary dysplasia)

This letter should be presented to each participating organisation before you commence your research at that site. The participating organisation is **University Hospitals of North Midlands NHS Trust.**

In accepting this letter, each participating organisation confirms your right of access to conduct research through their organisation for the purpose and on the terms and conditions set out below. This right of access commences on **23rd March 2017** and ends on **1st Septmeber 2019** unless terminated earlier in accordance with the clauses below.

You have a right of access to conduct such research as confirmed in writing in the letter of permission for research from **University Hospitals of North Midlands NHS Trust.** Please note that you cannot start the research until the Principal Investigator for the research project has received a letter from us giving confirmation from the individual organisation(s) of their agreement to conduct the research.

The information supplied about your role in research at the organisation(s) has been reviewed and you do not require an honorary research contract with the organisation(s). We are satisfied that such pre-engagement checks as we consider necessary have been carried out.

You are considered to be a legal visitor to the organisations premises. You are not entitled to any form of payment or access to other benefits provided by the organisation(s) or this organisation to employees and this letter does not give rise to any other relationship between you and the organisation(s), in particular that of an employee.

While undertaking research through the organisation(s) you will remain accountable to your substantive employer but you are required to follow the reasonable

L004 - Example letter of access for university researchers who do not require an honorary research contract
Version 2.3 August 2013
Research in the NHS: HR Good Practice Resource Pack   Page 1 of 3

University Hospitals of North Midlands **NHS**

NHS Trust

instructions of the organisation(s) or those instructions given on their behalf in relation to the terms of this right of access.

Where any third party claim is made, whether or not legal proceedings are issued, arising out of or in connection with your right of access, you are required to co-operate fully with any investigation by the organisation(s) in connection with any such claim and to give all such assistance as may reasonably be required regarding the conduct of any legal proceedings.
You must act in accordance with the organisations policies and procedures, which are available to you upon request, and the Research Governance Framework.

You are required to co-operate with the organisation(s) in discharging its/their duties under the Health and Safety at Work etc Act 1974 and other health and safety legislation and to take reasonable care for the health and safety of yourself and others while on the organisations premises. You must observe the same standards of care and propriety in dealing with patients, staff, visitors, equipment and premises as is expected of any other contract holder and you must act appropriately, responsibly and professionally at all times.

If you have a physical or mental health condition or disability which may affect your research role and which might require special adjustments to your role, if you have not already done so, you must notify your employer and each organisation prior to commencing your research role at that organisation.

You are required to ensure that all information regarding patients or staff remains secure and *strictly confidential* at all times. You must ensure that you understand and comply with the requirements of the NHS Confidentiality Code of Practice and the Data Protection Act 1998. Furthermore you should be aware that under the Act, unauthorised disclosure of information is an offence and such disclosures may lead to prosecution.

You should ensure that, where you are issued with an identity or security card, a bleep number, email or library account, keys or protective clothing, these are returned upon termination of this arrangement. Please also ensure that while on the organisations premises you wear your ID badge at all times, or are able to prove your identity if challenged. Please note that the organisation(s) do not accept responsibility for damage to or loss of personal property.

This organisation may revoke this letter and any organisation(s) may terminate your right to attend at any time either by giving seven days' written notice to you or immediately without any notice if you are in breach of any of the terms or conditions described in this letter or if you commit any act that we reasonably consider to amount to serious misconduct or to be disruptive and/or prejudicial to the interests and/or business of the organisation(s) or if you are convicted of any criminal offence. You must not undertake regulated activity if you are barred from such work. If you are barred from working with adults or children this letter of access is immediately terminated. Your employer will immediately withdraw you from undertaking this or any other regulated activity and you MUST stop undertaking any regulated activity immediately.

Your substantive employer is responsible for your conduct during this research project and may in the circumstances described above instigate disciplinary action against you.

L004 - Example letter of access for university researchers who do not require an honorary research contract
Version 2.3 August 2013
Research in the NHS: HR Good Practice Resource Pack

Page 2 of 3

University Hospitals of North Midlands **NHS**

NHS Trust

No organisation will indemnify you against any liability incurred as a result of any breach of confidentiality or breach of the Data Protection Act 1998. Any breach of the Data Protection Act 1998 may result in legal action against you and/or your substantive employer.

If your current role or involvement in research changes, or any of the information provided in your Research Passport changes, you must inform your employer through their normal procedures. You must also inform your nominated manager in each participating organisation and the R&D office in this organisation.

Yours sincerely

Mrs Heather Reidy,
Senior Research Governance Facilitator, UHNM

cc: Pensee Wu, Lecturer in O&G – Keele University
cc: Gill Farr, HR Administrator, Keele University

L004 - Example letter of access for university researchers who do not require an honorary research contract
Version 2.3 August 2013
Research in the NHS: HR Good Practice Resource Pack   Page 3 of 3

Appendix C: Ethical approval for the use of placentas for cell isolation

RESEARCH needs YOU

University Hospitals of North Midlands **NHS**
NHS Trust

RESEARCH AND DEVELOPMENT DEPARTMENT
Academic Research Unit
Courtyard Annexe – C Block
Newcastle Road
Stoke-on-Trent
ST4 6QG
Telephone: 01782 675387
Fax: 01782 675399

Email: Darren.Clement@uhns.nhs.uk
research.governance@uhns.nhs.uk

Ref: DC/CR

28th June 2016

Dr Pensee Wu
Consultant in Maternal Foetal Medicine
University Hospitals of North Midlands NHS Trust
Maternity Department
The Royal Stoke University Hospital
Newcastle Road
Stoke-on-Trent
ST4 6QG

Dear Dr Wu

Re: PERsonalised approach to FEtal stem Cell bank Use – do pregnancy
complications affect stem cell behaviour for autologous use? – PERFEC-U
Chief Investigator: Dr Pensee Wu
Sponsor/Co-Sponsor: University Hospitals of North Midlands NHS Trust
SSI Submission Date: 17/03/2016

I can confirm that the above project has been given NHS Permission for Research by the
Research & Development Department for the University Hospitals of North Midlands NHS
Trust and the details entered on to the R&D database.

I note that this research project has been approved by **West Midlands – Solihull**
Research Ethics Committee reference: 15/WM/0342

NHS permission for the above research has been granted on the basis described in the
application form, protocol and supporting documentation. The documents reviewed were:

Document	Version Number	Date
Protocol	2.1	03/03/16
PIS (C)	1.1	15/12/15
PIS (G)	1.1	15/12/15
PIS (P)	1.1	15/12/15
Consent Form (C)	1.1	15/12/15
Consent Form (G)	1.1	15/12/15

R&D ID: 1125 UKCRN ID: n/a CSP ID: n/a REC REF: 15/WM/0342

Consent Form (P)	1.1	15/12/15

The research sponsor or the Chief Investigator, or the local Principal Investigator at a research site, may take appropriate urgent safety measures in order to protect research participants against any immediate hazard to their health or safety. The R&D office should be notified that such measures have been taken. The notification should also include the reasons why the measures were taken and the plan for further action. The R&D office should be notified within the same time frame of notifying the REC and any other regulatory bodies.

Approval by the R&D Dept therefore assumes that you have read, understand and agree to comply with the:

- ❖ Research Governance Framework (www.gov.uk/government/publications/research-governance-framework-for-health-and-social-care-second-edition)
- ❖ Data Protection Act
- ❖ Health and Safety Act
- ❖ ICH Guidelines on good clinical practice
- ❖ All applicable Trust policies & procedures

In line with these requirements may I draw your attention to the need for you to provide the following documentation/notifications to the R&D Department throughout the course of the study and that all amendments (including changes to the local research team) need to be submitted to R&D in accordance with guidance in IRAS:-

- ❖ Annual Progress Report Form (sent to you by this department)
- ❖ End of Study Declaration Form (available on IRAS website)
- ❖ Changes to study start and end dates
- ❖ Changes in study personnel

Please note that the NHS organisation is required to monitor research to ensure compliance with the Research Governance Framework and other legal and regulatory requirements. This will be achieved by random audit by our department.

I would like to take this opportunity to wish you well with your research. If you need any further advice or guidance please do not hesitate to contact us.

Yours sincerely

Dr Darren Clement
R&D Manager – University Hospitals of North Midlands NHS Trust

Cc   Fidelma O'Mahony – Clinical Director Maternity, UHNM
      Darren Clement – Guy Hilton Research Centre, UHNM
      Li-Yun Chen – Student Researcher, Keele University
      Zara Richards – Postgraduate Research Administrator, Keele University
      Jill Stacey – Professional Head for Research Nursing, UHNM
      Helen Grocott – Information Governance Manager, UHNM
      Laura Longshaw – R&D Auditor & Monitor, UHNM
      Dawn Sirdefield – R&D Auditor & Monitor, UHNM

R&D ID: 1125 UKCRN ID: n/a CSP ID: n/a REC REF: 15/WM/0342